Dissertation

Submitted to the
Combined Faculties for the Natural Sciences and for Mathematics
of the Ruperto-Carola University of Heidelberg, Germany
for the Degree of
Doctor of Natural Sciences

Presented by
Dipl.-Biotechnol. Clemens Claudius Möller
Born in Karlsruhe
Oral Examination: 17.10.2007

Role of the Transient Receptor Potential Canonical 6 ion channel in genetic and acquired forms of proteinuric kidney disease

Referees: Prof. Dr. Michael Wink
Prof. Dr. Jochen Reiser

Table of Contents

Acknowledgments

Ich danke Prof. Dr. Michael Wink und Prof. Dr. Jochen Reiser für die exzellente Betreuung meiner Doktorarbeit.

Ich danke Prof. Dr. Gert Fricker und Prof. Dr. Thomas Braunbeck für ihre freundliche Bereitschaft, in meiner Prüfungskommission mitzuwirken.

Ich danke Prof. Dr. David Clapham, Prof. Dr. Iain Drummond, Prof. Dr. Raghuram Kalluri, Prof. Dr. Matthias Kretzler, Prof. Dr. Martin Pollak, Prof. Dr. Maria Rastaldi und Prof. Stuart Shankland für die Bereicherung meines Forschungsprojekts mit Ideen, Expertise, Reagentien, und dem Zugang zu ihren Laboratorien. Ich danke Prof. Dr. Peter Mundel und Dr. Christian Faul zudem für ihren wertvollen Rat.

Ich danke Dr. Mehmet Altintas, Dr. Changli Wei, Dr. Stefan Wawersik, Dr. Steven Mangos, Jing Li, Mélanie Becker und Jan Flesche für ihre kollegiale Hilfe.

Ich danke Petra Sgonina, Petra Fellhauer und Todd Erceg für die administrative Unterstützung meiner Arbeit.

Ich danke Cora Kaiser für ihre Hilfe mit Endnote.

Ich danke Yana Kamberov für ihre konstruktive Kritik.

Ich danke dem Deutschen Akademischen Austausch Dienst (DAAD) für die Förderung meiner Studien.

Vor allem danke ich meiner Mutter für ihre Liebe.

Publications

Moller, C. C., Wei, C., Altintas, M. M., Li, J., Greka, A., Ohse, T., et al. (2007). Induction of TRPC6 channel in acquired forms of proteinuric kidney disease. *J Am Soc Nephrol,* **18**(1), 29-36.

Reiser, J., Polu, K. R., Moller, C. C., Kenlan, P., Altintas, M. M., Wei, C., et al. (2005). TRPC6 is a glomerular slit diaphragm-associated channel required for normal renal function. *Nat Genet,* **37**(7), 739-744.

Moller, C. C., Pollak, M. R., & Reiser, J. (2006). The genetic basis of human glomerular disease. *Adv Chronic Kidney Dis,* **13**(2), 166-173.

Sever, S., Altintas, M. M.*, Nankoe, S. R.*, Moller, C. C.*, Ko, D., Wei, C., et al. (2007). Proteolytic processing of dynamin by cytoplasmic cathepsin L is a mechanism for proteinuric kidney disease. *J Clin Invest,* **117**(8), 2095-2104.
* equally contributing

Moller, C. C., Thomas, D., Van Dyk, D., Rylatt, D., & Sheehan, M. (2005). Preparative-scale fractionation by isoelectric trapping under nondenaturing conditions: separation of egg white protein isoforms on a modified Gradiflow unit. *Electrophoresis,* **26**(1), 35-46.

Moller, C. C., Mangos, S., Drummond, I. A., & Reiser, J. Expression profiles of TRPC1 and TRPC6 orthologs in zebrafish. *submitted*

Summary

Podocyte foot processes and the interposed glomerular slit diaphragm are critical components of the permeability barrier in the kidney. Mutations in several podocyte genes have been identified as the cause for progressive kidney failure and focal segmental glomerulosclerosis (FSGS). Podocyte injury is a hallmark of glomerular disease and usually involves the rearrangement of the podocyte actin cytoskeleton. Cell-specific therapies targeting podocyte injury are currently not available.

In 2004, a mutation in the TRPC6 ion channel was found to cosegregate with hereditary FSGS. Based on this finding it was hypothesized that TRPC6 is expressed in podocytes, and that TRPC6-mediated Ca^{2+} signaling contributes to the regulation of the podocyte actin cytoskeleton. According to this model, dysfunction of TRPC6 leads to a disruption of normal cytoskeletal organization, podocyte injury, and proteinuric disease. To test this hypothesis, four specific aims were outlined. First, to explore TRPC6 mutations in genetic FSGS. Second, to investigate its association with the glomerular filtration barrier. Third, to study TRPC6 expression in acquired forms of proteinuric kidney disease. Fourth, to investigate the molecular basis of TRPC6 contribution to the pathophysiology of proteinuric kidney disease

In genetic forms of FSGS, additional TRPC6 mutations were identified in five families with a history of FSGS. TRPC6-related FSGS presented as a late-onset disorder in individuals aged 17-57, and was not restricted to certain ethnic groups. All mutations occured in evolutionary conserved sites, and encoded amino acid substitutions at the amino- and carboxy-terminal ends of TRPC6. Two mutants, R895C and E897K, displayed increased current amplitudes, suggesting a pathogenic role of increased channel activity in TRPC6-related FSGS.

In an effort to understand the molecular basis for TRPC6 in the kidney, the association of TRPC6 with the glomerular filter was studied. TRPC6 was found to be expressed in podocytes near the glomerular slit diaphragm. TRPC6 colocalized and associated with the slit diaphragm proteins nephrin and podocin. The presence of TRPC6 in podocyte foot processes and its association with slit diaphragm proteins supports a role of TRPC6 in the regulation of glomerular filtration.

Since most proteinuric kidney diseases appear not as genetic but acquired disorders, TRPC6 was studied in humans with acquired glomerular diseases and in experimental models thereof. TRPC6 expression was induced in patients with minimal change disease and membranous glomerulopathy, as well as in passive Heymann nephritis (PHN) rats and puromycin aminonucleoside (PAN) rats. PAN-mediated podocyte injury correlated with increased receptor-operated calcium entry *in vitro*. TRPC6 gene delivery in mice was sufficient to induce proteinuria, and studies in cultured podocytes suggest that TRPC6 overexpression disrupts the actin cytoskeleton.

The present data suggest that in both genetic and acquired forms of proteinuric kidney disease, misregulation of TRPC6 – either by presence of mutated hyperactive channels, or by precence of too many wildtype channels – plays a pathogenic role. Together, the results of this work may have broad implications for the pathophysiology of TRPC6-related human kidney diseases, and promote the development of anti-proteinuric drugs interfering with TRPC6 channel function.

Zusammenfassung

Podozyten stellen mit ihren Fußfortsätzen und der sich dazwischen befindenden Schlitzmembran wichtige Bestandteile der glomerulären Filtrationsbarriere in der Niere dar. Mutationen in mehreren Genen für wichtige Proteine in Podozyten führen zu proteinurischen Nierenerkrankungen und fokaler segmentaler Glomerulosklerose (FSGS). Die meisten Nierenerkrankungen gehen mit einer Schädigung von Podozyten einher. Letztere äußert sich vor allem in einer Reorganisation des Aktin-Zytoskeletts. Derzeit gibt es keine zellspezifische Therapie bei Podozytenschädigung.

Im Jahr 2004 wurde über eine Mutation im Ionenkanal TRPC6 in Patienten mit hereditärer FSGS berichtet. Hieraus leitete sich die Hypothese dieser Arbeit ab: TRPC6 ist in Podozyten exprimiert und trägt in Podozyten zur Regulation des Aktin-Zytoskeletts bei. Dysregulation von TRPC6 führt demzufolge zu Störungen im Zytoskelett und Podozytenschädigung. Aus dieser Hypothese ergaben sich die Ziele dieser Arbeit: Untersuchung von TRPC6 (1) in hereditärer FSGS, (2) als Bestandteil des glomerulären Nierenfilters, (3) in erworbenen Formen proteinurischer Nierenerkrankungen sowie (4) Identifikation pathophysiologischer Mechanismen von TRPC6.

Um die Rolle von TRPC6 in hereditärer FSGS näher zu beleuchten, wurden 71 FSGS-Familien auf Mutationen im *TRPC6*-Gen untersucht. Es konnten fünf neue Mutationen identifiziert werden, darunter vier Missense-Mutationen in evolutionär konservierten Basenpaaren. Zwei Mutanten wiesen erhöhte Stromstärke-Amplituden auf. Letzteres wäre eine mögliche Erklärung für die Pathologie dieser Mutanten.

Um einen Zusammenhang zwischen TRPC6 und dem Nierenfilter zu prüfen, wurden Expressionsstudien durchgeführt. Es zeigte sich, dass TRPC6 in den Glomerula der Niere exprimiert ist; TRPC6 befindet sich u.a. in Podozytenfußfortsätzen nahe der Schlitzmembran. Ferner konnte nachgewiesen werden, dass TRPC6 mit den wichtigen Schlitzmembranproteinen Nephrin und Podocin kolokalisiert und mit diesen koimmunopräzipitiert. Dies deutet darauf hin, dass TRPC6 als Bestandteil der Schlitzmembran an der Regulation der glomerulären Filtration mitwirkt.

Tatsächlich ist der Großteil proteinurischer Nierenerkrankungen nicht hereditär, sondern erworben. Um zu klären, ob TRPC6 möglicherweise auch bei diesen Erkrankungen eine Rolle spielt, wurde zunächst die Expression von TRPC6 bei entsprechenden Patienten untersucht. Es zeigte sich, dass die Expression von TRPC6 bei Patienten mit minimal change Glomerulonephritis und membranöser Glomerulonephritis erhöht war. Ähnlich verhielt es sich in Tiermodellen sowie einem Zellkulturmodell von glomerulärer Nierenschädigung. Ferner war die Kalziumaufnahme geschädigter Podozyten *in vitro* höher als jene von normalen Podozyten. Der Gentransfer von TRPC6 in Mäusen führte zu Proteinurie. Eine mögliche Ursache hierfür könnte die Schädigung des Aktin-Zytoskeletts von Podozyten sein, wie sie bei der Überexprimierung von TRPC6 in kultivierten Podozyten beobachtet wurde.

Diese Arbeit impliziert eine Doppelrolle von TRPC6 in hereditären und erworbenen Formen glomerulärer, proteinurischer Nierenerkrankungen. Sowohl im Fall von TRPC6-Mutationen als auch für die erhöhte Expression des Wildtyp-Kanals legen die erhaltenen Daten nahe, dass eine erhöhte Kanalaktivität an der Schädigung von Podozyten beteiligt ist.

Abbreviations

ANOVA	analysis of variance
AP	alkaline phosphatase
CMV	cytomegalovirus
C_T method	comparative threshold method
C-terminal	carboxy-terminal
DAG	diacyl-glycerol
ddH_2O	double-distilled H_2O
DMEM	Dulbecco's modified Eagle's medium
(c)DNA	(complementary) deoxyribonucleic acid
EGF	epidermal growth factor
ELISA	enzyme linked immunosorbent assay
EPO	Erythropoietin
ESRD	end-stage renal disease
FRET	fluorescence resonance energy transfer
FSGS	focal segmental glomerulosclerosis
GAPDH	glyceraldehyde-3-phosphate dehydrogenase
GBM	glomerular basement membrane
(e)GFP	(enhanced) green fluorescent protein
GL-3	globotriaosylceramide
G protein	GTP-binding protein
HEK	human embryonic kidney
HEPES	N-2-hydroxyethylpiperazine-N'-(2-ethanesulphonic acid)
HIV	human immunodeficiency virus
hpf	hours post-fertilization
I-V	current-voltage
IFN-γ	interferon-γ
IgG	immunoglobulin G
IP_3(R)	inositol-1,4,5-trisphosphate (receptor)
LPS	lipopolysaccharide
MALDI-TOF	matrix assisted laser desorption/ionisation time-of-flight
MCD	minimal change disease
MGN	membranous glomerulonephritis
NCBI	National Center for Biotechnology Information
NFAT	nuclear factor of activated T-cells
NMMHC-IIA	nonmuscle myosin heavy chain IIA
N-terminal	amino-terminal

OAG	1-oleoyl-2-acetyl-*sn*-glycerol
P_{Ca}/P_{Na}	ratio of calcium permeability to sodium permeability
PAN	puromycin aminonucleoside
PBS(T)	phosphate buffered saline (Tween-20)
(RT-)PCR	(reverse transcription-) polymerase chain reaction
PDGF	platelet-derived growth factor
PIP_2	phosphatidylinositol-4,5-biphosphate
PHN	passive Heymann nephritis
PKC	protein kinase C
PKD	polycystic kidney disease
PLC	phospholipase C
PMA	phorbol-12-myristoyl-13-acetate
PTU	1-phenyl-2-thiourea
(m/r/t)RNA	(messenger/ribosomal/transfer) ribonucleic acid
SD	standard deviation
SDS	sodium dodecyl sulphate
S.E.M.	standard error of the mean
siRNA	small interfering ribonucleic acid
SNP	singe nucleotide polymorphism
SOCE	store-operated calcium entry
SV40	Simian vacuolating virus 40
TBMN	thin basement membrane nephropathy
TGF-β	transforming growth factor-β
TRP(C)	Transient Receptor Potential (Canonical)
VEGF(R)	vascular endothelial growth factor (receptor)

I. INTRODUCTION

I.1. Overview of kidney structure and function

The kidneys are two bean-shaped organs each weighing about 150 g. They are anatomically complex, consisting of many different types of specialized cells arranged in a highly organized three-dimensional pattern. The kidneys serve to maintain body composition, to excrete metabolic end products and foreign substances, and to produce and secrete important enzymes and hormones. Many important body functions heavily depend on the accurate regulation of body fluid composition and volume. For example, cardiac output and blood pressure are dependent on plasma volume, and most enzymes can carry out their physiological function only over rather narrow ranges of pH and ionic concentrations. Furthermore, the concentrations of potassium and calcium affect cell membrane potentials and excitability. As a consequence of food intake, metabolism, environmental factors, and exercise, the composition and volume of body fluids is subject to permanent change. It is the principal job of the kidneys to correct for any perturbations, thereby keeping the body fluid volume and the concentration of most ions within physiological range.

Each kidney is composed of functional units called nephrons. There are around one million nephrons in a human kidney; each nephron consists of a glomerulus and a long tubule (Fig. I.1.). The glomerulus is the site of blood filtration in the kidney. It is a twisted corpuscle of capillaries lines by endothelial cells, with the outside of the capillaries covered with specialized epithelial cells, called podocytes. Podocytes are large, highly differentiated cells that form an array of lace-like foot processes over the outer layer of the glomerular capillaries. An outer epithelial capsule, called Bowman's capsule, acts as a pouch to capture the filtrate, and to direct it into the beginning of the tubule.

The tubule is composed of a single layer of epithelial cells. In the tubule, the glomerular filtrate undergoes a series of modifications before becoming the final urine. These changes consist of reabsorption (removal) and secretion (addition) of solutes and fluid. Reabsorption, the movement of solute or water from the tubular lumen into blood, is the predominant process in the renal regulation of sodium, chloride, water, glucose, amino acids, proteins, phosphates, calcium, magnesium, urea, and uric acid. In contrast, secretion, i.e. the movement of solute from the blood or cell interior into the tubular lumen, is important in the regulation of H^+, potassium, ammonia, and a number of organic acids and bases.

The nephrons are packed together tightly to make up the kidney parenchyma, which can be divided into regions. The outer layer of the kidney is called the cortex; it contains all the glomeruli, much of the proximal tubule, and some of the more distal portions as well. The inner section, called the medulla, consists largely of the parallel arrays of the loops of Henle and collecting ducts. The medulla is formed into cone-shaped regions, called pyramids (the human kidney typically has seven to nine). The medulla is important for concentration of the urine: the extracellular fluid in this region of the kidney has much higher solute concentration than plasma – as much as four times higher – with highest solute concentrations reached at the papillary tips.

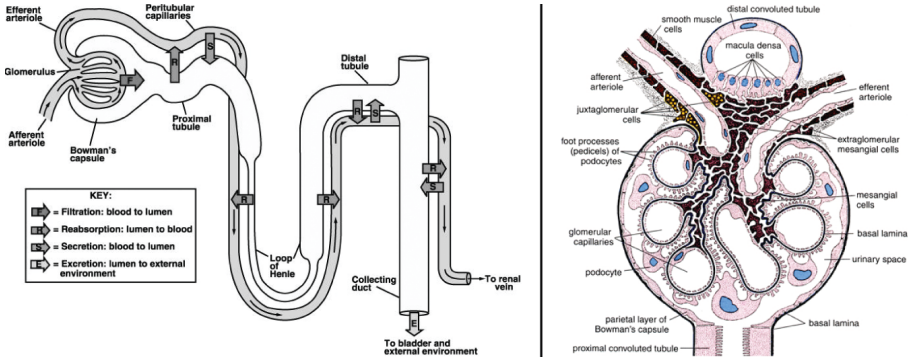

Fig. I.1. Organization of the nephron. (Left) The human kidney is made up of a million nephrons, one of which is shown schematically here. Each nephron consists of the following parts: glomerulus, proximal tubule, loop of Henle, and distal tubule. Several nephrons coalesce to empty into a collecting duct connecting the nephrons to the urether. Kidney filtration takes place in the glomerulus, a twisted corpuscle of capillaries. Blood enters the glomerular capillary tuft via the afferent arteriole, where an ultrafiltrate of plasma is formed, and exits the glomerulus via the efferent arteriole. The glomerular filtrate, consisting of water, small dissolved solutes and small proteins, passes the glomerular filtration barrier, and is collected in the lumen of Bowman's capsule. From there, it enters the renal tubular system, to be carried over a circuitous course, successively modified by exposure to the sequence of specialized tubular epithelial segments with different transport functions. The poximal tubule absorbs approximately two thirds of the glomerular filtrate. Fluid remaining at the end of the proximal tubule enters the loop of Henle, the distal tubule, and finally the collecting duct. Along the tubule, most of the glomerular filtrate is absorbed, but some additional substrates are secreted. After being processed by filtration, reabsorption, and secretion, the final urine enters the the ureter, collects in the bladder, and is finally excreted from the body. (Right) Schematic representation of the glomerulus (Source: courtesy of Prof. em. Dr. med. Wilhelm Kriz, Ruprecht-Karls-Universität Heidelberg, Germany.)

The kidney fulfills three essential functions in the body. These functions are maintenance of body composition, excretion of metabolic end products and foreign substances, and production and secretion of enzymes and hormones. The maintenance of body composition involves the coordinated regulation of blood osmolarity and acidity, as well as of the electrolyte concentrations in the blood, in particular sodium, potassium, chloride, calcium, magnesium, and phosphate. The kidney achieves this regulation by variation in the amounts of water and ions excreted in the urine. Among the substances that are excreted by the kidney are a number of products of metabolism, most notably urea, but also toxins and drugs belong into this category. The kidney is also an important endocrine organ and is responsible for the production

of Renin, Erythropoietin (EPO), and 1,25-Dihydroxyvitamin D3, the most active form of Vitamin D3, among others. Renin is an enzyme that catalyzes the conversion of angiotensinogen to angiotensin, a potent vasoconstrictor peptide contributing to salt balance and blood pressure regulation. Renin is produced in the kidney by the granular cells of the juxtaglomerular apparatus. Another important protein produced by the kidney is Erythropoietin (EPO), a glycosylated, 165-amino acid protein produced by renal cortical interstitial cells. EPO stimulates the maturation of erythrocytes in the bone marrow, and has become well known for its role in competitive sports doping practices. Finally, 1,25-Dihydroxyvitamin D3 is formed by kidney proximal tubule cells; this protein is a steroid hormone playing an important role in the regulation of body calcium and phosphate balance.

The characteristic events of filtration, reabsorption, and secrection in the kidney depend on a highly complex organization of blood circulation in this organ. The renal circulation is unusual in that in breaks into two separate capillary beds: the glomerular bed and the peritubular bed. These two capillary networks are arranged in series so that all the renal blood flow passes through both. As blood leaves the glomerulus, the capillaries coalesce into the efferent arteriole, but then bifurcate again to form the peritubular capillary network. This second network of capillaries is the site where the fluid reabsorbed by the tubules is returned to the circulation. Pressure in the first capillary bed, that of the glomerulus, is rather high (about 40-50 mmHg), whereas pressure in the peritubular capillaries is similar to that in capillary beds elsewhere in the body (about 5-10 mmHg). The renal artery, which enters the kidney at the renal hilum, carries about one fifth of the cardiac output; this represents the highest tissue-specific blood flow of all larger organs in the body (about 350 ml/min per 100 g tissue). As a consequence of this generous perfusion, the renal arteriovenous O_2 difference is much lower than that of most other tissues.

About one fourth of the plasma that enters the glomerulus passes through the filtration barrier to become the glomerular filtrate. Blood cells, most proteins, and about 75% of the fluid and small solutes stay in the capillary and leave the glomerulus via the efferent arteriole. This postglomerular blood, which has a relatively high concentration of protein and red cells, enters the peritubular capillaries, where the high osmotic pressure from the high protein concentration facilitates the reabsorption of fluid. The peritubular capillaries coalesce to form venules and eventually the renal vein.

I.1.1. The glomerular filtration barrier

The function of the glomerular filtration barrier is to retain plasma proteins in the blood on the basis of molecular size and charge. To reach from the vascular into the urinary space, molecules must pass through three distinct structures (Fig. I.2.).

The first structure is a fenestrated endothelium decorating the inner surface of glomerular capillaries. The second structure is the glomerular basement membrane (GBM), a thin sheet of specialized extracellular matrix. The third structure is formed by visceral glomerular epithelial cells (podocytes) and the interposed glomerular slit diaphragm. This complex three-layer barrier is freely permeable to water and small dissolved solutes, but retains most of the proteins and other larger molecules, as well as all blood particles.

The main determinant of passage through the glomerular filter is molecular size. A molecule such as inulin (5 kD) passes freely through the filter, and even a small protein such as myoglobin (17 kD) is filtered to a large extent. In contrast, substances of increasing size are retained with increasing efficiency, until at a size about 60-70 kD the amount filtered becomes very small. Filtration also depends on ionic charge, and negatively charged proteins, such as albumin, are retained to a greater extent than would be predicted by size alone.

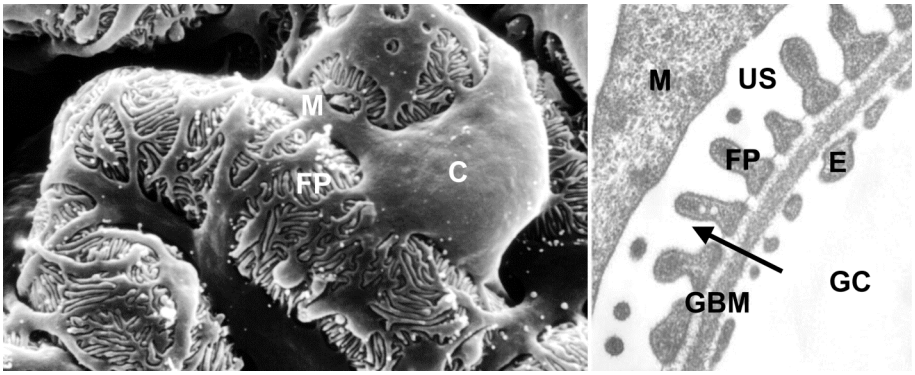

Fig. I.2. Ultrastructure of the glomerular filter. (Left) Scanning electron micrograph of normal rat glomerular capillaries. The urinary side of the capillary wall in covered by the highly branched podocytes. (Right) Cross-section through the glomerular filtration barrier. The arrow indicates the direction of fluid flow during glomerular filtration. C, podocyte cell body; M, podocyte major process; FP, podocyte foot processes; GBM, glomerular basement membrane; E, glomerular endothelial cells; US, urinary space; GC, glomerular capillary. (Source: adapted from Pavenstadt *et al.*; Physiol Rev. 2003, 83:253-307 [Pavenstadt *et al.*, 2003] and Mundel & Kriz; Anat Embryol (Berl). 1995, 192:385-397 [Mundel & Kriz, 1995].)

The fenestrated endothelium decorates the glomerular capillaries. The fenestrae between the endothelial cells are 70-100 nm in diameter. On their surface, the endothelial cells carry a complex of negatively-charged sialoproteins and proteoglycans that is referred to as the glycocalyx [Deen *et al.*, 2001]. While the

negative charge of the glycocalyx constitutes a potential barrier retarding anionic macromolecules, there is no evidence so far for such a role of the glycocalyx.

The glomerular basement membrane (GBM) is a thin sheet of specialized extracellular matrix [Miner, 2005] composed of four major components: laminin, type IV collagen, nidogen/entactin, and proteoglycans [Miner, 1999]. During glomerulogenesis, the GBM is built up in a combined effort by the underlying endothelial cells and overlying podocytes. As the case for the fenestrated endothelium, it is thought that that the presence of negatively-charged molecules within the GBM serves as a barrier retarding anionic macromolecules.

The final retention barrier consists of podocytes and the interposed glomerular slit diaphragm [Somlo & Mundel, 2000]. This explains why podocyte damage is typically associated with the development of proteinuria, i.e. the loss of proteins from the blood into the urine, which can lead to a permanent deterioration of the glomerular filter. Major advances in unraveling the structures necessary for proper podocyte function [Tryggvason & Wartiovaara, 2001] have pointed to the crucial role of podocytes in the maintenance of glomerular health and filtration. Podocytes are non-replicating, polarized epithelial cells that originate from precursor mesenchymal cells [Pavenstadt *et al.*, 2003]. During nephrogenesis, these cells undergo modification from a classic epithelial cell phenotype to a highly specialized octopus-shaped cell. Podocytes cover the external surface of adjacent capillaries and interact with the GBM through finger-shaped extensions called pedicels or foot processes. The basal surface of podocyte foot processes is anchored in the GBM via α3-/β1-integrins [Adler, 1992] and α-/β-dystroglycans [Regele *et al.*, 2000]. Podocyte foot processes interdigitate in a complex manner forming an intricate network surrounding the glomerular capillaries.

Adjacent foot processes bridge their narrow 300-400 Å wide gaps by a membrane-like structure, the glomerular slit diaphragm [Moller *et al.*, 2006]. The slit diaphragm is a specialized cell-cell junction. As a thin porous membrane, it is thought to form the major determinant of the size selectivity of the glomerular filtration barrier [Tryggvason & Wartiovaara, 2001]. The slit diaphragm appears early on in nephrogenesis. It is thought to be a modified adherens junction that allows for the passage of water and solutes from the blood into the kidney ultrafiltrate while inhibiting the loss of larger plasma molecules auch as albumin. The slit diaphragm has a zipperlike structure composed of a number of proteins with large extracellular domains including nephrin, neph1, neph2, neph3, P-cadherin, and FAT (Fig. I.3.).

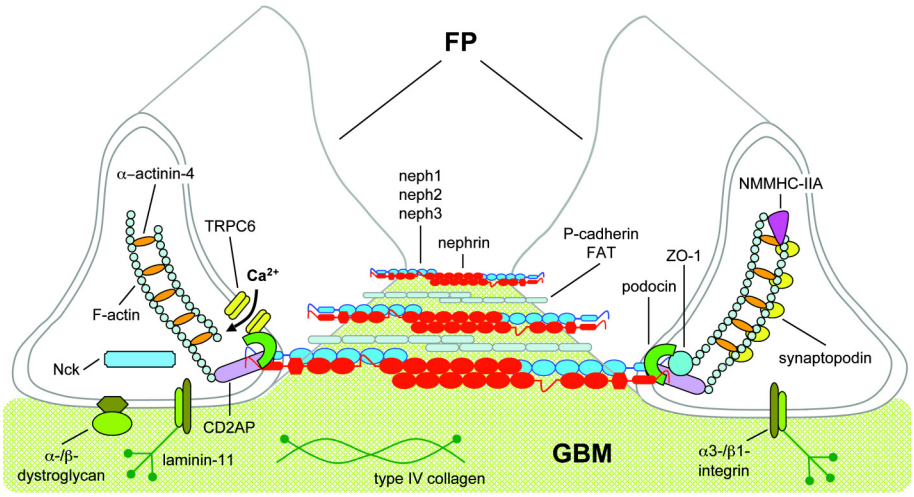

Fig. I.3. Schematic representation of podocyte foot processes and the interposed slit diaphragm. FP, podocyte foot processes; GBM, glomerular basement membrane. (Source: Moller *et al.*; Adv Chronic Kidney Dis. 2006, 13:166-173 [Moller *et al.*, 2006].)

Four distinct functions of the slit diaphragm multi-protein complex have been described [Huber & Benzing, 2005]. These are: i) function as molecular sieve, ii) function as cell-cell contact between podocytes, iii) function as a signaling platform, and iv) function as an organizing center regulating podocyte actin dynamics. The slit diaphragm proteins nephrin and its homologues neph1, neph2, and neph3 are important scaffolding molecules and key players in mediating extracellular signals into the podocyte cell body [Benzing, 2004]. Various adaptor proteins including podocin [Boute *et al.*, 2000], ZO-1 [Schnabel *et al.*, 1990], and CD2AP [Shih *et al.*, 1999] connect the slit diaphragm to the podocyte intracellular space. Furthermore, it has been shown that the α-actinin-4-binding protein densin and the src family protein tyrosine kinase Fyn are located at the slit diaphragm site [Ahola *et al.*, 2003; Verma *et al.*, 2003].

I.2. Glomerular kidney disease

Chronic kidney failure has become one of the biggest health care issues worldwide. In Germany alone, every year more than 15,000 patients are diagnosed with end-stage renal disease (ESRD), and more than 60,000 patients require dialysis. With life expectancy increasing and societies aging, kidney disorders are on the advance.

Whereas many of the acute kidney diseases originate in kidney tubules, most chronic kidney diseases originate in the glomerulus. In fact, glomerulopathies account for a significant fraction of end-stage renal disease (ESRD). The most important symptoms include proteinuria, hematuria, edema, and a reduced glomerular filtration rate. With respect to their pathological and clinicial manifestations, glomerular diseases are generally classified as falling into one of the broad categories with either an

inflammatory phenotype (nephritic syndrome) or a non-inflammatory phenotype (nephrotic syndrome). Nephritic syndrome is characterized pathologically by diffuse inflammatory changes in the glomeruli and clinically by abrupt-onset hematuria, mild proteinuria, and, often, hypertension, and edema. In contrast, nephrotic syndrome is characterized pathologically by a prolonged increase in the glomerular capillary wall permeability and clinically by heavy proteinuria and often hypoalbuminemia, severe edema, lipiduria, and lipemia. In many glomerular diseases, features of nephritic and nephrotic syndrome go hand in hand, making it difficult to identify the underlying cause of the disease. Likewise, many conditions referred to as glomerular diseases do not originate from a common, single disease-causing mechanism, but rather represent the pathological manifestation of a variety of associated diseases in the glomerulus.

Glomerular proteinuria is a hallmark of glomerular disease and results from an increased permeability of the glomerular filtration barrier. Normally, proteins larger than albumin do not enter the urinary space whereas lower molecular weight proteins are filtered and partially reabsorbed in the proximal tubule. Normal excretion levels of protein into the urine vary between 0 and 150 mg/d. Proteinuria is clinically characterized by a protein loss into the urine of more than 150 mg/d. Levels of 3 g of urinary protein per day are generally used to define “nephrotic-range” proteinuria.

While glomerular diseases can result from dysfunction in any glomerular cell type, including mesangial cells and endothelial cells, in many forms of glomerular diseases, proteinuria is correlated with podocyte injury and the podocyte has been suggested as the main culprit for glomerulosclerosis [Kriz *et al.*, 1998; Shankland 2006]. The complexity of interactions among podocyte proteins provides several targets for podocytopathy and disruption of the glomerular filtration barrier [Durvasula & Shankland, 2006], and studies in human diabetic nephropathy [Steffes *et al.*, 2001], the puromycin aminonucleoside (PAN) model of glomerulosclerosis [Kim *et al.*, 2001] and in TGF-β transgenic mice [Schiffer *et al.*, 2001] provide convincing evidence for a correlation between damage and loss of podocytes and progression of glomerular diseases.

Podocytes are injured in many forms of human (genetic and acquired) and experimental glomerular disease, including minimal change disease, focal segmental glomerulosclerosis (FSGS), diabetic nephropathy, membranous glomerulopathy, crescentic glomerulonephritis and Lupus nephritis [Endlich *et al.*, 2001], and loss of the integrity of the intricate structures of the podocyte can generally be seen in patients with nephrotic syndrome, who clinically present with hypertension, proteinuria, and progressive kidney disease.

In patients with glomerular disease, the ultrastructural examination of kidney biopsies often reveals the loss of normal podocyte foot process structure, resulting in a flattened phenotype, where foot processes form an epithelial monolayer lacking functional slit diaphragms; this condition is called foot process effacement (Fig. I.4.). Foot process effacement is often associated with proteinuria and is accompanied by a reorganization of the podocyte actin cytoskeleton [Kriz *et al.*, 1998].

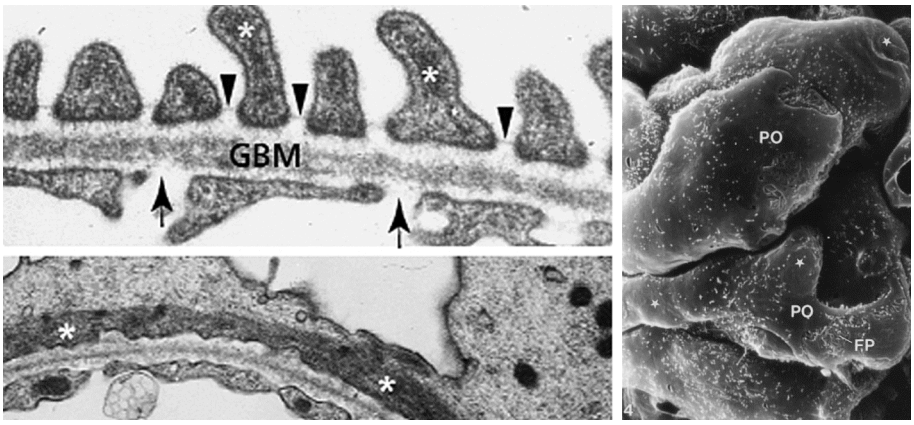

Fig. I.4. Podocyte foot process effacement. The normal glomerular filter (left upper panel) consists of three components: fenestrated endothelium (arrows), the glomerular basement membrane (GBM) and podocyte foot processes with the interposed slit diaphragm (arrowheads). Actin filaments are present in normal foot processes (asterisks). In nephrotic syndrome (left bottom panel), the effaced foot processes form a continuous band of cytoplasm containing a dense band of actin filaments (asterisks) running parallel to the GBM. On injured glomerular capillaries as seen in various glomerulopathies, podocyte cell bodies (PO) are attenuated and pulled over the outer surface of capillaries, thus covering major parts of the filtration area (right panel). Interdigitating foot processes (FP) are hardly visible due to foot process effacement. Moreover, pseudocysts (stars) begin to develop. (Source: adapted from Somlo & Mundel; Nat Genet. 2000, 24:333-335 [Somlo & Mundel, 2000] and Kriz *et al.*; Kidney Int. 1995, 48:1435-1450 [Kriz *et al.*, 1995].)

Recent insight into the molecular pathology of podocyte injury unraveled at least six major molecular causes of foot process effacement and proteinuria: i) interference with the negative surface charge of podocytes [Takeda *et al.*, 2001], ii) interference with the activity of GLEPP1, a membrane-bound tyrosine phosphatase [Wharram *et al.*, 2000], iii) interference with the actin cytoskeleton and its associated protein α-actinin-4 [Kaplan *et al.*, 2000], iv) interference with the GBM or the podocyte-GBM interaction [Kreidberg *et al.*, 1996], v) interference with the slit diaphragm [Kestila *et al.*, 1998], and vi) induction of podocyte B7-1 expression [Reiser *et al.*, 2004].

If early structural changes of podocytes are not reversed, severe and progressive glomerular damage is likely to develop [Reiser *et al.*, 2002]. This involves podocyte vacuolization, pseudocyst formation, detachment of podocytes from the GBM, and eventually podocyte cell death. Since the highly differentiated podocytes are unable to proliferate, the loss of single podocytes leads to podocyte depletion over time, which is a major determinant of glomerulosclerosis and chronic kidney failure.

I.2.1. Genetic forms of glomerular kidney disease

Clinical and molecular research aimed to understand glomerular disease has emerged to one of the most active areas in renal research at large. The unraveling of genetic causes resulting in proteinuria has helped to define roles for each component of the glomerular filtration barrier in the development of urinary protein loss.

Most of the inherited glomerular diseases have in common defects in the podocyte [Moller *et al.*, 2006], and a number of genetic mutations in several podocyte genes have been identified as culprits for progressive renal failure or increased glomerular disease susceptibility.

Recent progress in the eludication of genetic causes of glomerular disease revealed four groups of genetic disorders associated with podocyte injury: i) GBM-associated genetic podocytopathies, ii) cytoskeleton-associated genetic podocytopathies, iii) organelle-associated genetic podocytopathies, and iv) slit diaphragm-associated podocytopathies.

GBM-associated genetic podocytopathies

Basement membranes have been shown to influence cell proliferation, migration, and differentiation. Also in the kidney, an intact GBM is necessary for proper adhesion and function of the underlying endothelial cells and podocytes [Miner *et al.*, 2005]. Inherited disruption of two components of the GBM, type IV collagen and laminin-β2, have so far been shown to lead to glomerular disease.

Type IV collagen-related diseases, including Alport syndromes and thin basement membrane nephropathy (TBMN), originate from defects in the genes encoding the α-chains of type IV collagen [Kashtan, 2005]. In four of the six identified α-chain genes so far, mutations have been associated with progressive hereditary nephritis. With the exception of TBMN, all these gene defects lead to a thickened GBM and progressive hematuric glomerular disease, resulting in renal insufficiency and end-stage renal disease (ESRD). In contrast, patients with TBMN present with a thinnened GBM and asymptomatic microscopic hematuria. It is speculated that, in type IV collagen-related diseases, an increased fragility of the GBM accounts for pathogenesis.

The rare Nail-Patella syndrome is characterized by loss-of-function mutations in *LMX1B* encoding a transcription factor regulating the expression of *COL4A3*, *COL4A4*, *NPHS1* (nephrin), *NPHS2* (podocin), and *CD2AP*. In most patients with Nail-Patella syndrome, the GBM has a characteristic moth-eaten appearance and contains fibrillar collagen deposits. Whereas some individuals do not present with any clinical nephropathy, proteinuria occurs in 30-40% of patients and, in 5-10% of patients, the disease leads to progressive renal failure. While the phenotype of Nail-

Patella syndrome seems to be primarily confined to the GBM, it is likely that transcriptional dysregulation of slit diaphragm proteins contributes to the pathobiology of the disease.

Gene defects in *LAMB2* encoding the laminin-β2 chain lead to the rare Pierson syndrome. Laminin-β2 is abundantly expressed in the GBM where it is present in the adult GBM laminin-11 isoform (α5:β2:γ1). Laminin-11 plays a key role in anchoring and differentiation of podocyte foot processes. Laminin-11 malfunction due to a lack of of functional laminin-β2 is thought to be the cause for the disease, which leads to the onset of nephrosis soon after birth, rapid progression to end-stage renal disease (ESRD), and death in the first year.

Cytoskeleton-associated genetic podocytopathies

The major function of podocyte foot processes is to create the outer portion of the glomerular filtration barrier. Because the glomerular capillary wall undergoes cyclic distensions, a functional adaptive cytoskeleton, providing both mechanical strength and flexibility, is required for maintaining podocyte structural integrity. To match this unique challenge, podocytes have developed a highly dynamic cytoskeletal architecture involving microtubules, intermediate filaments and actin microfilaments. Whereas the podocyte cell body and primary processes are predominantly composed of microtubules and intermediate filaments, podocyte foot processes contain an actin-based contractile cytoskeletal network [Drenckhahn & Franke, 1988]. A group of cytoskeleton-associated proteins, including talin, paxillin, and vinculin, link actin filaments to the cell membrane-associated integrins at the GBM. Parts of the actin cytoskeleton are also linked to the slit diaphragm via catenins, ZO-1 or CD2AP.

Mutations in *ACTN4* encoding α-actinin-4 are associated with the development of familial focal segmental glomerulosclerosis (FSGS) [Pollak *et al.*, 2002]. The disease is characterized by onset in adolescence or early adulthood, slow progression, non-nephrotic proteinuria, and renal insufficiency. The protein α-actinin-4 is expressed in podocytes, where it crosslinks F-actin filaments in foot processes. The disease-causing mechanism appears to be linked to accelerated degradation of mutant α-actinin-4 by the proteasome. It is also thought that an increased affinity of mutant α-actinin-4 to F-actin may result in a dysregulation of actin filament formation in podocytes. Interestingly, α-actinin-4 is expressed throughout the body but the human phenotype associated with *ACTN4* mutations is apparent only in the kidney. This suggests that either a podocyte-specific protein-protein interaction is altered by human disease-associated mutations, or that the unique structure of the podocyte makes it particularly susceptible even to subtle changes in its cytoskeletal architecture.

Another group of cytoskeleton-associated mutations lead to podocyte injury by interference with the nonmuscle myosin heavy chain IIA (NMMHC-IIA), encoded by *MYH9* [Seri *et al.*, 2003]. MYH9-related diseases include the Epstein syndrome, Fechtner syndrome, May-Hegglin anomaly, and Sebastian syndrome. It has been suggested that these four sydromes are in fact not distinct entities but rather derive from a common single disorder with a continuous clinical spectrum characterized by a varying expressivity. Class II myosins play a well-characterized role in the contraction and force production in muscles and are required for cytokinesis, cell mobility, cell polarity, and cell architecture. In podocytes, NMMHC-IIA is thought to be a major component of the actin-myosin contractile apparatus in foot processes. The disease-causing mechanism leading to the glomerular phenotype of *MYH9*-related disease remains elusive.

Organelle-associated genetic podocytopathies

One podocyte organelle shown to be a target of genetic defects causing glomerular disease, is the mitochondrion. Expression of mitochondrial gene mutations follows a pattern of maternal inheritance. A typical example of a mitochondrial cytopathy is the A3243G transition in the mitochondrial gene *MTTL1* encoding for the tRNALeu(URR). This mutation leads to a defect in the Krebs cycle and has been associated with podocyte abnormalities and the development of focal segmental glomerulosclerosis (FSGS). Recently, an individual with steroid-resistant nephrotic syndrome, FSGS and evidence of abnormal mitochodria in the podocyte was presented [Lowik *et al.*, 2005]. The pathogenic impact of the A3243G mutation is not clearly understood. One hypothesis is that, because podocytes are terminally differentiated cells, they may be more susceptible to the effects of mitochondrial dysfunction as compared to neural and muscle cells. With the accumulation of abnormal mitochondria, the synthesis of mitochondrial proteins and appropriate oxidadive phosphorylation to generate energy for proper podocyte function may be absent. Most recently, another disease of potentially genetic origin was added to the list of mitochondria-associated podocytopathies: a mitochondrial respiratory chain deficiency was reported in one patient with congenital nephrotic syndrome and two siblings with severe congenital kidney disease and probable neprotic syndrome [Goldenberg *et al.*, 2005]. In all cases, mutations in the gene *NPHS1* (nephrin), which are the classic cause for congenital nephrotic syndrome of the Finnish type, were excluded. The authors suggest genetic deficiency in respiratory chain genes as a putative disease-causing mechanism. However, the genetic locus of such mutations remains elusive.

Another organelle associated to glomerular disease is the podocyte lysosome. The systemic Fabry disease, a defect in *galA* encoding the lysosomal enzyme α-galactosidase A leads to the formation of globotriaosylceramide (GL-3) deposits in nearly all glomerular cell types. Even though this mainly affects the vascular endothelium, there are particularly dense accumulations in podocytes and distal tubular epithelial cells [Warnock *et al.*, 2005]. The clinical outcome is azotemia, proteinuria and chronic kidney disease. In contrast to the majority of glomerular diseases, a promising therapeutic strategy exists with enzyme replacement therapy [Warnock, 2007] .

Slit diaphragm-associated podocytopathies

Due to the intricate organization of the slit diaphragm, it comes to no surprise that genetic defects in the associated proteins lead to podocyte injury. A number of genes associated with glomerular diseases have been identified in the past years and the respective clinical outcomes are well characterized [Pollak, 2002]. Among these diseases are the congenital nephrotic syndrome of the Finnish type caused by mutations in *NPHS1* encoding nephrin, and the steroid-resistant nephrotic syndrome of the podocin type caused by mutations in the *NPHS2* gene encoding podocin.

The Frasier syndrome and Denys-Drash syndrome are overlapping syndromes caused by mutations in *WT1* encoding Wilms' tumor protein, a transcription factor regulating a number of podocyte genes including *NPHS1* (nephrin) and *NPHS2* (podocin). Both syndromes are characterized by glomerular disease; while Frasier syndrome shows a pattern of focal segmental glomerulosclerosis (FSGS) in kidney biopsies, Denys-Drash syndrome is defined by diffuse mesangial sclerosis.

In two patients with primary focal segmental glomerulosclerosis (FSGS), a nucleotide variant leading to *CD2AP* haploinsufficiency was detected [Kim *et al.*, 2003]. The higher susceptibility of individuals carrying this mutation for glomerular disease demonstrates the pathogenic role of altered CD2AP expression levels. CD2AP is not only thought to be an important adaptor protein in podocytes, coupling the slit diaphragm to the actin cytoskeleton, but also implicated in endocytosis and lysosomal sorting. This, and the observation that, in $CD2AP^{+/-}$ mice, immunoglobulins accumulate in the GBM, led the authors to speculate that, in addition to its possible structural role, CD2AP may also be involved in targeting proteins to the degradative pathway. Immunoglobulin deposits in $CD2AP^{+/-}$ mice may reflect the impaired ability of the podocyte to clear plasma proteins from the GBM, suggesting a possible disease-causing mechanism in affected patients with *CD2AP* haploinsufficiency.

I.2.2. Acquired forms of glomerular kidney disease

In contrast to inherited forms of glomerular kidney disease, which originate due to a known genetic defect, acquired forms of glomerular kidney disease have no known underlying genetic cause. In fact, acquired forms of glomerular kidney disease account by far for most of the glomerular diseases since only a few of all disease states can currently be classified as genetic forms.

Among the acquired forms of glomerular kidney disease, one can differentiate between three groups. The first group is represented by disease states that are secondary to systemic disorders such as diabetes (diabetic nephropathy), infection with HIV (HIV-nephropathy), high blood pressure, or obesity. In fact, diabetes and high blood pressure are by far the most common culprits for acquired forms of glomerular kidney disease. The second group is represented by kidney diseases that develop due to the contact with certain toxins, or the (long-term) administration of certain drugs. The third group is represented by idiopathic diseases, i.e. forms of kidney disease for which the pathogenic cause remains completely unknown.

Due to the diversity of disease phenotypes and the possible causes thereof, and the lack of knowledge about the pathogenesis in most cases, the therapy of aquired forms of proteinuric kidney diseases remains a challenging task and in most cases, doctors are limited to ameliorating the symptoms of the disease and targeting the underlying systemic causes for the disease if such causes can be identified. A tissue- or cell-specific therapeutic targeting podocytes as the main cell type affected in most types of glomerular kidney diseases, is currently not available, and research on such drugs is lacking behind due to an incomplete understanding of the mechansims underlying glomerular filtration and the development of glomerular disease.

I.2.3. Focal segmental glomerulosclerosis (FSGS)

Focal and segmental glomerulosclerosis (FSGS) is a common, progressive pathological renal lesion observed in a disparate group of clinical disorders [Daskalakis & Winn, 2006]. Next to the aforementioned genetic predispositions associated with the development of FSGS, FSGS most often appears as an acquired glomerular kidney disease secondary to other disorders including HIV infection, obesity, hypertension and diabetes [Vincenti & Ghiggeri, 2005]. Furthermore, FSGS can also appear as an isolated, idiopathic condition.

FSGS is diagnosed by renal biopsy, with histopathological findings characterized by partial scarring of the glomerular capillary tuft in a significant proportion of glomeruli (Fig. I.5.). A FSGS-typical pattern has areas of glomerular scarring in several, but not all glomeruli (focal lesions), and the scarring usually affects only part

of the glomerular tuft, not the entire glomerulus (segmental lesions). Clinically, proteinuria and decreasing kidney function are the most common manifestations of FSGS. FSGS accounts for only 5-20% of cases of idiopathic nephrotic syndrome in children, but for as many as 35% of cases in adults [Haas *et al.*, 1995]. Often, renal insufficiency in FSGS progresses to end-stage renal disease (ESRD), a highly morbid state requiring either dialysis therapy or kidney transplantation.

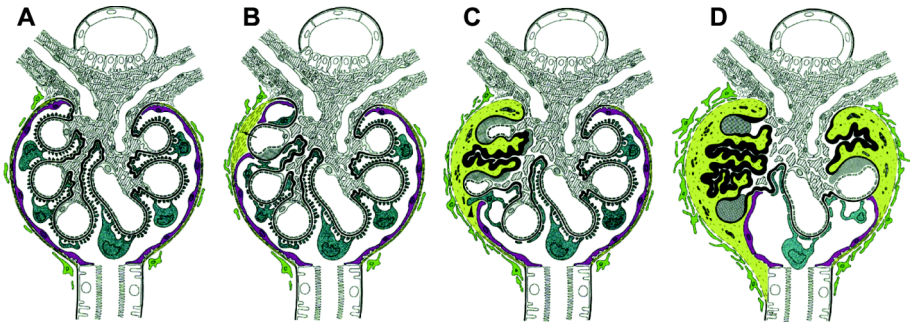

Fig. I.5. Schematic depicting the development of segmental glomerulosclerosis. (A) Normal glomerulus with vascular and urinary poles. Smooth muscles, extra glomerular mesangial, and mesangial cells proper are hatched; podocytes are shown in blue, parietal epithelial cells in red. The GBM is shown in black, the parietal basement membrane in yellow, tubular epithelia are shown in white. (B) A dilated and podocyte-denuded capillary is attached to Bowman's capsule. The attachment is accomplished by the affixation of parietal cells to the naked GBM. Thereby a gap in the parietal epithelium has come into existence, permitting filtration/exudation towards the cortical interstitium (arrow). (C) The adhesion has spread to neighboring capillaries resulting in either the collapse or in hyalinosis (shown in a dark grey pattern) of the involved capillaries. Podocytes at the flanks of the adhesion degenerate. The parietal epithelium may either appose those podocytes (arrowhead) or attach directly to the GBM at the flanks of the adhesion. Fluid leakage from perfused capillaries inside the adhesion has created a paraglomerular space (shown in yellow) that contains the sclerotic tuft remnants (that is, collapsed or hyalinized GBM formations). Towards the cortical interstitium this paraglomerular space has become separated by a layer of sheet-like fibroblast processes (shown in green). (D) Via the vascular pole the sclerotic process has reached a further lobule. A small "intact" tuft remnant protrudes into the urinary space still covered by the parietal epithelium. The sclerotic tuft remnants are located outside the parietal epithelium in the paraglomerular space that is separated from the cortical interstitium by a complete layer of cortical fibroblasts. Even in those late stages of injury perfused capillaries are regularly found within the sclerotic regions, probably accounting for the further expansion of the paraglomerular space that may extend onto the proximal tubule. In even later stages fibroblasts will invade the sclerotic area, resulting in fibrous organization. (Source: adapted from Kriz *et al.*; Kidney Int. 1998, 54:687-697. [Kriz *et al.*, 1998])

In searching for the molecular origins of FSGS, one has to consider all structures of the glomerular filter; during glomerulogenesis, the GBM is built by the combined effort of endothelial cells and podocytes, and malfunction of either component can interfere with the other two via multiple mechanisms. Over the last two decades, an enormous data set has evolved, correlating podocyte damage with progressive glomerulosclerosis [Kretzler, 2005]. Multiple reports underscore the concept that podocytes are the culprit for the majority of FSGS phenotypes, whether injured directly (e.g. defects in podocyte genes) or indirectly (secondary to other defects, e.g. in the GBM) [Kriz *et al.*, 1998; Kriz, 2002; Wiggins, 2007].

1.2.4. Model systems for the study of glomerular kidney disease

Podocyte cell culture

Podocytes have taken center stage in renal research as important regulators of glomerular filtration, and podocytopathy has been shown to be an important determinant of glomerular kidney disease [Shankland, 2006]. A major breakthrough for the research on podocytes occured around a decade ago when the first reports described the primary culture of podocytes in a way that these cells resembled structurally and functionally glomerular podocytes *in vivo* [Mundel *et al.*, 1996]. Soon afterwards, another milestone was achieved by generating conditionally immortalized differentiated podocytes cell lines, which can be maintained and studied in a straightforward and reproducible manner [Mundel *et al.*, 1997].

Primary cultures of podocyte are derived from glomeruli isolated from kidney cortex. The isolation of glomeruli can be carried out by a sieving technique under sterile conditions, passing kidney homogenates through a set of consecutive sieves with decreasing pore sizes, which eventually yields a glomerular preparation with minor contaminations of tubular cells and pariethal epithelium [Mundel *et al.*, 1997]. For higher purity of the glomerular preparation, an additional Ficoll-gradient centrifugation can be performed [Norgaard, 1976]. Ideally, cell culture is then started from manually selected glomeruli that have been decapsulated, i.e. glomeruli that are devoid of Bowman's capsule, thereby minimizing the presence of cell types other than podocytes.

A considerable pitfall of the early primary cultures of podocytes was that these cells very rapidly began to lose the cell type-specific properties of differentiated podocytes, including the characteristic cytoskeletal architecture and morphology and the expression of proteins normally found in differentiated podocytes, e.g. synaptopodin. The resulting phenotype was a cell exhibiting a cobblestone-like morphology, resembling undifferentiated podocyte precursor cells during early glomerular development [Mundel *et al.*, 1996].

Therefore, in the mid 1990s, novel studies addressed the improvement the cell culture of podocytes, aiming at generating a cell culture model of podocytes that would resemble more the *in vivo* phenotype – in particular with regard to the expression of the important podocyte marker synaptopodin. Among the many tested modifications in the cell culture protocol, the measure of simply avoiding a repeated subcultivation proved promising; this led to the conversion of many cells with the cobblestone-like appearance into cells with a characteristic arborized phenotype, very much resembling the morphology of podocytes *in vivo*, and in contrast to the cobblestone-

like precursor cells, these differentiated podocytes expressed synapopodin [Mundel *et al.*, 1996]. However, differentiation in these cells was correlated to growth arrest in these cells, rendering this model not suitable for a routine laboratory practice due to limited capability of propagation.

The solution to this problem came with the development of conditionally immortalized podocyte cell lines [Mundel *et al.*, 1997]. For the generation of these cell lines, podocytes were obtained from the Immortomouse [Jat *et al.*, 1991], a H-2K^b-tsA58 transgenic mouse carrying the thermolabile mutant of the proliferation-promoting SV40 large T antigen under the control of an interferon-γ (IFN-γ)–inducible promoter. Podocytes derived from the Immortomouse express functional T antigens and therefore grow continuously under permissive conditions at 33 °C in the presence of IFN-γ, and stop dividing when the activity and expression of the tumor antigen is suppressed by restrictive conditions without IFN-γ at 37 °C. Temperature shift from 33 °C to 37 °C renders the SV40 large T antigen inactive and induces growth arrest and differentiation of podocytes.

The most prominent phenotypic change during differentiation of immortalized podocytes is a dramatic rearrangement of the podocyte actin cytoskeletin inclucing an extension of actin stress fibers and microtubules into cellular processes reminiscent of podocyte major processes *in vivo*. As the case for the arborized, differentiated cells observed in modified podocytes primary culture, also in conditionally immortalized podocytes differentiation is accompanied by an onset of synaptopodin expression. Notably, these cells even form slit diaphragm-like cell-cell contacts and – when properly cultured – display virtually all proteins identified in podocytes *in vivo* including, among others, nephrin, podocin and CD2AP [Shankland *et al.*, 2007].

Nowadays, rat, mouse and human cultured podocytes are widely used throughout the world to study virtually all aspects of podocyte biology in health and disease including the podocyte actin cytoskeleton, cell cycle, signaling, cell-cell contacts, and matrix interaction. The availability of conditionally immortalized differentiated podocytes in culture has developed into an indispensable tool for the mechanistic analysis of podocyte function. In combination with animal models and human studies to confirm the *in vitro* results, the study of podocytes in culture is a valid and invaluable model system that will continue providing novel insight into the function of these unique cells in health and disease.

Models of podocyte damage and proteinuria

Studying glomerular disease is a challenging task due to heterogeneity of glomerular disorders; for example, glomerular kidney diseases can be genetic or non-genetic, acute or chronic, primary or secondary, and can occur as (in early stages) clinically undetectable or overt conditions. Furthermore, as is the case for almost all human diseases, exploring glomerular disease directly in human subjects is limited by factors such as limited patient number, heterogeneity of the patient population, and ethical considerations. Therefore, the use of experimental models involving cultured cell lines and animals is indispensable to investigate the pathogenesis of glomerular disease *in vitro* and *in vivo*. Indeed, the availability of experimental tools such as conditionally immortalized differentiated podocyte cell lines or genetically modified mice has significantly advanced our understanding of many aspects of glomerular kidney disease.

In this study, among others, two well-established experimental models of podocyte damage and proteinuria were used to study the role of TRPC6 in kidney podocytes: the puromycin aminonucleoside (PAN) model and the lipopolysaccharide (LPS) model.

Puromycin aminonucleoside (PAN) is an analogue of the antibiotic puromycin, a substance that causes premature chain termination during translation. In contrast to puromycin, puromycin aminonucleoside does not inhibit protein synthesis or induce apoptosis, but acts as a glomerular epithelial cell toxin, which can be used to induce nephropathy in rats [Trachtman *et al.*, 1995]. Progressive renal damage in the PAN model is partly mediated by excessive production of oxidant species. In puromycin aminonucleoside (PAN)-treated rats, podocyte foot process effacement and heavy proteinuria commence on day 4 after injection of PAN [Kim *et al.*, 2001]. On day 8, proteinuria peaks, and on day 30, rats have recovered with largely restored podocyte foot process structure and resolution of proteinuria. The PAN rat is a very well established model of chronic glomerular injury and focal segmental glomerulosclerosis (FSGS) and has already been used in more than 100 peer-reviewed publications.

In contrast to the PAN model, the lipopolysaccharide (LPS) model is a more acute murine model of podocyte damage and transient nephrotic syndrome [Reiser *et al.*, 2004]. Lipopolysaccharides are found in the cell walls of Gram-negative bacteria. LPS is an endotoxin, which induces a strong response from normal animal immune systems. The mechanism behind this response involves binding of LPS to the CD14/TLR4/MD2 receptor complex, which promotes the secretion of pro-inflammatory cytokines in many cell types, but especially in macrophages. It has

been found in podocytes that LPS induces expression of the B-cell costimulatory molecule B7-1 and a cytosolic form of the protease cathepsin L through CD14/TLR4-mediated signaling. Both receptors, TLR-4 and CD14, are constitutively expressed in podocytes. It has further been reported that injection of 200 µg LPS intraperitoneally in mice leads to foot process effacement and severe proteinuria within 24 h [Reiser & Mundel, 2004]. In animals that were analyzed for a prolonged time period, foot process effacement and proteinuria returned to baseline levels after 72 h. Notably, the effects of LPS-treatment are abrogated in B7-1$^{-/-}$ and cathepsin L$^{-/-}$ mice, implicating that B7-1 induction is necessary for the development of LPS-induced proteinuria. The LPS model has become a useful alternative to the other currently used models of podocyte injury, in particular because of its acute-onset nature and the reversibility of podocyte injury and proteinuria. An increasing number of laboratories worldwide have been utilizing the LPS model to study glomerular disease, a trend that is reflected by the increasing number of published reports featuring this model. A most recent example thereof is the combination of the LPS model with a transient gene delivery approach to elucidate the function of the GTPase dynamin in podocytes [Sever *et al.*, 2007] (appendix).

Finally, an important advantage of the PAN- and LPS models is that they can both be applied also *in vitro* on cultured podocytes. Whereas the administration of LPS to cultured podocytes has a similar time course as podocyte injury *in vivo*, including a peak phase of stress after 24 h and recovery after 72 h, the exposure of podocytes to PAN has a more prolonged course with the onset of structural changes occurring after 24-48 h. Podocyte damage in cell culture as a result of LPS administration is reversible, whereas higher doses of PAN result in more severe podocyte injury that is usually not reversible.

I.3. Transient Receptor Potential (TRP) channels

TRP channels were first identified in the fruit fly. Phototransduction in *Drosophila melanogaster* involves activation of membrane cation channels in photoreceptor cells leading to a sustained depolarizing current. The ionic basis for this sustained receptor potential is influx of calcium from the extracellular space. Cosens and Manning reported in 1969 that in one group of mutant flies this sustained receptor potential was compromised; these flies merely showed a transient receptor potential, and the mutant fly strain was named trp with the mutated gene being unknown [Cosens & Manning, 1969]. The *trp* gene was cloned in 1989 [Montell & Rubin, 1989] and subsequently shown to encode a calcium-permeable cation channel [Hardie & Minke, 1992]. Since the discovery of the original TRP protein in the fly, more than 80 other TRP-like proteins were identified in several organisms. TRP homologs are expressed

in the fruit fly, the zebrafish *Danio rerio*, the worm *Caenorhabditis elegans*, and in several mammalian species including mice and humans [Venkatachalam & Montell, 2007]. Together they represent the TRP superfamily of ion channel-forming proteins.

TRP subunits form voltage-independent cation-permeable ion channels in most mammalian cells, and based on similar structural motifs and amino acid homology, mammalian TRP proteins have been classified into TRPC (Canonical), TRPV (Vanilloid), TRPM (Melastatin), TRPP (Polycystin), TRPA (Ankyrin), and TRPML (Mucolipin) subfamilies [Ramsey *et al.*, 2006] (Fig. I.6.). Each TRP channel subunit consists of six putative transmembrane spanning segments (S1-6), a channel pore-forming loop between S5 and S6, and intracellularly located amino- and carboxy-termini. TRPC, TRPV, and TRPM channels share a highly conserved 25-amino acid motif termed the "TRP domain" [Montell, 2005].

A functional TRP ion channel is formed by homo- or heterooligomerization of four channel subunits, and the subunit composition is thought to be a major determinant of channel function, subcellular localization, and biophysical properties [Schaefer, 2005]. Oligomerization is thought to occur predominantly between closely related channel subunits of the same subfamily [Amiri *et al.*, 2003]. Yet, there also a few examples of channels that consist of unrelated subunits, or subunits from different subfamilies [Schaefer, 2005].

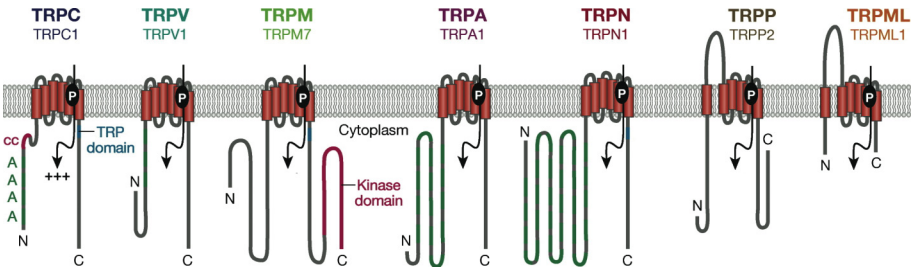

Fig. I.6. The TRP superfamily. A, ankyrin repeats; cc, coiled-coil domain; P, pore loop. (Source: adapted from Venkatachalam & Montell; Annu Rev Biochem. 2007, 76:387-417. [Venkatachalam & Montell, 2007].)

All TRP channels characterized thus far are permeable to calcium with the exception of TRPM4 and TRPM5, which are only permeable to monovalent cations. Most calcium-permeable TRP channels are only poorly selective for calcium, with a permeability ratio relative to sodium (P_{Ca}/P_{Na}) in the range between 0.3 and 10. Exceptions are TRPV5 and TRPV6, two highly calcium-selective TRP channels with $P_{Ca}/P_{Na} > 100$ [Owsianik *et al.*, 2006].

TRP channels are widespreadly expressed and serve very diverse functions ranging from thermal, tactile, taste, and osmolar sensing to fluid flow sensing [Clapham, 2003]. Functional diversity can even be seen within a single subfamily, indicating that structural similarity does not necessarily correspond to similar function.

As various as their functional properties are the modes of activation of TRP channels. TRP channels are gated by diverse stimuli that include the binding of intracellular and extracellular messengers, changes in temperature, and chemical and/or mechanical (osmotic) stress. In addition, some TRP channels appear to be constitutively open, whereas others seem to become activated upon depletion of intracellular calcium stores, although the latter mechanism, referred to as store-operated calcium entry (SOCE), remains an issue of intensive discussion [Clapham, 2003; Nilius, 2004]. Remarkably, the same channel can often be activated by more than one stimulus, illustrating the complexity of physiological roles played by TRP channels.

Recent studies of TRP channels indicate that they are involved in numerous fundamental cell functions and are considered to play an important role in the pathophysiology of many diseases [Nilius *et al.*, 2007]. Many TRP channels are expressed in the kidney along different parts of the nephron and growing evidence suggest that these channels are involved in hereditary as well as acquired kidney disorders [Hsu *et al.*, 2007]. For example, TRPM6 has been implicated in hypomagnesemia with secondary hypocalcemia, a rare autosomal-recessive disorder [Chubanov *et al.*, 2004], and mutations in *PKD1* (encoding the TRPP1 channel) and *PKD2* (encoding TRPP2), respectively, occur at a high frequency in individuals with polycystic kidney disease (PKD) [Wu & Somlo, 2000]. In addition, the highly calcium-selective channel TRPV5 contributes to several acquired mineral (dys)regulation diseases, such as diabetes mellitus, acid-base disorders, and vitamin D analogues-associated calcium imbalance, whereas TRPV4 may function as an osmoreceptor in kidney and participate in the (dys)regulation of sodium and water balance [Topala *et al.*, 2007; Hsu *et al.*, 2007].

Several studies highlight the potential of TRP channels as pharmaceutical targets [Wissenbach *et al.*, 2004; Hicks, 2006]. TRPC6 expressed in leukocytes is for example one of the most promising target molecules for potential anti-inflammatory drugs fighting diseases including chronic obstructive pulmonary disease and asthma [Gosling *et al.*, 2005].

I.3.1. The TRPC subfamily of ion channels

The Transient Receptor Potential Canonical (TRPC) subfamily is composed of proteins that are most highly related to the Drosophila TRP. It consists of seven mammalian members, TRPC1-7 [Venkatachalam & Montell, 2007].

In the human, the TRPC subfamily can be divided into three subgroups on the basis of amino acid homology: i) TRPC1, ii) TRPC4/5, and iii) TRPC3/6/7. TRPC2 is a pseudogene in the human but seems to encode an expressed protein in rat and mouse.

Whereas TRPC3, 6, and 7 share a number of similar features, e.g. with regard to their current-voltage relationships, they seem to have different basal activites [Dietrich *et al.*, 2003], and TRPC6 currents were shown to be enhanced by the cation channel blocker flufenamate, whereas TRPC3 and 7 were not [Inoue *et al.*, 2001]. The difference between the three channel types may indeed lie in their ion selectivity in that TRPC6 is somewhat calcium-selective ($P_{Ca}/P_{Na} = 5$), while TRPC3 and 7 are not.

Members of the TRPC subfamily are highly expressed in the central nervous system and to lesser degrees in many peripheral tissues, including kidney [Goel *et al.*, 2005; Ambudkar *et al.*, 2007].

TRPC channels contain three to four ankyrin repeats and a potential coiled-coil domain in the N-terminus. A proline-rich motif (LPXPFXXXPSPK) downstream of the EWKFAR motif is conserved in all members of the TRPC family and is thought to be responsible for interaction with Homer (for TRPC1) and/or immunophilins [Yuan *et al.*, 2003; Sinkins *et al.*, 2004].

A systematic analysis of the predicted pore region of TRPC family members has not been carried out yet. However, several studies have examined the effect of point mutations within the predicted pore region and extracellular loops bordering the pore. The change of a conserved LFW motif in the predicted pore helix of TRPC5 and TRPC6 to AAA resulted in dominant negative mutants [Hofmann *et al.*, 2002; Strubing *et al.*, 2003].

A number of studies aimed to elucidate the ability of TPRC proteins to form oligomers in the past years. Yet, the results show considerable inconsistence with regard to the suggested composition of native TRPC channels. Studies involving a systematic FRET approach to test possible combinations of TRPC channel complexes imply that TRPC channels exclusively form heteromers with members of their own subgroup (TRPC1, 4, 5 or TRPC3, 6, 7, respectively) [Hofmann *et al.*, 2002; Amiri *et al.*, 2003]. This is supported by findings that TRPC1 coimmunoprecipitated with TRPC4 and 5 but not with TRPC3, 6, and 7, and that – vice versa – TRPC3 coimmunoprecipitated with TRPC6 and 7 but not with TRPC1, 4, and 5 when

heterologously expressed in Sf9 insect cells or when tested endogenously from isolated rat brain preparations [Goel *et al.*, 2002]. Follow-up studies utilized TRPC isoform-specific antibodies to identify heterotypic TRPC interactions in rat and mammalian brain and revealed the presence of complexes containing either TRPC3 or 6, or TRPC1, 4 or 5 [Strubing *et al.*, 2001; Strubing *et al.*, 2003]. While these data point towards a subgroup-restricted oligomerization of TRPC channels, there are a number of studies demonstrating that oligomerization can also occur between members of different subgroups – and even beyond TRP channel subfamily borders. For example, it was shown that the *PKD2* gene product polycystin-2, which belongs to the TRPP subfamily, specifically associates with TRPC1 [Tsiokas *et al.*, 1999]. Consequently, the present evidence does currently not allow drafting a general model for TRPC oligomerization, and it still remains elusive how native TRPC channels are composed in the majority of cell types and tissues.

A common feature of all TRPC channels is that they all can function as receptor-operated channels downstream of G protein-coupled receptors via the phospholipase C pathway [Clapham, 2003]. Upon activation of the GPCR, stimulation of phospholipase C leads to the conversion of phosphatidylinositol-4,5-biphosphate (PIP_2) into inositol-1,4,5-trisphosophate (IP_3) and diacyl-glycerol (DAG). How the stimulation of phospholipase C translates into activation of the channel, is still under investigation, and multiple different mechanisms seem to be involved for each TRPC subunit. For example, TRPC2, 3, 6, and 7 can be directly activated by DAG or ist analogue 1-oleoyl-2-acetyl-*sn*-glycerol (OAG), whereas TRPC1, 4, and 5 are DAG-insensitive [Dietrich *et al.*, 2005].

Although the TRPC members of the mammalian transient receptor potential TRP cation channel family were the first to be described in 1995, the depth of knowledge of TRPC channels has fallen behind that of their counterparts in the TRPV and TRPM subfamilies in the intervening years. The complexities and controversies of TRPC channel composition and regulation have hindered their progress as therapeutic targets in the drug discovery environment to date, however embracing these challenges as opportunities may bring TRPC channels to the forefront of the discovery of novel therapies for many diseases.

I.3.2. Transient Receptor Potential Canonical 6 (TRPC6)

TRPC6 is expressed in multiple organs including brain, placenta and ovary, with the highest levels of transcript detected in lungs [Boulay *et al.*, 1997]. TRPC6 channels are believed to play an important role in pulmonary and vascular smooth muscle cells; the current evidence suggests that TRPC6 is activated downstream of the α1-adrenergic receptor [Inoue *et al.*, 2001] and the vasopressin receptor [Jung *et at.*,

2002], and mediates the regulation vascular and airway tone [Dietrich *et al.*, 2006]. In line with an important role of TRPC6 in these cell types, TRPC6 has been found to be upregulated in pulmonary artery smooth muscle cells in primary pulmonary hypertension and in response to hypoxia [Lin *et al.*, 2004; Yu *et al.*, 2004]. In the kidney, TRPC6 expression has been reported in glomeruli and tubules [Facemire *et al.*, 2004; Goel *et al.*, 2006; Sours *et al.*, 2006], where it is expressed in conjunction with several other TRPC members.

Like TRPC3 and 7, TRPC6 appears to form nonselective cation channels that show both inward and outward rectification, at negative and positive voltages, respectively [Trebak *et al.*, 2003]. The *I-V* relationships for these TRPCs demonstrate a far greater outward current (at positive voltages) than inward current (at negative voltages) with a reversal potential at around 0 mV. The single channel conductance of TRPC6 is 35 pS, with no second conductance state observed [Hofmann *et al.*, 1999].

With regard to the mode of activation, TRPC6 appears to function as a receptor-regulated, but not a store-regulated cation channel: Hofmann *et al.* showed that neither thapsigargin, ionomycin, PIP_2 nor IP_3 activated TRPC6, and it was therefore concluded that TPRC6 operates independently from extracellular stores [Hofmann *et al.*, 1999]. Furthermore, the phospholipase C inhibitor U73122 blocked agonist activation of TRPC6 leading the authors to conclude that TRPC6 is activated through PLC production of DAG, not by IP_3 or the IP_3-receptor, and not directly by G proteins. Another report describing a native TRPC6-like calcium channel in rabbit portal vein myocytes showed that those TRPC6-like channels could not be activated by IP_3; however, it was shown that IP_3 appears to synergize with DAG to produce greater TRPC6-like channel activation [Albert & Large, 2003]. It is important to mention that currently there is no known agonist or antagonist that is specific for TRPC6. However, when compared to the closely related subfamily members TRPC3 and 7, TRPC6 exhibited a distinct response: when expressed in HEK293 cells, TRPC6 currents were enhanced by the cation channel blocker flufenamate while TRPC3 and 7 currents were not [Inoue *et al.*, 2001].

Relatively little is known about proteins that interact with and regulate the trafficking and activity of TRPC6, although TRPC6 has been shown to bind to cytoskeletal proteins such as α-actinin, actin, and drebrin [Goel *et al.*, 2005] and endocytic vesicle-associated proteins such as dynamin, clathrin, and MxA [Goel *et al.*, 2005] and the plasmalemmal Na^+/K^+ ATPase pump [Goel *et al.*, 2005]. While cytoskeletal proteins can potentially exert an effect on channel trafficking, the role of these proteins in TRPC6 trafficking has not been directly demonstrated. Another determinant that may affect TRPC6 trafficking and activity is TRPC6 oligomerization: both, TRPC3 and TRPC6 are regulated by PIP_2 hydrolysis and

undergo translocation to the plasma membrane in response to agonist stimulation. Furthermore, TRPC6 has been shown to coimmunoprecipitate with TRPC3 and 7 [Hofmann *et al.*, 2002]. However, any direct impact of TRPC multimerization on TRPC6 trafficking remains elusive. In addition, it is also not clear whether trafficking of homomeric channels differs from that of heteromeric channels.

Despite the existence of multiple potential phosphorylation sites in the sequence of all TRPCs, few studies have specifically addressed the role of kinases in TRPC6 channel activity. Phorbol-12-myristoyl-13-acetate (PMA)-induced activation of protein kinase C has been shown to block OAG-induced activation of ectopically expressed mouse TRPC7 [Okada *et al.*, 1999] and rat TRPC6 [Zhang & Saffen, 2001], but unexpectedly had no effect on human TRPC6 [Estacion *et al.*, 2004]. In ^{32}P-labeled platelets, TRPC6 was significantly phosphorylated by protein kinase A and associated with other unidentified phosphoproteins; in this study, channel phosphorylation did not appear to affect either thrombin- or OAG-induced TRPC6 activity [Hassock *et al.*, 2002]. Recently, the possibility that tyrosine kinases might play a role in regulation of TRPC6 has received some attention. A recent report implicates the Src family kinase Fyn in epidermal growth factor (EGF)-dependent regulation of human TRPC6 [Hisatsune *et al.*, 2004]. In COS-7 cells overexpressing both Fyn and TRPC6, the channel was tyrosine phosphorylated following EGF-treatment, and Fyn phosphorylated TRPC6 in an *in vitro* kinase assay. Furthermore, Fyn and TRPC6 were shown to interact through the SH2 domain of Fyn and the channel N-terminal domain of TRPC6. In inside-out patches excised from TRPC6-expressing HEK293 cells, Fyn-dependent phosphorylation of TRPC6 increased OAG-induced channel activity.

In 2005, Gudermann *et al.* published the first report on constitutive TRPC6$^{-/-}$ mice. The authors found that these mice were viable [Dietrich *et al.*, 2005]. Fertility and litter sizes were comparable to those of wildtype mice. However, TRPC6$^{-/-}$ mice showed an elevated blood pressure and enhanced agonist-induced contractility of aortic rings as well as cerebral arteries. Furthermore, smooth muscle cells of TRPC6-deficient mice had higher basal cation entry, increased TRPC-carried cation currents, and more depolarized membrane potentials. When the authors knocked down expression of TRPC3 with siRNA in these cells, the higher basal cation entry was abolished; the same thing happened when they expressed exogenous TRPC6, suggesting that TRPC3 channels, which have a higher basal activity than TRPC6 channels [Dietrich *et al.*, 2003], were induced in TRPC6-deficient cells. Recently, the same group proposed TRPC6 as a key regulator of hypoxic pulmonary vasoconstriction, since this vitally important mechanism was absent in TRPC6-deficient mice challenged with hypoxic ventilation [Weissmann *et al.*, 2006]. Thus

far no study has addressed the renal phenotype of TRPC6-deficient mice. According to our current knowledge, young TRPC6$^{-/-}$ mice did not present with an overt kidney disease phenotype, and aged or experimentally challenged mice have not been studied yet (Dr. Thomas Gudermann, personal communication, TRP Meeting in Leuven, Belgium).

I.4. Specific aims

In 2004, Dr. Michelle Winn reported a mutation in the gene encoding the cation-permeable channel TRPC6. This mutation was genetically linked to the development of familial focal segmental glomerulosclerosis (FSGS) in a large family from New Zealand (Winn et al., public presentation, 5th International Podocyte Conference, Seattle, Washington, United States, June 18-20, 2004) [Winn *et al.*, 2004].

Based on this preliminary finding, indicating that genetic defects in an ion channel are associated with progressive kidney disease, and the notion that all previously described genes mutated in FSGS and nephrotic syndrome are highly expressed in the glomerular podocyte, the following hypothesis was developed:

The ion channel-forming protein TRPC6 is expressed in podocytes, and TRPC6-mediated Ca^{2+} signaling contributes to the regulation of the podocyte actin cytoskeleton. Malfunction of TRPC6 leads to a disruption of podocyte cytoskeletal organization, podocyte foot process effacement, glomerular dysfunction, and proteinuric kidney disease.

The studies outlined in this thesis were designed to test the aforementioned hypothesis with a focus on the following three specific aims:

- *Explore TRPC6 mutations in genetic forms of proteinuric kidney disease (FSGS)*
- *Investigate the association of TRPC6 with the glomerular filtration barrier*
- *Explore TRPC6 expression in acquired forms of proteinuric kidney disease*
- *Investigate the molecular basis of TRPC6 contribution to the pathophysiology of proteinuric kidney disease*

Appendix Chapter I

Moller, C. C., Pollak, M. R., & Reiser, J. (2006). The genetic basis of human glomerular disease. *Adv Chronic Kidney Dis,* **13**(2), 166-173.

The Genetic Basis of Human Glomerular Disease

Clemens C. Möller, Martin R. Pollak, and Jochen Reiser

Clinical and molecular research aimed to understand glomerular disease has emerged to one of the most active areas in renal research at large. The unraveling of genetic causes resulting in proteinuria has helped to define roles for each component of the glomerular filtration barrier in the development of urinary protein loss. Although most of the inherited glomerular diseases have in common defects in the podocyte, the glomerular basement membrane is also of critical importance for normal kidney permselectivity. This review summarizes recent progress in the eludication of genetic causes of glomerular disease and discusses their implications for the understanding of the pathogenic mechanisms, which can lead to disruption of the glomerular filtration barrier.

Index Words: Hereditary diseases; Glomerulonephritis; Nephrotic syndrome; Proteinuria; Podocytes

Glomerulopathies account for a significant fraction of end-stage renal disease (ESRD). The most important symptoms include proteinuria, hematuria, hypoproteinemia, edema, and a reduced glomerular filtration rate. With respect to their pathological and clinical manifestations, glomerular diseases are generally classified as falling into one of the broad categories with either an inflammatory phenotype (nephritic syndrome) or a noninflammatory phenotype (nephrotic syndrome [NS]). Nephritic syndrome is characterized pathologically by diffuse inflammatory changes in the glomeruli and clinically by abrupt-onset hematuria, mild proteinuria, and, often, hypertension, edema, and azotemia. In contrast, nephritic syndrome is characterized pathologically by a prolonged increase in the glomerular capillary wall permeability and clinically by heavy proteinuria and often hypoalbuminemia, severe edema, lipiduria, and lipemia. In many glomerular diseases, features of nephritic and nephrotic syndrome go hand in hand, making it difficult to identify the underlying cause of the disease. Likewise, many conditions referred to as glomerular diseases do not originate from a common, single disease-causing mechanism but in fact represent a characteristic pathological phenotype associated with several different diseases. Among these conditions, focal segmental glomerulosclerosis (FSGS) accounts for a significant proportion. FSGS describes a pathological lesion observed in a disparate group of clinical disorders. It is diagnosed by kidney biopsy, with histopathological findings characterized by partial scarring of the glomerular capillary tuft in a significant proportion of glomeruli. Patients with FSGS present with proteinuria and often develop kidney dysfunction that progresses to ESRD. It has become well known that genetic defects play a major role in the development of glomerulopathy. In this review, we summarize the present knowledge on genetic glomerular disorders and discuss the consequences of the recent findings for the understanding of glomerular disease. Although several of the discussed diseases are in fact systemic disorders, we focus here only on the glomerular phenotypes.

From the Nephrology Division, Department of Medicine, Massachusetts General Hospital and Harvard Medical School, Boston, MA; and Renal Division, Department of Medicine, Brigham and Women's Hospital and Harvard Medical School, Boston, MA.

MRP is supported by grants from the US National Institutes of Health. JR is supported by the KMD Foundation and the KUFA-ASN Research Grant. CCM is supported by a scholarship of the German Academic Exchange Service (DAAD).

Address correspondence to Jochen Reiser, MD, PhD, Massachusetts General Hospital, Harvard Medical School, Nephrology Division, MGH-East CNY-149-8230, 149 13th Street, Charlestown, MA 02129. E-mail: jreiser@partners.org

1548-5595/06/1302-0012$32.00/0
doi:10.1053/j.ackd.2006.01.009

The Glomerular Filtration Barrier

The function of the glomerular filtration barrier is to retain plasma proteins in the blood on the basis of molecular charge and size. To

reach from the vascular into the urinary space, molecules pass through 3 distinct structures. The first one is a fenestrated endothelium decorating the glomerular capillaries. The fenestrae between the endothelial cells are 70 to 100 nm in diameter. On their surface, the endothelial cells carry a complex of negatively charged sialoproteins and proteoglycans (glycocalyx). Although the negative charge of the glycocalyx constitutes a potential barrier retarding anionic macromolecules, there is no evidence so far for such a role of the endothelial glycocalyx. The second structure is the glomerular basement membrane (GBM), a thin sheet of specialized extracellular matrix composed of 4 major components: laminin, type IV collagen, nidogen/entactin, and proteoglycans. During glomerulogenesis, the GBM is built up in a combined effort of the underlying endothelial and overlying visceral epithelial cells (podocytes). As is the case for the fenestrated endothelium, it is thought that that the presence of negatively charged molecules within the GBM serves as a barrier retarding anionic macromolecules. The third structure consists of podocytes and the interposed glomerular slit diaphragm (SD). Podocytes are nonreplicating polarized epithelial cells that originate from precursor mesenchymal cells. During nephrogenesis, these cells undergo modification from a classic epithelial cell phenotype to a highly specialized octopus-shaped cell. Podocytes cover the external surface of adjacent capillaries and interact with the GBM through finger-shaped extensions called pedicels or foot processes (FP). The basal surface of podocyte FP is anchored in the GBM via α3-/β1-integrins and α-/β-dystroglycans. Podocyte FP interdigitate in a complex manner forming an intricate network surrounding the glomerular capillaries. Adjacent FP bridge their narrow 300 to 400 angstrom wide gaps by an electron-dense membrane-like structure, the SD (Fig 1). The SD is a thin porous membrane composed of a number of proteins. The SD multiprotein complex is thought to form the major determinant of the size permselectivity of the glomerular filtration barrier. It allows for the passage of water and solutes from the blood into the kidney ultrafiltrate while inhibiting the loss of larger plasma molecules.

Podocyte Injury and Proteinuria

Glomerular proteinuria is a hallmark of glomerular disease and results from an increased permeability of the glomerular filtration barrier. Normally, proteins larger than albumin do not enter the urinary space, whereas lower molecular weight proteins are filtered and partially reabsorbed in the proximal tubule. Normal excretion levels of protein into the urine vary between 0 and 150 mg/d. Proteinuria is clinically characterized by a protein loss into the urine of more than 150 mg/d. Levels of 3 (or 3.5) g of urinary protein per day are generally used to define "nephrotic-range" proteinuria. In many forms of glomerular diseases, proteinuria is correlated with podocyte injury. The complexity of interactions among podocyte proteins provides several targets for podocytopathy and disruption of the glomerular filtration barrier.[1] Loss of the integrity of the intricate structures of the podocyte can be seen in patients with NS, who clinically present with hypertension, proteinuria, and progressive kidney disease. Electron microscopic examination of kidney biopsy specimens reveals the loss of normal podocyte FP structure, resulting in a flattened podocyte phenotype, where FP forms an epithelial monolayer lacking functional SD (FP effacement). If early structural changes of podocytes are not reversed, severe and progressive glomerular damage is likely to develop. This involves podocyte vacuolization, pseudocyst formation, and detachment of podocytes from the GBM. Because the highly differentiated podocytes are unable to proliferate, the damage and loss of single podocytes lead to podocyte depletion over time, which is a major determinant in the development of glomerulosclerosis and chronic kidney failure.

GBM-Associated Genetic Podocytopathies

Basement membranes have been shown to influence cell proliferation, migration, and differentiation. Also in the kidney, an intact GBM is necessary for proper adhesion and function of the underlying endothelial cells and podocytes.[2] Inherited disruptions of 2 components of the GBM, type IV collagen and

laminin-β2, have so far been shown to lead to glomerular disease.

Type IV collagen-related diseases, including Alport syndromes and thin basement membrane nephropathy (TBMN), originate from defects in the genes encoding the α-chains of type IV collagen.[3] In 4 of the 6 identified α-chain genes so far, mutations have been associated with progressive hereditary nephritis. With the exception of TBMN, all these gene defects lead to a thickened GBM and progressive hematuric glomerular disease, resulting in renal insufficiency and ESRD. In constrast, patients with TBMN present with a thinnened GBM and asymptomatic microscopic hematuria. Kidney function usually remains normal in these individuals. It is speculated that, in type IV collagen-related diseases, an increased mechanical fragility of the GBM accounts for pathogenesis.

The rare Nail-Patella syndrome (NPS) is characterized by loss-of-function mutations in *LMX1B* encoding a transcription factor regulating the expression of *COL4A3* (type IV collagen α3 chain), *COL4A4* (type IV collagen α4 chain), *NPHS1* (nephrin), *NPHS2* (podocin), and *CD2AP*. In most patients with NPS, the GBM has a characteristic moth-eaten appearance and contains fibrillar collagen deposits. Whereas some individuals do not present with any clinical nephropathy, proteinuria occurs in 30% to 40% of patients and in 5% to 10% of patients the disease leads to progressive kidney failure. Although the phenotype of NPS seems to be primarily confined to the GBM, it is likely that transcriptional dysregulation of SD proteins contributes to the pathobiology of the disease.

Gene defects in *LAMB2* encoding the laminin-β2 chain lead to the rare Pierson syndrome. Laminin-β2 is abundantly expressed in the GBM where it is present in the adult GBM laminin-11 isoform (α5:β2:γ1). Laminin-11 plays a key role in anchoring and differentiation of podocyte FP. Laminin-11 malfunction, because of a lack of of functional laminin-β2, is thought to be the cause for the disease, which leads to the onset of nephrosis soon after birth, rapid progression to ESRD, and death in the first year.

Cytoskeleton-Associated Genetic Podocytopathies

The major function of the podocyte FP is to create the outer portion of the glomerular filtration barrier. Because the glomerular capillary wall undergoes cyclic distensions, a functional adaptive cytoskeleton, providing both mechanical strength and flexibility, is required for maintaining podocyte structural integrity. To match this unique challenge, podocytes have developed a highly dynamic cytoskeletal architecture involving microtubules, intermediate filaments, and actin microfilaments. Whereas the podocyte cell body and primary processes are predominantly composed of microtubules and intermediate filaments, podocyte FP contain an actin-based contractile cytoskeletal network. A group of cytoskeleton-associated proteins, including talin, paxillin, and vinculin, link actin filaments to the cell membrane-associated integrins at the GBM. Parts of the actin cytoskeleton are also linked to the SD via catenins and ZO-1, or via CD2AP. Under normal conditions, a dynamic actin cytoskeleton is part of the adaptive responses of the podocyte to changes in its microenvironment. Under disease conditions, the prolonged reorganization of actin bundles underlies the structural hallmark seen in FP effacement.

Mutations in *ACTN4* encoding α-actinin-4 are associated with the development of familial FSGS.[4] The disease is characterized by onset in adolescence or early adulthood, slow progression, nonnephrotic proteinuria, and renal insufficiency. α-Actinin-4 is expressed in podocytes, where it cross-links F-actin filaments in FP. The disease-causing mechanism appears to be linked to accelerated degradation of mutant α-actinin-4 by the proteasome. It is also thought that an increased affinity of mutant α-actinin-4 to F-actin may result in a dysregulation of actin filament formation in podocytes. Interestingly, α-actinin-4 is expressed throughout the body, but the human phenotype associated with *ACTN4* mutations is apparent only in the kidney. This suggests that either a podocyte-specific protein-protein interaction is altered by human disease-associated mutations or that the unique structure of the podocyte makes it particularly suscep-

tible even to subtle changes in its cytoskeletal architecture.

Another group of cytoskeleton-associated mutations lead to podocyte injury by interference with the nonmuscle myosin heavy chain IIA (NMMHC-IIA) encoded by *MYH9*.[5] *MYH9*-related diseases include the Epstein syndrome, Fechtner syndrome, May-Hegglin anomaly, and Sebastian syndrome. It has been suggested that these 4 sydromes are in fact not distinct entities but rather derive from a common single disorder with a continuous clinical spectrum characterized by a varying expressivity. Class II myosins play a well-characterized role in the contraction and force production in muscles and are required for cytokinesis, cell mobility, cell polarity, and cell architecture. In podocytes, nonmuscle myosin heavy chain IIA is thought to be a major component of the actin-myosin contractile apparatus in FP. The disease-causing mechanism leading to the glomerular phenotype of *MYH9*-related disease remains elusive.

Organelle-Associated Genetic Podocytopathies

One podocyte organelle shown to be a target of genetic defects causing glomerular disease is the mitochondrion. The mitochondrial genome is a set of extrachromosomal genes present in a circular genome. Expression of mitochondrial gene mutations follows a pattern of maternal inheritance. A typical example of a mitochondrial cytopathy is the A3243G transition in the mitochondrial gene *MTTL1* encoding for the $tRNA^{Leu(URR)}$. This mutation leads to a defect in the mitochondrial respiratory chain and has been associated with podocyte abnormalities and the development of FSGS. Most recently, an individual with steroid-resistant nephrotic syndrome, FSGS, and evidence of abnormal mitochodria in the podocyte was presented.[6] The pathogenic impact of the A3243G mutation is not clearly understood. One hypothesis is that because podocytes are terminally differentiated cells, they may be more susceptible to the effects of mitochondrial dysfunction compared with neural and muscle cells. With the accumulation of abnormal mitochondria, the synthesis of mitochondrial proteins and appropriate oxidadive phosphorylation to generate energy for proper podocyte function may be absent. Most recently, another disease of potentially genetic origin was added to the list of mitochondria-associated podocytopathies: a mitochondrial respiratory chain deficiency was reported in 1 patient with congenital NS and 2 siblings with severe congenital kidney disease and probable NS.[7] In all cases, mutations in the gene *NPHS1* (nephrin), which are the classic cause for congenital NS of the Finnish type, were excluded. The authors suggest genetic deficiency in respiratory chain genes as a putative disease-causing mechanism. However, the genetic locus of such mutations remains elusive.

Another organelle associated to glomerular disease is the podocyte lysosome. The systemic Fabry disease, a defect in *galA* encoding the lysosomal enzyme α-galactosidase A leads to the formation of globotriaosylceramide (GL-3) deposits in nearly all glomerular cell types. Even though this mainly affects the vascular endothelium, there are particularly dense accumulations in podocytes and distal tubular epithelial cells.[8] The clinical outcome is azotemia, proteinuria, and chronic kidney disease. In contrast to the majority of glomerular diseases, a promising therapeutic strategy exists with enzyme replacement therapy.

Slit Diaphragm-Associated Podocytopathies

The SD appears early in nephrogenesis. It is a modified adherens junction with a zipperlike structure composed of a number of proteins with large extracellular domains including nephrin; neph 1, 2, and 3; P-cadherin; and the protocadherin FAT.[9] Four distinct functions of the SD have been described.[10] These are function as molecular sieve, function as cell-cell contact between podocytes, function as signaling platform, and function as organizing center regulating podocyte actin dynamics. In particular, nephrin and its homologues neph 1, 2, and 3 have entered the stage serving not only as important scaffolding molecules but also as key players in mediating extracellular signals into the podocyte cell body, a process in which tyrosine phosphorylation appears to play a crucial role. The molecules composing

the SD are linked to the podocyte intracellular space via a number of transmembrane and cytoplasmic podocyte proteins located close to the SD site. Among them are various adaptor proteins including podocin, ZO-1, CD2AP, and catenins. Furthermore, it has been shown that the α-actinin-4-binding protein densin-180 and the src family protein tyrosine kinase Fyn are located at the SD site. Most recently, the calcium-permeable ion channel TRPC6 has been discovered as a part of the SD complex.[11] The complex interplay of SD proteins is thought to be a major determinant for the maintenance of the glomerular filtration barrier. So far, several protein-protein interactions have been shown at the SD site (eg, nephrin interacts with neph 1, podocin, CD2AP, and TRPC6; podocin itself interacts with CD2AP and TRPC6; and both nephrin and TRPC6 are phosphorylated by Fyn). Because of the intricate organization of the SD, it is no surprise that genetic defects in the associated proteins lead to podocyte injury. A number of genes associated with glomerular diseases have been identified in the past years, and the respective clinical outcomes are well characterized.[4] Among these diseases are the congenital NS of the Finnish type caused by mutations in *NPHS1* encoding nephrin and the steroid-resistant nephrotic syndrome of the podocin type caused by mutations in the *NPHS2* gene encoding podocin.

The Frasier syndrome and Denys-Drash syndrome are overlapping syndromes caused by mutations in *WT1* encoding the Wilms' tumor protein (WT1). WT1 is a transcription factor regulating a number of podocyte genes including *NPHS1* (nephrin) and *NPHS2* (podocin). Both syndromes are characterized by glomerular disease; whereas the Frasier syndrome shows a FSGS pattern in kidney biopsies, the Denys-Drash syndrome is defined by diffuse mesangial sclerosis. A recent study describes a patient with FSGS and slow progressive nephropathy carrying an F392L mutation in *WT1*.[12] Another report revealed the association between specific noncoding *WT1* single-nucleotide polymorphisms and FSGS in the black population.[13]

In 2 patients with primary FSGS, a nucleotide variant leading to CD2AP haploinsufficiency was detected.[14] The higher susceptibility of individuals carrying this mutation for glomerular disease shows the pathogenic role of altered CD2AP expression levels. CD2AP is not only thought to be an important adaptor protein in podocytes, coupling the slit diaphragm to the actin cytoskeleton, but also implicated in endocytosis and lysosomal sorting. This and the observation that in $CD2AP^{+/-}$ mice immunoglobulins accumulate in the GBM led the authors to speculate that, in addition to its possible structural role, CD2AP may also be involved in targeting proteins to the degradative pathway. Immunoglobulin deposits in $CD2AP^{+/-}$ mice may reflect the impaired ability of the podocyte to clear plasma proteins from the GBM, suggesting a possible diesease-causing mechanism in affected patients with CD2AP haploinsufficiency.

Most recently, mutations in the *TRPC6* gene encoding for the transient receptor potential canonical 6 (TRPC6) have been added to the list of glomerular disease-associated genes.[11,15] TRPC6 forms a calcium-permeable ion channel located at the SD site. In 6 families, mutations in *TRPC6* were associated with the development of FSGS. The disease presented in between 17 and 57 years of age and, in several patients, progressed to ESRD. Three mutations were shown to cause biologically gain-of-function effects, suggesting that an increased calcium influx at the SD site may contribute to the pathogenesis in affected individuals. How an increased calcium influx may lead to the disease phenotype and what the disease-causing mechanisms look like for the other 3 identified mutations remains elusive.

Conclusion and Outlook

Podocyte injury plays a key role in proteinuric glomerular diseases. The identification of a growing number of disease-associated genes involved in podocyte structure and function (Table 1) is in line with this paradigm. Recent years have brought substantial contributions to a better understanding of the podocyte and the SD. The observation that many of the recently identified genes are widely expressed but cause specific effects in the podocyte suggests that the related glomerular phenotypes

Table 1. Summary of the Most Important GBM-, Cytoskeleton-, Organelle-, and SD-Associated Primary and Secondary Genetic Glomerular Diseases With Podocytopathic Phenotype

	Disease	Gene	Locus	Heredity	Gene product	Onset
GBM-ASSOCIATED PODOCYTOPATHY	**type IV collagen-related diseases**					
	autosomal-recessive Alport syndrome	*COL4A3* or *COL4A4*	2q35-37	AR	type IV collagen α3 chain or α4 chain	late
	autosomal-dominant Alport syndrome			AD		
	thin basement membrane nephropathy (TBMN)			AD		
	X-linked Alport syndrome	*COL4A5*	Xq22.3	X-Linked	type IV collagen α5 chain	
	X-linked Alport syndrome with diffuse Leiomyomatosis (ATS-DL)	*COL4A5* and *COL4A6*			type IV collagen α5 chain and α6 chain	
	X-linked Alport syndrome with mental retardation (ATS-MR)	*COL4A5* and *FACL4*			type IV collagen α5 chain and long-chain acyl-CoA synthetase 4	
	Nail-Patella Syndrome (NPS)	*LMX1B*	9q34	AD	LMX1B	late
	Pierson syndrome	*LAMB2*	3p14-22	AR	laminin-β2 chain	infancy
CYTOSKELETON-ASSOCIATED PODOCYTOPATHY	***ACTN4*-related disease**	*ACTN4*	19q13	AD	α-actinin-4	late
	***MYH9*-related diseases**	*MYH9*	22q11.2	AD	non-muscle myosin heavy chain IIA (MYHIIA)	late
	Epstein syndrome					
	Fechtner syndrome					
	May-Hegglin anomaly					
	Sebastian Syndrome					
ORGANELLE-ASSOCIATED PODOCYTOPATHY	**A3243G mitochondrial cytopathy**	*MTTL1*	19q13	maternal	$tRNA^{Leu(URR)}$	in children / young adults
	mitochondrial respiratory chain deficiency	?	?	maternal suggested	complex V or complex II+V	infancy
	Fabry disease	□-*Gal A*	Xq22	X-linked	α-galactosidase A	adulthood
SD-ASSOCIATED PODOCYTOPATHY	**Congenital NS of the Finnish type (CNF)**	*NPHS1*	19q13.1	AR	nephrin	infancy
	Steroid-resistant NS of the podocin type	*NPHS2*	1q25-31	AR	podocin	3 mo to 5 yr, or late
	***WT1*-related diseases**	*WT1*	11p13	AD	WT1	infancy
	Denys-Drash syndrome (DDS)					
	Frasier syndrome (FS)					
	CD2AP haploinsufficiency	*CD2AP*	6p12	AD	CD2AP	adults
	***TRPC6*-related disease**	*TRPC6*	11q21-22	AD	TRPC6	late

may be the consequence of their particular roles in the unique organization of the glomerular filtration barrier and the increased susceptibility of podocytes even to subtle changes in certain pathways. Besides α-actinin-4, another good example thereof is CD2AP. Although being widespreadly expressed, it was possible to rescue $CD2AP^{-/-}$ lethality in mice with podocyte-targeted expression of CD2AP, highlighting the particular role of CD2AP in podocytes.[16]

In fact, the disease-causing mechanisms remain elusive for the majority of glomerular diseases, in particular those with late onset. Several factors hamper the efforts to elucidate the respective pathogenic mechanisms. First, podocytes are characterized by a high degree of instrinsic adaptability to external challenges because they have to be able to flexibly respond to changes in their microenvironment such as altered hemodynamics. In line with this notion is the observation that FP effacement itself is a reversible process and occurs, albeit rarely and partially, in every healthy individual. Podocytes may be able to temporarily overcome subtle pathophysiologic changes, which consequenly result in glomerular damage only over time. For example, in the cases of CD2AP haploinsufficiency and TRPC6 dysfunction, compensatory mechanisms mediated by homologous proteins (Cin85 or other TRP channels, respectively) may be able to retard the course of the disease.

Table 2. Genetic Glomerular Diseases With Rare Incidence, Unknown Genetic Cause, or Poorly Described Glomerular Phenotype

	Disease	Gene	Locus	Heredity	Gene product	Onset
	Infantile sialic acid storage disorder (ISSD)	*SLC17A5*	6q14-15	AR	Sialin	infancy
	Type I carbohydrate-deficient glycoprotein syndrome	*PMM2*	16p13.3-13.2	AR	Phosphomannomutase	infancy
	X-linked ichthyosis	*STS*	Xp22.32	X-linked	Steroid sulfatase (STS)	?
	Schimke Immuno-Osseous Dysplasia (SIOD)	*SMARCAL1*	2q34-q35	AR	SMARCAL1	?
	Autosomal-dominant nephropathy with features of Alport syndrome and FSGS	?	11q24	AD	?	?
	Familial IgA glomerulopathy	?	6q22-23	AD suggested	?	?
	Galloway-Mowat syndrome	?	?	AR	?	infancy
	Familial glomerulopathy with predominant fibronectin deposits	?	?	AD	?	?
	Collagenofibrotic glomerulopathy	?	?	AR suggested	?	?

Second, the use of mouse models is limited for many diseases of glomerular origin because the murine phenotypes often significantly differ from the manifestation in man. Knockout models are not always sufficient to simulate the intricate effects of the characterized gene defects, which may in fact be more subtle. Third, as proposed for *ACTN4* mutations, the disease manifestation may be dependent on a "second physiological hit" in some cases (eg, variations in glomerular capillary pressure or metabolic disturbances). Fourth, the manifold reasons for podocyte damage, deriving from distinct domains such as the SD, the GBM, or the actin cytoskeleton, can be difficult to emulate in vitro.

Albeit the given limitations, the clinical significance of proteinuria and the currently available experimental tools will continue to drive progress in the genetic and biologic understanding of glomerular diseases. Besides the genetic glomerulopathies described previously (Table 1), it will be interesting to see what we can learn from a number of other diseases whose glomerular phenotypes still require further characterization (Table 2). New genetic tools such as inducible podocyte-specific promoter elements that enable the conditional expression of transgenes exclusively in the glomerulus have become available.[17] They will help to overcome some of the limitations of murine knockout models and to better define the kidney phenotypes of systemic diseases. The establishment of conditionally immortalized podocyte cell lines and the development of experimental models of podocyte damage such as the puromycin aminonucleoside model and the lipopolysaccharide model have been invaluable achievements to study podocyte biology because they allow the investigation of the complex relationships between the components of the glomerular filtration barrier under various experimental conditions. The existing podocyte cell lines may be applied to study which SD-based protein interactions are disrupted in experimental podocyte injury, testing the hypothesis that perturbated protein interactions at the SD site are a major cause for podocytopathy. Of particular interest will also be to use the genetic findings for a better understanding of acquired forms of glomerular disease. For example, the detection of the calcium-permeable channel TRPC6 at the SD site and its implication in familial FSGS serve as a starting point to study the role of this channel in acquired forms of FSGS as well, adding the concept of calcium signaling at the SD site to the pool of potentially relevant pathogenic pathways.

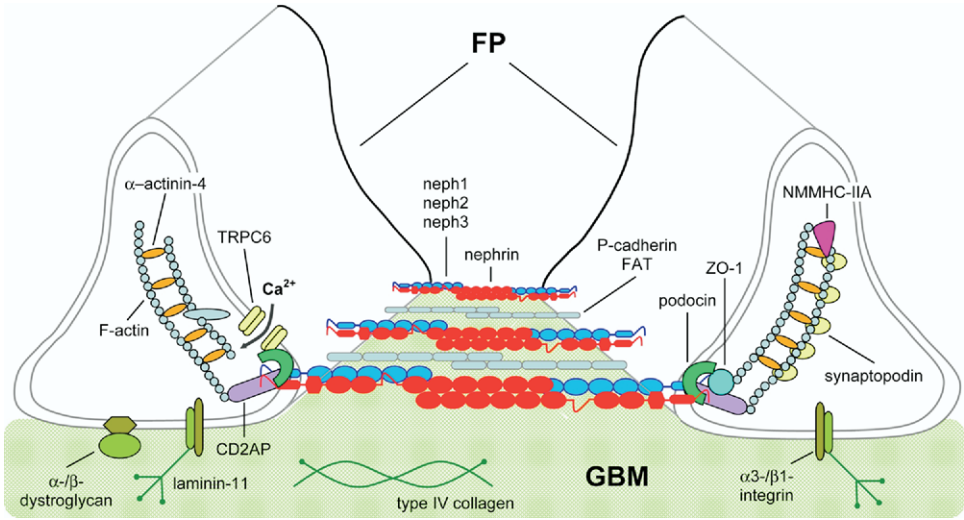

Figure 1. Schematic representation of podocyte foot processes (FP) and the interposed SD covering the outer aspect of the GBM.

References

1. Durvasula RV, Shankland SJ: Podocyte injury and targeting therapy: An update. Curr Opin Nephrol Hyperten 15:1-7, 2006
2. Miner JH: Building the glomerulus: A matricentric view. J Am Soc Nephrol 16:857-861, 2005
3. Kashtan CE: Familial hematurias: What we know and what we don't. Pediatr Nephrol 20:1027-1035, 2005
4. Pollak MR: Inherited podocytopathies: FSGS and nephrotic syndrome from a genetic viewpoint. J Am Soc Nephrol 13:3016-3023, 2002
5. Seri M, Pecci A, Di Bari F, et al: MYH9-related disease: May-Hegglin anomaly, Sebastian syndrome, Fechtner syndrome, and Epstein syndrome are not distinct entities but represent a variable expression of a single illness. Int J Mol Med 16:437-441, 2005
6. Lowik MM, Hol FA, Steenbergen EJ, et al: Mitochondrial tRNALeu (UUR) mutation in a patient with steroid-resistant nephrotic syndrome and focal segmental glomerulosclerosis. Nephrol Dial Transplant 20:336-341, 2005
7. Goldenberg A, Ngoc LH, Thouret MC, et al: Respiratory chain deficiency presenting as congenital nephrotic syndrome. Pediatr Nephrol 20:465-469, 2005
8. Warnock DG: Fabry disease: Diagnosis and management, with emphasis on the renal manifestations. Curr Opin Neprol Hyperten 14:87-95, 2005
9. Wartiovaara J, Ofverstedt LG, Khoshnoodi J, et al: Nephrin strands contribute to a porous slit diaphragm scaffold as revealed by electron tomography. J Clin Invest 114:1475-1483, 2004
10. Huber TB, Benzing T: The slit diaphragm: A signaling platform to regulate podocyte function. Curr Opin Nephrol Hypertens 14:211-216, 2005
11. Reiser J, Polu KR, Moller CC, et al: TRPC6 is a glomerular slit diaphragm-associated channel required for normal renal function. Nat Genet 37:739-744, 2005
12. Kaltenis P, Schumacher V, Jankauskiene A, et al: Slow progressive FSGS associated with an F392L WT1 mutation. Pediatr Nephrol 19:353-356, 2004
13. Orloff MS, Iyengar SK, Winkler CA, et al: Variants in the Wilms' tumor gene are associated with focal segmental glomerulosclerosis in the African American population. Physiol Genomics 21:212-221, 2005
14. Kim JM, Wu H, Green G, et al: CD2-associated protein haploinsufficiency is linked to glomerular disease susceptibility. Science 300:1298-1300, 2003
15. Winn MP, Conlon PJ, Lynn KL, et al: A mutation in the TRPC6 cation channel causes familial focal segmental glomerulosclerosis. Science 308:1801-1804, 2005
16. Grunkemeyer JA, Kwoh C, Huber TB, et al: CD2-associated protein (CD2AP) expression in podocytes rescues lethality of CD2AP deficiency. J Biol Chem 280:29677-29681, 2005
17. Moeller MJ, Soofi A, Sanden S, et al: An efficient system for tissue-specific overexpression of transgenes in podocytes in vivo. Am J Renal Physiol 289: F481-F488, 2005

II. TRPC6 MUTATIONS IN GENETIC FORMS OF PROTEINURIC KIDNEY DISEASE

II.1. Rationale

Based on the preliminary data by Winn *et al.* it remained unclear whether the identified mutation in TRPC6 represented a singular phenomenon in the isolated population of New Zealand, or does in fact represent a more widespread genetic cause for FSGS. Furthermore, nothing was known about the consequences of the identified mutation on TRPC6 function, for example whether the mutation leads to TRPC6 loss-of-function, or hyperactive TRPC6 channels, respectively.

Therefore, to investigate the abundance of mutations in the *TRPC6* gene across different ethnical backgrounds, 71 ethnically diverse families affected by familial focal segmental glomerulosclerosis (FSGS) were tested for the presence of mutations in the *TRPC6* gene in collaboration with the laboratory of Prof. Dr. Martin Pollak at the Brigham and Women's Hospital in Boston, Massachusetts, United States. In addition, to address the functional consequences of mutations in *TRPC6*, a patch-clamp setup enabling the electrophysiological characterization of wildtype and mutant TRPC6 channel currents was established in collaboration with Prof. Dr. David Clapham at the Children's Hospital in Boston, Massachusetts, United States.

II.2. Materials and Methods

II.2.1. Patient families

Blood was obtained from members of families with familial focal segmental glomerulosclerosis (FSGS) after informed consent was given in accordance with a protocol approved by the Institutional Review Board at the Brigham and Women's Hospital in Boston, Massachusetts, United States. In these families, the clinical history and pedigree information was obtained. DNA from FSGS-affected probands from 71 families was analyzed for mutations in the TRPC6 gene using bidirectional sequencing. Sequence analysis was performed using PCR-amplified genomic DNA. High-throughput capillary sequencing instrumentation and Sanger dideoxy DNA sequencing [Sanger, 1981] was used for mutation detection. Verification of sequence alterations in probands, family members, and control subjects was done using MALDI-TOF mass spectrometry-based singe nucleotide polymorphism (SNP) genotyping at the Harvard-Partners Core Genotyping Facility.

Family FG-BN

Family FG-BN is a two generation Colombian family. Clinical history was obtained in all twelve of the members and four were considered affected. Eight of the twelve members agreed to participate in the study. The mother was given a clinical diagnosis of nephrotic syndrome at age 52 and was still living in 2005. One daughter was diagnosed with FSGS at the age of 22 and confirmed by biopsy. She was never treated with steroids and has not been started on dialysis. Two brothers were diagnosed at the age 20 with renal disease. Neither was biopsied. One died at the age of 21 from end-stage renal disease (ESRD) and the other started dialysis 3 months after presenting with proteinuric renal disease. The father and six of the children are not affected. No clinical information could be obtained regarding the degree of proteinuria at the time of diagnosis in any of the affected members. None were treated with steroids and none have been transplanted. Two siblings, one boy and one girl, carry the S270T mutation, but have no clinical evidence of disease. At the time of screening, their ages and spot urine protein/Creatinine ratio were age 16 and 17 mg/gCr and age 27 and 3 mg/gCr, respectively.

Family FG-EA

Family FG-EA is a four generation African American family from the midwestern United States. Clinical history was obtained from 36 members. Of these, seven members were considered affected and two of these agreed to participate in the study. One was diagnosed at the age of 27 and presented with hypertension and proteinuria. A biopsy done at the time of presentation revealed FSGS. This individual was started on dialysis at the age of 30 and received a kidney transplant soon thereafter. The transplant failed after 11 years for unknown reasons. The brother of this individual was diagnosed with kidney disease at the age of 37. No biopsy was obtained and the patient was started on dialysis at age 39. Neither patient received corticosteroid therapy. None of the clinically unaffected members agreed to participate in the study.

Family FG-FQ

Family FG-FQ is a four generation family from Mexico. Clinical history was obtained from 25 members and nine were considered affected. A total of eleven members of the 25 agreed to participate in the study, 3 of whom are clinically affected. The proband was diagnosed with FSGS by biopsy at the age of 35 and developed end-stage renal disease (ESRD) at the age of 45. He is awaiting a transplant and was never treated with corticosteroids. Two of his brothers are affected. One brother was diagnosed at the age of 40 with biopsy showing FSGS. He developed ESRD and then received a kidney transplant. He has no evidence of

recurrence of FSGS in the transplanted kidney after six years of follow-up. His son was diagnosed with FSGS by biopsy at the age of 18. He has been treated with angiotensin converting enzyme inhibitors and has not needed renal replacement therapy after 6 years of follow-up. The second brother presented with ESRD at the age of 31 and was transplanted soon thereafter. He has had no evidence of recurrence of FSGS after 9 years of follow-up. The other affected members were considered affected based on clinical history of ESRD.

Family FS-XR

Family FS-XR is a four generation family of Irish/German descent from the northeastern United States. Clinical information was obtained from all twelve members of the family, of which two are affected. Four members agreed to participate in the study. One proband (affected female in the second generation of the pedigree) developed what was described as preeclampsia during her third pregnancy at the age of 24. The proteinuria resolved after delivery. During the fourth pregnancy at the age of 29, proteinuria developed again but persisted after delivery. No treatment or biopsy was pursued at that time. At the age of 49, the patient presented with uremic symptoms, a biopsy revealed FSGS and she was started on dialysis shortly thereafter. She was transplanted with a kidney from her son at the age of 50 and there is no evidence of recurrence in the transplanted kidney or development of kidney disease in the son. A biopsy of the transplant confirms absence of focal sclerosis or podocyte foot process effacement. Her daughter at the age of 27 developed proteinuria during her third pregnancy with persistent proteinuria after delivery. She reached end-stage renal disease (ESRD) within 8 years and is awaiting transplant. No biopsy was obtained. The third daughter developed preeclampsia which resolved after delivery. When genotyped, the third daughter carries the mutation (generation 3; fifth individual). At the time of her screening, she was 32 years old and her spot urine protein/Creatinine ratio was 145 mg/gCr (normal <150 mg/gCr) and has no clinical evidence of kidney disease.

Family FS-Z

Family FS-Z is a five generation family of western European descent. Clinical information was obtained from 53 members and twelve were considered affected. A total of 28 members agreed to participate, of which 6 were affected. Six of the total twelve affected individuals died of end-stage renal disease (ESRD). One of these developed hypertension and progressive renal failure prior to kidney biopsy which showed FSGS at the age of 55. Of the six affected individuals who participated in the study, one brother and his sister had kidney biopsy-confirmed FSGS. The sister

developed kidney disease after donating a kidney to her brother. The brother lost the first renal allograft as a result of FSGS in the transplanted kidney, a second cadaveric allograft due to acute rejection, and is currently awaiting a third transplant. Another of the six has reached ESRD and is on hemodialysis. One developed nephrotic syndrome at age 57 and then was transplanted and has been without evidence of recurrent disease in the transplanted kidney. Two have proteinuric renal disease (1.6 g/gCr and 2.7 g/gCr) and neither has progressed to ESRD as of 2005. Of these two, one developed kidney disease after donating a kidney to his affected father. In this family, there are nine individuals who carry the K874Stop mutation but do not have clinical evidence of kidney disease. Generation IV of this family includes four such individuals (3 women, 1 man) with age ranges between 37 and 44. Of these members, three of them provided urine specimens to estimate albumin excretion. The range of urinary albumin excretion in these individuals was between 5.6 mg/gCr and 28.3 mg/gCr. In generation V, there are five individuals with K874Stop mutations without clinical disease (2 women, 3 men) with age ranges between 13 and 18. The range of urinary albumin excretion was between 5.9 mg/gCr and 64.4 mg/gCr.

II.2.2. Sequence alignment

Sequence alignments were performed using the T-Coffee algorithm [Notredame *et al.*, 2000] comparing human TRPC6 protein sequences to other human TRPC channels (TRPC1; TRPC3-7) and TRPC6 protein sequences in fly (*Drosophila melanogaster*), rat (*Rattus norvegicus*), mouse (*Mus musculus*), Guinea pig (*Cavia porcellus*), and chimpanzee (*Pan troglodyte*). Protein sequence data was obtained from the National Center for Biotechnology Information (NCBI) database (http://www.ncbi.nlm.nih.gov).

II.2.3. Site-directed mutagenesis

Site-directed mutagenesis was performed to insert the variants identified into a full-length human TRPC6 cDNA clone (pcDNA3.1-TRPC6). Two mutagenic oligonucleotide primers were designed containing the desired mutation, flanked by unmodified nucleotide sequence. Mutagenesis was performed with an amplification reaction using the human TRPC6 cDNA template, mutagenic primers, and Pfu DNA polymerase (Stratagene, LaJolla, California, United States). Clones were then selected and sequenced to identify and verify mutants.

II.2.4. Patch-clamp electrophysiology

35 mm dishes of HEK293-M1 cells (human embryonic kidney cells stably transfected with the M1 muscarinic receptor) were transiently transfected with 2 μg of wild-type eGFP-TRPC6 or mutant eGFP-TRPC6 cDNA and 0.25 μg of eGFP cDNA (control) using Lipofectamine 2000 (Invitrogen, Carlsbad, California, United States). After transfection, cells were plated on glass coverslips at low density. Recordings were obtained from cells 24-72 hours after transfection. Cells were maintained at 37 °C in DMEM/Ham's F-12 (1:1), 10% fetal bovine serum, 100 U/mL penicillin, 100 μg/mL streptomycin and 100 μg/mL G-418 in 5% CO_2. eGFP-positive cells were visualized with a fluorescence microscope (Olympus, Center Valley, Pennsylvania, United States). Currents were recorded using an Axopatch 200B amplifier and pClamp8 software (Molecular Devices, Sunnyvale, California, United States). Voltage ramps from –100 mV to 100 mV over 150 ms were applied every 3.45 s from a holding potential of 0 mV. During voltage ramps, currents were sampled at 10 kHz and the recordings were filtered at 2 kHz. Current amplitude was normalized for cell capacitance. In each experiment the membrane potential was held either at –60 mV or 0 mV, and no differences were noted between experiments performed at a holding potential of –60 mV and 0 mV. Borosilicate glass pipettes with resistances of 2-4 MΩ were used for recording. The bath solution contained 135 mM NaCl, 5 mM CsCl, 2 mM $CaCl_2$, 1 mM $MgCl_2$, 10 mM HEPES, 10 mM Glucose, pH 7.4. The pipette solution contained 135 mM CsMES, 10 CsCl, 3 mM MgATP, 0.2 mM NaGTP, 0.2 mM EGTA, 0.13 mM $CaCl_2$, 10 mM HEPES, pH 7.3. The free calcium concentration in the pipette solution was approximately 100 nM as calculated by MaxChelator 2004 software [Patton *et al.*, 2004]. The average current amplitudes at –100 mV and 100 mV were compared with Student's *t* test. To determine the time to a 50%-decay of inward Ca^{2+} currents of wildtype and mutant TRPC6 channels, inward currents were recorded at –60 mV, and the time was measured starting when the inward current reached a maximum and ending when the current decayed to 50% of the peak amplitude.

II.3. Results

II.3.1. Families with TRPC6-related FSGS

To explore the role of *TRPC6* gene variation in kidney disease, probands of 71 pedigrees with familial FSGS were screened for alterations in the TRPC6 gene by DNA sequence analysis. Of the 71 families screened, 43 showed evidence of disease in members of multiple generations, and 28 showed evidence of disease in 2 or more members of a single generation (Fig. II.1.). Probands of 49% of the families were of

western European ancestry, 5% of African ancestry, and 27% described themselves as Hispanic. The phenotype in affected members of largest of these families (FS-Z) showed cosegregation only with chromosome 11q markers (with 2 point lod score examining linkage of affected individuals with the disease-associated haplotype equal to 1.8 at θ=0). Different heterozygous sequence variants were identified in five unrelated families with adult onset disease, all of which predicted changes in the encoded gene product: N143S, S270T, K874Stop, R895C and E897K (Table II.1.). Other available family members were also genotyped for the relevant variants; in all families, patterns of TRPC6 variant and disease inheritance followed a pattern of cosegregation with less than complete penetrance. In each family, inheritance was consistent with an autosomal-dominant pattern. 180 control individuals were also genotyped for the disease-associated variants. None of these disease associated variants were identified in the controls. In addition, none of these substitutions were found in the public SNP databases.

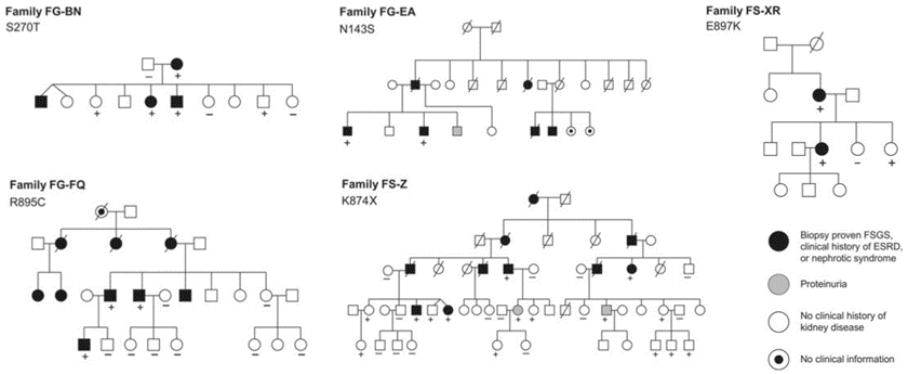

Figure II.1. Pedigrees of families with inherited FSGS. TRPC6 variants segregating in each family are indicated. Genotyped individuals are indicated as carrying (+) or not carrying (-) the variant identified in each family. ESRD, end-stage renal disease. (Data generated in collaboration with Prof. Dr. Martin Pollak, Brigham and Women's Hospital, Boston, Massachusetts, United States.)

Family	Ethnicity	Mutation	Exon	Age range at disease presentation (years)	Number of family members with ESRD
FG-EA	African-American	N143S	2	27-39	5 of 36
FG-BN	Colombian	S270T	2	17-52	3 of 12
FG-Z	Polish	K874Stop	12	27-57	9 of 53
FG-FQ	Mexican	R895C	13	18-46	6 of 25
FS-XR	Irish/German	E897K	13	24-35	2 of 12

Table II.1. Clinical manifestation of TRPC6-related FSGS.

II.3.2. Localization of mutations in the TRPC6 sequence

Each of the observed amino acid substitutions occurred in evolutionarily conserved residues (Fig. II.2.). Two mutations predict amino-acid substitutions in the N-terminal intracellular domain of TRPC6 (N143S, S270T), two predict amino-acid substitutions in the C-terminal intracellular domain (R895C, E897K), and one encodes a premature stop codon near the C terminus (K874Stop). Among the four missense mutations, three lead to conservative amino acid substitutions, substituting a hydrophilic-neutral amino acid with another hydrophilic-neutral one (N143S, S270T), or an hydrophilic-charged amino acid with another hydrophilic-charged one, respectively (E897K). In contrast, R895C is a non-conservative substitution, exchanging an hydrophilic-charged amino acid to a hydrophobic residue.

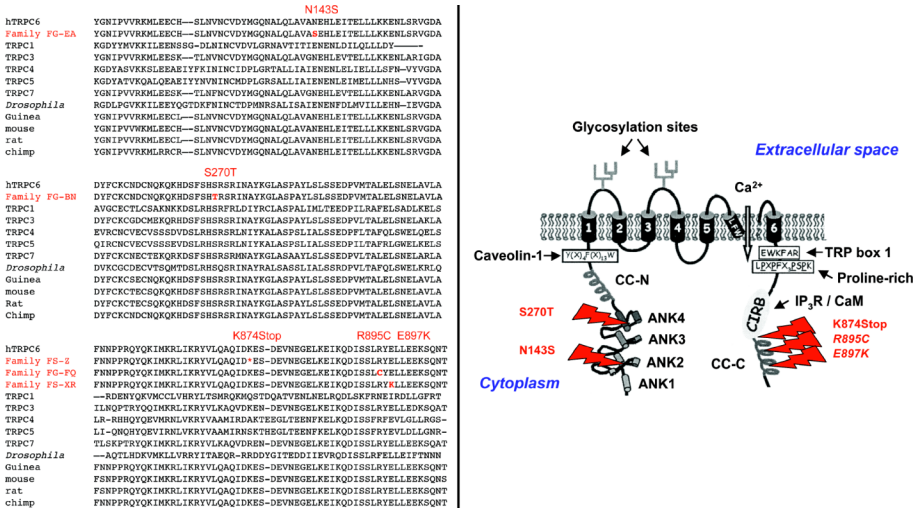

Fig. II.2. Localization of mutations in the TRPC6 sequence. (Left) Sequence alignments (using T-COFFEE) showing evolutionary conservation of mutated TRPC6 residues. All four missense mutations occur in conserved residues. (Right) Localization of mutations within the predicted TRPC6 protein structure. The amino-terminal cytoplasmic sequence contains several ankyrin repeats and a potential coiled-coil region. The carboxy-terminal cytoplasmic domain contains a conserved sequence found in TRPC, TRPV and TRPM proteins, termed the TRP box, and a potential coiled-coil sequence. The location and identity of mutations associated with familial forms of FSGS are indicated. ANK1–4, ankyrin repeats 1–4; CC-N, N-terminal potential coiled coil region; LFW, amino acid motif conserved in the putative pore region of all TRPC channels; CIRB, calmodulin/IP_3R binding region;. CC-C, C-terminal potential coiled coil region. (Source: adapted from Vazquez et al. (2004) Biochim Biophys Acta. 1742:21-36. [Vazquez *et al.*, 2004])

II.3.3. Electrophysiological analysis of mutant TRPC6 channels

To study whether mutations in TRPC6 affect calcium channel function, wild-type TRPC6 and the five mutant TRPC6 channels were expressed in HEK293 cells stably transfected with the $G\alpha_q$-coupled M1 muscarinic receptor. TRPC6 currents were recorded before and after activation of M1 receptors by carbachol. Currents from the N143S, S270T and K874Stop TRPC6 channels did not differ noticeably from wild type TRPC6 currents (data not shown). In contrast, currents from R895C and E897K mutant channels were significantly larger than wild type TRPC6 currents (Fig. II.3.). Notably, the non-conservative amino acid substitution R895C produced the most significant changes in current amplitude. Subtle differences in the rectification of the current-voltage relationship of these two mutants were also noted. However, the changes in rectification most likely result from the increased current density rather than directly from structurally related changes in channel gating or permeation.

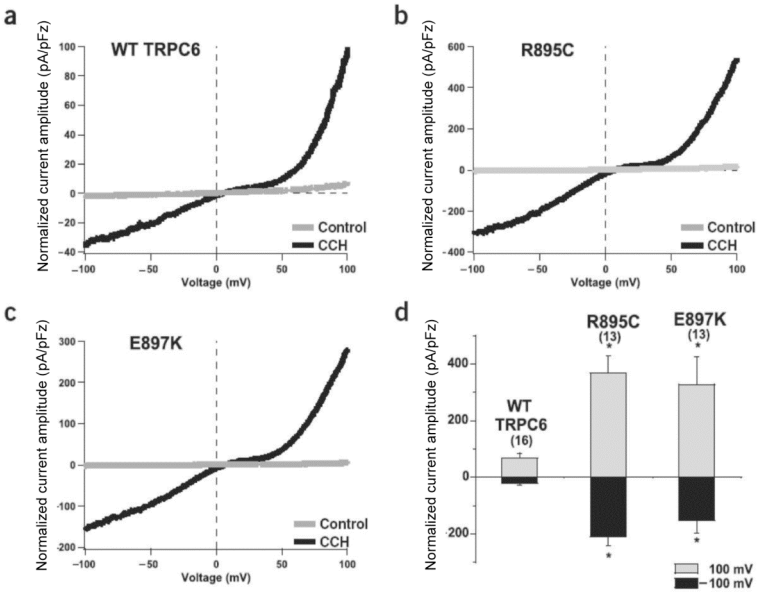

Fig. II.3. Inreased current amplitudes of mutant TRPC6 channels. Representative whole-cell currents measured from HEK293-M1 cells transiently transfected with cDNA encoding wild-type (WT) TRPC6 (a) or R895C (b) or E897K (c) mutant TRPC6. Current traces were recorded as cells were perfused with control bath solution (gray traces) or 100 μM carbachol (CCH, black traces). (d) Average normalized current amplitude measured at –100 mV (dark bars) and 100 mV (light bars) from cells expressing wild-type (WT) TRPC6 or R895C or E897K mutants. Current amplitudes from cells expressing R895C and E897K mutants were significantly higher at both –100 mV and 100 mV than those from cells expressing wild-type channels ($P < 0.01$). The number of experiments is shown in parentheses, and the error bars show the S.E.M. for each measurement. (Data generated in collaboration with Prof. Dr. David Clapham, Children's Hospital, Boston, Massachusetts, United States.)

The time to a 50%-decay of inward Ca^{2+} currents of wildtype and mutant TRPC6 was also studied. Inward currents were recorded at –60 mV, and the time was measured starting when the inward current reached a maximum and ending when the current decayed to 50% of the peak amplitude. Preliminary results suggest that the time to 50%-decay was prolonged in all of the tested TRPC6 mutants (Fig. II.4.). The mean values differed from the wildtype in a range from +54% (20 s for N143S vs. 13 s for wild-type) to +246% (45 s for E897K vs. 13 s for wild-type).

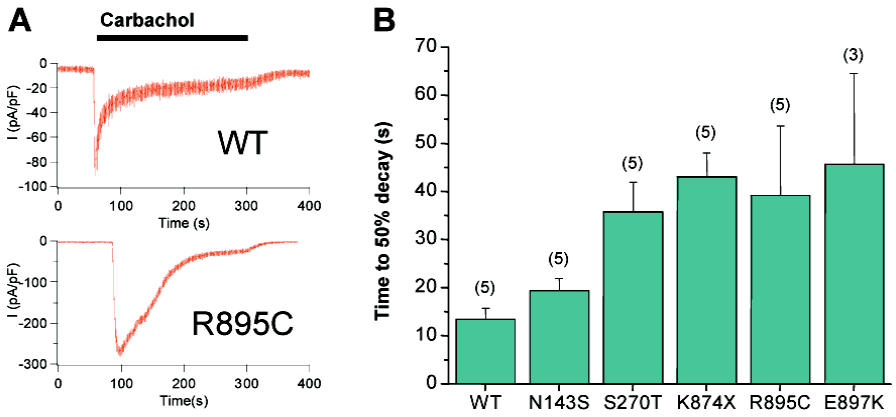

Fig. II.4. Prolonged time to 50%-decay for mutant TRPC6 channels. (A) Inward currents through wild-type TRPC6 (WT; upper panel) and mutant TRPC6 (R895C shown representatively; lower panel) channels were recorded at –60 mV following stimulation with carbachol. (B) The time to 50%-decay of the inward current appeared to be prolonged in all of the evaluated TRPC6 mutants. The number of experiments is shown in parentheses, and the error bars show the S.E.M. for each measurement. (Data generated in collaboration with Prof. Dr. David Clapham, Children's Hospital, Boston, Massachusetts, United States.)

II.4. Discussion

II.4.1. Clinical presentation of TRPC6-related FSGS

Mutations in several podocyte genes have been identified as culprits for progressive renal failure or increased glomerular disease susceptibility [Pollak *et al.*, 2002]. The presence of TRPC6 mutations cosegregating with kidney disease, the changes in channel current amplitude observed in two mutants, and the observed prolonged time to 50% decay suggest that TRPC6 channel function plays a role in normal renal ultrafiltration and the pathogenesis of glomerular disease.

The work presented suggests that TRPC6-related FSGS is not restricted to certain ethnic groups as TRPC6 mutations were found to cosegregate with kidney disease in families of African-American, Colombian, Polish, Mexican, and Irish/German descent alike. Second, TRPC6 mutations appear to account for a significant number of inherited FSGS cases. Given that among 71 tested families, five were positive for TRPC6 mutations, this relates to a relative frequency of TRPC6-related FSGS of about 7% among all cases of familial FSGS. Third, the age range at disease presentation was broad, ranging from 17-57 years. This classifies TRPC6-related FSGS as a disease with a rather late onset, in contrast to other genetic glomerulopathies that manifest in infancy such as congenital nephrotic syndrome of the Finnish type, steroid-resistant nephrotic syndrome of the podocin type, or Wilms' tumor protein 1 (WT1)-related diseases including Denys-Drash syndrome and Frasier syndrome. While in these diseases the early onset is most likely due to the severe damage that is inflicted on the molecular architecture of the slit diaphragm and the process of glomerular filtation as a result of nephrin or podocin disruption, the question remains why the onset of kidney disease in patients with TRPC6 mutations occurs at a relatively advanced age. One possible explanation is that mutations in TRPC6 may produce subtle changes in intracellular function that lead to irreversibly altered cell behavior only after time and in the presence of other renal insults [Pavenstadt *et al.*, 2002]. This would be similar to the adult onset and dominantly inherited form of FSGS due to mutations in the widely expressed protein α-actinin-4 [Kaplan *et al.*, 2000]. In addition, podocytes express several TRPC channel subunits other than TRPC6, and partial functional redundancy may also help account for the late onset of glomerular disease. Indeed, the ability of TRPC6 to form heteromers with other TRPC channels suggests a complex cellular regulation of calcium homeostasis [Schaefer *et al.*, 2005]. A similar explanation was also suggested for the late onset of disease in CD2AP haploinsufficiency, an autosomal-dominant genetic disorder [Kim *et al.*, 2003]. In this case the CD2AP-homolog Cin85 may partially be able compensate for decreased CD2AP levels [Tossidou *et al.*, 2007].

Finally, individuals with TRPC6-related FSGS did not present with any other pathological phenotype. TRPC6 is widely expressed in smooth muscle cells, where it is thought to contribute to the regulation of important physiological aspects such as airway resistance and vascular tone. However, TRPC6 mutations appear to exhibit their deleterious effect mainly in the kidney in absence of any other overt organ dysfunction. This suggests that the glomerular phenotype is the consequence of a unique role of TRPC6 in the organization of the glomerular filtration barrier and the increased susceptibility of this structure even to subtle changes in its microenvironment. Therefore, TRPC6 belongs to the same category of genes such as α-actinin-4 and CD2AP. Mutations in both genes foremostly lead to glomerular kidney disease while being widely expressed and associated with a plethora of different cellular functions in many cells throughout the body [Shih *et al.*, 1999; Kaplan *et al.*, 2000]. For example, in the case of CD2AP it was possible to rescue $CD2AP^{-/-}$ lethality in mice with podocyte-targeted expression of CD2AP, highlighting the particular role of CD2AP in podocytes [Grunkemeyer *et al.*, 2005].

II.4.2. Nature of TRPC6 mutations

Of the five TRPC6 mutations that were identified, all are located either at the N-terminal (N143S; S270T) or C-terminal (K874Stop; R895C ;E897K) intracellular tail of TRPC6. The two mutations at the N-terminus are both located within the sequence region spanning four ankyrin repeats. Ankyrin repeats fold into a helix-loop-helix-beta-hairpin/loop structure with several repeats stacked against one another to form a single domain with a protein-binding interface [Mosavi *et al.*, 2004]. In TRPC channels, the first ankyrin-like repeat is the minimum indispensable key structure for functional assembly of homo- and heteromeric TRPC4/TRPC5 channels [Schindl *et al.*, 2007]. Mutations in this region may therefore compromise the ability of TRPC6 to oligomerize with other TRPC subunits, or to interact with other binding partners. Ankyrin repeats have also been shown to be important determinants of proper plasma membrane targeting of TRPC channels [Wedel *et al.*, 2003; Smyth *et al.*, 2006]. Whereas not all ankyrin repeats seem to be crucial for the functional assembly of TRPC channels, a truncated variant of TRPC3 lacking all of the N-terminal ankyrin repeats no longer mediated agonist-induced Ca^{2+}-entry in HEK293 cells [Wedel *et al.*, 2003]. Finally, mutations within the ankyrin repeats of TRPC6 may prevent the channel from being correctly inserted into the plasma membrane. This is supported by findings of Cayouette *et al.* suggesting that TRPC6 levels at the plasma membrane are regulated by targeted membrane insertion [Cayouette *et al.*, 2004].

Notably, no changes in current amplitude were detected for the N-terminal N143S and S270T mutations and for the K874Stop non-sense mutation. Nevertheless, these mutations are likely to be disease-causing because of the nature of the changes (substitutions in very highly conserved residues), cosegregation with the disease phenotype, the absence of these changes from control individuals. Yet, this result suggests that an abnormality other than increased current amplitude is the cause of disease in the individuals with these mutations. The observed prolonged time to 50% decay may serve as a possible explanation. However, other factors may be involved as well, including altered channel regulation (despite normal current amplitude), altered interaction with slit diaphragm proteins, or altered protein turnover. Another possibility is that these mutations may exhibit altered current amplitudes only in the physiological context, e.g. when assembled into the proper heteromeric composition. Therefore, the effect of the studied mutations may not be visible when only the mutated TRPC6 subunits are expressed as monomeric channels in HEK293 cells.

Among the three mutations at the C-terminus, two (R895C; E897K) are located very close to each other in a putative coiled-coil domain. The coiled-coil is an ubiquitous protein motif that is commonly used for oligomerization. There is one potential coiled-coil motif in each of the cytosolic N- and C-termini of TRPCs. While no study has specifically investigated the importance of the C-terminal coiled-coil motif in TRPC channel, a recent study suggests that the C-terminal tail of TRPC4 and TRPC6 participates in channel oligomerization [Lepage *et al.*, 2006]. Importantly, the R895C and E897K mutations both resulted in TRPC6 channels with higher current amplitudes (Fig. II.3.) suggesting that disruption of the C-terminal putative coiled-coil motif in TRPC6 has a direct consequence on channel activity. Whether this is indeed due to an interference with the ability of TRPC6 to oligomerize with other channel subunits, will have to be addressed in future studies.

As is the case for the N143S and S270T mutations, also the mutation identified by Winn *et al.* in a large family from New Zealand (P112Q) is located at the N-terminal intracellular tail in the sequence region spanning the four ankyrin repeats [Winn *et al.*, 2005]. Similar to the increased channel activity that we observed for the R895C and E897K mutations, Winn *et al.* found the current amplitude increased for the TRPC6 P112Q channel [Winn *et al.*, 2005], indicating that interference with both, N- and C-terminal domains of TRPC6 can give rise to hyperactive channels. Winn *et al.* provide in their study a possible explanation for the increased current amplitude caused by the P112Q mutation: by carrying out surface biotinylation studies it was shown that mutant TRPC6 channels were more abundant in the plasma membrane when expressed heterologously in HEK293 cells than their wild-type counterparts.

II.4.3. TRPC$^{-/-}$ mice – a suitable model for TRPC-related FSGS?

To study the pathogenic mechanisms behind many inherited human diseases, important insights may be drawn from the study of genetic animal models. TRPC6-deficient mice have recently been characterized [Dietrich *et al.*, 2005]. As mentioned above, young TRPC6$^{-/-}$ mice appear to lack an overt renal phenotype. However, one has to take into account that thus far no study has explicitly addressed the renal phenotype of TRPC6-deficient mice. Moreover, given the late onset of the TRPC6-related human disease, in particular also aged mice would have to be considered.

One explanation is provided by the so-called second-hit hypothesis [Kriz, 2005]. For example, in the context of mutations in α-actinin leading to FSGS [Yao *et al.*, 2004], it has been suggested that, besides the presence of mutations, a second physiological hit such as a metabolic disturbance is required for the clinical manifestation of the disease. A similar mechanism may account for the absence of a disease phenotype in TRPC6$^{-/-}$ mice, which have not been experimentally challenged yet. Furthermore, as decribed above, a genetic second hit in the form of mutations in genes other than TRPC6 may be required for the disease onset as it was seen in bigenic mouse models of FSGS involving the pairwise interaction of CD2AP, synaptopodin, and Fyn [Huber *et al.*, 2006].

Also, the role of TRPC6 in the kidney may be different in the human and the mouse, and the findings in the animal model may not be applicable to the human disease phenotype. A recent example comes from a study indicating a key role of sialic acid in kidney development and function in mice [Galeano *et al.*, 2007]. Mice carrying a mutation in ManNAc kinase, a key enzyme in the sialic acid biosynthesis pathway die within 72 h after birth from severe glomerular disease including podocyte foot process effacement, structural damages in the glomerular basement membrane, hematuria and proteinuria. This is due to the disruption of sialic acid production. In contrast, disruption of the same enzyme does not cause any kidney damage in humans, where the disease mainly affects muscle function. This finding illustrates that there may be considerable differences in the organization of cellular functions between humans and widely applied animal models such as mice or rats, and one has to apply caution when trying to adapt experimental observations made in animal models to a human disease.

Finally, while TRPC6-deficient mice may reveal themselves as a suitable model to study the physiological role of TRPC6 in the kidney under an appropriate study design, they may not be suitable for studying the pathogenesis of TRPC6-related FSGS given that TRPC6 mutants appear to lead to increased channel function.

II.4.4. Consequences for the diagnosis of FSGS

The finding that mutations in the *TRPC6* gene are associated with familial forms of FSGS may be used for genotyping of candidate individuals in the future. Polymorphisms of TRPC6 may act as susceptibility or initiation factors for renal disease and may help determine which patients would benefit from early, aggressive therapy. Two examples of how genotyping may be applied to patients with glomerular disease can be found in nephrin and podocin mutations. In 1998, genetic mutations in the *NPHS1* gene encoding nephrin were shown to be associated with congenital nephrotic syndrome of the Finnish type [Kestila *et al.*, 1998]. Nephrin can be found in podocytes as an essential component of the slit diaphragm. In 2000, genetic mutations in another important podocyte protein, podocin, were shown to be associated with steroid-resistant nephrotic syndrome [Boute *et al.*, 2000]. Patients with this condition do not respond to standard treatment with the steroid prednisone. Consequently, the long-term prognosis for this steroid-resistant subgroup is poor because no satisfactory treatment exists. Like nephrin, podocin plays an important role in regulating kidney filtration at the slit diaphragm.

A genotyping assay has been developed that can be used to screen patients for the presence of nephrin or podocin mutations. This genetic test is now commercially available. The test results can detect the presence of the currently known mutations in either nephrin or podocin and therefore provide clarity about the cause of the disease and diagnostic clues for adequate treatment of patients. A similar approach to test for the presence of TRPC6 mutations in individuals with a family background of inherited FSGS will become available in the near future. Given the late onset of TRPC6-related glomerular disease, knowledge about genetic defects in the *TRPC6* gene may enable an earlier therapeutic intervention. It may also prompt the affected individuals to adopt a lifestyle aiming to preserve kidney function as long as possible, e.g. adhere to a low-salt diet. Whereas there are currently no therapies available that can specifically target TRPC6-related FSGS, this may still help improve the situation for the affected individuals.

III. TRPC6 ASSOCIATION WITH THE GLOMERULAR FILTRATION BARRIER

III.1. Rationale

The observation that mutations in TRPC6 are associated with a severe kidney phenotype in the absence of other overt organ dysfunction, points to a pivotal role of TRP6 channels in the kidney. However, the mechanism of TRPC6 involvement in kidney disease, and the role of TRPC6 in normal kidney function remain unclear. In an effort to understand the molecular mode of TRPC6 function for TRPC6 in the kidney, several key questions must be answered. Firstly, is TRPC6 expressed in podocytes? If so, what is the subcellular localization of TRPC6 in podocytes; in particular, is TRPC6 associated with the slit diaphragm, the key membranous structure often disrupted in focal segmental glomerulosclerosis? In an effort to reveal a possible link between TRPC6 and the glomerular filter, the expression of TRPC6 in podocytes and its association with the slit diaphragm were studied.

III.2. Materials and Methods

III.2.1. Cell culture

Conditionally immortalized mouse podocytes were cultured as described [Mundel *et al.*, 1997]. A GFP-TRPC6 construct, which included the complete mouse TRPC6 cDNA, was kindly provided by Mike Zhu (Ohio State University, Columbus, Ohio, United States). Cultured podocytes were transfected using Lipofectamine 2000 (Invitrogen, Carlsbad, California, United States) according to standard protocols.

III.2.2. Immunohistochemistry and Immunocytochemistry

Female adult Sprague-Dawley rats with a body weight of 200 g were perfused via the abdominal aorta with 2% paraformaldehyde in PBS for 3 min at 220 mmHg followed by cryoprotectant sucrose-PBS solution (800 mOsmol) for 5 min at 220 mmHg. For immunofluorescent labeling, sections were washed once with PBS and incubated with blocking solution (2% fetal calf serum, 2% bovine serum albumin, 0.2% fish gelatin) for 30 min at room temperature before incubation with the primary antibody for 1 h at room temperature. For double labeling, a second primary antibody was applied for 1 h. Antigen-antibody complexes were visualized with secondary antibodies conjugated with fluorochromes. Specimens were analyzed using a confocal microscope (Zeiss, Oberkochen, Germany). The following antibodies were used: mouse G1 monoclonal antibody to synaptopodin [Mundel *et al.*, 1997] and

rabbit polyclonal antiserum to TRPC6 (Alomone Labs, Jerusalem, Israel; 1:50 dilution) and polyclonal antibodies against CD2AP (gift from Dr. Andrew Shaw, Washington University, Saint Louis, Missouri, United States), nephrin and podocin (all in 1:200 dilution). As a control, the primary antibodies were either omitted or, in the case of TRPC6 staining, the primary antibody was pre-incubated with a TRPC6 control peptide for 1 h before use in the immunolabeling. Specimens were analyzed using a confocal microscope (Zeiss, Oberkochen, Germany). For immunofluorescent labeling of cultured podocytes, cells were processed as decribed before [Mundel *et al.*, 1997]. Mouse kidneys (wild-type and nephrin$^{-/-}$; kindly provided by Dr. Raghuram Kalluri, Beth Israel Deaconess Medical Center, Boston, Massachussets, United States) were harvested, snap-frozen and fixed with 4% formaldehyde after sectioning in ice-cold acetone for 10 min [Hamano *et al.*, 2002]. Sections were washed once with PBS and incubated with blocking solution (2% fetal calf serum, 2% bovine serum albumin, 0.2% fish gelatin) for 30 min at room temperature before incubation with the primary antibody for 1 h. For double labeling, a second primary antibody was applied for 1 h. Antigen-antibody complexes were visualized with secondary antibodies conjugated to fluorochromes. Specimens were analyzed using a confocal microscope (Zeiss, Oberkochen, Germany).

III.2.3. RT-PCR

Total RNA was isolated from murine cultured differentiated podocytes using Trizol reagent (Invitrogen, Carlsbad, California, United States) according to the manufacturer's instructions. cDNA synthesis was performed with SuperScript II Reverse Transcriptase (Invitrogen, Carlsbad, California, United States) using Oligo(dT)12-18 oligonucleotide primers according to the manufacturer's instructions.

III.2.4. Immunogold and Transmission Electron Microscopy

Immunogold labeling of ultrathin frozen sections of perfusion-fixed mouse kidney were incubated with the rabbit anti-TRPC6 antibody (Chemicon, Temecular, California, United States), followed by gold-labeled anti-rabbit secondary antibody. Images were obtained using a Philips CM10 electron microscope (Philips, Eindhoven, Netherlands).

III.2.5. Coimmunoprecipitation

Recombinant mouse GFP-TRPC6 was coexpressed with FLAG-tagged mouse CD2AP, nephrin and podocin, respectively, in HEK293 cells. FLAG-fusion proteins from cell lysates were immunoprecipitated using anti-FLAG-M2 beads and eluates were analyzed by Western blotting using anti-FLAG and anti-GFP antibodies (Sigma,

Saint Louis, Missouri, United States). For endogenous coimmunoprecipitation studies, whole cell extracts from cultured differentiated podocytes were prepared and incubated with anti-TRPC6 antibody overnight. The reaction was then incubated with protein G-coupled beads (Sigma, Saint Louis, Missouri, United States) for 2 h. Coimmunoprecipitated protein complexes were visualized by Western blotting using antibodies against TRPC6 (1:300 dilution), CD2AP (1:2,000), nephrin (1:300) and podocin (1:1,500). As a negative control, protein G-coupled beads without antibody were used.

III.3. Results

III.3.1. TRPC6 expression pattern in the kidney glomerulus

Confocal microscopy of adult rat kidney sections revealed widespread expression of TRPC6 throughout the kidney tubules and glomeruli (Fig. III.1.). Most TRPC6 expression within the glomerulus was confined to podocytes as shown by immunofluorescent double labeling with the podocyte marker synaptopodin resulting in a yellow staining pattern [Mundel *et al.*, 1997]. In addition, a signal was also detected in glomerular endothelial cells. Pre-incubation of TRPC6 antibody with a TRPC6 control peptide resulted in a negative signal.

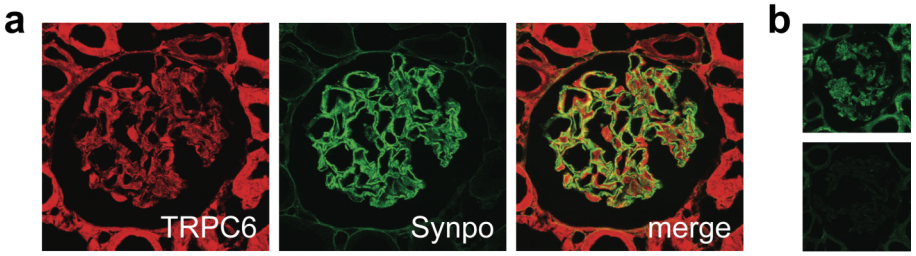

Fig. III.1. TRPC6 protein expression in the rat kidney glomerulus. (a) Confocal microscopy shows TRPC6 expression (red) in the glomerulus. TRPC6 colocalizes with the podocyte marker synaptopodin (green; overlap shown by yellow staining). (b) Compared with TRPC6 antibody labeling (green), preabsorption of TRPC6 antibody with control peptide results in negative staining.

Next, the expression of TRPC1-6 mRNAs in isolated glomeruli and cultured mouse podocytes was determined by RT-PCR (Fig. III.2., left). While expression of TRPC1-6 mRNAs was detected in isolated glomeruli, only TRPC1, 2, 5 and 6 mRNAs were detectably expressed in cultured podocytes. These data are consistent with other reports detecting TRPC6 mRNA in glomeruli [Winn *et al.*, 2005; Facemire *et al.*, 2004]. A TRPC6-specific antibody detected TRPC6 protein expression in cultured mouse podocytes in the nucleus as well as at the plasma membrane (Fig. III.2., right).

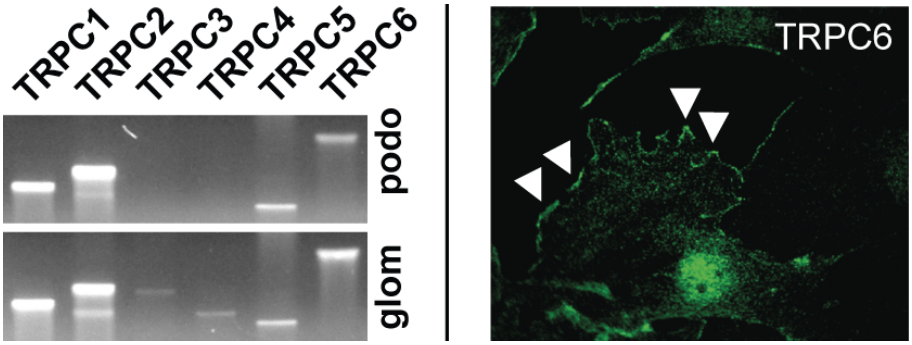

Fig. III.2. TRPC6 expression in cultured podocytes. (Left) Analysis of TRPC1-TRPC6 mRNA expression in cultured podocytes by RT-PCR. TRPC1, 2 5, and 6 mRNAs are detected in total podocyte RNA (podo). TRPC3 and 4 mRNAs are detected in total glomerular RNA (glom) but not in total podocyte RNA. (Right) TRPC6 protein expression in cultured podocytes. TRPC6 localizes to the cell membrane in cultured differentiated podocytes (arrowheads) as shown by immunostaining.

To determine the precise subcellular localization of TRPC6, immunogold labeling of ultrathin frozen sections from adult kidney cortex was performed. Gold particles were found in the cell body of podocytes and in primary processes (Fig. III.3., upper panel, white arrowheads). Clusters of gold particles were observed, indicating the presence of TRPC6-containing vesicles. In podocyte foot processes, gold particles labeled areas in close vicinity to the slit diaphragm region (Fig. III.3, upper panel, black arrowheads). TRPC6 expression was sometimes also detected in glomerular endothelial cells. The high power view of a section through the slit diaphragm area revealed the close association of TRPC6 with the slit diaphragm (Fig. III.3., lower panel, black arrowheads). The expression of TRPC6 near the slit diaphragm is consistent with a role for this channel in regulation of the glomerular filtration barrier.

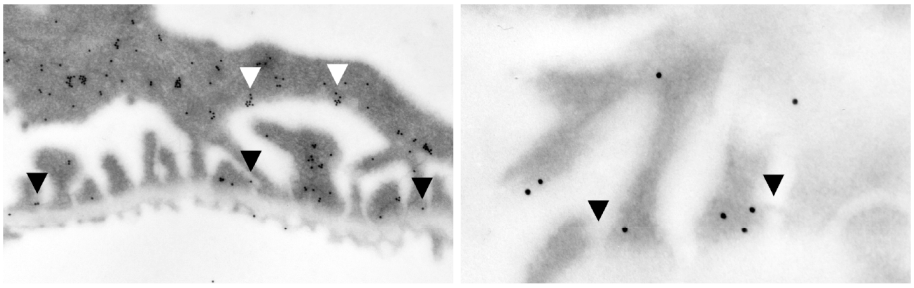

Fig. III.3. TRPC6 immunogold labeling. (Left) Immunogold labeling shows TRPC6 localization in podocyte major processes (white arrowheads) and foot processes. TRPC6 in podocyte foot processes is located in close vicinity to the slit diaphragm (black arrowheads). (Right) High-power view of slit diaphragm areas (arrowheads) displays heavy TRPC6 immunogold labeling.

III.3.2. TRPC6 association with the glomerular slit diaphragm

Given the central role of slit diaphragm disruption in kidney pathologies, the pattern of TRPC6 localization was further examined with respect to the disease-associated slit diaphragm proteins nephrin, podocin and CD2AP. Nephrin serves a molecular

scaffold and is involved in mediating extracellular signals into the podocyte cell body [Benzing, 2004]. Podocin is a stomatin protein family member with a predicted hairpin-like structure localizing to the insertion site of the slit diaphragm of podocytes [Boute *et al.*, 2000], where it is thought to recruit other proteins into nephrin-containing lipid raft signaling microdomains at the slit diaphragm [Schwarz *et al.*, 2001]. CD2AP is an important adapter protein, connecting the slit diaphragm complex to the podocyte actin cytoskeleton [Welsch *et al.*, 2005].

Since available antibodies against TRPC6 and slit diaphragm proteins are all rabbit-polyclonal, cultured podocytes were transfected with GFP-tagged TRPC6. Confocal microscopy of GFP-TRPC6-transfected podocytes stained with antibodies against nephrin, podocin and CD2AP revealed expression of GFP-TRPC6 at the podocyte cell membrane partially colocalizing with nephrin, podocin and CD2AP (Fig. III.4.). This further supported the notion that TRPC6 is associated with the slit diaphragm.

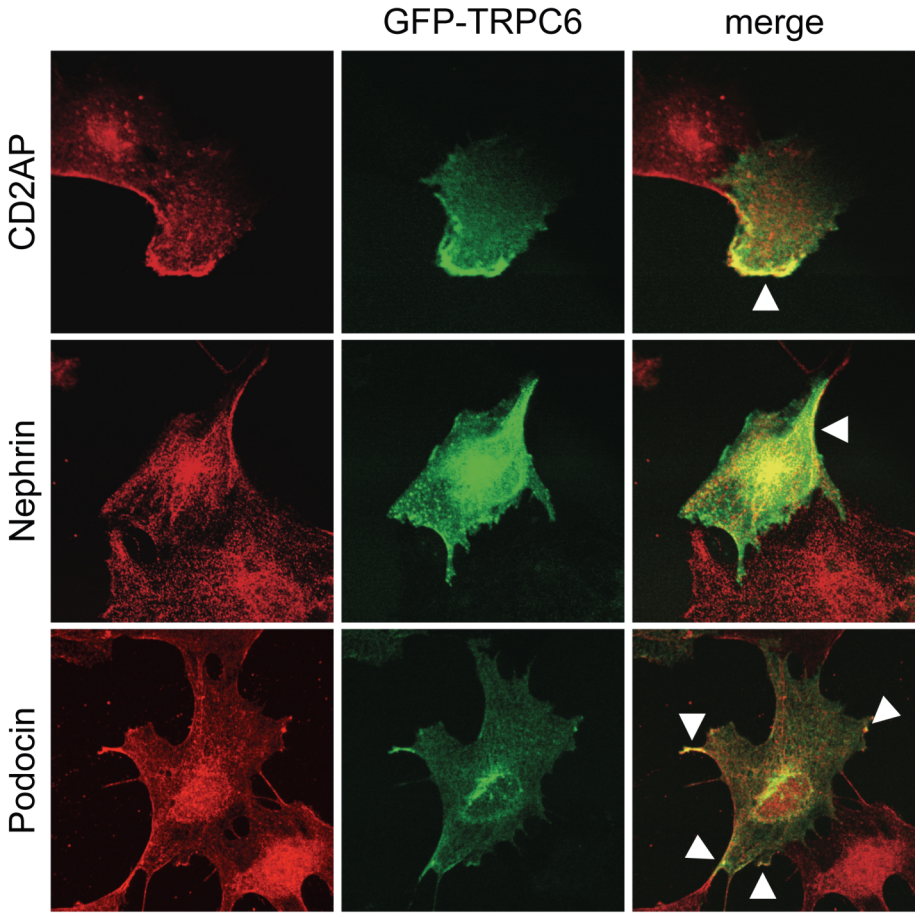

Fig. III.4. TRPC6 colocalizes with slit diaphragm proteins. GFP-TRPC6 colocalizes with CD2AP, nephrin and podocin at the cell membrane of cultured podocytes, as shown by confocal microscopy (arrowheads).

The colocalization of TRPC6 with nephrin, podocin and CD2AP raised the intriguing possibility that TRPC6 can interact with one or more of these key players at the slit diaphragm. To test this, coimmunoprecipitation studies were performed (Fig III.5.). Recombinant mouse GFP-TRPC6 was coexpressed with FLAG-tagged mouse nephrin, podocin, and CD2AP, respectively, in HEK293 cells. FLAG-fusion proteins from cell lysates were immunoprecipitated using anti-FLAG-M2 beads and eluates were analyzed by immunoblotting using anti-FLAG and anti-GFP antibodies. To detect the interaction of GFP-TRPC6 with FLAG-tagged nephrin, podocin or CD2AP, eluates were analyzed with anti-GFP antibody. GFP-TRPC6 was absent in eluates derived from cells cotransfected with FLAG-CD2AP. In contrast, GFP-TRPC6 was present in eluates derived from cells cotransfected with FLAG-nephrin and FLAG-podocin, indicating that TRPC6 can associate with nephrin and podocin.

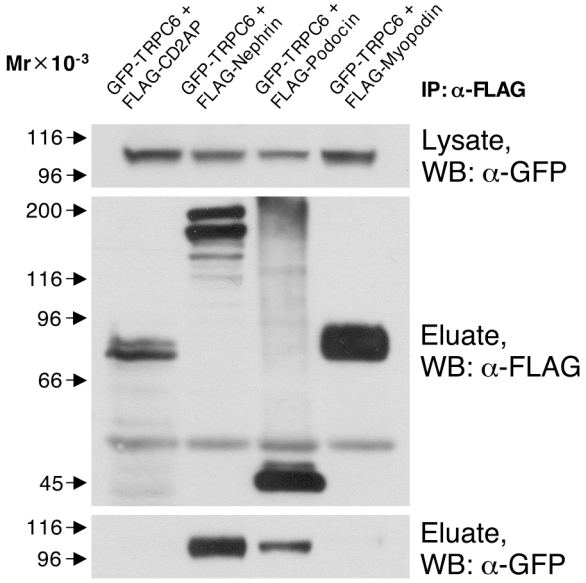

Fig. III.5. TRPC6 interacts with slit diaphragm proteins. GFP-TRPC6 associates with FLAG-tagged nephrin and podocin but not CD2AP in cotransfected HEK293 cells. GFP-TRPC6 was detected in total cell lysate bz Western blotting using an antibody to GFP (upper panel). FLAG-tagged fusion proteins were immunoprecipitated, eluted and visualized with an antibody to FLAG (middle panel). Coimmunoprecipitated GFP-TRPC6 was detected in eluate fractions (lower panel). FLAG-myopodin served as a negative control for TRPC6 binding. Apparent molecular weight is shown to the left in kDa.

Next, endogenous coimmunoprecipitation of TRPC6 with nephrin, podocin and CD2AP from cultured differentiated podocytes was carried out. Consistent with the overexpression data, TRPC6 coimmunoprecipitated with nephrin and podocin but not with CD2AP (Fig. III.6.). The association of TRPC6 with nephrin and podocin, key regulators of the the slit diaphragm points to an essential role of TRPC6 channels in the slit diaphragm protein complex.

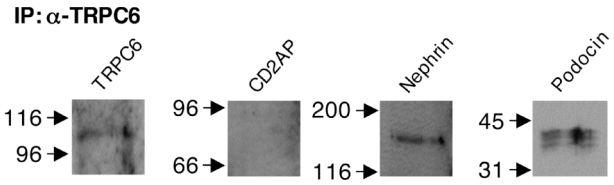

Fig, III.6. Endogenous coimmunoprecipitation of TRPC6 with slit diaphragm proteins from cultured podocytes. TRPC6 interacts with nephrin and podocin but not with CD2AP. Proteins were immunoprecipitated with antibody to TRPC6.

TRPC6 expression in glomeruli of nephrin$^{-/-}$-mice

Nephrin is a central component of the slit diaphragm and mice deficient in nephrin suffer from proteinuria and partial foot process effacement [Putaala *et al.*, 2001; Hamano *et al.*, 2002]. Given that nephrin interacts with TRPC6 in podocytes (Fig. III.6), the effect of nephrin deficiency on the localization of TRPC6 in the glomerulus was studied (Fig. III.7.). Neonatal wild-type mice displayed a barely detectable expression of glomerular TRPC6. In contrast, a strong signal in podocytes from nephrin knock-out mice pointed to an induction of podocyte TRPC6 expression. Actual levels of TRPC6 protein remain to be determined as immunofluorescence is not a quantitative technique. Immunofluorescence double labeling with the podocyte marker synaptopodin showed that TRPC6 was expressed in podocytes, resulting in a partial yellow overlap. Notably, nephrin$^{-/-}$ podocytes exhibited focal accumulation of TRPC6 protein. In summary, this suggests that lack of nephrin is correlated with altered subcellular localization of TRPC6, and possibly contributes to an induction of TRPC6 expression.

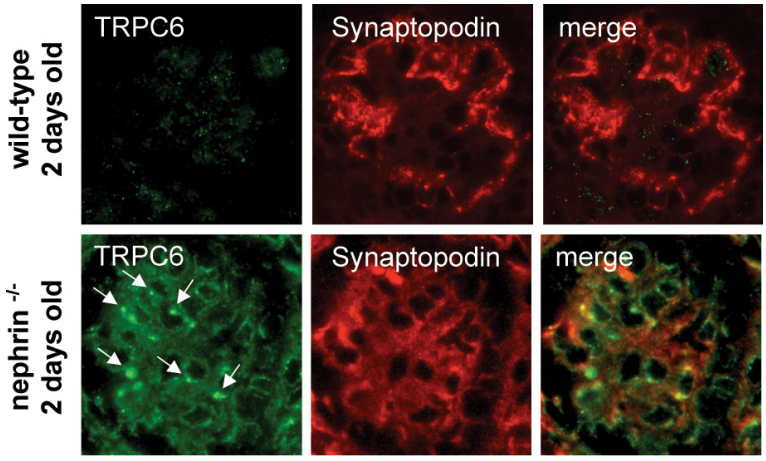

Fig. III.7. TRPC6 expression in neonatal wild-type and nephrin$^{-/-}$ mice. Weak TRPC6 expression was detected in glomeruli of 2 d old wild-type mice (upper panels). TRPC6 appeared to be induced in glomeruli of 2 d old nephrin-deficient mice (lower panels). TRPC6 formed aggregates in the glomerulus (white arrows). Double labeling of TRPC6 with the podocyte marker synaptopodin confirmed the localization of TRPC6 in kidney podocytes, resulting in a yellow overlap.

III.4. Discussion

III.4.1. Implications of the localization of TRPC6 in the glomerulus

TRPC6 is a novel podocyte protein involved in FSGS

Studies of familial nephrotic syndromes have delineated the importance of the podocyte in normal glomerular function [Kriz *et al.*, 1998]. Indeed, all previously described genes mutated in focal segmental glomerulosclerosis (FSGS) and nephrotic syndrome are highly expressed in the glomerular podocyte [Moller *et al.*, 2006]. The present data show that TRPC6 can potentially be added to the list of podocyte proteins involved in podocyte injury and FSGS development. Like other proteins shown be associated with podocytopathy, e.g. nephrin, podocin, α-actinin-4, or CD2AP, TRPC6 expression was detected in podocyte foot processes in close proximity to the slit diaphragm. TRPC6 is the first calcium-permeable channel detected at this site, suggesting that calcium signaling plays a role in regulation of the slit diaphragm.

TRPC6 expression in endothelial cells

TRPC6 expression in glomeruli was not exclusively limited to podocytes, but was also detected in glomerular endothelial cells. Given the interdependence of the constituents of the glomerular filtration barrier – the GBM is built and maintained in a combined effort by the underyling endothelial cells and overlying podocytes – this raises the possibility that TRPC6 mutation elicits its pathological effects in part through endothelial cells, and that podocytopathy may be a secondary effect of endothelial cell malfunction.

A possible pathogenic mechanism in endothelial cells may involve the vascular endothelial growth factor (VEGF), an important signaling protein involved in both vasculogenesis and angiogenesis. VEGF has recently been shown to play a critical role in maintaining the structure and function of the glomerulus [Eremina & Quaggin, 2004]. Loss of only one VEGF-A allele in podocytes leads to glomerular capillary endothelial cell dysfunction and proteinuria [Eremina *et al.*, 2003]. *In vitro*, VEGF-A and -C appear to enhance podocyte survival [Foster *et al.*, 2006; Guan *et al.*, 2006]. Notably, VEGF is also a potential activator of TRPC channels; TRPC channels have been implicated in mediating the calcium influx into endothelial cells, and changes in vascular permeability are seen in response to VEGF. TRPC6 and TRPC3 are capable of inducing calcium influx downstream of VEGFR2 when coexpressed in tissue culture [Pocock *et al.*, 2004; Cheng *et al.*, 2006]. In endothelial cells, increased

intracellular calcium leads to the activation of PKC-α and the Ca^{2+}/calmodulin-dependent myosin light chain kinase. These in turn enhance endothelial cell contraction and mediate disassembly of VE-cadherin cell–cell junctions, together allowing for increased fluid flow between cells [Tiruppathi *et al.*, 2002].

However, none of the known proteins associated with familial FSGS have thus far been shown to have a role in glomerular endothelial cells. In contrast, all appear to have important roles in podocytes. Therefore, it seems more likely that FSGS-associated TRPC6 mutations primarily affect podocytes, and that TRPC6 expression in glomerular endothelial cells plays a minor role. This is supported by the observation that TRPC6 mutations do not cause any detectable phenotype in the endothelial cells of other tissues. However, it is important to rule out this possibility by a suitable experimental approach, e.g. by cell type-specific knock-ins of one of the FSGS-assciated TRPC6 mutations in podocytes and endothelial cells, respectively.

III.4.2. Implications of the interaction of TRPC6 with podocin, nephrin

Two key questions arise from the findings that TRPC6 is expressed in podocyte foot processes near the slit diaphragm and interacts with the integral slit diaphragm proteins nephrin and podocin: first, what is the physiological role of these interactions in podocytes? Second, what is the molecular mechanism of TRPC6 malfunction leading to the development of FSGS? Addressing these questions is a challenging task given the current lack of understanding of FSGS pathogenesis and physiological TRPC6 channel function. However, a number of recent advances provide useful hints for the development of appropriate hypotheses:

TRPC6 forms a mechanosensor complex together with podocin

A recent report illustrates that podocin and the podocin homologue mec-2, which is known to function in mechanosensation in *Caenorhabditis elegans* [Huang *et al.*, 1995; O'Hagan *et al.*, 2005], regulate the activity of TRPC6 in a cholesterol-dependent manner [Huber *et al.*, 2006]. The authors of this study speculate that podocin, like mec-2 in the worm, participates in mechanosensation at the glomerular filtration barrier in a multiprotein complex containing the transmembrane proteins neph1, neph2, nephrin, the cytoplasmic adaptor protein CD2AP, and TRPC6, monitoring glomerular pressure or filtration rate. Such a concept would fit well with findings derived from the human genetics; as is the case for TRPC6, mutations in the *NPHS2* gene encoding podocin cause hereditary nephrotic syndrome in humans [Boute *et al.*, 2000]. Although TRPC6-associated disease displays a later onset of kidney failure and milder symptomps than the podocin disease, the similarity of the defects supports the notion that podocin modulates TRPC6 function.

Based on the observation that podocin colocalizes with TRPC6, one possibility is that podocin may regulate TRPC6 subcellular localization by acting to recruit TRPC6 to the slit diaphragm. The present data shows that TRPC6 was not only detected in podocyte foot processes but also in the cell body of podocytes. This is consistent with dynamic localization of TRPC6 in podocytes, which can be targeted for membrane insertion in a regulated manner. Similar regulatory mechanisms have been described for other TRPC channels. For example, TRPC3 insertion into the plasma membrane is regulated by VAMP2-dependent exocytosis [Singh *et al.*, 2004]; TRPC5 in hippocampal neurons has been shown to be translocated and rapidly inserted into the plasma membrane following stimulation of the epidermal growth factor receptor (EGFR) [Bezzerides *et al.*, 2004]. TRPC6 has been shown to be inserted into the plasma membrane upon G protein-coupled receptor activation in HEK293 cells [Cayouette *et al.*, 2004]. According to this model, in order for TRPC6 to reach the slit diaphragm in podocyte foot processes, TRPC6 protein has to be transported from the cell body to the foot processes. Podocin is a candidate to target TRPC6 to its proper place in the plasma membrane. Podocin is present as high-order oligomers in erythrocyte lipid rafts where it may serve a scaffolding function, and in podocytes it is anchored to the plasma membrane at the insertion site of the slit diaphragm [Schwarz *et al.*, 2001]. Moreover, mutations in *NPHS2* encoding podocin have been shown to disrupt nephrin targeting to lipid raft microdomains [Huber *et al.*, 2003].

Recent evidence substantiates the concept that TRPC6 and podocin may be part of a putative mechanosensor complex at the slit diaphragm. As discussed in more detail in Chapter IV, podocytes exhibit contractile responses and have been found to respond to both stretch [Endlich & Endlich, 2006] and shear stress [Friedrich *et al.*, 2006]. Thus far it remains unclear how podocytes are able to sense mechanical stimuli. The idea of a mechanosensor near the slit diaphragm seems probable given that the slit diaphragm is subject to mechanical force in a vertical direction from fluid flow across the membrane and in a lateral direction from the contact between neighboring podocytes As described previously, the work of several groups has suggested that podocin participates in mechanosensation at the glomerular filtration barrier [Huang *et al.*, 1995; O'Hagan *et al.*, 2005]. Hence, TRPC may be part of this complex through its association with podocin.

It has also been suggested that TRP channels can sense mechanical stretch directly, i.e. that the channel pore becomes permeable due to conformational changes induced by stretch of the plasma membrane [Lin & Corey, 2005; Dietrich *et al.*, 2006]. Examples thereof are TRPM3 [Grimm *et al.*, 2003], TRPM7 [Oancea *et al.*, 2006], TRPP1 and TRPP2 [Nauli & Zhou, 2004; Praetorius & Spring, 2005], as well as TRPC1 [Maroto *et al.*, 2005]. TRPC6 has been shown to respond to pressure stimuli

in patches even in the presence of phospholipase C blockers, arguing against second-messenger activation and in favor of direct activation through membrane stretch [Spassova *et al.*, 2006]. The authors of this study suggest a common molecular basis for lipid-mediated membrane stretch activation and the well-known activation of TRPC6 via diacyl-glycerol (DAG) in that in both cases the mechanism underlying channel activation is a conformational change rendering TRPC6 channels permeable.

Future studies will have to address the mechanistic relevance of the podocin-TRPC6 association by providing answers to the following questions: how does podocin modulate TRPC6 activity? Does TRPC6 act downstream of podocin as a mechanosensor? Can TRPC6 function as a mechanosensor by itself? Eventually, the elucidation of the podocin-TRPC6 interplay may help draft a model of the long-sought mechanosensory complex at the slit diaphragm.

TRPC6 is associated with nephrin-mediated signaling at the slit diaphragm

A number of studies suggest that the slit diaphragm may serve as a platform mediating the signals required for sustained podocyte structure and function. The slit diaphragm protein nephrin was shown to associate with signaling microdomains, also known as lipid rafts [Benzing, 2004]. Nephrin itself appears to be a signaling molecule generating podocyte survival signals [Huber & Benzing, 2005], and its disruption from the slit diaphragm has been reported in secondary forms of FSGS [Schmid *et al.*, 2003]. Tyrosine phosphorylation, a key event in signal transduction, has been shown to occur at the slit diaphragm site: the Src protein tyrosine kinase Fyn has been shown to bind and phosphorylate nephrin [Verma *et al.*, 2003]. Nephrin phosphorylation then induces binding of Nck adapter proteins, which in turn reorganizes the actin cytoskeleton [Verma *et al.*, 2006; Tanaka & Sabry, 1995]. Also TRPC6 has been shown to also be a target of phosphorylation by Fyn [Hisatsune, 2004], and phosphorylation by Fyn has been shown to enhance TRPC6 channel activity [Shi *et al.*, 2004]. Treatment of cultured podocytes with PAN induces structural changes leading to an increased tyrosine phosphorylation [Reiser *et al.*, 2000], and a recent study demonstrated that treatment of human podocyte cells with the plasma of nephrotic patients induced an alteration of intracellular Ca^{2+} signaling mediated by tyrosine phosphorylation [Coward *et al.*, 2005].

Given that TRPC6 interacts with nephrin in podocytes (Fig. III.6.), and nephrin deficiency has a profound effect on TRPC6 localization in glomeruli (Fig III.7.) this suggests that TRPC6 may be assembled in a complex together with nephrin and Fyn and that this complex is regulated by tyrosine phosphorylation of nephrin and/or TRPC6. TRPC6 as a component or downstream target of such a signaling platform could be involved in monitoring the integrity of the slit diaphragm in podocytes.

Appendix Chapters II and III

Reiser, J., Polu, K. R., Moller, C. C., Kenlan, P., Altintas, M. M., Wei, C., et al. (2005). TRPC6 is a glomerular slit diaphragm-associated channel required for normal renal function. *Nat Genet,* **37**(7), 739-744.

nature genetics

TRPC6 is a glomerular slit diaphragm-associated channel required for normal renal function

Jochen Reiser[1], Krishna R Polu[2], Clemens C Möller[1], Peter Kenlan[2], Mehmet M Altintas[1], Changli Wei[1], Christian Faul[3], Stephanie Herbert[2], Ivan Villegas[4], Carmen Avila-Casado[5], Mary McGee[6], Hikaru Sugimoto[7], Dennis Brown[6], Raghu Kalluri[7], Peter Mundel[3], Paula L Smith[8], David E Clapham[8] & Martin R Pollak[2]

Progressive kidney failure is a genetically and clinically heterogeneous group of disorders. Podocyte foot processes and the interposed glomerular slit diaphragm are essential components of the permeability barrier in the kidney. Mutations in genes encoding structural proteins of the podocyte lead to the development of proteinuria, resulting in progressive kidney failure and focal segmental glomerulosclerosis. Here, we show that the canonical transient receptor potential 6 (TRPC6) ion channel is expressed in podocytes and is a component of the glomerular slit diaphragm. We identified five families with autosomal dominant focal segmental glomerulosclerosis in which disease segregated with mutations in the gene *TRPC6* on chromosome 11q. Two of the TRPC6 mutants had increased current amplitudes. These data show that TRPC6 channel activity at the slit diaphragm is essential for proper regulation of podocyte structure and function.

Proteinuria is a common feature of kidney dysfunction of glomerular origin and is itself a risk factor for both renal and extrarenal disease[1]. The glomerular podocyte is a central component of the renal filtration

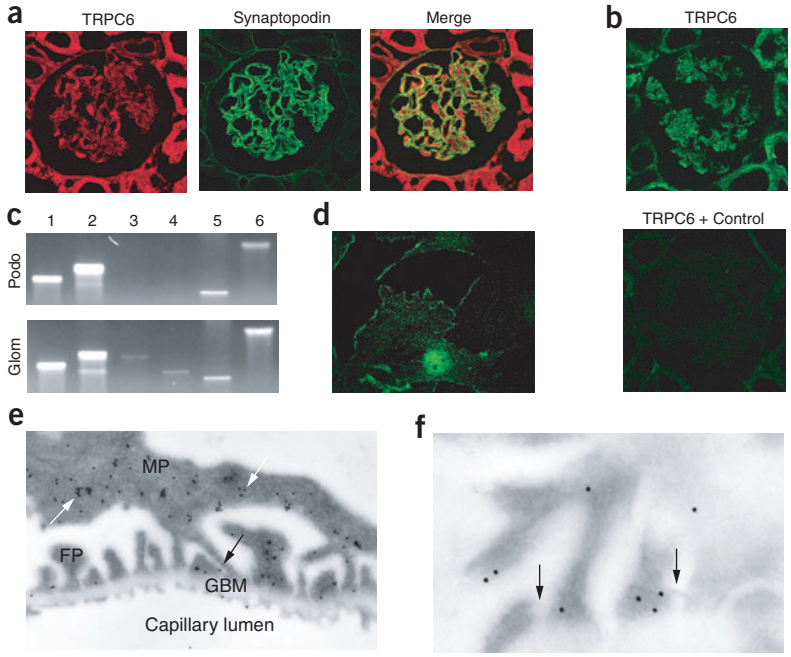

Figure 1 TRPC6 expression in the kidney glomerulus. (**a**) Confocal microscopy shows TRPC6 expression (red) in the glomerulus. TRPC6 colocalizes with the podocyte marker synaptopodin (green; overlap shown by yellow staining). (**b**) Compared with the TRPC6 antibody labeling (green), preabsorption of TRPC6 antibody with the control peptide results in negative staining. (**c**) Analysis of *TRPC1–TRPC6* mRNA expression (lanes 1–6, respectively) in cultured podocytes by RT-PCR. *TRPC6*, *TRPC1*, *TRPC2* and *TRPC5* mRNAs are detected in total podocyte RNA (Podo). *TRPC3* and *TRPC4* mRNAs are detected in total glomerular RNA (Glom) but not in total podocyte RNA. (**d**) TRPC6 localizes to the cell membrane in cultured podocytes, as shown by immunostaining (green). (**e**) Immunogold labeling shows TRPC6 localization in podocyte major processes (MP, white arrows) and foot processes (FP). TRPC6 in podocyte foot processes is located in close vicinity to the slit diaphragm (black arrows). GBM, glomerular basement membrane. (**f**) High-power view of slit diaphragm areas (arrows) shows heavy TRPC6 immunogold labeling.

[1]Renal Unit, Department of Medicine, Massachusetts General Hospital and Harvard Medical School, Boston, Massachusetts 02129, USA. [2]Renal Division, Department of Medicine, Brigham and Women's Hospital and Harvard Medical School, Boston, Massachusetts 02115 USA. [3]Department of Medicine, Mount Sinai School of Medicine, New York, New York 10029 USA. [4]Renal Unit, Instituto del Riñon-Fresenius Medical Care, Colombia. [5]Department of Pathology, Instituto Nacional de Cardiologia Ignacio Chavez, Mexico D.F. 14080, Mexico. [6]Program in Membrane Biology and Renal Unit, Massachusetts General Hospital and Harvard Medical School, Boston, Massachusetts 02129, USA. [7]Center for Matrix Biology, Department of Medicine, Beth Israel Deaconess Medical Center and Harvard Medical School, Boston, Massachusetts 02115, USA. [8]Howard Hughes Medical Institute, Children's Hospital, Department of Cardiology, Boston, Massachusetts 02115, USA. Correspondence should be addressed to J.R. (jreiser@partners.org) or M.R.P. (mpollak@rics.bwh.harvard.edu).

Published online 27 May 2005; doi:10.1038/ng1592

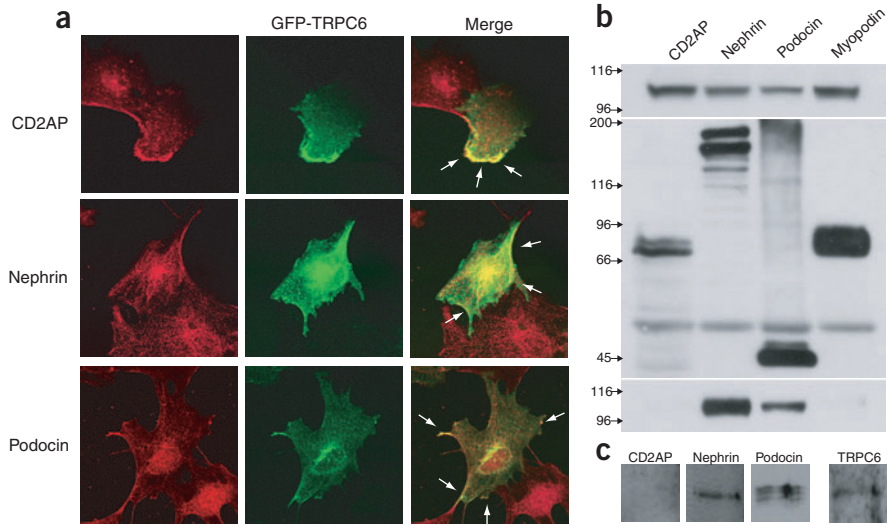

Figure 2 TRPC6 colocalizes and directly interacts with slit diaphragm proteins. (**a**) GFP-TRPC6 colocalizes with CD2AP, nephrin and podocin at the cell membrane of cultured podocytes, as shown by confocal microscopy (arrows). (**b**) GFP-TRPC6 associates with FLAG-tagged nephrin and podocin but not CD2AP in cotransfected HEK293 cells. GFP-TRPC6 was detected in total cell lysate by immunoblotting using an antibody to GFP (upper panel). FLAG-tagged fusion proteins were immunoprecipitated, eluted and visualized with an antibody to FLAG (middle panel). Coimmunoprecipitated GFP-TRPC6 was detected in eluate fractions (lower panel). FLAG-myopodin served as a negative control for TRPC6 binding. Apparent molecular weight is shown to the left in kDa. (**c**) Endogenous coimmunoprecipitation of TRPC6 with slit diaphragm proteins from cultured podocytes. TRPC6 interacts with nephrin and podocin but not with CD2AP. Proteins were immunoprecipitated with antibody to TRPC6.

barrier[2]. Podocytes (glomerular visceral epithelial cells) are located in the glomerulus. Their complex cytoarchitecture includes cellular extensions (foot processes) that connect to the glomerular basement membrane on the outer aspect of the glomerular capillaries. Together with the interposed slit diaphragm, a specialized multiprotein junction, they form a crucial component of the ultrafiltration barrier[3]. This explains why structural damage of the podocyte may lead to the development of proteinuria. Mutations in *ACTN4* (α-actinin-4), *NPHS1* (nephrin) and *NPHS2* (podocin) lead to the development of proteinuric kidney disease[4]. Winn and colleagues identified a family with autosomal dominant focal segmental glomerulosclerosis (FSGS) that segregated with a point mutation in the gene *TRPC6* on chromosome 11q (ref. 5). This prompted us to examine the renal expression and interactions of TRPC6 as well as the spectrum and function of *TRPC6* genetic variants in families with FSGS.

TRPC6 is a member of the transient receptor potential (TRP) superfamily of cation-selective ion channels. The TRPC subfamily (TRPC1–TRPC7) is a group of calcium-permeable cation channels that are important for the increase in intracellular Ca^{2+} concentration after the engagement of G protein–coupled receptors and receptor tyrosine kinases[6]. TRPCs form homo- and heterotetramers that can interact with a variety of other proteins[7]. Because all genes previously described to be mutated in FSGS and nephrotic syndrome are highly expressed in the glomerular podocyte, we examined the expression of TRPC6 in the kidney to define its localization. Confocal microscopy of adult rat kidney sections showed broad expression of TRPC6 throughout the kidney in tubules and glomeruli (**Fig. 1a**). This observation is consistent with recent reports detecting *TRPC6* mRNA in glomeruli[5,8]. Most TRPC6 expression in the glomerulus was confined to podocytes (**Fig. 1a**), as shown by immunofluorescent double labeling with the podocyte marker synaptopodin, resulting in a yellow staining pattern (**Fig. 1a**)[9]. TRPC6 was also expressed in glomerular endothelial cells. Whereas TRPC6 labeling with the antibody to TRPC6 produced strong glomerular staining and staining in tubules (**Fig. 1b**), preincubation of TRPC6 antibody with a TRPC6 control peptide resulted in a negative signal (**Fig. 1b**).

Next, we studied the expression of *TRPC1–TRPC6* mRNAs in isolated glomeruli and cultured mouse podocytes by RT-PCR (**Fig. 1c**). Whereas *TRPC1–TRPC6* were all expressed in the glomerulus, only *TRPC1*, *TRPC2*, *TRPC5* and *TRPC6* were expressed in cultured podocytes. We analyzed TRPC6 expression in a cultured mouse podocyte cell line[10] and detected labeling at the cell membrane (**Fig. 1d**). To determine the precise subcellular localization of TRPC6, we carried out immunogold labeling of ultrathin frozen sections from adult kidney cortex (**Fig. 1e**). Gold particles were found in the cell body of podocytes and in primary processes (**Fig. 1e**). In podocyte foot processes, gold particles labeled areas in close vicinity to the slit diaphragm region (**Fig. 1e**). We also detected TRPC6 expression in glomerular endothelial cells (**Fig. 1e**) and on a few mesangial cells (data not shown). In order for TRPC6 to reach the slit diaphragm in podocyte foot processes, it must be transported from the cell body through the major processes into the foot processes. Membrane proteins with high protein turnover can be found in various subcellular localizations. Similarly, podocalyxin, a major sialoprotein in podocytes, is detected intracellularly throughout the entire exocytotic pathway, consistent with a high rate of synthesis[11]. High-power

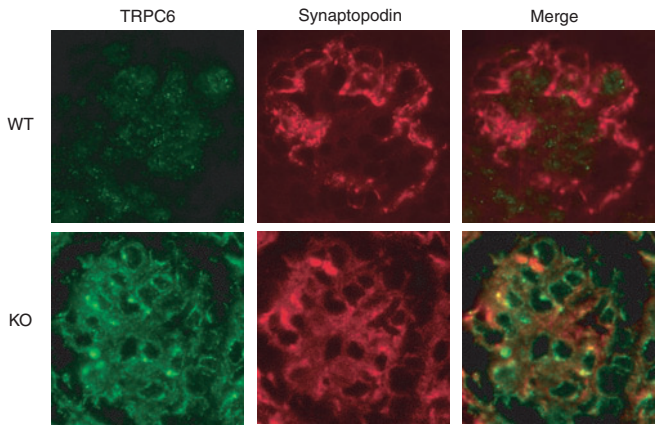

Figure 3 TRPC6 is upregulated in glomeruli of 2-d-old nephrin-deficient mice, as shown by fluorescence microscopy. Weak TRPC6 expression was detected in glomeruli of 2-d-old wild-type mice (WT; upper panels). TRPC6 was upregulated in glomeruli of 2-d-old nephrin-deficient mice (KO; lower panels). TRPC6 forms aggregates in the glomerulus. Double labeling of TRPC6 with the podocyte marker synaptopodin shows the localization of TRPC6 in kidney podocytes, resulting in yellow staining.

Table 1 Characteristics of TRPC6 mutations

Family	Ethnicity	Mutation	Exon	Age at disease presentation	Number of family members with ESRD	Change in current amplitude
FG-EA	African American	N143S	2	27–39	5 of 36	No
FG-BN	Colombian	S270T	2	17–52	3 of 12	No
FS-Z	Polish	K874X	12	27–57	9 of 53	No
FG-FQ	Mexican	R895C	13	18–46	6 of 25	Yes
FS-XR	Irish and German	E897K	13	24–35	2 of 12	Yes

Summary of families and TRPC6 variants identified, including range of ages at disease presentation (in y), number of family members known to have end-stage renal disease (ESRD) and indication of whether the variant protein produced an altered current amplitude when expressed in HEK cells. Additional clinical details are given in **Supplementary Note** online.

magnification of a section through the slit diaphragm area showed that TRPC6 was closely associated with the slit diaphragm (**Fig. 1f**).

Next, we tested whether TRPC6 colocalizes with the human disease-associated slit diaphragm proteins nephrin, podocin and CD2AP. Because available antibodies against TRPC6 and slit diaphragm proteins are all rabbit polyclonal, we transfected cultured podocytes with green fluorescent protein (GFP)-tagged TRPC6. Confocal microscopy of podocytes transfected with GFP-TRPC6 constructs and stained with antibodies against nephrin, podocin and CD2AP (**Fig. 2a**) showed that GFP-TRPC6 was expressed at the podocyte cell membrane and partially colocalized with endogenous nephrin, podocin and CD2AP[12–14]. These findings suggest that in podocytes, TRPC6 is at least in part associated with the slit diaphragm.

To test whether TRPC6 interacts with nephrin, podocin or CD2AP, we carried out coimmunoprecipitation studies (**Fig. 2b**). We coexpressed recombinant mouse GFP-TRPC6 with FLAG-tagged mouse nephrin, podocin or CD2AP in human embryonic kidney (HEK293) cells. We immunoprecipitated FLAG fusion proteins from cell lysates using anti-FLAG-M2 beads and analyzed eluates by immunoblotting using antibodies to FLAG and to GFP. To detect the interaction of

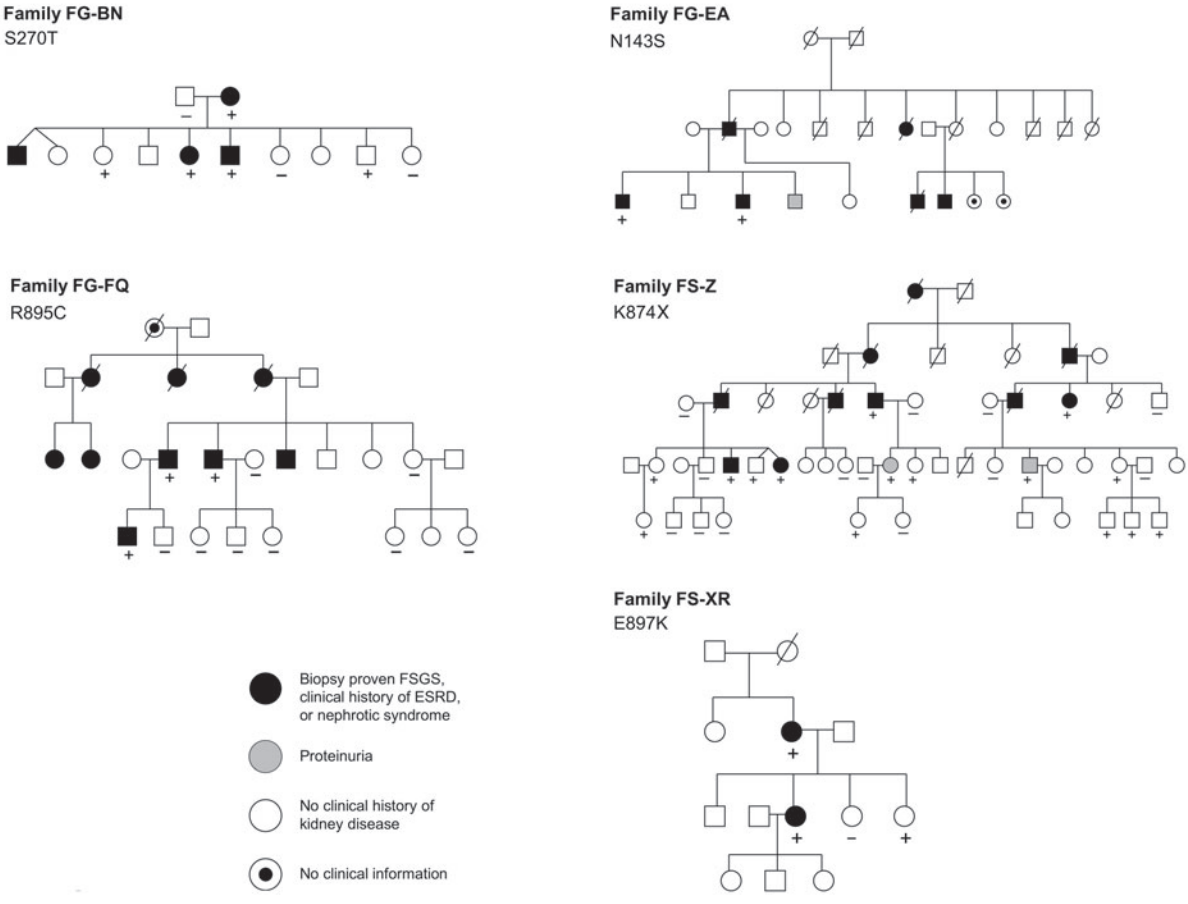

Figure 4 Pedigrees of families with inherited FSGS. *TRPC6* variants segregating in each family are indicated. Genotyped individuals are indicated as carrying (+) or not carrying (–) the variant identified in each family. ESRD, end-stage renal disease.

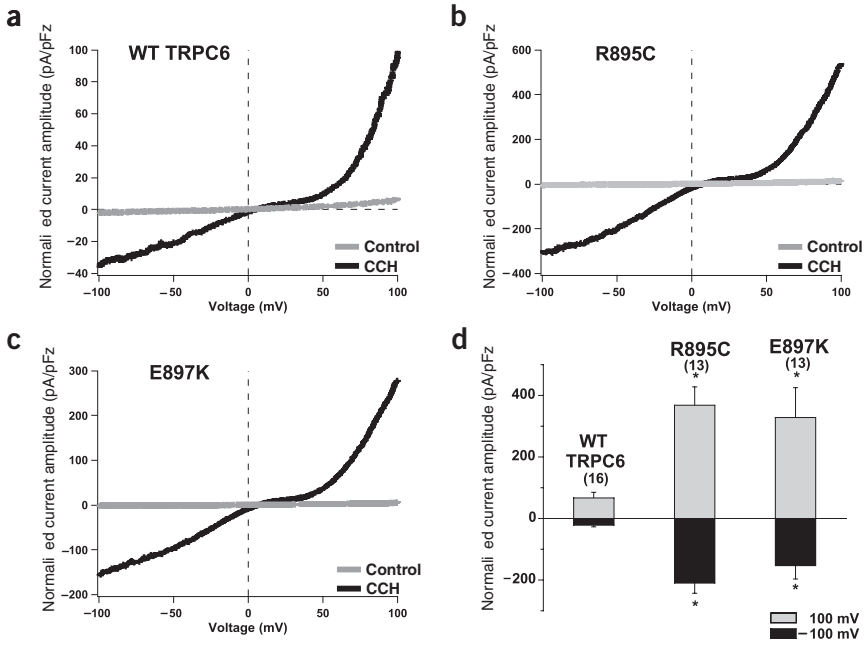

Figure 5 Electrophysiological analysis of mutant TRPC6 channels. Representative whole-cell currents measured from HEK293-M1 cells transiently transfected with cDNA encoding wild-type (WT) TRPC6 (**a**) or R895C (**b**) or E897K (**c**) mutant TRPC6. Current traces were recorded as cells were perfused with control bath solution (gray traces) or 100 μM carbachol (CCh, black traces). Voltage ramps from –100 mV to 100 mV over 150 ms were applied every 3.45 s from a holding potential of 0 mV. Current amplitude was normalized for cell capacitance. (**d**) Average normalized current amplitude measured at –100 mV (dark bars) and 100 mV (light bars) from cells expressing wild-type (WT) TRPC6 or R895C or E897K mutant TRPC6. Current amplitudes from cells expressing R895C and E897K mutant channels were significantly higher at both –100 mV and 100 mV than those from cells expressing wild-type channels ($*P < 0.01$). The number of experiments for each is shown in parentheses, and the error bars show the s.e.m. for each measurement.

GFP-TRPC6 with FLAG-tagged nephrin, podocin or CD2AP, we analyzed eluates with antibody to GFP. Immunoblotting showed that GFP-TRPC6 was absent from the eluates derived from cells cotransfected with FLAG-CD2AP (**Fig. 2b**). In contrast, GFP-TRPC6 was present in eluates derived from cells cotransfected with FLAG-nephrin and FLAG-podocin, indicating that TRPC6 had a direct biochemical interaction with nephrin and podocin but not with CD2AP. We also carried out the reverse coimmunoprecipitation, using FLAG-TRPC6 and GFP-tagged slit diaphragm fusion proteins (data not shown). These experiments yielded identical results. We also carried out endogenous coimmunoprecipitation using whole cellular extracts from cultured differentiated podocytes known to express the vital slit diaphragm components nephrin, podocin and CD2AP[15]. The immunoprecipitation with antibody to TRPC6 antibody showed that TRPC6 had an interaction with nephrin and podocin but not with CD2AP (**Fig. 2c**).

Nephrin is a central component of the slit diaphragm, and mice deficient in nephrin suffer from proteinuria and partial foot-process effacement[16,17]. We therefore examined the effect of nephrin deficiency on the localization of TRPC6 in the glomerulus (**Fig. 3**). Neonatal wild-type mice had low levels of expression of glomerular TRPC6 (**Fig. 3**). Some expression was detected in podocytes, as shown by immunofluorescence double labeling with the podocyte marker synaptopodin, resulting in a partial yellow overlap (**Fig. 3**). The targeted deletion of nephrin led to an induction of podocyte TRPC6 expression and to focal accumulation of TRPC6 (**Fig. 3**). These data suggest that the lack of nephrin induces podocyte TRPC6 expression and leads to altered cellular localization of TRPC6.

To explore the role of *TRPC6* gene variation in kidney disease, we screened probands of 71 pedigrees with familial FSGS for alterations in *TRPC6* by DNA sequence analysis. Of these 71 families, 43 showed evidence of disease in members of multiple generations, and 28 showed evidence of disease in two or more members of a single generation. Probands of 49% of the families were of western European ancestry; 5% were of African ancestry, and 27% described themselves as Hispanic. The phenotype in affected members of the largest of these families (FS-Z) cosegregated only with chromosome 11q markers (two-point lod score examining linkage of affected individuals with the disease-associated haplotype equaled 1.8 at $\theta = 0$). We identified different heterozygous sequence variants in five unrelated families with adult-onset disease, all of which predicted changes in the gene product: N143S, S270T, K874X, R895C and E897K (**Table 1**). We genotyped the relevant variants in other available family members. In all families, *TRPC6* variant and disease inheritance followed a pattern of cosegregation (with less than complete penetrance). In each family, inheritance was consistent with an autosomal dominant pattern (**Fig. 4** and **Supplementary Note** online). Each of the observed amino-acid substitutions occurred in evolutionarily highly conserved residues (**Supplementary Fig. 1** online). Two mutations predict amino-acid substitutions in the N-terminal intracellular domain of TRPC6; two predict amino-acid substitutions in the C-terminal intracellular domain; and one encodes a premature stop codon near the C terminus (**Supplementary Fig. 1** online). We genotyped 180 control individuals for the disease-associated variants but found none of them. None of these substitutions were found in the public SNP databases either.

To study whether mutations in *TRPC6* affect calcium channel function, we expressed wild-type or one of the five mutant TRPC6 channels in HEK293-M1 cells stably transfected with the Gαq-coupled M1 muscarinic receptor. We recorded TRPC6 currents before and after activation of M1 receptors by carbachol. Currents from N143S, S270T and K874X mutant TRPC6 channels did not differ noticeably from those from wild-type TRPC6 channels (data not shown). In contrast, currents from R895C and E897K mutant channels were significantly larger than those from wild-type TRPC6 channels (**Fig. 5**). Similarly, Winn and coworkers identified increased current amplitude with the disease-associated TRPC6 P112Q channel[5]. We also noted subtle differences in the rectification of the current-voltage relationship of these two mutants. We believe that these changes in rectification result from the increased current density rather than directly from structure-related changes in channel gating or permeation. If the currents through R895C and E897K mutant TRPC6 channels are similarly increased *in vivo*, these mutations could lead to a gain-of-function alteration in activity and, thus, increased calcium influx.

Three of the *TRPC6* mutations that we identified did not produce apparent changes in current amplitude. Nevertheless, we believe that

these mutations cause disease because of their nature (substitutions in very highly conserved residues or premature stop codon), their cosegregation with the disease phenotype and their absence from control individuals. This suggests that an abnormality other than increased current amplitude is the cause of disease in individuals with these mutations. The several possibilities include altered channel regulation (despite normal amplitude), altered interaction with other slit-diaphragm proteins and altered protein turnover.

Mutations in several podocyte genes have been implicated in susceptibility to progressive renal failure or increased glomerular disease[4]. The presence of *TRPC6* mutations cosegregating with kidney disease; the evolutionary conservation of the altered amino acids, slit-diaphragm localization and interactions; and the gain-of-function changes observed in two mutants suggest that TRPC6 channel function is essential for normal renal ultrafiltration. The question remains why the onset of kidney disease in individuals with *TRPC6* mutations occurs at a relatively advanced age. Like the adult onset and dominantly inherited form of FSGS caused by mutations of the widely expressed protein α-actinin-4, gain-of-function mutations of *TRPC6* might produce subtle changes in intracellular function that lead to irreversible alterations of cell behavior only after time and in the presence of other renal insults[18]. In addition, podocytes express several other TRPC channels, including *TRPC1*, *TRPC2* and *TRPC5* (**Fig. 1b**). Partial functional redundancy might also account for the late onset of glomerular disease. The ability of TRPC6 to form heterotetramers with other TRPC channels is suggestive of a complex cellular regulation of calcium homeostasis.

Podocyte electrophysiology has been under investigation for many years[19]. Published work has been focused on measurements of the membrane potential and whole-cell conductance in rodent podocytes and their response to vasoactive agonists[19]. The location of podocytes within the glomerulus, surrounding the glomerular capillaries, exposes these cells to the transmural hydrostatic pressure driving ultrafiltration. Podocyte foot processes contain a contractile apparatus that may be regulated by slit diaphragm–derived calcium signaling[20]. Mature podocytes express several types of receptors and second messenger systems[3]. These include receptors for muscarine, angiotensin, prostaglandin E2 and atrial natriuretic peptide, all of which activate intracellular Ca^{2+}, phospholipase C, inositol 1,4,5-triphosphate, cAMP and cGMP signaling cascades. Thus, podocytes may use foot process– and slit diaphragm–derived intracellular signals to respond to their cellular environment. Nephrin itself is a signaling molecule that generates podocyte survival signals[21]. Fyn kinase is associated with nephrin[22] and regulates TRPC6 channel opening by tyrosine phosphorylation[23]. The disruption of nephrin from the slit diaphragm, as has been reported in secondary forms of FSGS[24], might mediate its effects on podocytes by modulating TRPC6-originated calcium flux. Changes in TRPC6 calcium currents in podocyte foot processes seem to be central to the ability of the podocyte to regulate its intracellular and cytoskeletal behavior over its lifetime.

METHODS

Immunohistochemistry and immunoelectron microscopy. We perfused female adult Sprague-Dawley rats (body weight = 200 g) through the abdominal aorta with 2% paraformaldehyde in phosphate-buffered saline for 3 min at 220 mm Hg and then with cryoprotectant sucrose–phosphate-buffered saline solution (800 mOsmol) for 5 min at 220 mm Hg. We collected kidneys from wild-type and nephrin-deficient mice, snap-froze them in accordance with standard protocols, sectioned them in ice-cold acetone and then fixed them with 4% formaldehyde. For immunofluorescent labeling, we washed sections once with phosphate-buffered saline and incubated them with blocking solution (2% fetal calf serum, 2% bovine serum albumin and 0.2% fish gelatin) for 30 min at room temperature before further incubation with the primary antibody for 1 h at room temperature. For double labeling, we applied a second primary antibody for 1 h. We visualized antigen-antibody complexes with secondary antibodies conjugated with fluorochromes. We analyzed specimens using a confocal microscope (Zeiss). We incubated immunogold-labeled ultrathin frozen sections of perfusion-fixed mouse kidney with the rabbit antibody to TRPC6 (Chemicon) and then with gold-labeled secondary antibody to rabbit. We obtained images using a Philips CM10 electron microscope.

We used the following antibodies: mouse monoclonal antibody G1 to synaptopodin; rabbit polyclonal antisera to TRPC6 (Chemicon, Sigma, Alomone 1:50 dilution); and polyclonal antibodies against CD2AP (gift from A. Shaw, Washington University), nephrin and podocin (all at 1:200 dilution). As a negative control, we either omitted the primary antibodies or, in the case of TRPC6 staining, preincubated the primary antibody with a TRPC6 control peptide for 1 h before immunolabeling. We analyzed specimens analyzed using a confocal microscope (Zeiss). For immunofluorescent labeling of cultured podocytes, we processed cells as described before[10]. We carried out immunofluorescent labeling of nephrin-deficient kidneys as described previously[17].

Coimmunoprecipitation studies. We expressed recombinant mouse GFP-TRPC6 with FLAG-tagged mouse CD2AP, nephrin or podocin in HEK293 cells. We immunoprecipitated FLAG fusion proteins from cell lysates using anti-FLAG-M2 beads and analyzed eluates by immunoblotting using antibodies to FLAG or to GFP (Sigma).

For endogenous coimmunoprecipitation studies, we prepared whole-cell extracts from cultured differentiated podocytes and incubated them with antibody to TRPC6 overnight. We then incubated the reaction with protein G–coupled beads (Sigma) for 2 h. We visualized coimmunoprecipitated protein complexes by western blotting using antibodies against TRPC6 (1:300 dilution), CD2AP (1:2,000), nephrin (1:300) or podocin (1:1,500). As a negative control, we used protein G–coupled beads without antibody.

Cell culture and transfection. We cultured wild-type mouse podocytes as described[9,25]. The GFP-TRPC6 construct, which included the complete mouse *Trpc6* cDNA, was provided by M. Zhu (Ohio State University, Columbus, Ohio, USA). We transfected cultured podocytes using standard protocols.

RT-PCR. We isolated total RNA from cultured mouse podocytes using the Trizol reagent (Invitrogen) in accordance with the manufacturer's instructions. We synthesized cDNA using SuperScript II Reverse Transcriptase (Invitrogen) and $Oligo(dT)_{12\text{-}18}$ oligonucleotide primers in accordance with the manufacturer's instructions.

Clinical recruitment. We obtained blood from members of families with familial FSGS after informed consent was given in accordance with a protocol approved by the Institutional Review Board at Brigham and Women's Hospital. We also obtained clinical history and pedigree information for these families. We measured albumin excretion in urine using a DCA 2000 microalbumin/creatinine analyzer (Bayer). We isolated genomic DNA from peripheral blood leukocytes using Qiagen columns.

Genotyping. We analyzed DNA from probands from 71 families with familial FSGS for mutations in *TRPC6* using bidirectional sequencing. We carried out sequence analysis using PCR-amplified genomic DNA. We used high-throughput capillary sequencing instrumentation and Sanger dideoxy DNA sequencing to detect mutations. Sequence alterations in probands, family members and control subjects were verified using MALDI-TOF mass spectrometry (Sequenom)-based SNP genotyping at the Harvard-Partners Core Genotyping Facility. Primer sequences are given in **Supplementary Table 1** online.

Sequence alignment. We generated sequence alignments using the T-Coffee program comparing human TRPC6 protein sequences to sequences of other human TRPC channels (TRPC1 and TRPC3–TRPC7) and of TRPC6 proteins in fly (*Drosophila melanogaster*), rat (*Rattus norvegicus*), mouse (*Mus musculus*), guinea pig (*Cavia porcellus*) and chimpanzee (*Pan troglodytes*)[26]. We obtained protein sequence data from the National Center for Biotechnology Information database.

Site-directed mutagenesis. We used site-directed mutagenesis to insert the variants identified into a full-length human *TRPC6* cDNA clone (pcDNA3.1-TRPC6). We designed two mutagenic oligonucleotide primers containing the desired mutation and flanked by unmodified nucleotide sequence. We carried out mutagenesis with an amplification reaction using the *TRPC6* cDNA template, mutagenic primers and *Pfu* DNA polymerase. We then selected and sequenced clones to identify and verify mutants.

Electrophysiological analysis of mutant and wild-type TRPC6. We transiently transfected 35-mm dishes of HEK293-M1 cells (human embryonic kidney cells stably transfected with the M1 muscarinic receptor) with 2 μg of wild-type or mutated *TRPC6* cDNA and 0.25 μg of eGFP cDNA using Lipofectamine 2000 (Invitrogen). We then plated transfected cells on glass coverslips at low density. We took recordings from cells 24–72 h after transfection. We maintained cells at 37 °C in Dulbecco's modified Eagle medium and Ham's F-12 medium (1:1), 10% fetal bovine serum, 100 U ml^{-1} penicillin, 100 μg ml^{-1} streptomycin and 100 μg ml^{-1} G-418 in 5% CO_2.

We visualized eGFP-positive cells with a fluorescence microscope (Olympus) and recorded currents using an Axopatch 200B amplifier and pClamp8 software (Axon Instruments). During voltage ramps, we sampled currents at 10 kHz and filtered the recordings at 2 kHz. In each experiment, we held the membrane potential at either –60 mV or 0 mV (no differences were noted between these experiments). We used borosilicate glass pipettes with resistances of 2–4 MΩ for recording. The bath solution contained 135 mM NaCl, 5 mM CsCl, 2 mM $CaCl_2$, 1 mM $MgCl_2$, 10 mM HEPES buffer and 10 mM glucose (pH 7.4). The pipette solution contained 135 mM CsMES, 10 CsCl, 3 mM MgATP, 0.2 mM NaGTP, 0.2 mM EGTA, 0.13 mM $CaCl_2$ and 10 HEPES buffer (pH 7.3). Free calcium concentration in the pipette solution was ~100 nM as calculated by MaxChelator. We compared average current amplitudes at –100 mV and 100 mV using the Student's *t*-test.

Note: Supplementary information is available on the Nature Genetics website.

ACKNOWLEDGMENTS

We thank the family members for their participation in these studies and M.A. Arnaout for discussions about the manuscript. This work was supported by grants from the US National Institutes of Health (M.R.P., P.M. and R.K.) as well as the Howard Hughes Medical Institute (P.L.S. and D.E.C.). J.R. was supported by the KMD Foundation and the KUFA-ASN Research Grant.

COMPETING INTERESTS STATEMENT

The authors declare that they have no competing financial interests.

Received 12 April; accepted 23 May 2005
Published online at http://www.nature.com/naturegenetics/

1. Zandi-Nejad, K., Eddy, A.A., Glassock, R.J. & Brenner, B.M. Why is proteinuria an ominous biomarker of progressive kidney disease? *Kidney Int. Suppl.*, S76–S89 (2004).
2. Somlo, S. & Mundel, P. Getting a foothold in nephrotic syndrome. *Nat. Genet.* **24**, 333–335 (2000).
3. Pavenstadt, H., Kriz, W. & Kretzler, M. Cell biology of the glomerular podocyte. *Physiol. Rev.* **83**, 253–307 (2003).
4. Pollak, M.R. Inherited podocytopathies: FSGS and nephrotic syndrome from a genetic viewpoint. *J. Am. Soc. Nephrol.* **13**, 3016–3023 (2002).
5. Winn, M.P. *et al.* A mutation in the TRPC6 cation channel causes familial focal segmental glomerulosclerosis. *Science*, published online 5 May 2005 (doi:10.1126/science.1106215).
6. Montell, C. The TRP superfamily of cation channels. *Sci. STKE* **2005**, re3 (2005).
7. Clapham, D.E. TRP channels as cellular sensors. *Nature* **426**, 517–524 (2003).
8. Facemire, C.S., Mohler, P.J. & Arendshorst, W.J. Expression and relative abundance of short transient receptor potential channels in the rat renal microcirculation. *Am. J. Physiol. Renal Physiol.* **286**, F546–F551 (2004).
9. Mundel, P. *et al.* Synaptopodin: an actin-associated protein in telencephalic dendrites and renal podocytes. *J. Cell Biol.* **139**, 193–204 (1997).
10. Mundel, P. *et al.* Rearrangements of the cytoskeleton and cell contacts induce process formation during differentiation of conditionally immortalized mouse podocyte cell lines. *Exp. Cell Res.* **236**, 248–258 (1997).
11. Schnabel, E., Dekan, G., Miettinen, A. & Farquhar, M.G. Biogenesis of podocalyxin–the major glomerular sialoglycoprotein–in the newborn rat kidney. *Eur. J. Cell Biol.* **48**, 313–326 (1989).
12. Boute, N. *et al.* NPHS2, encoding the glomerular protein podocin, is mutated in autosomal recessive steroid-resistant nephrotic syndrome. *Nat. Genet.* **24**, 349–354 (2000).
13. Kestila, M. *et al.* Positionally cloned gene for a novel glomerular protein–nephrin–is mutated in congenital nephrotic syndrome. *Mol. Cell* **1**, 575–582 (1998).
14. Kim, J.M. *et al.* CD2-associated protein haploinsufficiency is linked to glomerular disease susceptibility. *Science* **300**, 1298–1300 (2003).
15. Reiser, J. *et al.* Induction of B7–1 in podocytes is associated with nephrotic syndrome. *J. Clin. Invest.* **113**, 1390–1397 (2004).
16. Putaala, H., Soininen, R., Kilpelainen, P., Wartiovaara, J. & Tryggvason, K. The murine nephrin gene is specifically expressed in kidney, brain and pancreas: inactivation of the gene leads to massive proteinuria and neonatal death. *Hum. Mol. Genet.* **10**, 1–8 (2001).
17. Hamano, Y. *et al.* Determinants of vascular permeability in the kidney glomerulus. *J. Biol. Chem.* **277**, 31154–31162 (2002).
18. Kaplan, J.M. *et al.* Mutations in ACTN4, encoding alpha-actinin-4, cause familial focal segmental glomerulosclerosis. *Nat. Genet.* **24**, 251–256 (2000).
19. Pavenstadt, H. & Bek, M. Podocyte electrophysiology, *in vivo* and *in vitro*. *Microsc. Res. Tech.* **57**, 224–227 (2002).
20. Drenckhahn, D. & Franke, R.P. Ultrastructural organization of contractile and cytoskeletal proteins in glomerular podocytes of chicken, rat, and man. *Lab. Invest.* **59**, 673–682 (1988).
21. Huber, T.B. *et al.* Nephrin and CD2AP associate with phosphoinositide 3-OH kinase and stimulate AKT-dependent signaling. *Mol. Cell. Biol.* **23**, 4917–4928 (2003).
22. Verma, R. *et al.* Fyn binds to and phosphorylates the kidney slit diaphragm component Nephrin. *J. Biol. Chem.* **278**, 20716–20723 (2003).
23. Hisatsune, C. *et al.* Regulation of TRPC6 channel activity by tyrosine phosphorylation. *J. Biol. Chem.* **279**, 18887–18894 (2004).
24. Bandyopadhyay, B.C. *et al.* Apical localization of a functional TRPC3/TRPC6-Ca2+-signaling complex in polarized epithelial cells. Role in apical Ca2+ influx. *J. Biol. Chem.* **280**, 12908–12916 (2005).
25. Reiser, J., Kriz, W., Kretzler, M. & Mundel, P. The glomerular slit diaphragm is a modified adherens junction. *J. Am. Soc. Nephrol.* **11**, 1–8 (2000).
26. Notredame, C., Higgins, D.G. & Heringa, J. T-Coffee: A novel method for fast and accurate multiple sequence alignment. *J. Mol. Biol.* **302**, 205–217 (2000).

IV. TRPC6 INDUCTION IN ACQUIRED FORMS OF PROTEINURIC KIDNEY DISEASE

IV.1. Rationale

TRPC6 mutations provide important novel clues towards the understanding of hereditary forms of proteinuric glomerular disease. For example, the current evidence indicates that TRPC6 mutations lead to more active ion channels, indicating that the pathological effect of TRPC6 mutations is due to hyperactivity of the channel rather that TRPC6 loss-of-function. However, from a global healthcare perspective the small number of families with TRPC6 mutations limits the enthusiasm to develop TRPC6 antagonists specifically for this type of disease. On the other hand, the presence of TRPC6 at the slit diaphragm raises another key question: Is malfunction of wild-type TRPC6 a more general cause of glomerular disease – also occuring in the far more common acquired forms? Similar to increased channel function due to genetic mutation, altered TRPC6 activity may also be observed in acquired forms of proteinuric kidney disease and represent a common pathogenic feature in this clinically heterogenous class of disorders. Based on this notion, expression levels of TRPC6 were explored in human kidney biopsies and in experimental models of acquired glomerular failure. Furthermore, the potential consequences of increased TRPC6 levels were addressed in a set of mechanistic *in vitro* and *in vivo* studies.

IV.2. Materials and Methods

IV.2.1. Human kidney biopsies

Glomerular total cDNA samples were obtained from human kidney biopsies and renal samples from a tumor-free part of a nephrectomy specimen in a multicenter study for renal gene expression analysis (the European Renal cDNA Consortium) [Cohen *et al.*, 2002]. Informed consent was obtained according to the respective local ethical committee guidelines. Kidney microdissection, RNA quality control by microfluid electrophoresis, and reverse transcription were performed in accordance with the standard protocols of the European Renal cDNA Consortium. Microdissected glomeruli from 34 patients with proteinuric diseases and 8 control subjects were analyzed. Patients were stratified according to their histologic diagnosis into focal segmental glomerulosclerosis (FSGS; n = 9), minimal change disease (MCD; n = 13), and membranous glomerulonephritis (MGN; n = 28). For control biopsies, renal tissue was derived from healthy poles of tumor nephrectomies (CON; n = 9).

IV.2.2. Quantitative real-time PCR

TRPC6 mRNA levels in human glomerular diseases

Quantitative real-time PCR on glomerular total cDNA samples obtained from human kidney biopsies was performed on a Applied Biosystems 7300 Real-Time PCR System using heat-activated Amplitaq Gold TaqDNA polymerase (Applied Biosystems, Foster City, California, United States). All real-time PCR reagents were supplied by Applied Biosystems (Foster City, California, United States). Predeveloped TaqMan assay reagent was used for TRPC6 and the internal standard 18S ribosomal RNA. The primers for human TRPC6 were cDNA-specific and did not amplify genomic DNA. PCR conditions were as follows: 2 min at 50 °C, 10 min at 95 °C, followed by 40 cycles of 15 s at 95 °C, 60 s at 60 °C. Quantification of the templates was performed using a standard curve [Giulietti *et al.*, 2001]. Quantities of TRPC6 cDNA were normalized against the amount of 18S rRNA. All measurements were performed in duplicate, and controls that consisted of ddH_2O were negative in all runs. Data were given as means ± SD. Statistical analysis was performed by using the unpaired *t* test with the significance level set to $P < 0.05$.

TRPC6 mRNA levels in puromycine aminonucleoside (PAN)-treated rats

For the assessment of glomerular TRPC6 mRNA levels in PAN-rats, rat glomeruli were isolated by standard differential sieve-technique [Shankland *et al.*, 2007] and total mRNA was isolated using Trizol reagent (Invitrogen, Carlsbad, California, United States). cDNA synthesis was performed with SuperScript II Reverse Transcriptase (Invitrogen, Carlsbad, California, United States) using Oligo(dT)12-18 oligonucleotide primers. Quantitative real-time PCR was performed essentially as described above with cDNA-specific primers for rat TRPC6 and rat GAPDH as endogenous control. Relative quantities of TRPC6 were normalized against the relative quantities of GAPDH. An untreated control sample was used as calibrator and its expression level was set to 100%. Fold-expression changes were calculated using the comparative threshold (C_T) method for relative quantitation with the equation $2^{-\Delta\Delta CT}$ [Livak & Schmittgen, 2001]. All measurements were performed in triplicate, and controls that consisted of ddH_2O were negative in all runs. Data were given as means ± standard deviation (SD). Statistical analysis was performed by using the unpaired *t* test with the significance level set to $P < 0.05$.

IV.2.3. Immunohistochemistry and Immunocytochemistry

Human glomerular biopsies were fixed in cold acetone and stained with anti-TRPC6 antibody (Abcam, Cambridge, Massachusetts, United States) and mouse G1 monoclonal antibody to synaptopodin [Mundel *et al.*, 1997] following standard protocols. Immunocytochemistry on cultured podocytes was done on cells that were grown on coverslips as described [Reiser *et al.*, 2004]. The podocyte actin cytoskeleton was visualized with the Alexa Fluor 594 phalloidin conjugate (Molecular Probes, Eugene, Oregon, United States). Renal biopsies from passive Heymann nephritis (PHN) rats were fixed in methyl Carnoy's solution and embedded in paraffin. Indirect immunoperoxidase staining [Pippin *et al.*, 2003] was performed on 4 μm sections using TRPC6 primary antibody (omitted in controls). Glomeruli were scored from 1 to 4 on the basis of the percentage of positively stained podocytes in each glomerulus (0 to 25% positive = 1; 26 to 50% positive = 2; 51 to 75% positive = 3; 76 to 100% positive = 4). Scoring values were statistically analyzed by one-way ANOVA, and Bonferroni multiple comparison test was performed. At all time points, the increase in TRPC6 expression was statistically significant. Immunogold and transmission electron microscopy were performed according to standard protocols as described previously [Reiser *et al.*, 2005].

IV.2.4. Podocyte cell culture

Conditionally immortalized mouse podocyte cell lines were cultured as previously described [Mundel *et al.*, 1997]. Podocytes were grown in 75 cm^2 plastic tissue cell culture flasks (Becton Dickinson, Franklin Lakes, New Jersey, United States) in a humidified atmosphere and 5% CO_2. Cells were maintained under permissive conditions at 33 °C in medium containing RPMI-1640, 10% fetal bovine serum, 100 U/ml penicillin-streptomycin (all from Invitrogen, Carlsbad, California, United States), and supplemented with 100 U/ml γ-interferon (Cell Sciences, Canton, Massachusetts, United States). Cells were allowed to differentiate by shift to 37 °C for growth under non-permissive conditions in medium without γ-interferon.

IV.2.5. C5b-9 treatment

To determine the expression of TRPC6 in podocytes stimulated with complement *in vitro*, conditionally immortalized mouse podocytes [Mundel *et al.*, 1997] were used. All studies were performed between days 15 and 17 of growth-restrictive conditions at 37 °C. For induction of sublytic C5b-9 attack, mouse podocytes were stimulated with sheep anti-mouse podocyte IgG and complement as described previously [Pippin *et al.*, 2003]. In group C6+, podocytes were sensitized with medium that contained 0.5 mg/ml sheep anti-mouse podocyte IgG at 37 °C for 30 min. Sensitized podocytes

were then exposed to a sublytic amount of complement for 30 min, washed three times, and incubated in growth medium for 48 h. In group C6–, which served as control, podocytes were sensitized with sheep anti-mouse podocyte IgG and exposed to complement that lacked C6 for 30 min. Whole-cell lysates were isolated in RIPA buffer, and Western blotting analysis was performed according to standard procedures using anti-TRPC6 antibody and monoclonal anti-actin antibody (Sigma, Saint Louis, Missouri, United States) as a loading control.

IV.2.6. Induction of passive Heymann nephritis (PHN)

The passive Heymann nephritis (PHN) model of membranous nephropathy was induced in male Sprague-Dawley rats (Simonsen Laboratories, Gilroy, California, United States) by intraperitoneal injection (5 ml/kg body weight) of sheep antibody to Fx1A [Perkinson *et al.*, 1985]. Rats that received an injection of normal sheep serum (5 ml/kg body weight) served as controls for the anti-Fx1A antibody. Control and PHN rats were sacrificed at 5, 11, and 28 d (n = 5 for each time point) for renal biopsies and glomerular isolation. All animal studies were approved by the Subcommittee on Research Animal Care of the Massachusetts General Hospital.

IV.2.7. Induction of puromycin aminonucleoside (PAN) nephropathy

Rats were obtained from male Sprague-Dawley rats (Simonsen Laboratories, Gilroy, California, United States). For studying TRPC6 protein expression in glomeruli, rats were given a single injection of puromycin aminonucleoside (PAN; Sigma, Saint Louis, Missouri, United States) (50 mg/kg body weight) at day 0. At days 0, 4, 8, and 28, rats were killed and kidneys were collected. For assessment of TRPC6 mRNA levels and PAN-induced albuminuria, rats were given three consecutive injections of PAN (50 mg/kg body weight) at days 0, 10, and 20. At days 27 and 34, rats were killed and kidney were collected. All animal studies were approved by the Subcommittee on Research Animal Care of the Massachusetts General Hospital.

IV.2.8. Fluo-4 calcium imaging

Cultured differentiated podocytes were treated for 24 h with 10 or 50 µg/ml puromycin aminonucleoside (PAN). Cells then were loaded with the Fluo-4 calcium indicator (Invitrogen, Carlsbad, California, United States) in 0.1 mM Ca^{2+} for 1 h. Receptor-operated channels were activated by addition of 100 µM 1-oleoyl-2-acetyl-*sn*-glycerol (OAG), followed by changing the extracellular buffer to 2 mM Ca^{2+} to distinguish membrane-associated channel-dependent changes in calcium.

IV.2.9. Cytochalasin D treatment

Cultured differentiated podocytes were treated with cytochalasin D (Sigma, Saint Louis, Missouri, United States) as described before [Reiser *et al.*, 2000]. 60 min after addition of cytochalasin D, cells were washed twice with PBS.

IV.2.10. GFP-TRPC6 overexpression *in vitro*

Cultured differentiated podocytes were transiently transfected with GFP-TRPC6 using Lipofectamine 2000 (Invitrogen, Carlsbad, California, United States). After 48h, cells were fixed with paraformaldehyde and stained with phalloidin (Invitrogen, Carlsbad, California, United States) to visualize the actin-based cytoskeleton.

IV.2.11. *In vivo* gene delivery

FLAG-TRPC6 plasmids were introduced into C57BL6 mice (Bar Harbor, Maine, United States) using the TransIT In Vivo Gene Delivery System (Mirus Bio, Madison, Wisconsin, United States) [Herweijer & Wolff, 2007]. 15 µg of plasmid DNA was mixed with 15 µl of Mirus polymer solution and 170 µl of endotoxin-free H_2O. It then was topped with 1.8 ml of Mirus delivery solution before injection through tail vein. All animal studies were approved by the Subcommittee on Research Animal Care of the Massachusetts General Hospital. For measuring luciferase activity, mice were gene-delivered with 10 µg of pGL3 luciferase reporter plasmid (Promega, Madison, Wisconsin, United States). Kidneys from 5 mice were harvested 12 h after gene delivery, and luciferase activity was assayed using the Luciferase Assay System (Promega, Madison, Wisconsin, United States). Kidneys from 7 uninjected control mice were also tested. Light intensity was measured on a SpectraMax M5 plate reader luminometer (Molecular Devices, Sunnyvale, California, United States).

IV.2.12. Assessment of proteinuria and albuminuria

For assessment of proteinuria in mice, spot urine samples were cleared by centrifugation at 3,000 rpm for 5 min at 4 °C. Total urinary protein was determined using the Bio-Rad Protein Assay (Bio-Rad, Hercules, California, United States) according to the method of Bradford [Bradford, 1976]. 2 µL of pre-cleared urine was mixed with 200 µL of 1x dye solution. After incubation at room temperature for 5 min, the absorbance at a wavelength of 585 nm was measured using a SpectraMax $M2^e$ plate reader spectrophotometer (Molecular Devices, Sunnyvale, California, United States). A standard curve was obtained by measuring serial dilutions of bovine serum albumin (Bio-Rad, Hercules, California, United States). Albuminuria in PAN-

treated rats was assessed by collection of urine from each animal for 24 h in metabolic cages (Nalgene, Rochester, New York, United States) and measurement of the albumin concentration by ELISA using the Neph-Rat Kit (Exocell, Philadelphia, Pennsylvania, United States). For verification of efficiency of anti-Fx1A injection in passive Heymann nephritis (PHN) rats, urinary protein was determined using the sulfosalicylic acid method before control and PHN rats were killed [Shankland *et al.*, 1996] (data not shown).

IV.3. Results

IV.3.1. TRPC6 induction in human acquired glomerular diseases

Elevated TRPC6 mRNA expression in human acquired glomerular diseases

TRPC6 mRNA expression was analyzed in isolated glomeruli from patients with focal segmental glomerulosclerosis (FSGS), minimal change disease (MCD), and membranous glomerulonephritis (MGN) (Fig. IV.1.). Control samples were obtained from the healthy kidney poles of individuals who underwent tumor nephrectomies. By real-time quantitative PCR, the ratio of TRPC6 mRNA to 18S ribosomal RNA was determined. Levels of TRPC6 mRNA were significantly increased in patients with MCD (n = 13; P = 0.006) and MGN (n = 28; P = 0.024) as compared with control patients (n = 9). In patients with FSGS (n = 9), the increase in TRPC6 mRNA did not reach statistical significance.

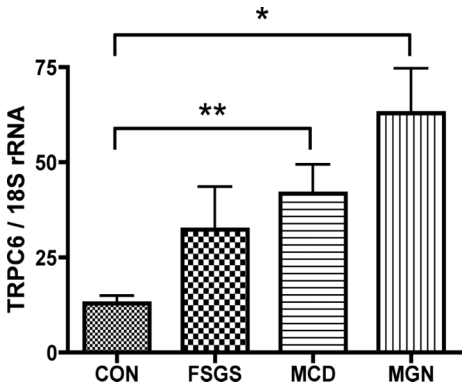

Fig. IV.1. TRPC6 mRNA expression in human acquired glomerular diseases. The ratio of human TRPC6 mRNA versus 18S ribosomal RNA (18S rRNA) was determined by quantitative real-time PCR. Compared with control kidneys (CON; n = 9), TRPC6 mRNA was statistically significantly upregulated in kidneys from patients with minimal change disease (MCD; $^{**}P$ = 0.0063; n = 13) and with membranous glomerulonephritis (MGN; $^{*}P$ = 0.0238; n = 28). In kidneys from patients with FSGS (n = 9), the increase in TRPC6 mRNA did not reach statistical significance.

TRPC6 protein expression in human acquired glomerular diseases

To determine the spatial distribution of TRPC6 protein, immunostaining of TRPC6 was performed on human kidney biopsies of normal tissue and of glomeruli from FSGS, MCD, and MGN kidneys (Fig. IV.2.). In control glomeruli, TRPC6 labeling was found throughout the glomerulus and in particular at the outer aspects of capillary loops; double labeling with synaptopodin showed that glomerular TRPC6 was localized in podocytes represented by yellow overlap (Fig. IV.2., CON). In FSGS, TRPC6 staining appeared clustered and aggregated as well as segmentally more intense (Fig. IV.2., FSGS). TRPC6 staining in MCD displayed a similar pattern as FSGS but with less intensity (Fig. IV.2., MCD). In MGN, glomerular TRPC6 expression was granular and particularly intense in podocytes (Fig. IV.2., MGN).

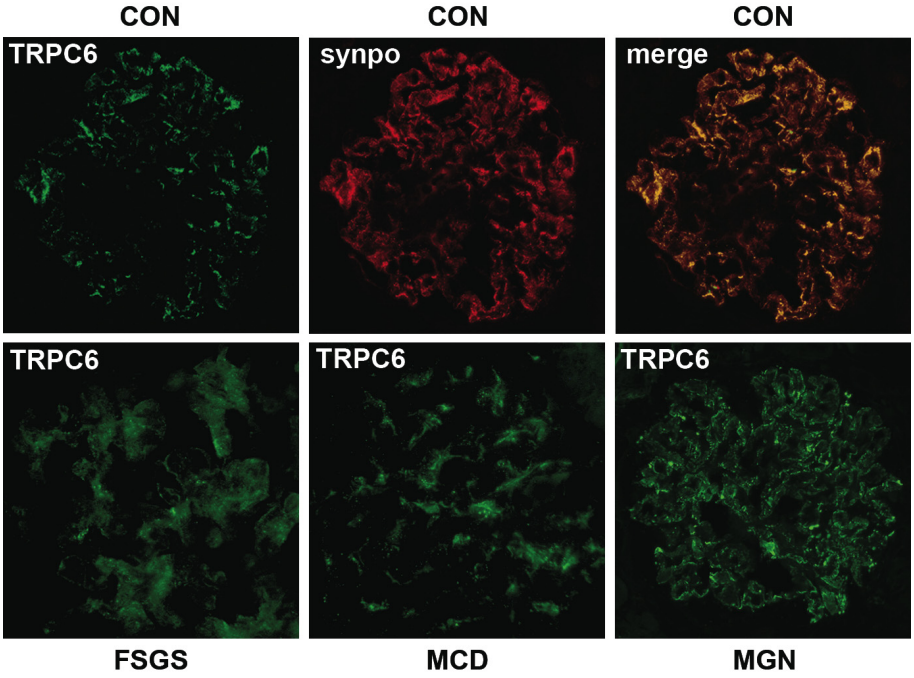

Fig. IV.2. TRPC6 protein expression in human acquired glomerular diseases. Kidneys were examined by indirect immunofluorescence using a primary antibody against TRPC6. Double labeling with the podocyte marker synaptopodin led to a yellow overlap (merge). In FSGS and MCD kidneys, TRPC6 staining was induced and appeared clustered. TRPC6 intensity was stronger in FSGS than in MCD. TRPC6 staining was strongest and appeared granulated in glomeruli during MGN.

IV.3.2. TRPC6 induction in the C5b-9 cell culture model of membranous disease

The described TRPC6 mRNA and protein studies suggested that TRPC6 expression was highest in MGN. This is of particular significance given that membranous nephropathy is the most common cause of idiopathic nephrotic syndrome in white adults, accounting for about one fifth of cases [Ronco & Debiec, 2006]. In about 40% of patients, membranous nephropathy leads to end-stage renal disease (ESRD) after

10 years [Wasserstein, 1997; Glassock, 2004]. Eighty percent of cases are classified as idiopathic, which reflects the current lack of knowledge with respect to the pathogenic mechanisms behind membranous disease. There is currently no effective treatment option available, and the appropriate treatment of membranous disease remains a subject of continuing debate [Glassock, 2004]. In membranous nephropathy, subepithelial immune deposits form in situ as a result of circulating antibodies against one or several antigens that remain yet to be identified in the human [Imai *et al.*, 1997]. Hand in hand with the formation of immune deposits goes activation of complement leading to assembly of C5b-9 membrane attack complexes on podocyte plasma membranes. This represents the main culprit for sublethal podocyte injury and the onset of proteinuria [Pippin *et al.*, 2003]. It has also been reported that the damage of podocytes mediated by complement C5b-9 complex is associated with an activation of (the TRPC6-associated) phospholipase C, and an increase in intracellular calcium [Cybulsky *et al.*, 1990].

Since immunfluorescence studies do not allow quantitative measurements of TRPC6 protein in podocytes, TRPC6 expression was examined in a well-established *in vitro* model of membranous disease. In this model, cultured differentiated mouse podocytes were exposed to anti-podocyte antibody [Ronco & Debiec, 2006] and serum with or without complement as a model to mimic the effects of the complement system in membranous glomerular disease [Cybulsky *et al.*, 2005]. Western blotting of TRPC6 in treated cells showed significantly increased TRPC6 expression in cells that were stimulated with C6+ serum when compared to cells that were stimulated by C6– serum lacking functional complement ($n = 3$, $P < 0.05$; Fig. IV.3.). The finding that TRPC6 expression is elevated in the C5b-9 model is consistent with the *in vivo* data from human biopsies and establishes a useful *in vitro* model for studying TRPC6 in membranous disease.

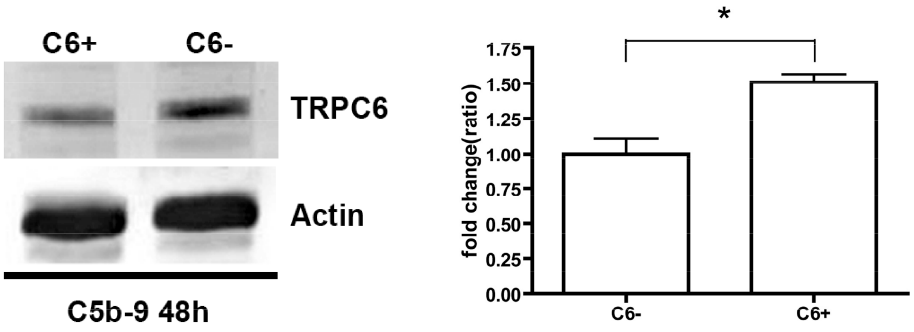

Fig. IV.3. TRPC6 levels are increased in the C5b-9 *in vitro* model of membranous disease. (Left) Cultured differentiated podocytes were stimulated with antipodocyte antibody and C6- or C6+ serum. Western blotting shows that the expression of TRPC6 increased in cells that were stimulated with C6+ serum when compared with cells that were stimulated by C6- serum. (Right) Densitometric analysis of three Western blots revealed a significant increase of TRPC6 in podocytes that were stimulated with C6+ serum compared with C6- serum ($P < 0.05$).

IV.3.3. TRPC6 induction in two animal models of acquired glomerular disease

TRPC6 induction in the passive Heymann nephritis (PHN) rat

To establish wheater glomerular injury by C5b-9 could also induce podocyte TRPC6 expression *in vivo*, the passive Heymann nephritis (PHN) model of membranous nephropathy was used [Perkinson *et al.*, 1985]. In the PHN model, rats are administered an injection of anti-Fx1A antibody, which induces the formation of subepithelial immune deposits. This in turn causes the activation of the C5b-9 membrane attack complex of complement and the subsequent development of severe proteinuria. Sprague-Dawley rats that received an injection of normal sheep serum served as controls for anti-Fx1A. Control and PHN rats were sacrificed at 5, 11, and 28 d (n = 5 for each time point) for immunohistochemical analysis of glomeruli. TRPC6 protein expression was strongly induced in glomeruli in rats with PHN (Fig. IV.4.). While induced TRPC6 staining was observed predominantly along capillary loops resembling a podocyte staining pattern, expression was also detected in glomerular endothelial cells.

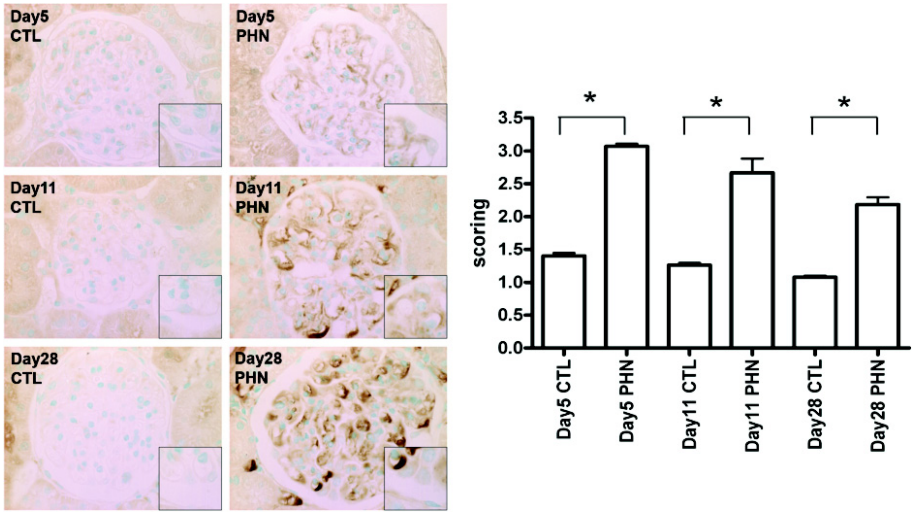

Fig. IV.4. TRPC6 levels are increased in the passive Heymann nephritis (PHN) *in vivo* model of membranous disease. (Left) Immunostaining for TRPC6 shows increased glomerular TRPC6 expression levels at days 5, 11, and 28. While TRPC6 expression predominantly followed a podocyte staining pattern, few endothelial also were positively stained. (Right) Semiquantitative scoring of glomerular TRPC6 immunostaining (score from 1 to 4) of the percentage of positively stained podocytes. Scoring values were statistically analyzed by one-way ANOVA. At all time points, the increase in TRPC6 expression was statistically significant.

TRPC6 induction in rats treated with puromycin aminonucleoside (PAN)

TRPC6 expression levels were also explored in the puromycin aminonucleoside (PAN) rat model of podocyte injury and nephrotic syndrome [Kim *et al.*, 2001]. TRPC6 levels were significantly induced in the glomeruli of PAN-injected rats

4 d after treatment at the peak of PAN-mediated injury (Fig. IV.5., a). Induced TRPC6 protein was detected mainly in podocytes as shown by double labeling with the podocyte marker synaptopodin. Eight days after PAN treatment, TRPC6 expression levels were still elevated. Twenty-eight days after PAN treatment, which is the timepoint representing recovery from PAN-mediated injury, TRPC6 expression levels had returned to baseline. By quantitative real-time PCR, an upregulation of TRPC6 mRNA in rats was detected upon PAN-mediated injury (Fig. IV.5., b). This correlated with the development of albuminuria (Fig. IV.5., c). Consistent with a role of TRPC6 in the establishement or progression of acquired glomerular kidney disease, TRPC6 induction accompanied proteinuria in the PAN rat.

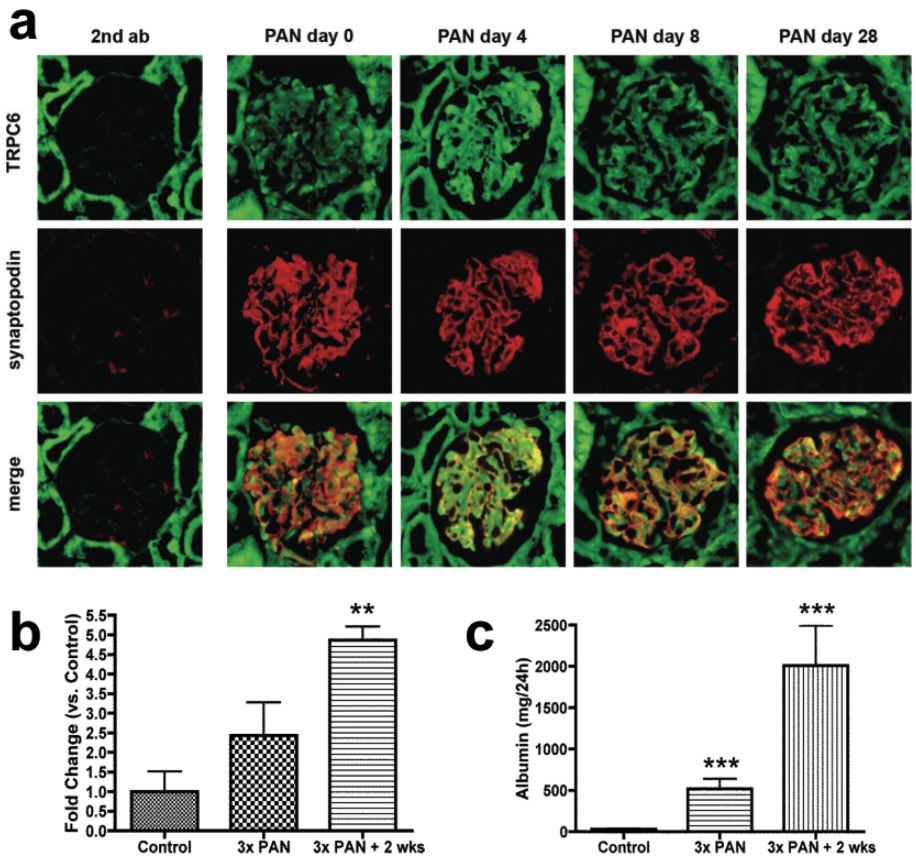

Fig. IV.5. TRPC6 levels are induced in podocytes *in vivo* after treatment of rats with puromycin aminonucleoside (PAN). (a) Frozen rat kidney sections were immunostained using antibodies that were specific for TRPC6 and the podocyte marker synaptopodin. When primary antibodies were omitted in the staining procedure (2nd ab), a background signal for TRPC6 in tubules but no signal in glomeruli and no signal for synaptopodin was detected. In the glomeruli of untreated rats (PAN day 0), TRPC6 was expressed predominantly in podocytes as shown by a partial overlap with synaptopodin. Four days after PAN treatment, in the peak phase of PAN-induced stress, TRPC6 expression was induced dramatically in podocytes. Eight days after PAN treatment, TRPC6 levels still seemed to be elevated, and 28 d after PAN treatment (= recovery) TRPC6 expression returns to baseline levels. (b) Rats were injected with 3 consecutive doses of PAN. Two weeks after the third injection, TRPC6 mRNA levels were 4.9-fold elevated in glomeruli ($P < 0.01$). (c) One week after the third injection, albuminuria was determined to be 519 mg/24 h ($P < 0.001$). Two weeks after the third injection, the average amount was determined to be 2,009 mg/24 h ($P < 0.001$).

IV.3.4. OAG-induced Ca^{2+} influx upon PAN-mediated podocyte injury

In an effort to elucidate the consequence of elevated TRPC6 expression in injured podocytes, calcium influx in cultured podocytes after PAN-treatment was studied (Fig. IV.6.). Twenty-four hours after the application of PAN on cultured podocytes, receptor-operated calcium channels were activated by addition of the diacylglycerol analog 1-oleoyl-2-acetyl-*sn*-glycerol (OAG). In PAN-treated podocytes, an elevated calcium influx was observed compared to untreated control cells, suggesting that increased calcium influx is a component of PAN-mediated podocyte injury.

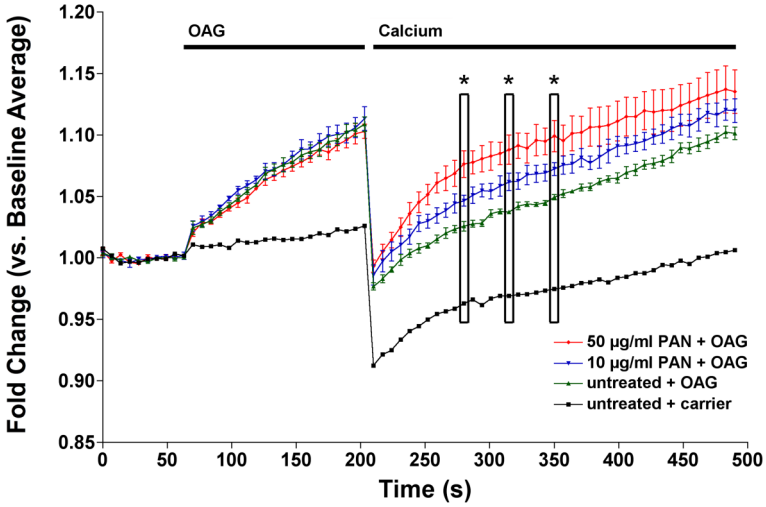

Fig. IV.6. Increased Ca^{2+} levels in cultured podocytes after treatment with puromycin aminonucleoside (PAN). Cultured differentiated podocytes were treated for 24 h with 10 or 50 µg/ml PAN. Cells then were loaded with Fluo-4 in 0.1 mM Ca^{2+} for 1 h. Receptor-operated channels were activated by addition of 100 µM OAG followed by changing the extracellular buffer to 2 mM Ca^{2+} to distinguish membrane-associated channel-dependent changes in calcium. Differences were statistically significant at the time points indicated ($P < 0.05$).

IV.3.5. Rapid-onset proteinuria after TRPC6 overexpression *in vivo*

The data from the human biopsies and the experimental models suggested a link between TRPC6 expression level and glomerular injury. To determine if TRPC6 overexpression is sufficient to cause disease, an *in vivo* hydrodynamic gene delivery approach was used to induce transient overexpression of TRPC6 in mice. Urinary protein excretion was measured as a marker for glomerular injury.

In recent years hydrodynamic gene delivery via injection into the tail vein has been established as a novel method for transient gene transfer into small rodents such as mice and rats [Herweijer & Wolff, 2007]. Hydrodynamic delivery of plasmid DNA expression vectors allows for a broad range of *in vivo* experiments, including the testing of regulatory elements, antibody generation, evaluation of gene therapy approaches, basic biology, and disease model creation [Hodges & Scheule, 2003].

The current understanding of the mechanism of hydrodynamic gene delivery is that upon rapid injection of a solution into the tail vein, fluids enter the vena cava where the fluids back up, as the large volume cannot be pumped rapidly enough through the heart. This creates increased pressure in the vena cava and pushes the plasmid DNA solution into draining vasculature, in particular the large hepatic vein. There, the fluid is forced out of the capillaries into the tissue and the nucleic acids (or other compounds present in the solution) enter into the parenchymal cells. Although nucleic acid uptake and expression has been measured in all major organs, the majority (> 90%) is found in the liver. Two anatomic features account for this; first, the liver has larger access vessels to the vena cava than other organs, absorbing the bulk of the injected plasmid DNA solution; second, liver vessels contain a higher number of large pores allowing for easier fluid/plasmid DNA extravasation.

It is conceivable that podocytes are particularly susceptible target cells for gene delivery by tail vein injection because of their exposed location in close contact to the glomerular blood vessels. For example, it was previosuly shown that gene delivery of a plasmid DNA encoding the calcium-dependend serine protease Furin lead to strong expression of Furin in podocytes [Mayer *et al.*, 2003].

To study the phenotype of mice after overexpression of wild-type TRPC6 in podocytes, wild-type FLAG-tagged TRPC6 was transiently overexpressed in mouse kidneys using a gene delivery approach. FLAG-TRPC6 was often detected in podocyte foot processes in close proximity to the slit diaphragm 12 h after injection (Fig. IV.7., a). When mice were administered an injection of the pGL3 luciferase reporter vector, luciferase activity was detected in whole-kidney homogenates 12 h after injection (Fig. IV.7., b). Mice that were administered an injection of FLAG-TRPC6 displayed transient proteinuria 15 h after injection (Fig. IV.7., c). These data demonstrate that transient TRPC6 overexpression in mice was sufficient to cause proteinuria.

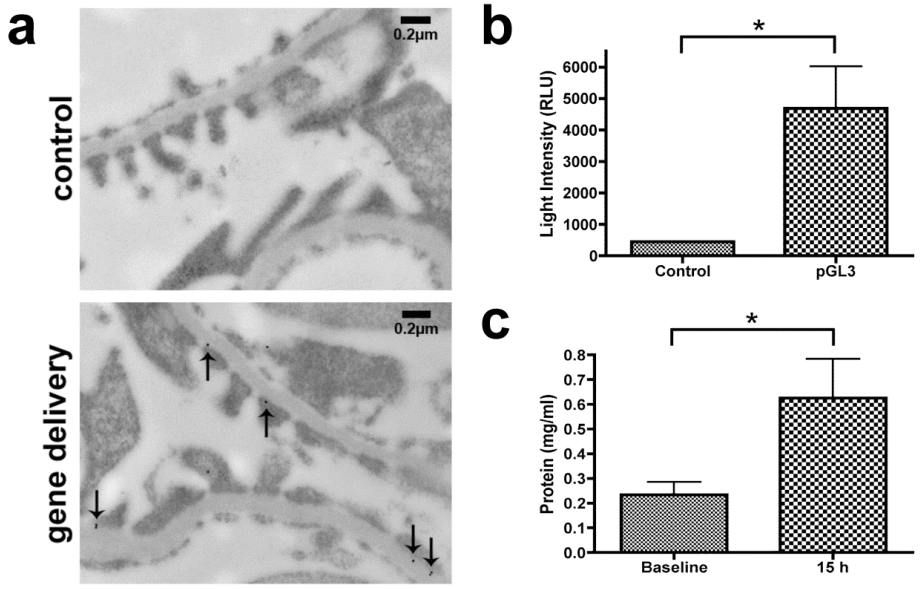

Fig. IV.7. TRPC6 *in vivo* gene delivery leads to transient overexpression of exogenous TRPC6 in podocytes and is associated with the development of proteinuria. (a) A construct coding for a FLAG-TRPC6 fusion protein was gene-delivered into mice via tail vein injection. Twelve hours after gene transfer, mouse kidneys were processed for immunogold analysis with anti-FLAG antibody. Immunogold labeling of FLAG-TRPC6 was detected in podocyte foot processes in close vicinity of the slit diaphragm. (b) Gene delivery of the pGL3 luciferase reporter vector led to the detection of luciferase activity in kidneys 12 h after gene transfer ($P = 0.0158$). (c) FLAG-TRPC6 was gene-delivered into mice and proteinuria was assessed by Bradford assay. Before gene delivery, baseline urine protein excretion averaged to 0.23 mg/ml. Fifteen hours after gene delivery, mice developed proteinuria with an average urine protein excretion of 0.63 mg/ml ($P = 0.0275$).

IV.3.6. Effects of TRPC6 overexpression on the podocyte actin cytoskeleton

Podocytes possess a highly dynamic cytoskeletal architecture involving microtubules, intermediate filaments, and actin microfilaments [Ichimura *et al.*, 2007]. This architecture provides the mechanical stability for podocytes to resist the high intraluminal hydrostatic pressure driving ultrafiltration. Perturbation of the cytoskeletal architecture plays a major role during podocyte injury and foot process effacement [Pavenstadt *et al.*, 2003]. Therefore, it was hypothesized that TRPC6 may exert its biological effects in podocytes through a similar mechanism. This would be in line with reports suggesting a functional interplay between TRP channels and the actin cytoskeleton. [Arikawa *et al.*, 1990; Smith *et al.*, 1991; Monk *et al.*, 1996; Montell, 1997; Wyszynski *et al.*, 1997].

Effect of cytochalasin D on TRPC6 localization in podocytes

It was tested whether disruption of the actin cytoskeleton in cultured podocytes with cytochalasin D affects the localization of TRPC6. Cytochalasin D disrupts actin filaments and inhibits actin polymerization [Schliwa, 1982]. After depolymerization of F-actin in cultured podocytes using cytochalasin D [Reiser *et al.*, 2000], TRPC6

appeared to be internalized and was closely associated with depolymerized clusters of actin (Fig. IV.8.). Upon removal of cytochalasin D, TRPC6 relocalized to the plasma membranel, indicating that TRPC6 subcellular distribution could be governed by the cytoskeleton.

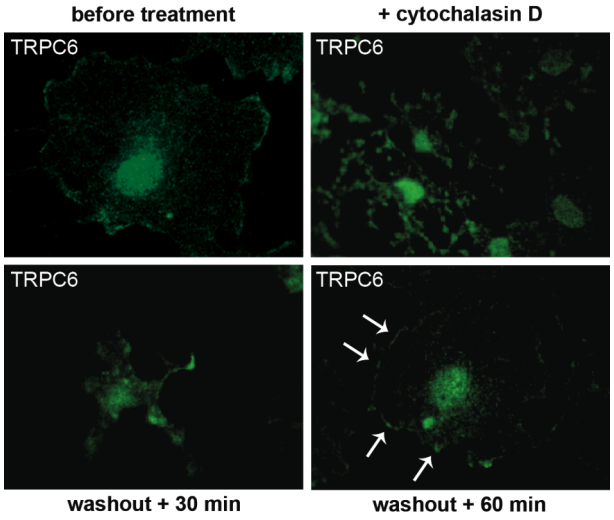

Fig. IV.8. Effect of cytochalasin D treatment on TRPC6 subcellular localization. Six hours after cytochalasin D incubation, TRPC6 localized with depolymerized actin clusters within the cell body (top right). Thirty minutes after washout of cytochalasin (partial recovery), TRPC6 started to redistribute within the cell (bottom left). Sixty minutes after washout (full recovery), most of TRPC6 was relocalized at the cell membrane (bottom right, arrows).

TRPC6 overexpression in vitro leads to disruption of the podocyte actin cytoskeleton

To study whether TRPC6 overexpression affects the actin cytoskeleton directly, we transiently overexpressed green fluorescence protein (GFP)-tagged TRPC6 [Reiser *et al.*, 2005] in cultured podocytes. Cells that expressed GFP-TRPC6 displayed a marked loss of actin stress fibers (Fig. IV.9.) when compared to untransfected control cells. Transfection of empty GFP vector had no effect on the podocyte actin cytoskeleton, nor did transfection of GFP-tagged TRPC5. These studies suggest that induction of TRPC6 channel could result in pathology by affecing cytoskeletal organization.

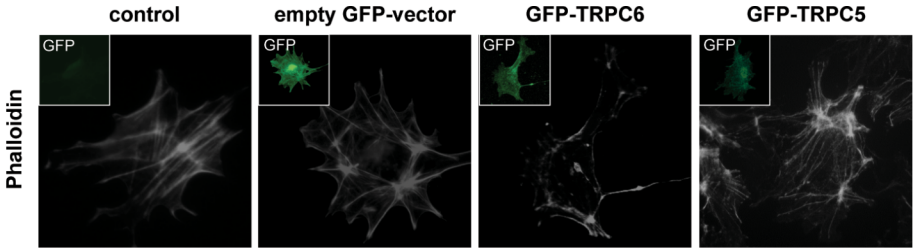

Fig. IV.9. TRPC6 overexpression leads to the loss of stress fibers in podocytes. Cultured podocytes were transfected with a green fluorescence protein (GFP)-TRPC6 fusion protein (green) and stained with phalloidin to visualize actin stress fibers. Cells were analyzed by confocal microscopy. Cells that were transfected with GFP-TRPC6 show a significant loss of stress fibers and exhibit a more cortical actin cytoskeleton than untransfected control cells, or cells that were transfected with empty GFP vector.

IV.4. Discussion

IV.4.1. Dual role for TRPC6 in genetic and acquired forms of proteinuric kidney disease

The presented studies show that TRPC6 was induced in a subset of acquired human proteinuric kidney diseases. This was also the case in experimental *in vitro* and *in vivo* models of acquired glomerular disease. These results are consistent with hyperactivity of mutated TRPC6 channels in genetic FSGS. Taken together, these data indicate that TRPC6 plays a pivotal role in both, genetic and non-genetic forms of glomerular disease. TRPC6 is therefore the first known example of a protein involved in both, genetic and acquired forms of glomerular kidney disease. Whereas in TRPC6-related FSGS TRPC6 hyperactivity or misregulation is due to genetic mutation leading to podocyte damage, in acquired forms of proteinuric diseases perturbed podocyte function appears to be a consequence of wild-type TRPC6 protein induction, due to increased TRPC6 transcription or altered protein turn-over. Based on the data presented, a putative mechanism for TRPC6 regulation of podocytes could include modulation of calcium signaling and/or modification of the actin cytoskeleton. To test this hypothesis, TRPC6 loss-of-function studies in podocytes are the next step. These could involve TRPC6 knock-down in podocytes, or the use of a published dominant-negative variant of TRPC6 [Hofmann *et al.*, 2002].

Of particular significance is the induction of TRPC6 in membranous disease. The presented data show that TRPC6 mRNA levels were significantly elevated in glomeruli from patients with membranous glomerulonephritis (MGN). The assessment of TRPC6 localization in glomeruli from patients with MGN by immunostaining revealed strong expression of TRPC6 in podocytes and the formation of aggregates. Furthermore, induction of TRPC6 was also observed in the passive Heymann nephritis (PHN) *in vivo* model and the C5b-9 *in vitro* model of membranous disease. These findings open a whole new series of possible

investigations. For example, it will be important to study the mechanism of TRPC6 regulation by complement, and to investige the downstream effects of elevated TRPC6 activity in membranous disease. Notably, among the cellular mechanisms leading to proteinuria in membranous nephropathy are cytoskeletal changes similar to what is observed upon TRPC6 overexpression [Topham *et al.*, 1999].

IV.4.2. Possible role of TRPC6 in podocytes

TRPC6 as a regulator of the podocyte contractile apparatus

Disruption of the actin cytoskeleton in cultured podocytes led to the delocalization of TRPC6 from the plasma membrane and the association of TRPC6 with clusters of depolymerized actin. This suggests that TRPC6 channels are associated with the podocyte actin cytoskeleton (Fig. IV.8.)**.** In addition, overexpression of a GFP-TRPC6 fusion protein in cultured podocytes lead to a marked reduction of stress fibers and the development of a more cortical actin cytoskeleton (Fig. IV.9.), further supporting that there may be a functional link between TRPC6 and the podocyte actin cytoskeleton. Together this data point to a regulatory role for TRPC6 with regard to the actin cytoskeleton in podocytes.

It has long been hypothesized that podocyte foot processes contain an actin-based contractile cytoskeletal network since they contain several proteins of the contractile apparatus normally found in muscle [Drenckhahn & Franke, 1988]. Experimental evidence that podocytes respond to mechanical stimuli by reorganization of their actin cytoskeleton comes from the work of several groups. Interestingly, Endlich *et al.* reported that mechanical stress induced a reversible reorganization of the podocyte actin cytoskeleton in a Ca^{2+}- and Rho kinase-dependend manner [Endlich *et al.*, 2001]. These data provided a link between Ca^{2+}-signaling and the actin cytoskeleton in podocytes. In 2004, it was discovered that human podocytes possess a stretch-sensitive, calcium-activated K^+ channel, which in vascular smooth muscle cells functions to moderate the degree of membrane depolarization [Kirber *et al.*, 1992]. Electrophysiological studies of this channel revealed that its activity was increased when suction was applied to the patch pipette, indicating that the channel was stretch-sensitive. Recently it was also shown that the podocyte actin cytoskeleton is reorganized in response to fluid shear stress *in vitro* [Friedrich *et al.*, 2006]. Finally, mature podocytes express several types of receptors for substances know to be involved in the contraction and relaxation of smooth muscle cells [Rebibou *et al.*, 1992; Mundel *et al.*, 1995; Pavenstadt, 2000].

The podocyte contractile apparatus has been proposed to render the podocyte capable of reacting to changes in glomerular capillary tone and to adjust for the size of the filtration surface area [Kriz *et al.*, 1994]. Podocyte hypertrophy has been suggested as a major consequence of podocyte (mal)adaption to mechanical strain [Shirato *et al.*, 1996]. According to this model, podocyte foot process effacement represents an adaptive change in cell shape resulting in increased surface area coverage by podocytes [Kriz *et al.*, 1994; Kretzler *et al.*, 1994, Petermann *et al.*, 2005].

The contractile cyoskeletal network could also equip podocytes to regulate the strength of the capillary wall [Kriz *et al.*, 1995]. Such a system could underlie several possible regulatory functions. First, varying restoring forces at a given transmural pressure difference might result in changes of the filtration surface area. Second, if the hydraulic permeability of the GBM were a function of its elastic distension and/or compression, then an adjustable system influencing local distension of a large part of the GBM would serve to stabilize the hydraulic permeability in the face of changes in the wall stress of the glomerulus.

Hints about the functional role of TRPC6 in podocytes may also be derived from smooth muscle cells, which share a number of structural and functional properties with podocytes, and for which important roles for TRPC6 have been described [Dietrich *et al.*, 2006]. In smooth muscle cells, ion channels initiate and regulate contraction and tone; apart from voltage-gated calcium channels, non-selective cation channels have also been identified as important players in the regulation of vascular tone by mediating the entry of cations like calcium, sodium, and magnesium. Several studies point to a pivotal role of TRPC6 in vascular and pulmonary smooth muscle cells. TRPC6 appears to play a similar function as the α1-adrenoceptor-activated non-selective cation channel in vascular smooth muscle cells [Inoue *et al.*, 2001], and the vasopressin-, 5-HT-, PDGF-activated cation channel in the aortic smooth muscle cell line A7r5 [Jung *et al.*, 2002]. In addition, TRPC6 appears to play a critical role in the intravascular pressure-induced depolarization and constriction of small arteries and arterioles [Welsh *et al.*, 2002] known as the Bayliss effect. Studies in TRPC6 knock-out mice reveal a crucial role for TRPC6 in the control of airway and vascular smooth muscle contractility [Dietrich *et al.*, 2005; Weissmann *et al.*, 2006].

TRPC6 as a modulator of the podocyte transcriptional machinery

Calcium responses can be subdivided into short-term, rapid responses that do not involve transcriptional changes, and long-term modifications that require changes in gene transcription [Berridge *et al.*, 1998]. One or both of these mechanisms may occur downstream of TRPC6 activation.

It has been shown that sustained increased intracellular calcium can directly affect gene transcription. For example, the genes encoding AP-1 transcription factor components are calcium-sensitive, and elevation of calcium upregulates their transcription [Fantozzi *et al.*, 2003]. AP-1 transcription factors modulate many cellular processes including proliferation, migration and apoptosis, and play an important regulatory role in podocytes. For example, nephrin signaling has been shown to activate AP-1 transcription factors [Huber *et al.*, 2001], and increased AP-1 binding activity to DNA has been suggested to underlie the induction of endothelin-1 protein in podocytes in response to protein overload [Morigi *et al.*, 2005].

It was recently reported that TRPC6 is a key component of a Ca^{2+}-dependent regulatory loop that drives pathologic cardiac remodeling via the calcineurin-NFAT pathway [Kuwahara *et al.*, 2006]. Nuclear factor of activated T-cells (NFAT) transcription complexes are translocated into the nucleus upon dephosphorylation by the phosphatase calcineurin, which is itself activated by calcium signaling pathways. The authors demonstrated that calcineurin activation lead to TRPC6 upregulation. This is thought to result through direct regulation of the TRPC6 promoter by NFAT. Whereas it remains unclear what the implications of a putative NFAT-signaling pathway involving TRPC6 could be, an abstract presented at the ASN Renal Week 2005 [Franz *et al.*, 2005] suggests that calcineurin signaling may also be of importance in podocytes: cultured differentiated podocytes express calcineurin, and that treatment of podocytes with the calcineurin inhibitor cyclosporine A increased the expression of the cytoskeletal regulator synaptopodin [Asanuma *et al.*, 2006].

Podocyte loss - the ultimate consequence of TRPC6 malfunction?

Alterations in the intracellular calcium concentration may ultimately cause the irreversible damage and loss of podocytes (podocytopenia). Differentiated podocytes cannot proliferate and there is no known molecular mechanism of podocyte regeneration. Consequently, there appears to be no compensatory mechanism for podocyte loss. Podocyte depletion inevitably results in decreasing kidney function. This is believed to be one of the underlying causes for both disease and age-related deterioration of the kidneys [Pagtalunan *et al.*, 1997; Kim *et al.*, 2001; Mundel & Shankland, 2002]. Podocyte apoptosis and detachment from the GBM have been proposed as putative mechanisms leading to podocyte loss.

Firstly, a sustained increase in intracellular calcium has the potential to cause podocyte apoptosis due to calcium overload [Shankland, 2006]. This may be caused by an ability of TRPC6 to augment the deleterious effects of angiotensin II, an activator of G protein-coupled receptors upstream of TRPC6 [Pavenstadt *et al.*, 2003]. Angiotensin II induces apoptosis in cultured rat podocytes and perhaps TRPC6 enhances this pathway of programmed cell death [Ding *et al.*, 2002].

Detachment is another mechanism of podocyte loss. Hara and colleagues have shown that cells obtained from the urine of patients with various glomerular diseases stained positive for the podocyte marker podocalyxin, indicating that podocytes detached from the GBM [Hara *et al.*, 2001]. Similar results have been shown in a PAN model of podocyte injury in rats [Kim *et al.*, 2001]. While the mechanisms of podocyte detachment remain unknown, they are likely to involve the abnormal function of integrins [Regele *et al.*, 2000]. Since calcium is a known regulator of integrin function, an increase of intracellular calcium mediated by TRPC6 channels may interfere with the podocyte ability to adhere to the GBM. This could eventually lead to the detachment of podocytes from the GBM.

IV.4.3. Potential of gene delivery to study TRPC6 function and as a therapeutic intervention

The ectopic expression of TRPC6 in mice resulted in transient proteinuria, suggesting that TRPC6 can drive the manifestation of proteinuric kidney disease. Similar to endogenous TRPC6, gene-delivered TRPC6 was expressed in close proximity to the slit diaphragm, indicating that the exogenous protein was properly targeted. Whereas this observation illustrates the potential of the gene delivery approach to study TRPC6 function *in vivo*, the important question of tissue- or cell-specificity must be addressed since hydrodynamic tail vein delivery mainly results in expression in the liver and only lower levels of expression (100- to 1000-fold) are found in the spleen, heart, kidneys and lungs.

It has been shown that by delivering the plasmid DNA solution directly into vessels supplying an organ, it is possible to direct a majority of the expression to that organ. For example, Maruyama *et al.* demonstrated that delivery into the renal vein resulted in high reporter gene expression levels in the kidneys [Maruyama *et al.*, 2004; Kameda *et al.*, 2004]. While such approaches allow for the testing of expression constructs in particular organs, the surgical nature of these delivery approaches prevents routine use. Another approach to achieve tissue- or cell type-specific expression of the delivered plasmid DNA is the use of target-specific promoters. For podocyte-specific gene delivery this option became available with cloning of the p2.5P podocin-promoter [Moeller *et al.*, 2002]. Since podocin expression is almost

exclusively limited to podocytes, p2.5P enables podocyte-specific targeting [Gawlik & Quaggin, 2005]. Given that in the present work, gene delivery was carried out with plasmids encoding for TRPC6 under the control of the constitutive cytomegalovirus (CMV) promoter, which lead to overexpression of TRPC6 in podocytes but also in other cell types in the glomerulus and other organs, it will be important to validate the obtained findings by delivering TRPC6 in a podocyte-specific fashion under the control of the p2.5P podocin-promoter.

The results of the gene delivery experiments illustrate the potential of the gene delivery technique to investigate TRPC6 function in podocytes. In contrast to genetic mouse models, whose generation is costly and time-consuming, hydrodynamic gene delivery can easily be carried out in high throughput. In addition, an advantage of this approach is the flexibility to overcome strain-specific and gene-dosage effects. The feasibility of gene-transfer allows to test protein overexpression in different rodent strains with the ability to gauge the level of protein expression by varying different concentrations of gene-transferred plasmid. It will be interesting to see the effects of gene delivery of the FSGS-associated variants of TRPC6, or simultaneous gene delivery of TRPC6 with other channel subunits in a podocyte-specific manner.

Another popular application of hydrodynamic gene delivery is the evaluation of gene therapy approaches. Gene delivery has been used to test gene therapy approaches for genetic and acquired diseases including treatments for diabetic nephropathy [Dai *et al.*, 2004] and crescentic glomerulonephritis [Higuchi *et al.*, 2003]. Recent work on the GTPase dynamin illustrates the potential of hydrodynamic tail vein delivery as a therapeutic intervention [Sever *et al.*, 2007] (appendix): During proteinuric kidney disease, induction of a cytoplasmic form of the lysosomal protease cathepsin L leads to cleavage of dynamin at an evolutionary conserved site, resulting in reorganization of the podocyte actin cytoskeleton and proteinuria. Dynamin mutants that lack the cathepsin L site, or render the cathepsin L site inaccessible through dynamin self-assembly, are resistant to cathepsin L cleavage. When gene-delivered into mice, these mutants restored podocyte function and resolve proteinuria. With respect to TRPC6, a possible therapeutic approach lies in blocking the hyperactive channel. In light of the absence of small molecule inhibitors specifically targeting TRPC6, a gene delivery approach involving a dominant-negative TRPC6 pore mutant [Hofmann *et al.*, 2002] could be an interesting alternative to block TRPC6 channel activity *in vivo*.

Appendices Chapter IV

Moller, C. C., Wei, C., Altintas, M. M., Li, J., Greka, A., Ohse, T., et al. (2007). Induction of TRPC6 channel in acquired forms of proteinuric kidney disease. *J Am Soc Nephrol,* **18**(1), 29-36.

Sever, S., Altintas, M. M.*, Nankoe, S. R.*, Moller, C. C.*, Ko, D., Wei, C., et al. (2007). Proteolytic processing of dynamin by cytoplasmic cathepsin L is a mechanism for proteinuric kidney disease. *J Clin Invest,* **117**(8), 2095-2104.
* equally contributing

Induction of TRPC6 Channel in Acquired Forms of Proteinuric Kidney Disease

Clemens C. Möller,* Changli Wei,* Mehmet M. Altintas,* Jing Li,* Anna Greka,* Takamoto Ohse,† Jeffrey W. Pippin,† Maria P. Rastaldi,‡ Stefan Wawersik,§ Susan Schiavi,§ Anna Henger,‖ Matthias Kretzler,‖ Stuart J. Shankland,† and Jochen Reiser*

**Department of Medicine, Nephrology Division, Massachusetts General Hospital and Harvard Medical School, Boston, Massachusetts; †Division of Nephrology, University of Washington, Seattle, Washington; ‡Renal Immunopathology Laboratory, Associazione Nuova Nefrologia and Fondazione D'Amico per la Ricerca sulle Malattie Renali, c/o San Carlo Borromeo Hospital, Milan, Italy; §Endocrine and Renal Sciences, Genzyme Corporation, Framingham, Massachusetts; and ‖Nephrologisches Zentrum, Medizinische Poliklinik, Ludwig-Maximilians-Universität München, Munich, Germany*

Injury to podocytes and their slit diaphragms typically leads to marked proteinuria. Mutations in the *TRPC6* gene that codes for a slit diaphragm–associated, cation-permeable ion channel have been shown recently to co-segregate with hereditary forms of progressive kidney failure. Herein is shown that induced expression of wild-type TRPC6 is a common feature of human proteinuric kidney diseases, with highest induction observed in membranous nephropathy. Cultured podocytes that are exposed to complement upregulate TRPC6 protein. Stimulation of receptor-operated channels in puromycin aminonucleoside–treated podocytes leads to increased calcium influx in a time- and dosage-dependent manner. Mechanistically, it is shown that TRPC6 is functionally connected to the podocyte actin cytoskeleton, which is rearranged upon overexpression of TRPC6. Transient *in vivo* gene delivery of TRPC6 into mice leads to expression of TRPC6 protein at the slit diaphragm and causes proteinuria. These studies suggest the involvement of TRPC6 in the pathology of nongenetic forms of proteinuric disease.

J Am Soc Nephrol 18: 29–36, 2007. doi: 10.1681/ASN.2006091010

Podocytes are specialized cells that reside in the kidney glomerulus and cover the outer surface of the filtering capillaries (1). Their foot processes form a complex interdigitating pattern with slits that are bridged by extracellular protein–protein contacts to form the slit diaphragm (2). Podocyte foot processes and slit diaphragms contribute to the formation of the glomerular filter, combining a seal to macromolecules with high hydraulic conductivity that is subject to regulation. These two characteristics both are perturbed in most glomerular kidney diseases, resulting in a leakage of proteins into the urine, which may give rise to progressive damage and decline in GFR (3). Mutations in genes that are specific for podocyte development and function have taken center stage in understanding glomerular kidney diseases that cause various degrees of proteinuria and, potentially, the progression to ESRD (4).

Recently, a mutation in the cation-permeable ion channel TRPC6 was identified as a culprit for a familial form of FSGS (5). Our group subsequently characterized TRPC6 as a component of the slit diaphragm, suggesting that it functions as critical regulator of normal renal function (6).

TRPC6 belongs to the TRP superfamily of ion channel-forming proteins. TRP channel genes encode subunits that form ion channels in many cell types (7,8). Members of the TRP superfamily have been identified on the basis of amino acid sequence and structural similarity and are classified into seven subfamilies (9). TRPC6 is a member of the TRPC subfamily and has been reported to be Ca^{2+} selective. Ca^{2+} entry through other TRPC channels has been shown to increase cytoplasmic Ca^{2+}, allowing for phosphorylation of signal transduction proteins and transcription factors or for the regulation of cytoskeletal dynamics (10). Mutations of TRP proteins produce many renal diseases, including Mg^{2+} wasting, hypocalcemia, and polycystic kidney diseases (11). The discovery of mutations in the TRPC6 gene as cause for hereditary FSGS as well as the localization of TRPC6 at the slit diaphragm open a whole series of questions about the physiologic and pathophysiologic role of this channel in podocytes. On the basis of our previous findings in hereditary FSGS, we hypothesized that also in acquired forms of kidney disease, TRPC6 expression levels and channel function may contribute to glomerular disease pathogenesis *via* a dysregulated Ca^{2+} influx at the slit diaphragm site. In this article, we provide evidence that, in addition to the effects of gain-of-function mutations in the *TRPC6* gene, elevated levels

Published online ahead of print. Publication date available at www.jasn.org.

M.K.'s current affiliation is Department of Medicine, Division of Nephrology, University of Michigan, Ann Arbor, Michigan.

Address correspondence to: Dr. Jochen Reiser, Department of Medicine, Nephrology Division, Massachusetts General Hospital and Harvard Medical School, MGH-East, 149 13th Street, Boston, MA 02129. Phone: 617-726-9363; Fax: 617-726-5669; E-mail: jreiser@partners.org

ISSN: 1046-6673/1801-0029

of wild-type TRPC6 protein in acquired glomerular diseases lead to podocyte dysfunction. We discuss a role of elevated TRPC6 levels in the reorganization of the podocyte actin cytoskeleton and the development of proteinuria.

Materials and Methods

Animals and Treatments

All animal studies were approved by the Subcommittee on Research Animal Care of the Massachusetts General Hospital. C57BL6 mice were obtained from Jackson Laboratory (Bar Harbor, ME). The passive Heymann nephritis (PHN) model of experimental membranous nephropathy was induced in male Sprague-Dawley rats (Simonsen Laboratories, Gilroy, CA) by intraperitoneal injection (5 ml/kg body wt) of sheep antibody to Fx1A (12). Rats that received an injection of normal sheep serum (5 ml/kg body wt) served as controls for the anti-Fx1A antibody. Control and PHN rats were killed at 5, 11, and 28 d ($n = 4$ to 5 for each time point) for renal biopsies and glomerular isolation. For verification of efficiency of anti-Fx1A injection, urine protein excretion was determined using the sulfosalicylic acid method before control and PHN rats were killed (13) (data not shown). For assessment of TRPC6 mRNA levels and puromycin aminonucleoside (PAN)-induced albuminuria, rats were given three consecutive injections of PAN (50 mg/kg body wt) at days 0, 10, and 20. At days 27 and 34, rats were killed and kidneys were collected. Glomeruli were isolated using standard sieve technique. TRPC6 mRNA levels were analyzed by quantitative real-time reverse transcriptase–PCR according to standard protocols. Albuminuria was assessed by collection of urine from each animal for 24 h in metabolic cages (Nalgene, Rochester, NY) and measurement of the albumin concentration by ELISA using the Neph-Rat Kit (Exocell, Philadelphia, PA). For TRPC6 immunostainings, rats were given a single injection of PAN (50 mg/kg body wt) at day 0. At days 0, 4, 8, and 28, rats were killed and kidneys were collected. Kidneys were processed for immunostaining as described before (6).

Patients

Human kidney biopsies, obtained in a multicenter study for renal gene expression analysis (the European Renal cDNA Consortium), were processed as described (14). Informed consent was obtained according to the respective local ethical committee guidelines. Histologies were stratified by the reference pathologists of the European Renal cDNA Consortium. Predeveloped TaqMan assay reagent was used for TRPC6 and the internal standard 18S rRNA. Quantification of the given templates was performed according to the standard curve method. All measurements were performed in duplicate; controls that consisted of bi-distilled H_2O were negative in all runs. Microdissected glomeruli from 34 patients with proteinuric diseases and eight control subjects were analyzed. Patients were stratified according to their histologic diagnosis into FSGS ($n = 9$), minimal-change disease (MCD; $n = 13$), and membranous glomerulonephritis (MGN; $n = 28$). For control biopsies, renal tissue was derived from healthy poles of tumor nephrectomies (CON; $n = 9$).

Cell Culture

To determine the expression of TRPC6 in podocytes that were stimulated with complement *in vitro*, we used conditionally immortalized mouse podocytes (15). All studies were performed between days 15 and 17 of growth-restrictive conditions. For induction of sublytic C5b-9 attack, mouse podocytes were stimulated with sheep anti-mouse podocyte IgG and complement as described previously (16). In group C6+, podocytes were sensitized with medium that contained 0.5 mg/ml sheep anti-mouse podocyte IgG at 37°C for 30 min. Sensitized podocytes then were exposed to a sublytic amount of complement for 30 min, washed three times, and then incubated in growth medium for 48 h. In group C6−, which served as control for C5b-9–attacked cells, podocytes were sensitized with sheep anti-mouse podocyte IgG and exposed to complement that lacked C6 for 30 min. Whole-cell lysates were isolated in RIPA buffer, and Western blot analysis was performed according to standard procedures using anti-TRPC6 antibody and anti-actin antibody as a loading control.

Immunohistochemistry, Immunocytochemistry, and Electron Microscopy

Human glomerular biopsies were fixed in cold acetone and stained with anti-TRPC antibody (Abcam, Cambridge, MA) and monoclonal anti-synaptopodin antibody (15) following standard protocols. Immunocytochemistry on cultured podocytes was done on cells that were grown on coverslips as described previously (6). Actin cytoskeleton was visualized with the Alexa Fluor 594 phalloidin conjugate (Molecular Probes, Eugene, OR). Renal biopsies from PHN rats were fixed in methyl Carnoy's solution and embedded in paraffin. Indirect immunoperoxidase staining (16) was performed on 4-μm sections using TRPC6 primary antibody (omitted in controls). Glomeruli were scored from 1 to 4 on the basis of the percentage of positively stained podocytes in each glomerulus (0 to 25% positive = 1; 26 to 50% positive = 2; 51 to 75% positive = 3; 76 to 100% positive = 4). Scoring values were statistically analyzed by one-way ANOVA, and Bonferroni multiple comparison test was performed. At all time points, the increase in TRPC6 expression was statistically significant. Transmission electron microscopy and immunoelectron microscopy were performed according to standard protocols as described previously (6).

Calcium Flux Studies

Differentiated cultured podocytes were treated for 24 h with 10 or 50 μg/ml PAN. Cells then were loaded with the Fluo-4 calcium indicator in 0.1 mM Ca^{2+} for 1 h. Receptor-operated channels were activated by addition of 100 μM 1-oleoyl-2-acetyl-sn-glycerol, followed by changing the extracellular buffer to 2 mM Ca^{2+} to distinguish membrane-associated channel-dependent changes in calcium.

In Vivo *Gene Delivery*

FLAG-TRPC6 plasmids were introduced into C57BL6 mice using the TransIT *in vivo* gene delivery system (Mirus Bio, Madison, WI). In brief, 15 μg of plasmid DNA was mixed with 15 μl of Mirus polymer solution and 170 μl of endotoxin-free H_2O. It then was topped with 1.8 ml of Mirus delivery solution before injection through tail vein. Fifteen hours after gene delivery, proteinuria was assessed by Bradford protein assay (Bio-Rad, Hercules, CA). Mice that received an injection showed significant proteinuria as compared with baseline urine protein excretion ($P = 0.0275$). For the luciferase activity assay, kidneys were harvested from eight mice 12 h after gene delivery of 10 μg of pGL3 luciferase reporter plasmid, and luciferase activity was assayed using the Luciferase Assay System (Promega, Madison, WI). We also tested kidneys from eight control mice that did not receive an injection. Light intensity was measured on a plate reader luminometer.

Statistical Analyses

Unless stated otherwise, statistical analyses were performed by using the unpaired t test, and the null hypothesis was rejected at the 0.05 level. Values are presented as means ± SD.

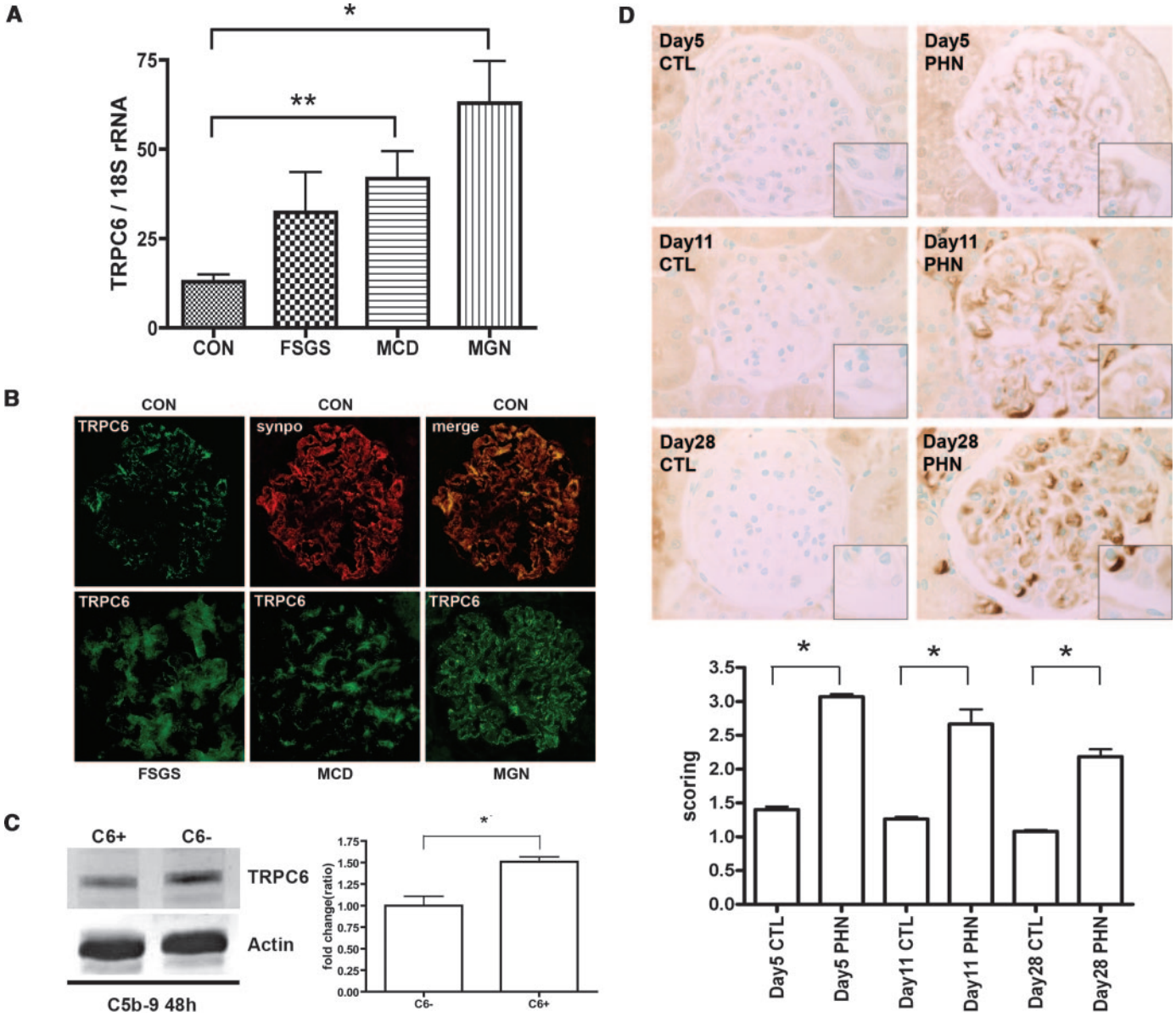

Figure 1. TRPC6 mRNA and protein expression in human glomerular disease. (A) The ratio of human TRPC6 mRNA *versus* 18S ribosomal RNA was determined by quantitative real-time reverse transcriptase–PCR. Compared with control kidneys (CON; $n = 9$), TRPC6 mRNA was statistically significantly upregulated in kidneys from patients with minimal-change disease (MCD; $^{**}P = 0.0063$; $n = 13$) and with membranous glomerulonephritis (MGN; $^{*}P = 0.0238$; $n = 28$). In kidneys from patients with FSGS ($n = 9$), the increase in TRPC6 mRNA did not reach statistical significance. (B) Kidneys were examined by indirect immunofluorescence using a primary antibody against TRPC6. Double labeling with the podocyte marker synaptopodin leads to a yellow overlap (merge). In FSGS and MCD kidneys, TRPC6 staining was induced and appeared clustered. TRPC6 intensity was stronger in FSGS than in MCD. TRPC6 staining was strongest and appeared granulated in glomeruli during MGN. TRPC6 levels are increased in models of MGN. (C) Cultured podocytes were differentiated for 15 to 17 d and stimulated with antipodocyte antibody and C6− or C6+ serum. Western blot analysis shows that the expression of TRPC6 increased in cells that were stimulated with C6+ serum when compared with cells that were stimulated by C6− serum (left). Densitometric analysis of three Western blots revealed a significant increase of TRPC6 in podocytes that were stimulated with C6+ serum compared with C6− serum (right; $P < 0.05$). (D) Immunostaining for TRPC6 shows increased glomerular TRPC6 expression levels at days 5, 11, and 28 of passive Heymann nephritis (top). Although TRPC6 expression predominantly followed a podocyte staining pattern, few endothelial also were positively stained. Semiquantitative scoring of glomerular TRPC6 immunostaining (score from 1 to 4) of the percentage of positively stained podocytes was performed (bottom). Scoring values were statistically analyzed by one-way ANOVA. At all time points, the increase in TRPC6 expression was statistically significant.

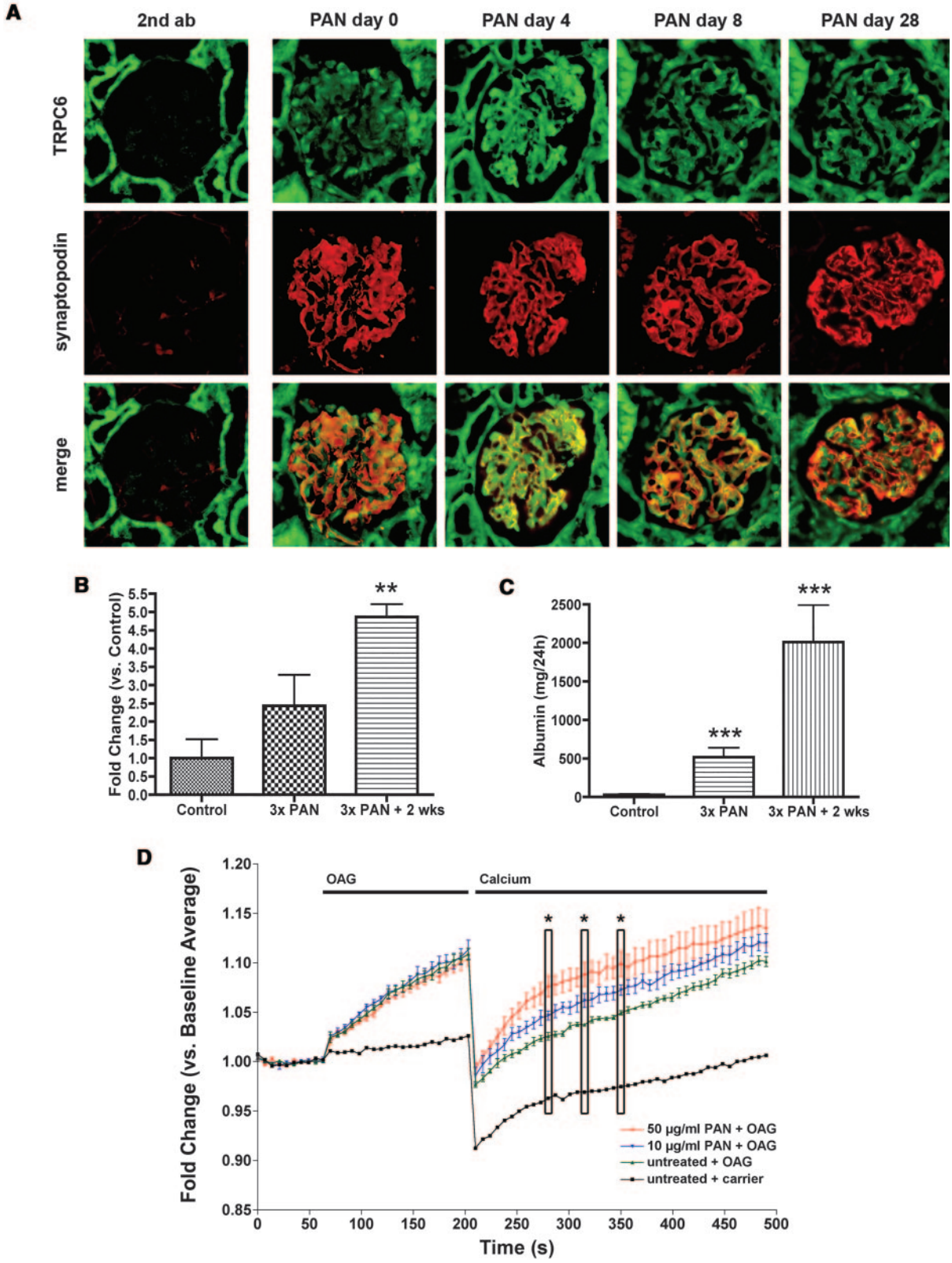

Figure 2. TRPC6 levels are induced in podocytes *in vivo* after treatment of rats with puromycin aminonucleoside (PAN). (A) Frozen rat kidney sections were stained using antibodies that were specific for TRPC6 and the podocyte marker synaptopodin. When primary antibodies were omitted in the staining procedure (second antibody), we could detect a high background signal for TRPC6 in tubules but no signal in glomeruli and no signal for synaptopodin. In the glomeruli of untreated rats (PAN day 0), TRPC6 is expressed predominantly in podocytes as shown by a partial overlap with synaptopodin. Four days after PAN treatment, in the peak phase of PAN-induced stress, TRPC6 expression is induced dramatically in podocytes. Eight days after

Results and Discussion

In this study, we first examined the expression of TRPC6 in nongenetic forms of human proteinuric kidney diseases. We analyzed TRPC6 mRNA expression in isolated glomeruli from patients with FSGS, MCD, and MGN (Figure 1A). Control samples were obtained from the healthy kidney poles of individuals who underwent tumor nephrectomies. By real-time quantitative PCR, we determined the ratio of TRPC6 mRNA to 18S ribosomal RNA (17). We found significantly increased levels of TRPC6 mRNA in patients with MCD ($n = 13$, $P = 0.006$) and MGN ($n = 28$, $P = 0.024$) as compared with control patients ($n = 9$). In patients with FSGS ($n = 9$), the increase in TRPC6 mRNA did not reach statistical significance. Immunostaining of TRPC6 was performed on human kidney biopsies of normal tissue and of glomeruli during FSGS, MCD, and MGN (Figure 1B). In control glomeruli, TRPC6 labeling was found throughout the glomerulus and in particular at the outer aspects of capillary loops (Figure 1B, CON). Double labeling with the podocyte marker synaptopodin showed that glomerular TRPC6 was localized in podocytes represented by a yellow overlap (Figure 1B, CON). In FSGS, TRPC6 staining appeared clustered and aggregated as well as segmentally more intense (Figure 1B, FSGS). TRPC6 staining in MCD displayed a similar pattern as FSGS but with less intensity (Figure 1B, MCD). In MGN, glomerular TRPC6 expression was granular and dramatically induced in podocytes (Figure 1B, MGN).

Given our observation that TRPC6 mRNA and protein were strongest in MGN, we next exposed cultured differentiated mouse podocytes to antipodocyte antibody and serum with or without complement. Treatment of cultured podocytes with sublytic amounts of C5b-9 mimics the effects of the complement system as a potent mediator of glomerular injury in membranous glomerular disease. Consequences of sublytic C5b-9 attack include the release of calcium and the activation of signaling pathways in the podocyte (16). Western blot analysis of TRPC6 in treated cells showed significantly increased TRPC6 expression in cells that were stimulated with C6+ serum when compared with cells that were stimulated by C6− serum that lacked functional complement ($n = 3$, $P < 0.05$; Figure 1C).

To test the hypothesis that C5b-9 induces podocyte TRPC6 expression *in vivo*, we used the PHN model of experimental membranous nephropathy (12). In the PHN model, rats are administered an injection of anti-Fx1A antibody, inducing formation of subepithelial immune deposits, the activation of the C5b-9 membrane attack complex of complement, and the development of severe proteinuria. Sprague-Dawley rats that received an injection of normal sheep serum served as controls for the anti-Fx1A antibody. Control and PHN rats were killed at 5, 11, and 28 d ($n = 4$ to 5 for each time point) for immunohistochemical analysis of glomeruli. TRPC6 protein expression was strongly induced in glomeruli in rats with PHN (Figure 1D). While induced TRPC6 staining was observed predominantly along capillary loops that resembled a podocyte staining pattern, we also found noticeable expression in glomerular endothelial cells.

Next, we explored TRPC6 expression levels in the PAN experimental model of podocyte injury and nephrotic syndrome (18). TRPC6 levels were induced significantly in the glomeruli of PAN-injected rats 4 d after treatment at the peak of PAN-mediated injury (Figure 2A). Induced TRPC6 protein was detected mainly in podocyte as shown by double labeling with the podocyte marker synaptopodin (Figure 2A). Eight days after PAN treatment, TRPC6 expression levels still were upregulated slightly. Twenty-eight days after PAN treatment, which represents the recovery from PAN-mediated injury, TRPC6 expression levels returned to baseline (Figure 2A). By real-time quantitative PCR, we determined an upregulation of TRPC6 mRNA levels in rats upon PAN-mediated injury (Figure 2B). The increase in TRPC6 mRNA correlated with the development of albuminuria in these rats (Figure 2C).

To understand better whether induction of wild-type TRPC6 is associated with changes in intracellular calcium, we examined the calcium influx in cultured podocytes after injury with PAN (18) (Figure 2C). Twenty-four hours after the application of PAN on cultured podocytes, receptor-operated calcium channels were activated by addition of the diacylglycerol analog 1-oleoyl-2-acetyl-sn-glycerol. We observed elevated calcium influx in PAN-treated podocytes compared with untreated control cells, suggesting that increased influx of calcium is a component of podocyte injury, possibly mediated by TRPC6 channels (Figure 2C).

In the next step, we focused on the molecular mechanisms that may account for the pathogenic effect of induced TRPC6 protein. TRP channels are known to be associated with the actin cytoskeleton (19), the proper organization of which is essential for normal podocyte function (20). Therefore, we first tested whether the disruption of the actin cytoskeleton in cultured podocytes (15) would affect the localization of TRPC6. After

PAN treatment, TRPC6 levels still seem to be elevated, and 28 d after PAN treatment, which represents the recovery from PAN-induced stress, TRPC6 expression returns to baseline levels. The upregulation of TRPC6 mRNA in isolated glomeruli correlates with the development of albuminuria in PAN-treated rats. (B) Rats were administered injections of three consecutive doses of PAN. Two weeks after the third injection, TRPC6 mRNA levels were 4.9-fold elevated in isolated glomeruli ($P < 0.01$). (C) Rats were administered injections of three consecutive doses of PAN. One week after the third injection, the average amount of albumin in the urine was determined to e 519 mg/24 h ($P < 0.001$). Two weeks after the third injection, the average amount of albumin in the urine was determined to be 2009 mg/24 h ($P < 0.001$). PAN treatment is correlated with increased calcium influx in cultured podocytes. (D) Differentiated podocytes were treated for 24 h with 10 or 50 μg/ml PAN. Cells then were loaded with Fluo-4 in 0.1 mM Ca^{2+} for 1 h. Receptor-operated channels were activated by addition of 100 μM 1-oleoyl-2-acetyl-sn-glycerol, followed by changing the extracellular buffer to 2 mM Ca^{2+} to distinguish membrane-associated channel-dependent changes in calcium. Differences in intracellular calcium concentration were statistically significant at the time points indicated. *$P < 0.05$.

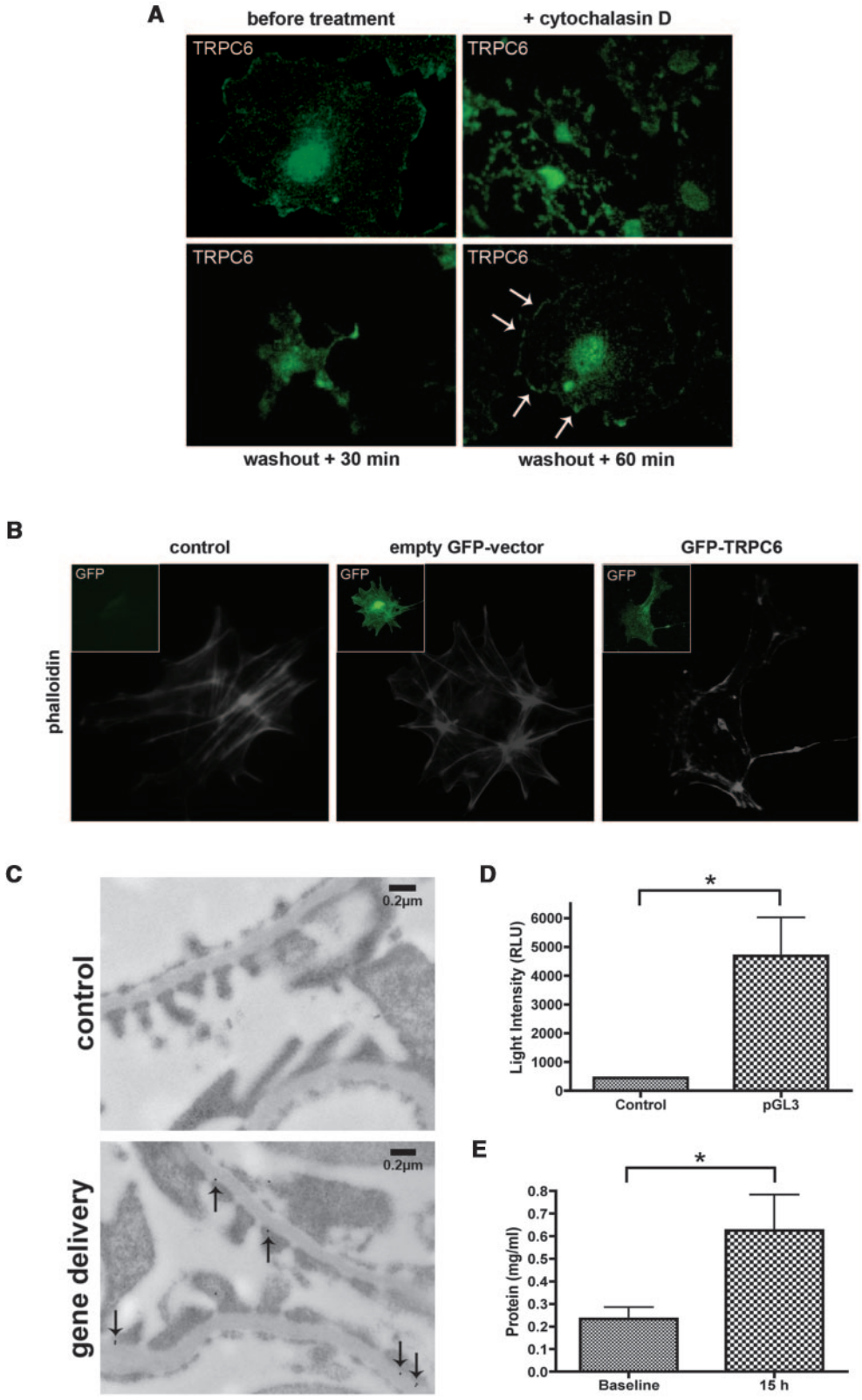

Figure 3. TRPC6 is associated with the podocyte actin cytoskeleton. (A) Effect of cytochalasin D treatment on TRPC6 subcellular localization. Six hours after cytochalasin D incubation, TRPC6 localizes with depolymerized actin clusters within the cell body (top right). Thirty minutes after washout of cytochalasin (partial recovery), TRPC6 starts to redistribute within the cell (bottom left). Sixty minutes after washout (full recovery), most of TRPC6 is re-localized at the cell membrane (bottom right, arrows). (B) TRPC6 overexpression leads to the loss of stress fibers in podocytes. Differentiated podocytes were transfected with a green fluorescence protein (GFP)-TRPC6 fusion protein (green) and stained with phalloidin to visualize actin stress fibers. Cells were analyzed by confocal microscopy. Cells that were transfected with GFP-TRPC6 (right) show a significant loss of stress fibers and exhibit a more

depolymerization of F-actin in cultured podocytes using cytochalasin D (18), we found TRPC6 closely associated with depolymerized clusters of actin (Figure 3A, top right). The removal of cytochalasin D allows the reorganization of the actin cytoskeleton; consequently, TRPC6 started to redistribute to its original localization at the cell membrane (Figure 3A, bottom).

To study whether TRPC6 overexpression affects the actin cytoskeleton directly, we overexpressed green fluorescence protein (GFP)-tagged TRPC6 (6) in cultured differentiated podocytes (Figure 3B). Cells that expressed GFP-TRPC6 displayed loss of actin stress fibers (Figure 3B, right) that normally are found in untransfected control cells (Figure 3B, left). Transfection of the empty GFP vector had no effect on the podocyte actin cytoskeleton (Figure 3B, middle). These studies suggest that TRPC6 is functionally associated with the actin cytoskeleton in podocytes and that induction of TRPC6 channel directly affects cytoskeletal organization in these cells.

If such a functional association of TRPC6 with podocyte actin cytoskeleton were true, we wondered, then, whether we could observe a phenotype in mice when overexpressing wild-type TRPC6 in podocytes. Therefore, we used a transient gene delivery approach to deliver wild-type FLAG-tagged TRPC6 in mouse kidneys (21). With this approach, we found gene-transferred FLAG-TRPC6 in podocyte foot processes often in close vicinity to the slit diaphragm 12 h after gene injection (Figure 3C, arrows). When mice were administered an injection of the pGL3 luciferase reporter vector, we were able to detect luciferase activity in whole-kidney lysates 12 h after gene injection (Figure 3D). Functionally, mice that were administered an injection of FLAG-TRPC6 displayed transient proteinuria 15 h after gene injection (Figure 3E).

The discovery that mutations in the TRPC6 gene cause hereditary FSGS together with the finding that TRPC6 is a component of the slit diaphragm multiprotein complex raises questions regarding the mechanisms that are involved in the physiologic and pathophysiologic role of this channel in podocytes. In this study, we provide evidence that, in addition to the effects of gain-in-function mutations in *TRPC6*, pathophysiologically elevated expression levels of TRPC6 are detected in acquired glomerular diseases. Our data in cultured podocytes suggest that the consequences of elevated TRPC6 include reorganization of the podocyte actin cytoskeleton and altered calcium regulation. Importantly, overexpression of wild-type TRPC6 seems to be sufficient to cause proteinuria in healthy mice. Taken together, these data indicate that TRPC6 plays a pivotal role in nongenetic forms of glomerular disease, suggesting that functional TRPC6 blockade may provide an effective treatment for genetic and acquired forms of proteinuric kidney disease, in particular in MGN.

Acknowledgments

C.C.M. was supported by a scholarship of the German Academic Exchange Service (DAAD). J.R. was supported by the KMD Foundation and the KUFA-ASN Research Grant.

Parts of this work were selected for oral presentations at the annual meetings of American Society of Nephrology, November 8 through 13, 2005, Philadelphia, PA and November 14 through 19, 2006, San Diego, CA.

We thank Mary McKee from the Program in Membrane Biology at Massachusetts General Hospital and Harvard Medical School for technical assistance with electron microscopy.

Disclosures

None.

References

1. Somlo S, Mundel P: Getting a foothold in nephrotic syndrome. *Nat Genet* 24: 333–335, 2000
2. Pavenstadt H, Kriz W, Kretzler M: Cell biology of the glomerular podocyte. *Physiol Rev* 83: 253–307, 2003
3. Kriz W, Lemley KV: The role of the podocyte in glomerulosclerosis. *Curr Opin Nephrol Hypertens* 8: 489–497, 1999
4. Tryggvason K, Pikkarainen T, Patrakka J: Nck links nephrin to actin in kidney podocytes. *Cell* 125: 221–224, 2006
5. Winn MP, Conlon PJ, Lynn KL, Farrington MK, Creazzo T, Hawkins AF, Daskalakis N, Kwan SY, Ebersviller S, Burchette JL, Pericak-Vance MA, Howell DN, Vance JM, Rosenberg PB: A mutation in the TRPC6 cation channel causes familial focal segmental glomerulosclerosis. *Science* 308: 1801–1804, 2005
6. Reiser J, Polu KR, Moller CC, Kenlan P, Altintas MM, Wei C, Faul C, Herbert S, Villegas I, Avila-Casado C, McGee M, Sugimoto H, Brown D, Kalluri R, Mundel P, Smith PL, Clapham DE, Pollak MR: TRPC6 is a glomerular slit diaphragm-associated channel required for normal renal function. *Nat Genet* 37: 739–744, 2005
7. Pedersen SF, Owsianik G, Nilius B: TRP channels: an overview. *Cell Calcium* 38: 233–252, 2005
8. Nilius B, Voets T: Diversity of TRP channel activation. *Novartis Found Symp* 258: 140–149, 2004
9. Clapham DE: TRP channels as cellular sensors. *Nature* 426: 517–524, 2003
10. Li Y, Jia YC, Cui K, Li N, Zheng ZY, Wang YZ, Yuan XB: Essential role of TRPC channels in the guidance of nerve

cortical actin cytoskeleton than untransfected control cells (left) or cells that were transfected with empty GFP vector (middle) displaying a regular actin cytoskeleton. TRPC6 *in vivo* gene delivery leads to transient overexpression of exogenous TRPC6 in podocytes and is associated with the development of proteinuria. (C) A construct coding for a FLAG-TRPC6 fusion protein was gene-delivered into mice *via* tail-vein injection. Twelve hours after gene transfer, mouse kidneys were processed for immunogold analysis with anti-FLAG antibody. Immunogold labeling of FLAG-TRPC6 was detected in podocyte foot processes in close vicinity of the slit diaphragm site. (D) Gene delivery of the pGL3 luciferase reporter vector leads to the detection of luciferase activity in kidneys 12 h after gene transfer ($P = 0.0158$). (E) FLAG-TRPC6 was gene-delivered into mice and proteinuria was assessed by Bradford assay. Before gene delivery, baseline urine protein excretion averaged to 0.23 mg/ml. Fifteen hours after gene delivery, mice developed proteinuria with an average urine protein excretion of 0.63 mg/ml ($P = 0.0275$).

growth cones by brain-derived neurotrophic factor. *Nature* 434: 894–898, 2005
11. Thebault S, Hoenderop JG, Bindels RJ: Epithelial Ca2+ and Mg2+ channels in kidney disease. *Adv Chronic Kidney Dis* 13: 110–117, 2006
12. Perkinson DT, Baker PJ, Couser WG, Johnson RJ, Adler S: Membrane attack complex deposition in experimental glomerular injury. *Am J Pathol* 120: 121–128, 1985
13. Shankland SJ, Pippin J, Pichler RH, Gordon KL, Friedman S, Gold LI, Johnson RJ, Couser WG: Differential expression of transforming growth factor-beta isoforms and receptors in experimental membranous nephropathy. *Kidney Int* 50: 116–124, 1996
14. Cohen CD, Frach K, Schlondorff D, Kretzler M: Quantitative gene expression analysis in renal biopsies: A novel protocol for a high-throughput multicenter application. *Kidney Int* 61: 133–140, 2002
15. Mundel P, Reiser J, Zuniga Mejia Borja A, Pavenstadt H, Davidson GR, Kriz W, Zeller R: Rearrangements of the cytoskeleton and cell contacts induce process formation during differentiation of conditionally immortalized mouse podocyte cell lines. *Exp Cell Res* 236: 248–258, 1997
16. Pippin JW, Durvasula R, Petermann A, Hiromura K, Couser WG, Shankland SJ: DNA damage is a novel response to sublytic complement C5b-9-induced injury in podocytes. *J Clin Invest* 111: 877–885, 2003
17. Schmid H, Henger A, Cohen CD, Frach K, Grone HJ, Schlondorff D, Kretzler M: Gene expression profiles of podocyte-associated molecules as diagnostic markers in acquired proteinuric diseases. *J Am Soc Nephrol* 14: 2958–2966, 2003
18. Reiser J, Pixley FJ, Hug A, Kriz W, Smoyer WE, Stanley ER, Mundel P: Regulation of mouse podocyte process dynamics by protein tyrosine phosphatases rapid communication. *Kidney Int* 57: 2035–2042, 2000
19. Lockwich T, Singh BB, Liu X, Ambudkar IS: Stabilization of cortical actin induces internalization of transient receptor potential 3 (Trp3)-associated caveolar Ca2+ signaling complex and loss of Ca2+ influx without disruption of Trp3-inositol trisphosphate receptor association. *J Biol Chem* 276: 42401–42408, 2001
20. Asanuma K, Yanagida-Asanuma E, Faul C, Tomino Y, Kim K, Mundel P: Synaptopodin orchestrates actin organization and cell motility via regulation of RhoA signalling. *Nat Cell Biol* 8: 485–491, 2006
21. Mayer G, Boileau G, Bendayan M: Furin interacts with proMT1-MMP and integrin alphaV at specialized domains of renal cell plasma membrane. *J Cell Sci* 116: 1763–1773, 2003

Proteolytic processing of dynamin by cytoplasmic cathepsin L is a mechanism for proteinuric kidney disease

Sanja Sever,[1] Mehmet M. Altintas,[1] Sharif R. Nankoe,[1] Clemens C. Möller,[1] David Ko,[1] Changli Wei,[1] Joel Henderson,[2] Elizabetta C. del Re,[1] Lianne Hsing,[3] Ann Erickson,[4] Clemens D. Cohen,[5] Matthias Kretzler,[6] Dontscho Kerjaschki,[7] Alexander Rudensky,[3,8] Boris Nikolic,[1] and Jochen Reiser[1]

[1]Department of Medicine, Nephrology Division and Program in Glomerular Disease, Massachusetts General Hospital (MGH) and Harvard Medical School, Boston, Massachusetts, USA. [2]Department of Pathology, Brigham and Women's Hospital, Harvard Medical School, Boston, Massachusetts, USA. [3]Department of Immunology, University of Washington, Seattle, Washington, USA. [4]Department of Biochemistry and Biophysics, The University of North Carolina, Chapel Hill, North Carolina, USA. [5]Medizinische Poliklinik, University of Munich, Munich, Germany. [6]Department of Internal Medicine, Division of Nephrology, University of Michigan Medical School, Ann Arbor, Michigan, USA. [7]Clinical Institute of Pathology, Vienna Medical University, Vienna, Austria. [8]Howard Hughes Medical Institute, University of Washington School of Medicine, Seattle, Washington, USA.

Kidney podocytes and their foot processes maintain the ultrafiltration barrier and prevent urinary protein loss (proteinuria). Here we show that the GTPase dynamin is essential for podocyte function. During proteinuric kidney disease, induction of cytoplasmic cathepsin L leads to cleavage of dynamin at an evolutionary conserved site, resulting in reorganization of the podocyte actin cytoskeleton and proteinuria. Dynamin mutants that lack the cathepsin L site, or render the cathepsin L site inaccessible through dynamin self-assembly, are resistant to cathepsin L cleavage. When delivered into mice, these mutants restored podocyte function and resolve proteinuria. Our study identifies dynamin as a critical regulator of renal permselectivity that is specifically targeted by proteolysis under pathological conditions.

Introduction

In the US alone, kidney diseases affect some 20 million people, twice as many as it did 2 decades ago. Renal ultrafiltration occurs in glomeruli, specialized structures that ensure permselectivity of the kidney filter so that essential plasma proteins are retained in the blood. A sign of glomerular dysfunction is the loss of protein in the urine (termed proteinuria or nephrotic syndrome if protein loss exceeds 3.5 g/d). Proteinuria often leads to progressive renal failure, eventually requiring dialysis or kidney transplantation (1). Podocytes are specialized cells within the glomerulus that are essential for ultrafiltration (Supplemental Figure 1A; supplemental material available online with this article; doi:10.1172/JCI32022DS1). Podocytes form foot processes (FPs), highly dynamic cellular extensions that are connected by slit diaphragms. Together with the glomerular basement membrane (GBM) and the glomerular endothelial cells, podocytes form a key component of the kidney permeability barrier. Most forms of proteinuria are characterized by a reduction of podocyte membrane extensions in number and size as well as transformation of podocyte FPs into a band of cytoplasm (referred to as FP effacement). Familial mutations underlie only a small percentage of kidney diseases (2) and therefore do not readily explain the molecular mechanisms underlying the far more common acquired causes of FP effacement and proteinuria. In this study, we show that dynamin is essential to maintain the filtration barrier in kidneys due to a role in regulating actin dynamics in podocytes. We further demonstrate that CatL is responsible for FP effacement. CatL affects podocyte function by cleaving dynamin in the cytoplasm. The cleavage of dynamin by CatL is inhibited when dynamin is induced to self-assemble. Gene delivery of dynamin mutants that are prone to self-assemble into higher-order structures, or that contain a mutated CatL cleavage site, can prevent and reverse podocyte FP effacement and proteinuria in a mouse model of proteinuria.

Nonstandard abbreviations used: CatL, cathepsin L; FP, foot process; PAN, puromycin aminonucleoside.

Conflict of interest: The authors have declared that no conflict of interest exists.

Citation for this article: *J. Clin. Invest.* **117**:2095–2104 (2007). doi:10.1172/JCI32022.

Results

Cathepsin L is necessary for podocyte FP effacement and proteinuria in a mouse model. Cathepsin L (CatL) belongs to a subclass of cysteine proteases termed lysosomal cathepsins, which are involved primarily in protein breakdown within the lysosomal compartment. Interestingly, CatL is strongly induced in rodent nephrotic podocytes (3). Moreover, earlier studies showed that inhibitors of cysteine proteases reduced proteinuria in rats, possibly by inhibiting degradation of the GBM (4). Recently, Goulet and colleagues described a novel role for CatL in processing of the CDP/Cux transcription factor in the nucleus during the S phase (5). Together, these findings raise many possibilities for the potential site of CatL action during the pathogenesis of proteinuria, including the cytoplasm. To explore the relevance of CatL in human kidney disease, we examined CatL mRNA levels using quantitative real-time PCR (rt-PCR) in microdissected glomeruli from patients with acquired proteinuric diseases (6). *CatL* mRNA levels were 2-fold or greater in biopsy samples from patients with 3 types of proteinuric kidney diseases — membranous glomerulonephritis, focal segmental glomerulosclerosis, and diabetic nephropathy — compared with control samples (Figure 1A). Samples from patients with minimal change disease, which is characterized by reversible podocyte FP effacement, showed only a minor increase. There was also a signifi-

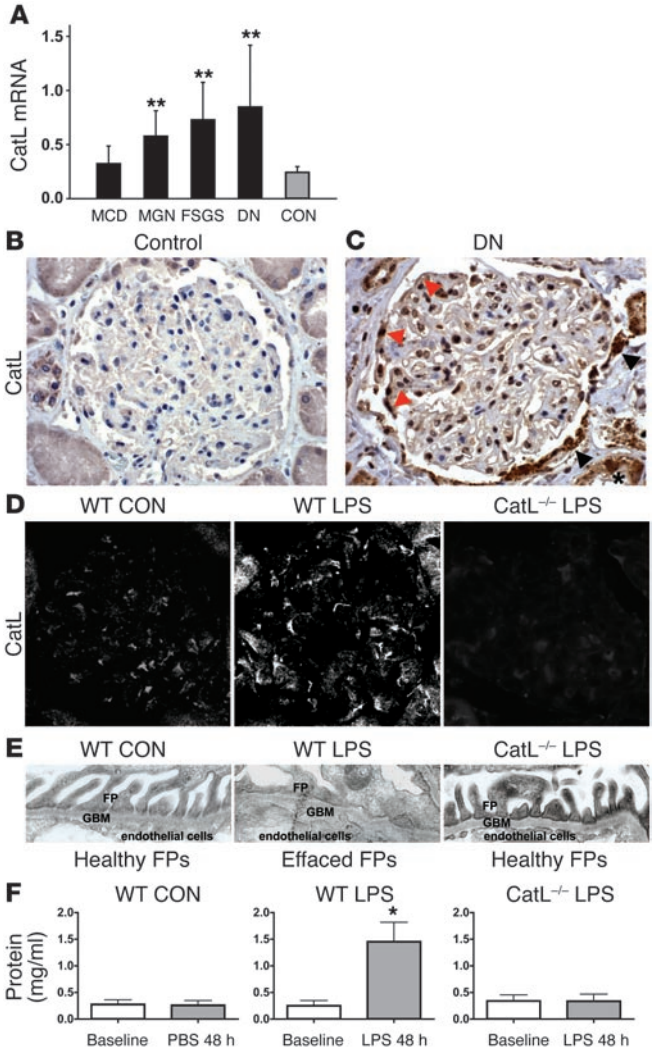

Figure 1
CatL is essential for proteinuric kidney diseases. (**A**) Quantitative rt-PCR of microdissected glomeruli from human biopsies of patients with acquired proteinuric diseases: minimal change disease (MCD; $n = 7$), membranous glomerulonephritis (MGN; $n = 9$), focal segmental glomerulosclerosis (FSGS; $n = 7$), and diabetic nephropathy (DN; $n = 10$). $^{**}P < 0.01$. CON, control ($n = 8$). (**B**) CatL labeling of normal human kidney. (**C**) CatL labeling of human kidney with diabetic nephropathy, mildly reduced renal function, and nephrotic range proteinuria. (**D**) Immunocytochemistry of mouse glomeruli using monoclonal anti-CatL antibody. WT mice received either PBS (WT CON) or LPS (WT LPS). LPS was also injected into $CatL^{-/-}$ mice ($CatL^{-/-}$ LPS). Original magnification, ×400 (**C** and **D**). (**E**) Electron micrographs of FPs. (**F**) Urinary protein levels determined using the standard Bradford protein assay. Urine was collected immediately before (Baseline) and 48 hours after addition of LPS. Each bar represents at least 8 animals.

cant increase in staining for CatL in glomeruli of patients with diabetic nephropathy (in Figure 1, compare B and C). The glomerulus contains 4 major cell types: podocytes, endothelial cells, mesangial cells, and cells of the Bowman capsule. CatL was induced in the nuclei of glomerular cells, in line with its role in cleaving transcription factors (5). There was also a strong increase in CatL within cells of the Bowman capsule (Figure 1C, arrowheads) and proximal tubular cells as shown before in proteinuric states (Figure 1C, asterisk; ref. 7). Finally, CatL staining was also elevated in the cytoplasm of podocytes (Figure 1C, red arrows).

We next examined whether a similar upregulation of CatL occurs in the LPS mouse model of proteinuria (3). Immunocytochemistry using anti-CatL antibodies (8, 9) detected weak CatL staining in normal glomeruli (Figure 1D, left). Glomerular CatL labeling increased within 24 hours after a single LPS injection (Figure 1D, middle) but not in mice lacking CatL (Figure 1D, right) (10). LPS treatment resulted in FP effacement in control mice (Figure 1E, left and middle) but not in the LPS-treated $CatL^{-/-}$ mice (Figure 1E, right). Finally, urinary protein increased from a baseline level of approximately 0.25 mg/ml to 1.2 ± 0.15 mg/ml in control mice but remained unchanged in LPS-treated $CatL^{-/-}$ mice (0.25 ± 0.11 mg/ml) (Figure 1F). These data provide genetic evidence that CatL is essential for proteinuria.

LPS induces expression of cytoplasmic CatL. To investigate how CatL triggers proteinuria, we examined its subcellular activity before and after LPS treatment in cultured podocytes. Subcellular sites of CatL and CatB activity were visualized by a fluorogenic substrate, CV-$(FR)_2$, which emits light upon cleavage by CatL or CatB (3). In untreated podocytes, protease activities were restricted to lysosomes (Figure 2A, left column). LPS treatment dramatically increased protease activity, which now extended outside lysosomes into the cytoplasm (Figure 2A, middle column). The vast majority of cytoplasmic cathepsin activity after LPS administration could be attributed to CatL, since it was sensitive to the CatL inhibitor Z-FF-FMK, which does not inhibit CatB (Figure 2A, right column; notice only perinuclear red staining). In line with the CatL activity in the cytoplasm, CatL protein colocalized with the lysosome-associated membrane protein LAMP-2 in lysosomes of control cells (Figure 2B, left column). After LPS treatment, there was a dramatic increase in overall CatL staining, some of which was present in the cytosol as well as in the nucleus (Figure 2B, right column). In addition, induced CatL was detected in LAMP-2–positive vesicles extending in podocyte processes close to the plasma membrane, which likely represent vesicles targeted for secretion (Supplemental Figure 1B and ref. 9). The relocalization of CatL upon LPS treatment was specific, since other lysosomal proteases such as CatB (Figure 2C) and mannosidase α (Supplemental Figure 1C) colocalized exclusively with LAMP-2 before and after LPS treatment. Finally, the presence of CatL in the cytoplasm was not due to lysosomal leakage (Supplemental Figure 1D).

The mRNA for CatL contains several AUG codons (Figure 2D). After translation from the first AUG, CatL is processed to yield a 30-kDa lysosomal form, called single-chain CatL (Figure 2D, black arrows). However, alternative translation initiation from a downstream AUG produces a CatL isoform devoid of the lysosomal targeting sequence (called short CatL), which localizes to the cytoplasm (Figure 2D, red arrow; ref. 5). To test whether LPS induces expression of short CatL, subcellular fractionation experiments using cultured podocytes were performed. The particulate fraction contains membranes, including lysosomes, whereas the soluble fraction represents cytoplasm. GAPDH was used as a marker for soluble cytosolic proteins and the efficiency of lysis. As expected, lysosomal single-chain CatL (30 kDa) was present in the particulate fraction, which also contained LAMP-2, CatB, and mannosidase α (Figure 2E, lane 2). LPS treatment for 24 hours led to strong induction of a 34-kDa short CatL, which was present exclusively in the

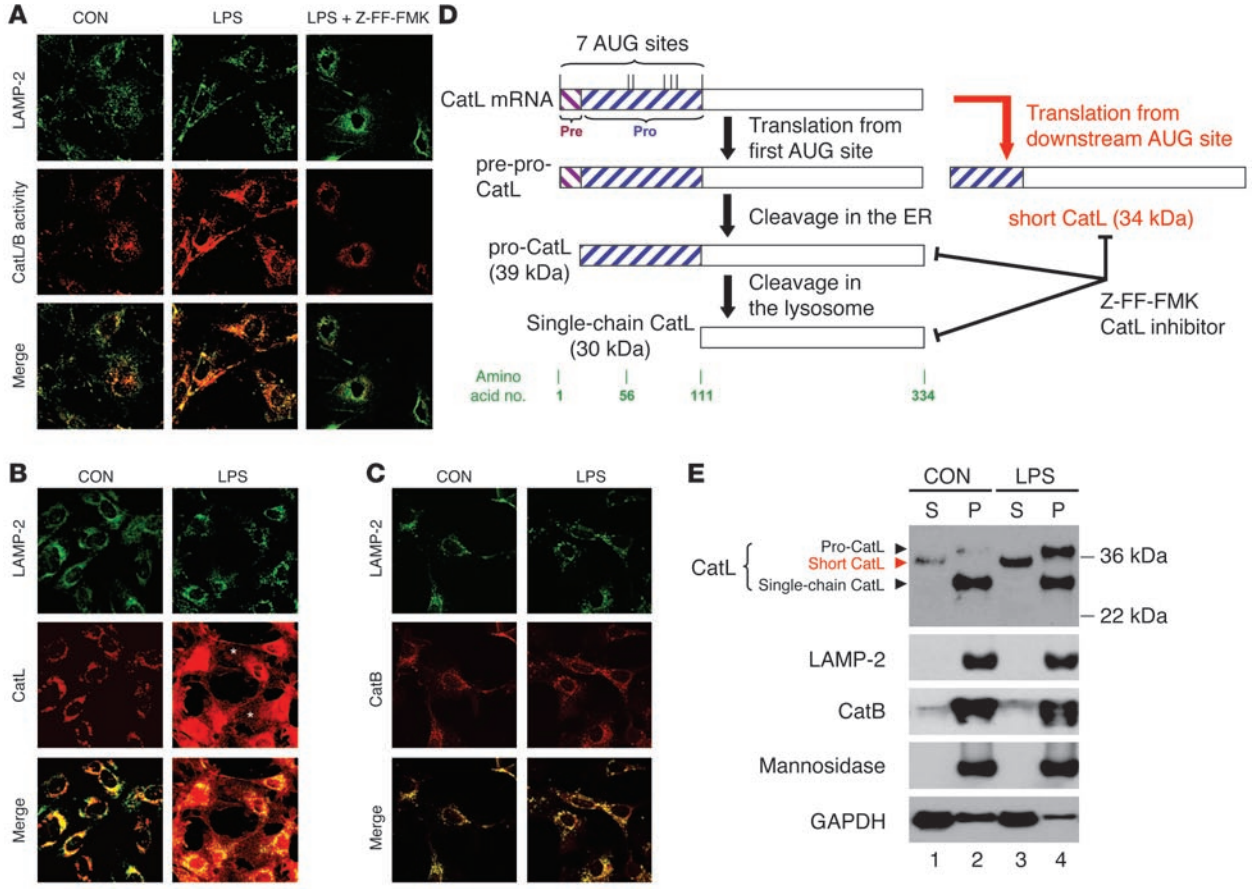

Figure 2

Induction of cytoplasmic CatL protein and activity by LPS. (**A**) Cultured podocytes were stained using anti–LAMP-2 antibodies and the BIOMOL CV-CatL/B activity detection kit. Control cells, cells treated with 50 μg/ml of LPS for 24 hours, and cells treated with LPS and 1 μM of the selective CatL inhibitor Z-FF-FMK are shown. (**B**) Labeling of cultured podocytes using anti-CatL antibody, untreated or after treatment with 50 μg/ml of LPS for 24 hours. (**C**) Labeling of cultured podocytes using anti-CatB antibody, untreated or after treatment with 50 μg/ml of LPS for 24 hours. (**D**) Schematic of CatL mRNA and resulting proteins. (**E**) Subcellular fractionation of podocytes in isotonic sucrose prior to and 24 hours after LPS treatment. Total proteins from the soluble (S) and the particulate (P) fractions were analyzed by Western blotting.

cytoplasm (Figure 2E, compare lanes 1 and 3). In contrast, there was no significant increase in the amount of the single-chain form, LAMP-2, or mannosidase α (Figure 2E, lanes 2 and 4). In addition, the soluble fractions were not contaminated with nuclear proteins such as the transcription factor Wilms tumor 1 (Supplemental Figure 1E), indicating that the soluble short form of CatL did not come from the nuclear compartment. Interestingly, addition of LPS also induced expression of the 39-kDa pro-CatL, which is known to be secreted (Figure 2E and Supplemental Figure 1B). The ability of CatL mRNA to allow downstream AUG translation and thus generate cytoplasmic CatL was confirmed by transfecting *CatL*$^{-/-}$ fibroblasts with a cDNA in which the first AUG codon had been mutagenized (Supplemental Figure 1, F and G; ref. 5).

Loss of dynamin staining in podocytes correlates with the proteinuria and is CatL dependent. We next attempted to identify a target of cytoplasmic CatL. The computer-based algorithm PEPS (Prediction of Endopeptidase Substrates; ref. 11) identified the GTPase dynamin as a potential CatL substrate (data not shown). Dynamin is a large GTPase essential for the formation of clathrin-coated vesicles at the plasma membrane (12), and it has also been implicated in the regulation of actin dynamics in certain cell types (13). We first examined dynamin distribution in podocytes using immunogold EM. Dynamin antigenic sites were detected within the center of podocyte FPs (Figure 3A, left, asterisk) and in electron-dense areas rich in cortical actin cytoskeleton (Figure 3A, left, a). In addition, a high-power view localized dynamin on the cytoplasmic side of vesicular structures, which are most likely clathrin-coated pits (Figure 3A, right, v). Next, we examined dynamin staining in mice before and after LPS treatment. As expected based on the EM data, immunocytochemistry in control mice detected dynamin staining in glomeruli (Figure 3B, left), in a pattern consistent with podocyte expression. Twenty-four hours after a single LPS injection, dynamin labeling in the glomerulus appeared weaker and clustered (Figure 3B, middle panel), but it remained unchanged in tubules (data not shown). A similar dynamin staining pattern was observed in a rat model for proteinuric kidney disease in which animals are injected with puromycin aminonucleoside (PAN) (Supplemental Figure 2A; ref. 14), suggesting that changes in glomerular dynamin staining are associated with proteinuria. Importantly, dynamin staining was preserved in *CatL*$^{-/-}$ mice treated with

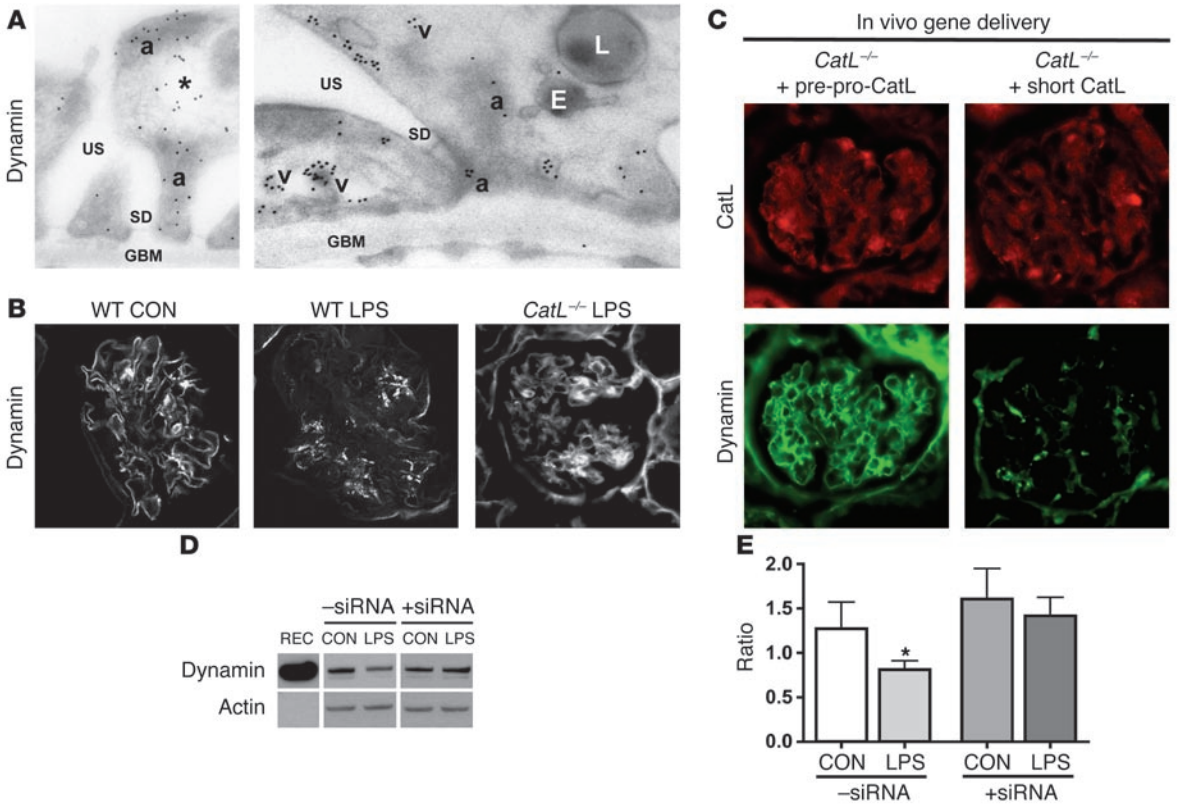

Figure 3
Altered dynamin staining in glomerulus after LPS treatment is CatL dependent. (**A**) Immunogold analysis of dynamin in podocyte FPs of rat glomerulus. Low-power view (left) depicts dynamin within the center of podocyte FPs (asterisk) as well as in electron-dense areas rich of cortical actin (a) (original magnification, ×30,000). High-power view shows gold particles, which are associated with the cytoplasmic side of vesicles (v) and with electron-dense actin areas (a) (original magnification, ×45,000). E, endosome; GBM, glomerular basement membrane; Ly, lysosome; SD, slit diaphragm; US, urinary space. (**B**) Immunocytochemistry of dynamin in glomeruli of *WT* mice before and after injection of LPS and of *CatL*$^{-/-}$ mice after injection of LPS. (**C**) Immunocytochemistry of samples from *CatL*$^{-/-}$ mice for glomerular dynamin and CatL. *CatL*$^{-/-}$ mice had been reconstituted with either Pre-Pro-CatL (left) or with short CatL (right) using transient gene transfer. Twenty-four hours after gene transfer, glomeruli were stained using anti-CatL and anti-dynamin hudy 1 antibody. Original magnification, ×400 (**B** and **C**). (**D**) Immunoblot of endogenous dynamin in cultured podocytes in response to LPS. Recombinant dynamin (REC), extracts of *WT* and *CatL*$^{-/-}$ podocytes, were analyzed. (**E**) Quantitation of dynamin in cell extracts shown in **D**. Dynamin signal was adjusted to actin levels.

LPS (Figure 3B, right). We hypothesize that the alteration of dynamin staining in vivo is due to proteolysis by cytoplasmic CatL. To investigate this possibility, DNAs encoding for short-form CatL or pre-pro-CatL were injected in *CatL*$^{-/-}$ mice using transient gene delivery (15, 16). Both DNA constructs led to glomerular CatL expression (Figure 3C, top row). Strikingly, expression of the short CatL specifically altered dynamin staining in a manner similar to that seen with LPS (Figure 3C, bottom row). Together with the fact that dynamin is a substrate of CatL in vitro (see below), these data are consistent with dynamin being cleaved by CatL in kidney after LPS treatment. Because isolated glomeruli from animals also contain other resident cells, we quantified dynamin abundance before and after LPS treatment using cultured podocytes. Western blotting of podocyte lysates revealed an approximately 30% decrease in the amount of endogenous dynamin after LPS treatment (Figure 3, D and E). Dynamin reduction was CatL dependent, since it did not occur when *CatL* was downregulated using siRNA (Figure 3D and Supplemental Figure 2, B and C). Together, these data suggest that the cytoplasmic CatL targets dynamin in rodent models of proteinuria.

CatL cleaves dynamin:GTP in vitro and in vivo. If dynamin is a CatL target in the cytoplasm, then recombinant dynamin should be cleavable by CatL at neutral pH. The PEPS algorithm identified a potential recognition sequence (ELSGGA) within dynamin between amino acids 354 and 359. Interestingly, the ELSGGA motif is highly conserved among several species (Figure 4A). CatL did not cause significant cleavage of dynamin at pH 7.0 (Figure 4C, compare lanes 1 and 2). Strikingly, addition of GTP resulted in the generation of a prominent proteolytic fragment with a molecular weight of approximately 40 kDa (p40) (Figure 4C, lane 3). p40 is the predicted size of the N-terminal fragment after cleavage at the ELSGGA sequence (Figure 4A). Another fragment, p55, is observed in the absence of added protease (Figure 4C, lane 1). Thus, p55 is not a precursor of p40. Furthermore, incubation of dynamin with CatB generated p55 in a nucleotide-independent manner (Figure 4C, lanes 5–8), whereas the protease furin was unable to cleave dynamin (Figure 4C, lanes 9–12). Thus, while p55 is produced by a number of proteases and thus represents a "hot spot" for proteolysis (17), p40 is generated by CatL *only* when dynamin is in the GTP-bound conformation. Interestingly, addition of

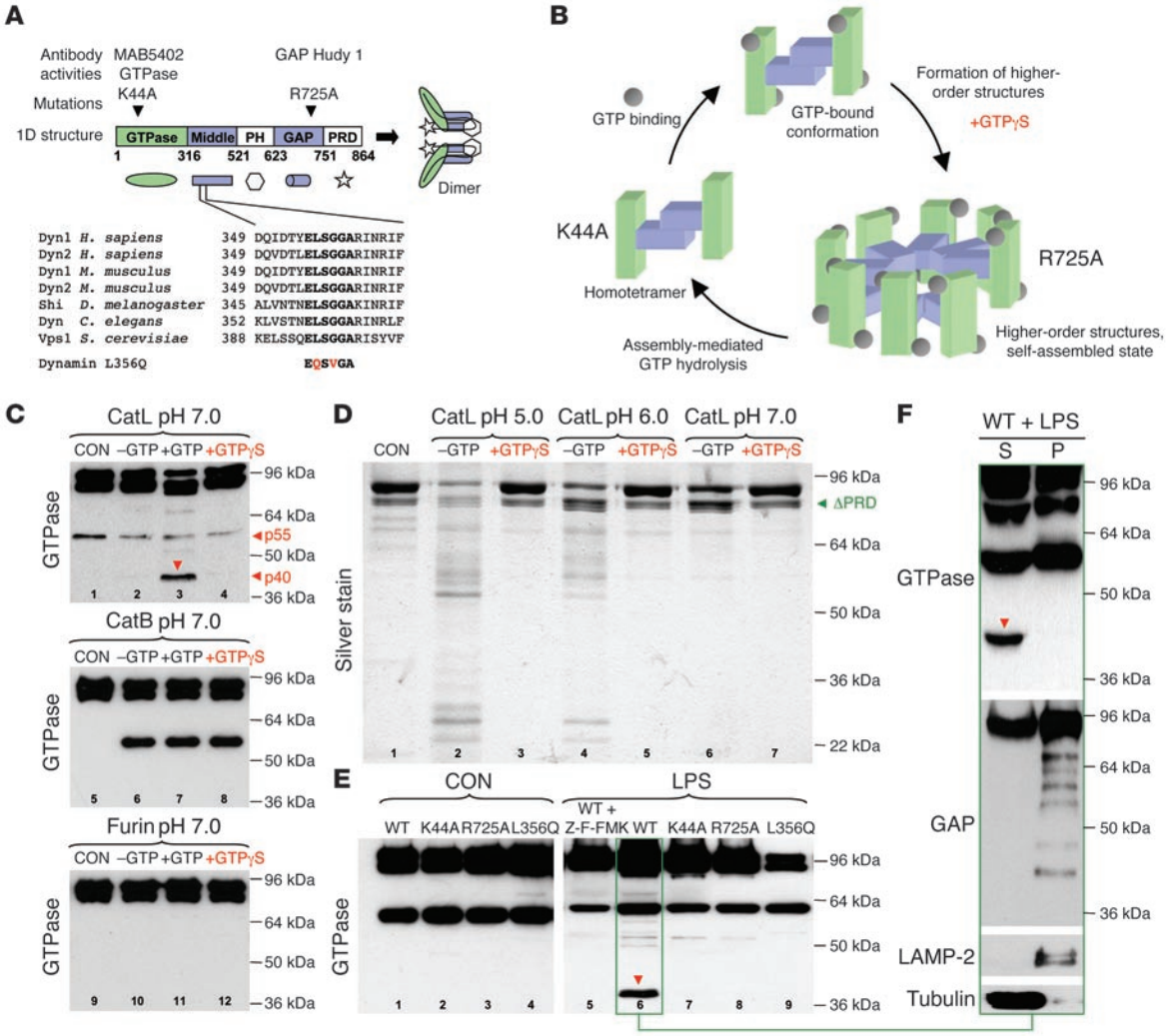

Figure 4

Effects of the nucleotide-bound and assembly state of dynamin on CatL cleavage in vitro and in vivo. (**A**) Domain structure of dynamin, corresponding antibodies, and amino acid sequence of predicted CatL cleavage sites. Note that the ELSGGA sequence is a highly conserved motif throughout the species. PH, pleckstrin homology domain; PRD, proline-arginine rich domain; Shi, dynamin homolog in *Drosophila*; Vsp1, dynamin homolog in yeast. (**B**) Schematic depiction of dynamin GTPase cycle. In its basal state, dynamin is a homotetramer. Self-assembly into higher-order structures such as rings or spirals can be promoted by GTPγS and activates assembly-mediated GTP hydrolysis, which in turn drives disassembly. Dynamin's middle domain is located inside the spiral. (**C**) Recombinant dyn1 (20 pmol) (CON) was mixed with CatL (1 pmol) (top panel), CatB (middle panel), or Furin (bottom panel). The reactions were performed at pH 7.0 under nonassembly conditions (200 mM NaCl). Where indicated, 200 μM GTP or 1 mM GTPγS was present. Proteolytic products were detected by monoclonal anti-dynamin antibody against the GTPase domain. (**D**) Silver staining of recombinant dyn1 incubated with CatL at different pHs in the presence or absence of GTPγS. (**E**) Western blot analysis using GTPase antibody of podocyte extracts infected with various dynamin mutants before or after addition of 100 μg/ml LPS for 20 hours. Note the appearance of a 40-kDa fragment (arrow). When indicated, podocytes were treated with 1 μM of the selective CatL inhibitor Z-FF-FMK for the duration of the LPS treatment. (**F**) Western blot analysis of subcellular fractionation of podocytes expressing dyn^{WT} for 24 hours after LPS treatment. Extracts were blotted using antibodies against the GTPase domain (N-terminal), GAP domain (C-terminal), LAMP-2, and tubulin.

GTPγS (nonhydrolyzable GTP analog) did *not* stimulate cleavage by CatL (Figure 4C, lane 4). These data can be explained in terms of dynamin's oligomerization status. In its basal state, dynamin is a homotetramer that can self-associate into rings or spirals when bound to GTP (Figure 4B). These higher-order dynamin structures exhibit elevated GTPase activity, which in turn drives their disassembly. GTPγS stabilizes oligomerized dynamin due to inhibition of GTP hydrolysis (18). Dynamin oligomerization is mediated by the middle and GAP domains of dynamin (19), and based on a cryo-EM reconstruction of assembled dynamin (20), amino acids ELSGGA (located in the middle domain) are predicted to be inaccessible when dynamin is self-assembled (Figure 4B). To test the idea that dynamin self-assembly protects against CatL cleavage, we performed additional cleavage experiments at an acidic pH where CatL is more active. At pH 5.0 and 6.0, CatL was highly reactive toward recombinant dynamin, even in the absence of GTP (Figure 4D, lanes 2 and 4). Strikingly, this proteolysis was inhibited by addition of GTPγS (Figure 4D, lanes 3 and 5). Together, our data

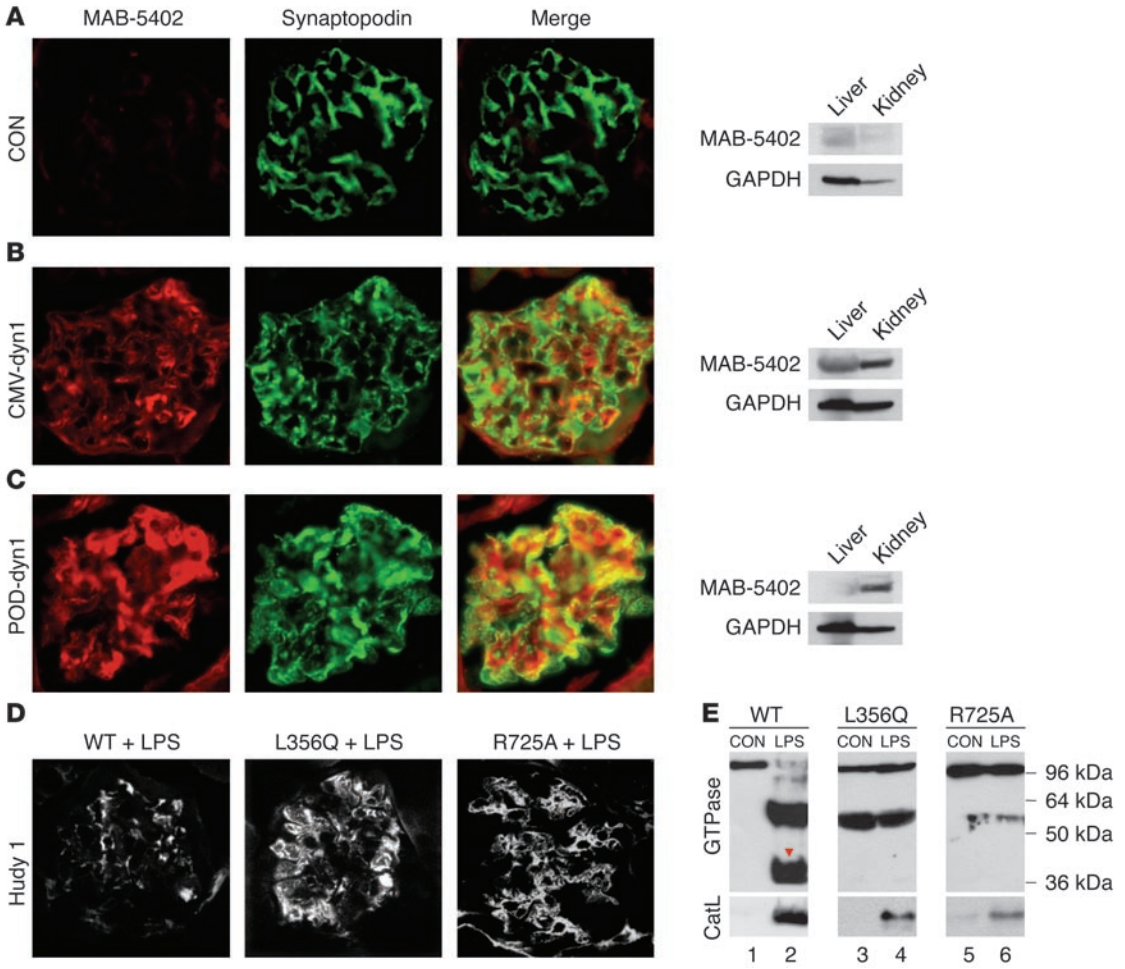

Figure 5
LPS-induced dynamin cleavage in mouse kidneys. (**A**–**C**) Double immunofluorescence of dyn1 (MAB-5402 antibody; red) and the podocyte marker synaptopodin (green). Mice were injected with podocin-driven expression vector lacking the dynamin gene (**A**), CMV-dyn1 expression vector (**B**), and POD-dyn1 expression vector (**C**). Western blot analysis of total kidney and liver extracts isolated from animals injected with different cDNAs as indicated in the figure. (**D**) Immunocytochemistry of glomeruli from mice that were injected with LPS. Twenty-four hours after LPS injections, animals received cDNA expressing dyn^{WT}, dyn^{L356Q}, and dyn^{R725A} and were sacrificed 14 hours later. Glomeruli were stained using monoclonal anti-dynamin hudy 1 antibody. Original magnification, ×400 (**A**–**D**). (**E**) Western blot analysis of kidney extracts after gene delivery of different dyn1 cDNAs using the GTPase and CatL antibody before and after addition of LPS.

are consistent with the hypothesis that the primary site recognized by CatL is within a domain that becomes inaccessible upon dynamin self-assembly.

To further explore CatL-mediated dynamin cleavage, we infected cultured podocytes with adenoviruses encoding different dynamin mutants (Figure 4A) and subsequently treated them with LPS. As expected, addition of LPS to cells expressing dyn^{WT} resulted in generation of p40 (Figure 4E, lane 6), which was inhibited by the addition of the CatL inhibitor Z-FF-FMK (Figure 4E, lane 5). Importantly, LPS treatment of podocytes expressing dyn^{K44A} (a mutant that cannot bind GTP) did not result in detectable levels of p40 (Figure 4E, lane 7), consistent with our data that in vitro cleavage of dynamin by CatL at neutral pH is GTP dependent. To confirm the identity of the cleavage site, we created dyn^{L356Q}, in which the ELSGGA sequence was mutated to EQSVGA. The addition of LPS to cultured podocytes overexpressing dyn^{L356Q} yielded no p40 (Figure 4E, lane 9). Finally, we examined a GTPase-defective dynamin mutant carrying a mutation in its GAP domain (dyn^{R725A}). This mutant dynamin oligomerizes, but is impaired in assembly-stimulated GTP hydrolysis (Figure 4B; ref. 19). dyn^{R725A} is therefore predicted to live longer in the assembled state. Consistent with our model, LPS treatment of cells expressing dyn^{R725A} did not generate p40 (Figure 4E, lane 8). To demonstrate that dynamin cleavage by CatL occurred in the cytoplasm, we performed subcellular fractionation experiments. Thus, the N-terminal p40 was detected only in the supernatant fraction (Figure 4F, left lane, GTPase), whereas the C-terminal part of dynamin was found degraded in the pellet fraction (Figure 4F, right lane, GAP). Together, these data support a model in which CatL specifically targets the GTP-bound form of dynamin in the cytoplasm by recognizing an evolutionally conserved ELSGGA motif and that dynamin self-assembly into higher-order structures such as rings or spirals prevents CatL cleavage.

To demonstrate that dynamin is cleaved by cytoplasmic CatL during proteinuric kidney disease, we looked for p40 in mouse kid-

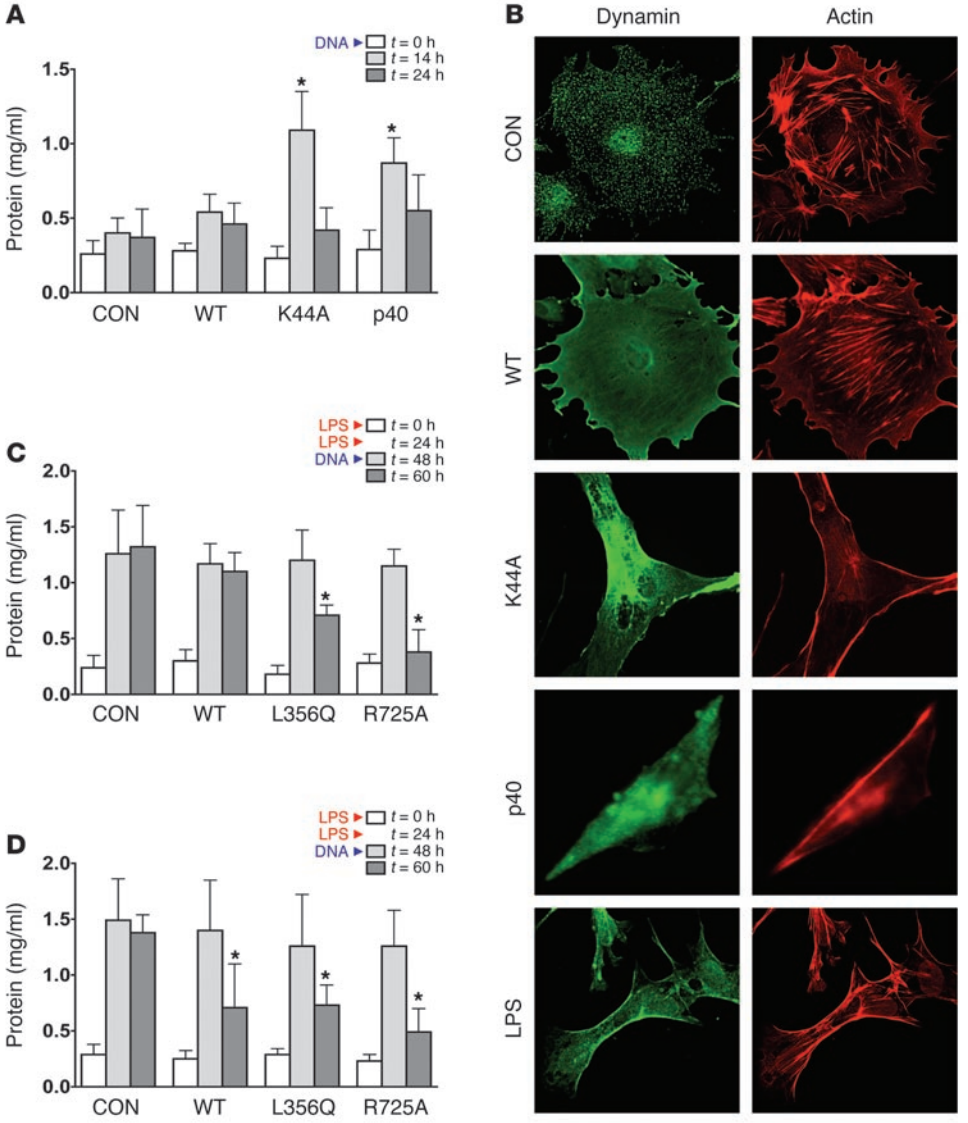

Figure 6
The effects of dynamin mutants on proteinuria and podocyte morphology. (**A**) Urinary protein levels determined using the standard Bradford protein assay. Urine was collected immediately before (0 h) and 14 and 24 hours after injection of podocin-driven expression vectors containing different dynamin constructs as indicated in the figure. Each bar represents at least 10 animals. (**B**) Cultured podocytes were infected with adenoviruses expressing the indicated dynamin constructs. Eighteen hours after infection, cells were stained with hudy 1 (green) to visualize dynamin and rhodamine phalloidin (red) to visualize F-actin. (**C**) Urinary protein levels determined using the standard Bradford protein assay. Mice were injected at 0 and 24 hours with LPS to induce proteinuria. At 48 hours (peak proteinuria), mice received empty vector, CMV-dyn^{WT}, CMV-dyn^{L356Q}, or CMV-dyn^{R725A}. Urinary protein levels were determined 12 hours after injection. Each data point represents at least 10 animals. (**D**) Urinary protein levels determined using the standard Bradford protein assay. Mice were injected at 0 and 24 hours with LPS to induce proteinuria. At 48 hours (peak proteinuria), mice received empty vector, POD-dyn^{WT}, POD-dyn^{L356Q}, or POD-dyn^{R725A}. Urinary protein levels were determined 12 hours after injection. Each bar represents at least 10 animals.

ney extracts after LPS treatment. Since the GTPase antibody, which recognizes p40, was not sufficiently sensitive to detect endogenous dynamin cleavage fragments (data not shown), we used a gene-delivery protocol to express dynamin in mouse kidneys (15, 16). We delivered dyn1 because overexpression of dyn2 sometimes induces apoptosis (21). rt-PCR showed that podocytes normally express *dyn2* (ubiquitous form) and some *dyn3* (predominantly expressed in testis), but no *dyn1* (neuronal isoform; Supplemental Figure 3A). Dyn1 was expressed from a CMV promoter (CMV-dyn) or from the podocyte-specific podocin promoter (POD-dyn; ref. 22). Gene-delivered dyn1 was distinguished from endogenous dyn2 using the monoclonal dynamin antibody MAB-5402, which predominantly recognizes dyn1 (Supplemental Figure 3B). As expected, MAB-5402 weakly stained control glomeruli (Figure 5A), whereas it strongly stained glomeruli 14 hours after delivery of CMV-dyn1 (Figure 5B) or POD-dyn1 (Figure 5C). The CMV promoter directed expression of dyn1 in the liver and kidney (Figure 5B, Western blot), and dyn1 was detected in virtually all resident cell types of the glomerulus including podocytes, as seen from colocalization with synaptopodin (Figure 5B, Merge). In contrast, the podocin promoter directed expression exclusively in the kidney (Figure 5C, Western blot), and dyn1 localized predominantly in podocytes (Figure 5C, Merge). The presence of dyn1 in FPs of podocytes was demonstrated using EM (Supplemental Figure 3C). Importantly, LPS treatment led to altered staining of gene-delivered dyn1^{WT} in glomeruli, whereas the staining of dyn^{L356Q} and dyn^{R725A} remained unchanged (Figure 5D). Moreover, LPS treatment resulted in generation of p40, but only in mice expressing dyn^{WT} (Figure 5E, lane 2) and not in mice expressing dyn^{L356Q} and dyn^{R725A} (Figure 5E, lanes 4 and 6). Generation of p40 required the presence of CatL, since it was not detected in *CatL*$^{-/-}$ mice injected with LPS (Supplemental Figure 3D). Western blotting also detected a dynamin fragment of approximately 55 kDa. As in cultured podocytes, the presence of this fragment was LPS and CatL independent (Figure 5E, lanes 3 and 5, and Supplemental Figure 3D), supporting the idea that it is generated by other proteases during extract preparation. These experiments extend our observations in the cultured podocytes and indicate that LPS induces CatL-dependent cleavage in live mice.

Dynamin is required for normal glomerular function. The hypothesis that cleavage of dynamin by CatL leads to proteinuria implies that

dynamin is essential for podocyte morphology in healthy kidneys. In support of this notion, expression of dominant-negative dyn^{K44A} in mouse podocytes caused severe proteinuria (Figure 6A and Supplemental Table 1) and FP effacement (Supplemental Figure 4B, 14 hours). Proteinuria and FP effacement were maximum 14 hours after gene delivery and returned to baseline after loss of dyn^{K44A} expression (Supplemental Figure 4, A and B, and data not shown). Expression of dyn^{WT} did not cause changes in FP architecture (data not shown) or significant proteinuria (Figure 6A and Supplemental Table 1), demonstrating specificity of the dyn^{K44A} phenotype. Importantly, expression of p40 also caused proteinuria (Figure 6A and Supplemental Table 1), demonstrating that this dynamin fragment has dominant-negative characteristics with respect to podocyte function.

Since podocyte FP effacement is primarily driven by the rearrangement of the actin cytoskeleton (23), we examined actin morphology in cultured podocytes expressing dyn^{K44A} and p40. Podocytes were infected using an adenoviral expression system, which allows greater than 90% infection efficiency (24). The experiments were performed using the neuronal isoform of dyn1 (Figure 6B) as well as the ubiquitously expressed dyn2 (Supplemental Figure 5). The 2 isoforms yielded identical results, demonstrating that the observed phenotypes in podocytes were not isoform specific (compare F-actin staining in cells expressing dyn^{WT} and dyn^{K44A} in Figure 6B and Supplemental Figure 5). Podocyte actin is organized in parallel bundles of stress fibers and a cortical ring of filamentous actin (Figure 6B, CON). Expression of dyn^{WT} did not significantly alter the F-actin staining pattern (Figure 6B, WT). In contrast, the expression of dyn^{K44A} or p40 abolished stress fibers while enhancing the cortical actin web, resulting in a polygonal cellular shape (Figure 6B). Similar actin and cell morphology phenotypes were associated with LPS (Figure 6B) and PAN treatments (25). Thus, occurrence of proteinuria in mice expressing dyn^{K44A} or p40 (Figure 6A) correlates with changes in podocyte morphology due to changes in actin cytoskeleton (Figure 6B).

If dynamin is a target of CatL, then dyn^{L356Q} and dyn^{R725A}, which are resistant to CatL cleavage, might be beneficial during LPS-induced proteinuria. At peak proteinuria (48 hours after initial LPS), mice were injected with empty vector, dyn^{WT}, dyn^{L356Q}, or dyn^{R725A} either from the CMV promoter (Figure 6C) or the podocin promoter (Figure 6D), and the degree of proteinuria was analyzed 12 hours after DNA injection. Strikingly, expression of dyn^{R725A} led to almost complete resolution of proteinuria, whereas expression of dyn^{L356Q} reduced proteinuria by approximately 50% (Figure 6, C and D; 60-hour time point). Interestingly, while CMV-dyn^{WT} had no affect on proteinuria (Figure 6C), podocin-driven expression reduced proteinuria by 50% (Figure 6D). The ability of POD-dyn^{WT} to overcome proteinuria is likely due to the higher level of podocyte-specific dynamin expression expected from the podocin promoter. Indeed, kidney extracts from animals expressing POD-dyn^{WT} contained the same level of dynamin as extracts from animals expressing CMV-dyn^{WT}, even though the latter was expressed in all cell types in the glomerulus (Figure 5, B and C). Thus, while expression of a high level of dyn^{WT} can partially reverse LPS-induced FP effacement, dyn^{L356Q} and dyn^{R725A} are more potent. Interestingly, dyn^{R725A} is the most powerful, most likely due to restoration of optimal cellular levels of dynamin:GTP.

Discussion

In this study, we investigated the role of the protease CatL and the large GTPase dynamin in healthy and diseased kidney podocytes. We show that dynamin is normally required to maintain the ultrafiltration barrier in kidneys, possibly via regulation of the actin cytoskeleton in podocytes. Using a mouse model for inducible kidney failure, we found that cleavage of dynamin by a cytoplasmic form of CatL leads to podocyte failure and proteinuria. Gene delivery of CatL-resistant dynamin mutants can prevent and even reverse proteinuria. Our data define a new role for cytoplasmic CatL (trigger) and dynamin (target) in the pathogenesis of glomerular proteinuria and open new potential avenues for pharmacological intervention of kidney disease.

Previous inhibitor studies suggested that CatL is involved in proteinuric kidney disease (4), and our current (Figure 1D) and previous work (3) has shown that CatL is upregulated in rodent models for nephropathy. Consistent with these findings, we observed an increase in levels of glomerular *CatL* mRNA in a number of human proteinuric diseases (Figure 1A) that correlated with a dramatic increase in the protein level in glomeruli (Figure 1C). Using knockout mice, we provide definitive evidence that CatL is essential to cause nephropathy in response to LPS in a mouse model (Figure 1, D–F). Furthermore, we have shown that after LPS treatment, CatL appears in the cytoplasm, due to expression of the short form of the protein. Together, the data indicate that localization of CatL to the cytoplasm represents a key event in the induction of glomerular kidney disease. Consistent with this model, we show that dynamin, a cytoplasmic protein, is essential for kidney function and that it is cleaved by CatL after LPS treatment. Importantly, the dynamin p40 fragment generated by CatL cleavage functions as a dominant-negative inducer of proteinuria. Thus, the activity of the cytoplasmic CatL, in contrast to its lysosomal counterpart, seems to be specific and to yield a functional product (p40). These data argue that complete destruction of dynamin is not necessarily required to cause kidney failure.

Intriguingly, the CatL cleavage site is highly conserved among dynamin family members (Figure 4A), and its accessibility is suppressed by dynamin oligomerization. Moreover, cytoplasmic CatL targets only the GTP-bound form of dynamin, implying that only a portion of dynamin is cleaved in vivo. Our previous experiments indicate that dynamin:GTP is the active form of the enzyme (19, 26), so it is tempting to speculate that CatL functions to switch off dynamin much like the result of dynamin self-assembly. It remains to be seen whether this novel switch-off mechanism is ever used during normal cell physiology.

EM revealed 2 populations of actin in FPs of podocytes; one is the actin bundle running above the level of slit diaphragms, and the other is the cortical actin network located beneath the plasmalemma (27). Our data show that dynamin colocalizes with both of these populations (Figure 3B). It appears that FPs have the molecular makeup for constant morphological rearrangement in order to accommodate glomerular filtration. This membrane reshaping is most likely driven by rapid changes in the actin network (28), and our study suggests that it requires functional dynamin. On its C terminus, dynamin contains a proline-arginine rich domain (PRD) that binds directly to the Src homology 3 (SH3) domains of multiple proteins, some of which are actin-regulating or -binding proteins including profilin, Nck, Grb2, syndapin, intersectin, cortactin, mABP1, and tuba (reviewed in ref. 13). It is through these interactions that dynamin is thought to coordinate membrane remodeling and actin filament dynamics during endocytosis, cell morphogenesis, and cell migration. Despite these links between dynamin and actin, it is still unclear how exactly dynamin regulates

actin dynamics. Our results identify podocytes, with their complex actin dynamics, as an appropriate cell type for investigating the interplay between dynamin's role in endocytosis and its ability to regulate the actin cytoskeleton. Indeed, formation of a cortical actin cytoskeleton in cells expressing dyn^{K44A} or p40 or that have been treated with LPS (Figure 6B) could result from the inhibition of endocytosis, misregulation of actin dynamics, or both. While at present we have no direct evidence for a direct connection between actin and dynamin, addition of LPS does not inhibit endocytosis in cultured podocytes (Supplemental Figure 6), suggesting that loss of endocytosis per se is not sufficient to generate a cortical actin network. In agreement with this conclusion are experiments showing that expression of a known endocytosis inhibitor, dominant-negative $auxilin^{H875Q}$ (29), impaired endocytosis to the same extend as dyn^{K44A} (Supplemental Figure 6A), yet it did not alter actin morphology (Supplemental Figure 6B). In addition, nondifferentiated podocytes contained predominantly cortical actin (Supplemental Figure 6B), yet they exhibited WT levels of endocytosis (Supplemental Figure 6A). In sum, there seems to be no correlation between levels of endocytosis and actin dynamics in podocytes, raising the possibility that dynamin mutants might primarily act on podocyte actin dynamics. This conclusion is also in line with the observation that CatL reduced endogenous dynamin by only 30% (Figure 3D), possibly maintaining dynamin's role in endocytosis. Regardless of these observations, dynamin is clearly present on clathrin-coated pits in podocytes (Figure 3A), and changes in endocytosis have been implicated in some forms of podocyte failure (30). Clearly, more work is needed to define the exact role(s) of dynamin in podocytes.

Proteinuria was resolved by expression of dyn^{R725A}, dyn^{L356Q}, and to some degree dyn^{WT}. While our study shows that dynamin is efficiently delivered and expressed in podocytes, it is unlikely that every podocyte received dynamin. We propose that damaged podocytes may be particularly amenable to uptake of DNA presented in polymers (8, 31). Alternatively, it is conceivable that the effects of gene-delivered dynamin has multiple effects in podocytes. For example, it seems possible that restoration of podocyte actin has a salutary effect on the slit diaphragm function. Finally, gene-delivered dynamin in podocytes may have a non–cell-autonomous effect on other resident glomerular cells such as glomerular endothelial cells. Whatever the precise mechanism, the use of dynamin mutants as a treatment for human kidney disease is an attractive subject for future experiments.

Methods

Cells, antibodies, reagents, and standard techniques. Mouse podocyte cell lines were grown as described previously (32). Dynamin antibodies included anti-dynamin (hudy 1) from Upstate Technology; mouse anti-dyn1 5402 from Chemicon; VAM-SV041 from Stressgen. Two rabbit antisera against CatL were used as described previously (8, 33). $CatL^{-/-}$ fibroblasts were maintained as described previously (34). Stable CatL-knockdown cell lines were generated with a vector-based siRNA directed against CatL (target sequence 5′-GTGGACTGTTCTCACGCT-3′). Quantitative PCR was performed on an Applied Biosystems 7300 Real-Time PCR System. Fold expression changes were calculated using the comparative C_T method for relative quantitation with the equation $2^{-\Delta\Delta CT}$. Protein expression levels for dynamin and CatL were calculated using results of densitometric analysis from 7 independent experiments with Kodak 1D Image Analysis software. Statistical significance was assessed with the unpaired Student's *t* test with Welch's correction. *P* less than 0.05 was considered statistically significant. Transfections with CatL constructs were performed using Lipofectamine 2000 (Invitrogen). Immunocytochemical analysis of cultured podocytes was performed as described previously (3). BIOMOL CV-CatL/B activity kit was utilized as described in the manufacturer's instructions. The fluorophore cresyl violet [CV-$(FR)_2$] substrate becomes florescent after CatL/B cleavage of the attached Phe-Arg groups. This substrate easily penetrates the cell membrane and the membranes of the internal cellular organelles, enabling the detection of cathepsin activity within living podocytes. Immunoperoxidase labeling of human tissue was done on formalin-fixed kidney biopsy samples embedded in paraffin. Transmission electron microscopy and immunoelectron microscopy were performed as described previously (35). Subcellular fractionation was performed as described (36).

Animals and treatments. All animal studies were approved by the MGH Subcommittee for Research Animal Care. *C57BL/6* mice were obtained from The Jackson Laboratory. *CatL*$^{-/-}$ mice were on a pure *C57BL/6* background (10). The mouse model LPS-induced proteinuria was utilized as previously described (3). The rat PAN nephrosis model was induced as described (37).

Patients and quantitative glomerular rt-PCR. Microdissected glomeruli from patients with proteinuric diseases and from control subjects were analyzed. Biopsies were obtained from patients and donors after informed consent and with approval of the local ethical committees. For control biopsies, renal tissue was derived from pretransplantation kidney biopsies during cold ischemia time from 7 living and 1 cadaveric donor ($n = 8$) (38). Statistical analysis was performed using the Kruskal-Wallis test and Mann-Whitney *U* test. *P* less than 0.05 was considered statistically significant.

Processing of dynamin by CatL in vitro. Recombinant dynamin was purified as described previously (39). One microgram of dynamin (10 pmol) was diluted in buffer containing 200 mM NaCl, 10 mM HEPES pH 7.0, 2 mM EGTA, 1 mM $MgCl_2$, and 1 mM DTT. When indicated, 200 μM of GTP or 1 mM of $GTP\gamma S$ was added, and dynamin was allowed to bind nucleotides for 10 minutes on ice. The reaction was initiated by addition of 0.5 μl of purified CatL (specific activity 4.13 U/mg of protein from Sigma-Aldrich), and samples were placed at 37°C in the water bath for 10 minutes. Total assay volume was 20 μl. The reaction was terminated with addition of E-64d inhibitor (Sigma-Aldrich) and sample buffer. For Western blot analysis, 5 μl of the samples was run on 10% SDS-PAGE. When CatB (specific activity 3.00 U/mg of protein from Sigma-Aldrich) or recombinant human furin (from R&D Systems) were used, 2 μl of the enzymes were added in the assay.

Adenoviral infections of cultured podocytes. Podocytes were grown to 70% confluency. Cells were washed twice with 1× PBS and infected with 1.2 ml of serum-free DMEM medium containing 100 μl transactivator virus and 100 μl virus expressing dyn1 or dyn2. After 2 hours of infection at 37°C, medium containing virus was replaced with full DMEM. If cells were treated with LPS or PAN, 50 μg/ml of LPS or 50 μg/ml PAN was added at this point. Eighteen to 24 hours after infection, cells were detached using trypsin and either processed for subcellular fractionation or tested in the motility assays as described in ref. 3. When indicated, 20 μM of Z-FF-FMK CatL specific inhibitor (Calbiochem) was added simultaneously with LPS.

Kidney extracts. Four mouse kidneys were homogenized in buffer containing 20 mM HEPES pH 7.5, 100 mM NaCl, 1 mM $MgCl_2$, 1 mM PMSF, proteinase inhibitors, calpain inhibitor (Calbiochem), and E-64d using Dounce homogenizer. Subsequently, cytosol was centrifuged for 10 minutes at 4,600 *g*. Proteins were solubilized by 1% Triton X, 1 hour at 4°C, before it was spun at 70,000 *g* for 1 hour.

In vivo gene delivery. CatL plasmids encoding short and long CatL (5), dyn1 plasmids (all pcDNA), or p2.5 podocin-promoter driven (22) were introduced into mice ($n > 10$, each construct) using the *Trans*IT in vivo gene delivery system according to the manufacturer's instructions (Mirus). Proteinuria was assessed using Multistix 8 SG strips (Bayer) (data not shown) and the Bradford protein assay (Sigma-Aldrich).

Acknowledgments

This work was supported by the American Society for Nephrology (to S. Sever and J. Reiser) and the NIH (R01 DK64787 to S. Sever and R01 DK073495 to J. Reiser). J. Reiser was also supported by the KMD foundation. M.M. Altintas was supported by an NIH training grant and T32DK007540, and C.C. Möller by a Deutscher Akademischer Austausch Dienst (DAAD) Predoctoral Scholarship. The authors are grateful for the analysis of CatL cleavage sites by Thomas Reinheckel and Tobias Lohmueller, University of Freiburg. The authors are indebted to Johannes Walter for critically reading the manuscript. The fluorescence and electron microscopy work was performed in the Microscopy Core facility of the MGH Program in Membrane Biology, supported by an NIH Program Project grant (DK38452), the NIH Boston Area Diabetes and Endocrinology Research Center (DK57521), and the NIH Center for the Study of Inflammatory Bowel Disease (DK43341). We thank all members of the European Renal cDNA Bank and their patients for their support (for participating centers at the time of the study see ref. 38).

Received for publication March 5, 2007, and accepted in revised form May 9, 2007.

Address correspondence to: Sanja Sever or Jochen Reiser, Department of Medicine, Nephrology Division and Program in Glomerular Disease, MGH and Harvard Medical School, MGH-East, CNY-149, 13th Street, Boston, Massachusetts 02129, USA. Phone: (617) 724-8922; Fax: (617) 726-5669; E-mail: ssever@partners.org (S. Sever). Phone: (617) 726-9363; Fax: (617) 726-5669; jreiser@partners.org (J. Reiser).

Mehmet M. Altintas, Sharif R. Nankoe, and Clemens C. Möller contributed equally to this work.

1. Zandi-Nejad, K., Eddy, A.A., Glassock, R.J., and Brenner, B.M. 2004. Why is proteinuria an ominous biomarker of progressive kidney disease? *Kidney Int. Suppl.* **66**:S76–S89.
2. Tryggvason, K., Patrakka, J., and Wartiovaara, J. 2006. Hereditary proteinuria syndromes and mechanisms of proteinuria. *N. Engl. J. Med.* **354**:1387–1401.
3. Reiser, J., et al. 2004. Podocyte migration during nephrotic syndrome requires a coordinated interplay between cathepsin l and alpha3 integrin. *J. Biol. Chem.* **279**:34827–34832.
4. Baricos, W.H., O'Connor, S.E., Cortez, S.L., Wu, L.T., and Shah, S.V. 1988. The cysteine proteinase inhibitor, E-64, reduces proteinuria in an experimental model of glomerulonephritis. *Biochem. Biophys. Res. Commun.* **155**:1318–1323.
5. Goulet, B., et al. 2004. A cathepsin L isoform that is devoid of a signal peptide localizes to the nucleus in S phase and processes the CDP/Cux transcription factor. *Mol. Cell.* **14**:207–219.
6. Cohen, C.D., and Kretzler, M. 2003. Gene-expression analysis of microdissected renal biopsies. *Methods Mol. Med.* **86**:285–293.
7. Olbricht, C.J., Cannon, J.K., and Tisher, C.C. 1987. Cathepsin B and L in nephron segments of rats with puromycin aminonucleoside nephrosis. *Kidney Int.* **32**:354–361.
8. Ahn, K., et al. 2002. An alternate targeting pathway for procathepsin L in mouse fibroblasts. *Traffic.* **3**:147–159.
9. Asanuma, K., Shirato, I., Ishidoh, K., Kominami, E., and Tomino, Y. 2002. Selective modulation of the secretion of proteinases and their inhibitors by growth factors in cultured differentiated podocytes. *Kidney Int.* **62**:822–831.
10. Nakagawa, T., et al. 1998. Cathepsin L: critical role in Ii degradation and CD4 T cell selection in the thymus. *Science.* **280**:450–453.
11. Lohmuller, T., et al. 2003. Toward computer-based cleavage site prediction of cysteine endopeptidases. *Biol. Chem.* **384**:899–909.
12. Kirchhausen, T. 2000. Three ways to make a vesicle. *Nat. Rev. Mol. Cell Biol.* **1**:187–198.
13. Schafer, D.A. 2004. Regulating actin dynamics at membranes: a focus on dynamin. *Traffic.* **5**:463–469.
14. Inokuchi, S., et al. 1996. Re-evaluation of foot process effacement in acute puromycin aminonucleoside nephrosis. *Kidney Int.* **50**:1278–1287.
15. Mayer, G., Boileau, G., and Bendayan, M. 2003. Furin interacts with proMT1-MMP and integrin alphaV at specialized domains of renal cell plasma membrane. *J. Cell Sci.* **116**:1763–1773.
16. Moller, C.C., et al. 2007. Induction of TRPC6 channel in acquired forms of proteinuric kidney disease. *J. Am. Soc. Nephrol.* **18**:29–36.
17. Muhlberg, A.B., Warnock, D.E., and Schmid, S.L. 1997. Domain structure and intramolecular regulation of dynamin GTPase. *EMBO J.* **16**:6676–6683.
18. Akagi, Y., et al. 1997. Transcriptional activation of a hybrid promoter composed of cytomegalovirus enhancer and beta-actin/beta-globin gene in glomerular epithelial cells in vivo. *Kidney Int.* **51**:1265–1269.
19. Sever, S., Muhlberg, A.B., and Schmid, S.L. 1999. Impairment of dynamin's GAP domain stimulates receptor-mediated endocytosis. *Nature.* **398**:481–486.
20. Zhang, P., and Hinshaw, J.E. 2001. Three-dimensional reconstruction of dynamin in the constricted state. *Nat. Cell Biol.* **3**:922–926.
21. Fish, K.N., Schmid, S.L., and Damke, H. 2000. Evidence that dynamin-2 functions as signal-transducing GTPase. *J. Cell Biol.* **150**:145–154.
22. Moeller, M.J., Sanden, S.K., Soofi, A., Wiggins, R.C., and Holzman, L.B. 2003. Podocyte-specific expression of cre recombinase in transgenic mice. *Genesis.* **35**:39–42.
23. Verma, R., et al. 2006. Nephrin ectodomain engagement results in Src kinase activation, nephrin phosphorylation, Nck recruitment, and actin polymerization. *J. Clin. Invest.* **116**:1346–1359. doi:10.1172/JCI27414.
24. Damke, H., Freundlieb, S., Gossen, M., Bujard, H., and Schmid, S.L. 1995. Tightly regulated and inducible expression of a dominant interfering dynamin mutant in stably transformed HeLa cells. *Methods Enzym.* **257**:209–221.
25. Reiser, J., et al. 2000. Regulation of mouse podocyte process dynamics by protein tyrosine phosphatases. *Kidney Int.* **57**:2035–2042.
26. Sever, S., Damke, H., and Schmid, S.L. 2000. Dynamin:GTP controls the formation of constricted coated pits, the rate limiting step in clathrin-mediated endocytosis. *J. Cell Biol.* **150**:1137–1148.
27. Ichimura, K., Kurihara, H., and Sakai, T. 2003. Actin filament organization of foot processes in rat podocytes. *J. Histochem. Cytochem.* **51**:1589–1600.
28. Moeller, M.J., and Holzman, L.B. 2006. Imaging podocyte dynamics. *Nephron Exp. Nephrol.* **103**:e69–e74.
29. Sever, S., et al. 2006. Physical and functional connection between auxilin and dynamin during endocytosis. *EMBO J.* **25**:4163–4174.
30. Kim, J.M., et al. 2003. CD2-associated protein haploinsufficiency is linked to glomerular disease susceptibility. *Science.* **300**:1298–1300.
31. Eyre, J., et al. 2006. Statin-sensitive endocytosis of albumin by glomerular podocytes. *Am. J. Physiol. Renal Physiol.* **292**:F674–F681.
32. Mundel, P., et al. 1997. Rearrangements of the cytoskeleton and cell contacts induce process formation during differentiation of conditionally immortalized mouse podocyte cell lines. *Exp. Cell Res.* **236**:248–258.
33. Ishidoh, K., and Kominami, E. 1994. Multi-step processing of procathepsin L in vitro. *FEBS Lett.* **352**:281–284.
34. Hsieh, C.S., deRoos, P., Honey, K., Beers, C., and Rudensky, A.Y. 2002. A role for cathepsin L and cathepsin S in peptide generation for MHC class II presentation. *J. Immunol.* **168**:2618–2625.
35. Regele, H.M., et al. 2000. Glomerular expression of dystroglycans is reduced in minimal change nephrosis but not in focal segmental glomerulosclerosis. *J. Am. Soc. Nephrol.* **11**:403–412.
36. Damke, H., Baba, T., Warnock, D.E., and Schmid, S.L. 1994. Induction of mutant dynamin specifically blocks endocytic coated vesicle formation. *J. Cell Biol.* **127**:915–934.
37. Kim, S.W., et al. 2004. Increased expression and apical targeting of renal ENaC subunits in puromycin aminonucleoside-induced nephrotic syndrome in rats. *Am. J. Physiol. Renal Physiol.* **286**:F922–F935.
38. Schmid, H., et al. 2003. Gene expression profiles of podocyte-associated molecules as diagnostic markers in acquired proteinuric diseases. *J. Am. Soc. Nephrol.* **14**:2958–2966.
39. Damke, H., et al. 2001. Expression, purification, and functional assays for self-association of dynamin-1. *Methods Enzymol.* **329**:447–457.

V. EXPRESSION PATTERNS OF TRPC1 AND TRPC6 ORTHOLOGS IN ZEBRAFISH (*DANIO RERIO)*

V.1. Rationale

In an attempt to understand the complex functions of the kidney, investigators have taken advantage of tractable animal model systems. Lipopolysaccharide (LPS)-treated mice and puromycin aminonucleoside (PAN)-treated rats are well-established animal models used to study kidney pathologies. Another important group of animal models is represented by lower vertebrates such as the frog, *Xenopus laevis*, and the zebrafish, *Danio rerio*. In particular the latter is an emerging model system that becomes more and more widely used in basic life science research [Drummond, 2000].

The zebrafish offers a number of experimental advantages that make it a very attractive system for studies of kidney development and disease. First, zebrafish embryos develop in freshwater outside of the mother and are transparent, allowing observation of internal organs without dissection. Second, development occurs rapidly and embryos progress from fertilized eggs to free-swimming fish larvae in roughy 2.5 days. Third, zebrafish can be bred in very high numbers, which makes high-throughput approaches such as large-scale screening studies possible. Fourth, the sequencing of the zebrafish genome is nearing completion and has already yielded a huge body of genetic information that can be directly exploited in experiments, for example, by targeted disruption of single genes in order to assess their function. In comparison to gene knock-out in mice, which is a tedious and expensive task, zebrafish genes can be rapidly disrupted by morpholino anti-sense knock-down. Together, these features make the zebrafish a useful model for studying organ development and progression of disease, as well as the role of particular genes in these processes.

The simplicity of the kidney in developing zebrafish larvae, the zebrafish pronephros, makes the study of this organ particularly interesting [Drummond, 2003]. In contrast to human kidneys, which each contain up to one million nephrons organized in a very complex fashion, the zebrafish pronephros consists of only two nephrons with glomeruli fused at the midline, pronephic tubules connect directly to the glomeruli via a neck segment, and paired bilateral pronephric ducts that convey the blood filtrate outside the animal. While the functional pronepros is remarkably simple, it represents a fully-functioning organ and, in free-swimming larvae of fish and amphibians, it performs the essential kidney functions of blood filtration and regulation of blood pressure. This feature allows efficient mechanistic studies of the

kidney, looking on single nephrons. The zebrafish is a powerful tool that can be manipulated with ease to rapidly determine the function of genes and the importance of cell-cell interactions that underly the development of all kidney forms.

A recent study demonstrated that nephrin and podocyte orthologs are specifically expressed in zebrafish pronephric podocytes and are required for the development of pronephric podocyte cell structure [Kramer-Zucker *et al.*, 2005]. Disruption of nephrin or podocin expression in zebrafish resulted in a loss of slit diaphragms and failure to form normal podocyte foot processes.

Based on the potential of the zebrafish model system for the study of TRPC channel function in the kidney, the expression of TRPC6 and TRPC1 orthologs in the developing zebrafish was studied. The focus was on TRPC6 due to its known pathogenic implications in genetic and acquired forms of glomerular kidney disease and its association with the slit diaphragm. TRPC1 expression was also examined as this is a prominent member of the counterpart TRPC1/4/5 subgroup within the TRPC subfamily.

V.2. Materials and Methods

V.2.1 Zebrafish embryos

Wild-type TL or TÜAB zebrafish lines were maintained and raised as previously described [Westerfield, 1995]. Embryos were reared at 28.5 °C in E3 solution with 0.003% PTU (1-Phenyl-2-thiourea, Sigma, Saint Louis, Missouri, United States) added to retard pigment formation. Embryonic staging was performed as previously described [Westerfield, 1995]. All animal studies were approved by the Subcommittee on Research Animal Care of the Massachusetts General Hospital.

V.2.2. Cloning of zebrafish TRPC1 and TRPC6

For zebrafish TRPC1 only hypothetical sequence information was available in public databases. Therefore, the TRPC1 ortholog was cloned from zebrafish total mRNA. Total RNA was isolated from 2-day old zebrafish embryos using Trizol reagent (Invitrogen, Carlsbad, California, United States) and reverse transcription was performed with Oligo(dT)12-18 oligonucleotide primers. Based on hypothetical sequence information predicted by automated computational analysis available in the National Center for Biotechnology Information (NCBI) CoreNucleotide database (http://www.ncbi.nlm.nih.gov; Accession Number XM_694363), 5’ (5’-ATGGCTG-CTCTATATCAGG-GC-3’) and 3’ (5’-TTAGCTTCTGGGGTAGAACATG-3’) primers were designed to amplify the full length zebrafish TRPC1 ortholog. TRPC1

was subcloned into the pCRII-TOPO vector (Invitrogen, Carlsbad, California, United States) and four clones containing the TRPC1 open reading frame were sequenced using T7 and SP6 primers. The obtained sequence was aligned to known TRPC1 homologs in other species using the ClustalW algorithm [Thompson *et al.*, 1994]. For zebrafish TRPC6, sequence information recently became available (Accession Number NM_001030282). TRPC6 was cloned as done with TRPC1; the obtained sequence was identical to the entry in the NCBI CoreNucleotide database.

V.2.3. TRPC1 and TRPC6 in situ hybridization

Whole-mount in situ hybridization was performed as previously described [Thisse & Thisse, 1998]. For TRPC1 and TRPC6 antisense probes, the templates (pCRII-TOPO-TRPC1 and pCRII-TOPO-TRPC6) were linearized with *Not*I (New England Biolabs, Ipswich, Massachusetts, United States) and antisense riboprobes were transcribed using SP6 RNA polymerase (Ambion, Austin, Texas, United States). Embryos were hybridized with digoxigenin-labeled riboprobes. Anti-DIG-AP (1:5,000) and the NBT/BCIP substrate (Roche Diagnostics, Basel, Switzerland) were used to detect the probe. After the color reaction was stopped, embryos were washed with methanol and equilibrated in clearing solution (1/3 benzoyl-alcohol and 2/3 benzoyl-benzoate) and photographed using a Leica MZ12 dissecting microscope (Leica, Solms, Germany). Histological analysis on embryos after in situ hybridization analysis was carried out after stained embryos were fixed in 4% paraformaldehyde then dehydrated through a series of methanol/PBST washes of 25%/75%, 50%/50%, 75%/25%, and finally 100% methanol for 10 min each followed by embedding in JB-4 (Polysciences, Warrington, Pennsylvania, United States). A Riechert–Jung Supercut 2065 (Leica, Solms, Germany) microtome was used to generate 10 μm sections. A Nikon E800 microscope equipped with a Spot Image digital camera was used for photography (Nikon, Melville, New York, United States).

V.3. Results

V.3.1. Sequence analysis of zebrafish TRPC1

Four different clones including the TRPC1 open reading frame were sequenced to obtain the full-length TRPC1 sequence. Each base was identical in at least three clones. This sequence was then compared to the preliminary genomic sequence from zebrafish clone CH211-193E5 (Accession Number CT573382) and was confirmed as the zebrafish TRPC1 ortholog with one base being different (A2227 vs. T103578).

The TRPC1 sequence is highly conserved across species (Fig. V.1.) and zebrafish TRPC1 shares 81% sequence identity with human TRPC1. The zebrafish TRPC1

gene encodes a protein of 783 amino acids, derived from an mRNA transcript with 13 exons. Of note, mino acid E709 encoded by the GAA codon including base A2227 is a highly conserved one, there is a chance that the preliminary sequence entry for zebrafish clone CH211-193E5 may be incorrect in position T103578 since in this case a GTA codon would encode V709 instead of the highly conserved E709.

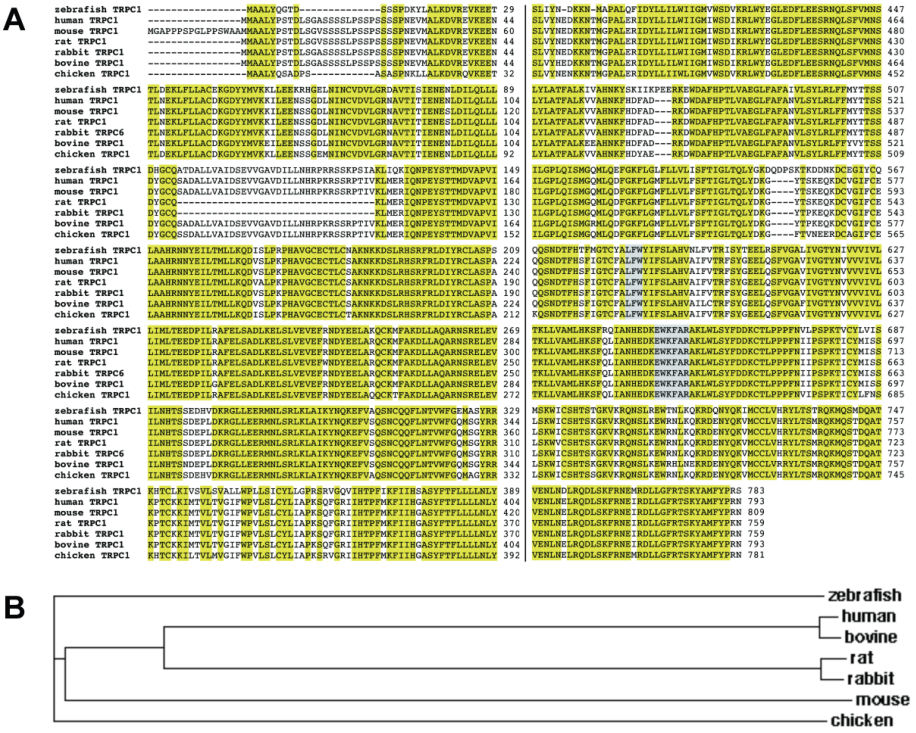

Fig. V.1. Sequence analysis of zebrafish TRPC1. (A) Alignment of the zebrafish TRPC1 sequence to known TRPC1 homologs in other species using the ClustalW algorithm. Conserved amino acids are highlighted in yellow. (B) Phylogenetic tree representative of evolutionary relationships between the zebrafish TRPC1 ortholog and cloned full length TRPC1 channels of other species. Branch length is proportional to evolutionary distance.

V.3.2. Expression pattern of TRPC1 in zebrafish

The expression of zebrafish TRPC1 mRNA was studied by whole mount in situ hybridization and histological analysis of zebrafish embryos. TRPC1 expression was ubiquitous throughout all stages of development up to and including 24 hours post-fertilization (hpf) (Fig. V.2.). At 56 hpf, expression was restricted to the head with no detectable expression in the trunk, and strong head expression of TRPC1 persisted until 72 hpf. At 72 hpf, expression of TRPC1 was also detected in cells surrounding the inflow tract of the heart. In addition, expression of TRPC1 was detected in the ganglion cell layer and the inner nuclear layer of the eye.

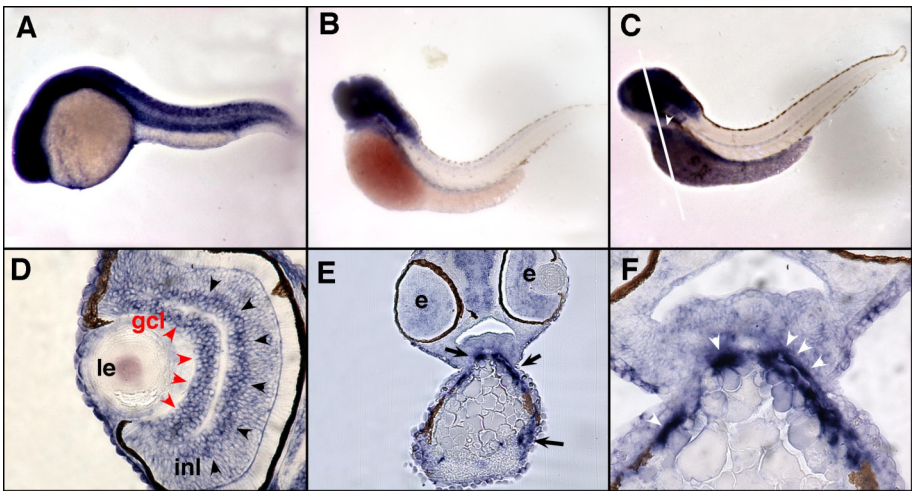

Fig. V.2. Expression of zebrafish TRPC1 by whole mount in situ hybridization and histological analysis. The expression of TRPC1 mRNA is ubiquitous in all stages tested up to and including 24 hpf (A / data not shown). At 56 hpf, expression is restricted to the head with no detectable expression in the trunk (B). Strong head expression of TRPC1 persists until 72 hpf (C), in addition to detectable expression in the inflow tract of the heart (white arrowhead). Histological examination of 72 hpf embryos reveals specific expression of TRPC1 in the ganglion cell layer (gcl, red arroheads) and in the inner nuclear layer (inl, black arrowheads). The plane of section as denoted by the white line in panel C confirms the expression of TRPC1 in the inflow track (E, black arrows). A magnified view (F) shows a high level of expression in the cells surrounding the inflow tract (white arrowheads). Le=lens, e=eye, gcl=ganglion cell layer, inl=inner nuclear layer.

V.3.3. Expression pattern of TRPC6 in zebrafish

The expression of zebrafish TRPC6 mRNA was studied by whole mount in situ hybridization and histological analysis of zebrafish embryos (Fig. V.3.). The expression of TRPC6 mRNA was ubiquitous in all stages tested up to and including 24 hours post-fertilization (hpf) (data not shown). At 48 hpf, expression became restricted to the head, pectoral fins, and the area of the gut extending to the posterior end. This pattern of TRPC6 expression persisted to 72 hpf, where expression in the most posterior region of the gut remained high while more proximal regions of the gut showed diminished expression. The histological examination revealed that TRPC6 expression in the pectoral fins was restricted to the dorsal surface. Sectioning through the trunk of 72 hpf embryos showed that TRPC6 mRNA was expressed in cells lining the dorsal aorta. A closer examination of the gut revealed that TRPC6 was highly expressed in cells that surround and encapsulate the gut. These cells are believed to be precursors of intestinal smooth muscle cells.

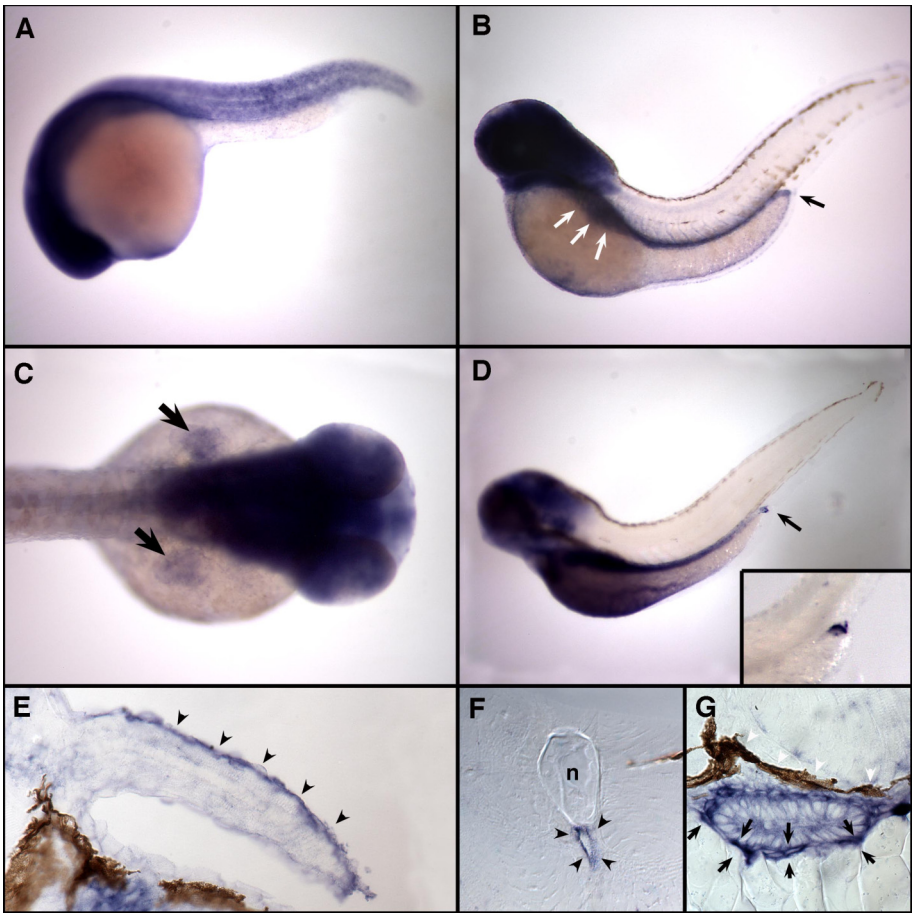

Fig. V.3. Expression of zebrafish TRPC6 by whole mount in situ hybridization and histological analysis. The expression of TRPC6 mRNA is ubiquitous in all stages tested up to and including 24 hpf (A / data not shown). At 48 hpf, expression becomes restricted to the head, pectoral fins (black arrowhead), the area of the gut (white arrows) extending to the posterior end (black arrow). A dorsal view shows the extent of the expression of TRPC6 in the pectoral fins (C, black arrows). This pattern of TRPC6 expression persists to 72 hpf, where expression in the most posterior region of the gut (black arrow and inset) remains high while more proximal regions of the gut show diminished expression (D). Histological examination reveals that TRPC6 expression in the pectoral fins is restricted to the dorsal surface (E, black arrowheads). Sectioning through the trunk of 72 hpf embryos shows that TRPC6 mRNA is expressed in cells lining the dorsal aorta (F, black arrowheads). A closer examination of the gut reveals that TRPC6 is highly expressed in cells that surround and encapsulate the gut (G, demarcated by black arrows).

V.4. Discussion

In zebrafish, five TRP channel genes have thus far been described. TRPM7 was identified as the gene defective in the mutant touchtone/nutria [Elizondo *et al.*, 2005] which exhibits altered skeletal structure, a diminished response to touch, and kidney stones. TRPM7 is expressed in mesonephric kidney tubules, corpuscles of Stannius, and the liver. TRPA1 and TRPN (NOMPC) have been shown to contribute to ear and lateral line hair cell function [Corey *et al.*, 2004; Sidi *et al.*, 2003]. TRPC2, which is a pseudogene in humans, is expressed in the adult olfactory epithelium superficial layer [Sato *et al.*, 2005]. Recently, the osmosensory channel TRPV4 has been detected in multiple developing organs in zebrafish [Mangos *et al.*, 2007].

This study demonstrates that both TRPC1 and TRPC6 are expressed in zebrafish during development. In line with the published work on TRPC1 expression in the heart [Dietrich *et al.*, 2007], TRPC1 expression was detected in cells surrounding the inflow tract of the heart. This suggest a role for TRPC1 in the zebrafish cardiovasculature. In addition, TRPC1 was expressed in the zebrafish eye retina, consistent with the general role of TRPC channels in sensory physiology [Clapham, 2003], and the immunolocalization of TRPC1 in the chicken retina [Crousillac *et al.*, 2003]. TRPC1 was present in 72 hpf embryos in the ganglion cell layer and in the inner nuclear layer [Dahm *et al.*, 2007]. These structures contain neuronal cells appearing early on the second day post-fertilization [Hu & Easter, 1999]. This observation indicates that TRPC1 may play a role in zebrafish vision, analogue to the role of the original *trp* gene in *Drosophila* photoreceptors [Montell, 1997].

TRPC6 expression was detected on the dorsal surface of the pectoral fins. The pectoral fin is composed of two simple muscles, the abductor and adductor [Thorsen & Hale, 2005], as well as large dorsal and ventral nerve branches [Thorsen & Hale, 2007]. It remains to be determined in which of these cell types TRPC6 is expressed. Further studies involving double labeling neuronal and muscle cell markers will be necessary to answer this question. TRPC6 was also found in cells that surround and encapsulate the gut at 48 hpf. Given that this is the stage in development when the first detectable smooth muscle cell markers were detected in the vicinity of the gut [Georgijevic *et al.*, 2007], it appears that TRPC6 could be expressed in gastrointestinal smooth muscle cells. A possible role for TRPC6 in these cells would be to contribute to the stability, contractiliy and elasticity of the zebrafish gut. Finally, TRPC6 expression was also detected in cells lining the aorta. Based on the many recently published reports indicating an important role of TRPC6 for the cardiopulmonary vasculature [Dietrich *et al.*, 2007], it is probable that TRPC6 fulfills a similar role in the zebrafish.

The lack of detectable TRPC6 expression in zebrafish podocytes could be due to low abundance of TRPC6 channels in these cells. It is also possible that TRPC6 expression may only be upregulated under pathophysiological conditions. Finally, TRPC6 expression could simply occur in later stages of development. This is the most likely situation given the situation in neonatal mice, where no expression of TRPC6 was detected. To test this, further studies of TRPC6 expression in genetic and inducible zebrafish models of glomerular injury will be necessary, and TRPC6 expression must also be investigated in adult fish.

VI. CONCLUDING REMARKS

Focal Segmental Glomerulosclerosis (FSGS) is a condition diagnosed in around one fifth of all patients with end-stage renal disease (ESRD). The proportion of end-stage renal disease attributed to FSGS has increased more than 10-fold over the past two decades [Kitiyakara et al., 2004]. Therefore, identifying the molecular mechansims involved in the development of FSGS is of high priority.

In this study five mutations in the calcium-permeable ion channel TRPC6 were associated with the development of familial forms of FSGS. All mutations occured in evolutionary conserved sequence motifs at the N-terminal and C-terminal intracellular tails of TRPC6, and two mutations lead to increased channel current amplitudes when expressed in HEK293 cells. TRPC6 was found to be in glomeruli, where it is located in podocytes in close proximity to the slit diaphragm. Furthermore, it was shown TRPC6 interacts with the slit diaphragm proteins podocin and nephrin.

In addittion to *NPHS1* (nephrin), *NPHS2* (podocin), *ACTN4* (α-actinin-4), and *CD2AP*, *TRPC6* represents the fifth known gene associated with inherited nephrotic syndrome and FSGS. Moreover, TRPC6 is the first example of a protein suggested to play a dual role in both, genetic and acquired forms of glomerular disease. Finally, TRPC6 is the first calcium-permeable ion channel shown to be associated with the slit diaphragm multiprotein complex, substantiating the role of calcium signaling for the molecular regulation of glomerular filtration at the slit diaphragm site.

It was demonstrated that wild-type TRPC6 was induced in a number of acquired human and experimental glomerular diseases, in particular in Membranous Glomerulonephritis (MGN) and *in vitro* and *in vivo* models thereof [Moller et al., 2007]. Elevated TRPC6 levels were correlated with albuminuria and increased intracellular calcium in the rat puromycin aminonucleoside (PAN) model of podocyte injury. Overexpression of TRPC6 in cultured podocytes lead to a disruption of the podocyte actin cytoskeleton. TRPC6 overexpression in mice using gene delivery was sufficient to induce transient proteinuria. These data provide the first experimental evidence that TRPC6 can play a pathological role in glomerular kidney disease.

The present work opens a series of questions that have to be addressed in the future. Due to the clinical significance of FSGS and nephrotic syndrome, the focus will be on the elucidation of the physiological and pathophysiological roles of TRPC6 channels in podocyte foot processes (Fig. VI.1.). Promising future lines of investigation will include the study of TRPC6 protein-protein interactions, the identification of upstream and downstream effectors, and the screening for specific channel agonists and antagonists in podocytes.

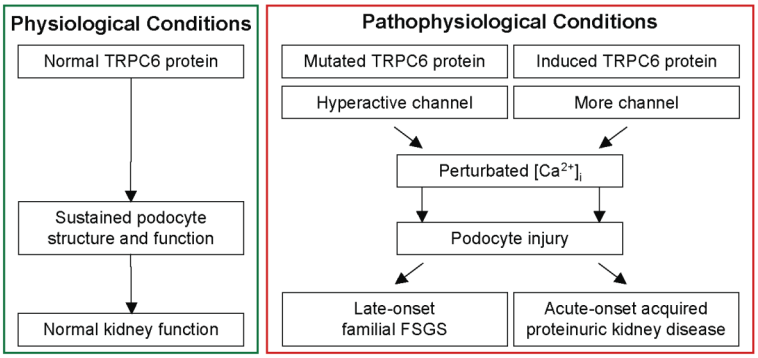

Fig. VI.1. Working Model.

The development of suitable model systems to study TRPC6 function is also of great importance. The presented work shows that, next to to genetic mouse models of TRPC6 dysfunction, the experimental approach of *in vivo* gene delivery can be a useful alternative. Furthermore, it is demonstrated that *Danio rerio* expresses at least two TRPC channel orthologs, TRPC1 and TRPC6, suggesting the zebrafish as an animal model for the study of TRPC6.

The significance of the presented observations is reflected by a number of recent articles highlighting the importance of the questions that will have to be addressed with regard to the role of TRPC6 in glomerular kidney disease [Gudermann, 2005; Walz, 2005; Kriz, 2005; Winn et al., 2006; Mukerji et al., 2007; Oh, 2007]. Future studies on TRPC6 in podocytes will benefit from the increased attention that both areas of research, podocyte biology and TRPC6 physiology, have been receiving in the past years (Fig. VI.2). They will help refine the understanding of glomerular disease and provide hope to the many individuals affected by glomerular disorders.

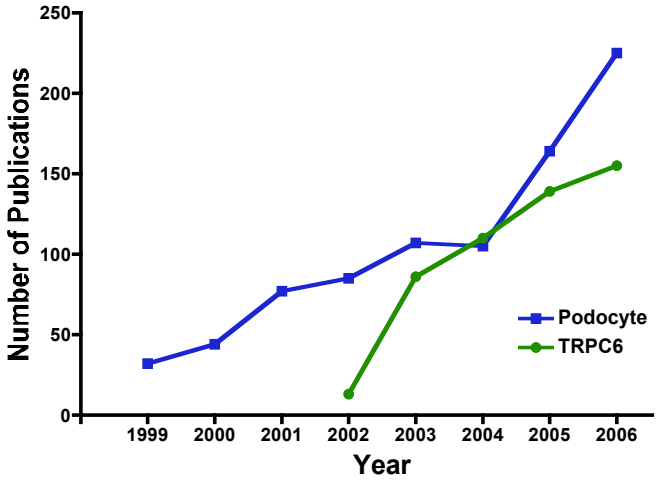

Fig. VI.2. The number of publications returned from a PubMed search with the keywords "Podocyte" and "TRPC6" (http://www.ncbi.nlm.nih.gov).

VII. REFERENCES

Adler, S. (1992). Characterization of glomerular epithelial cell matrix receptors. *Am J Pathol,* **141**(3), 571-578.

Ahola, H., Heikkila, E., Astrom, E., Inagaki, M., Izawa, I., Pavenstadt, H., et al. (2003). A novel protein, densin, expressed by glomerular podocytes. *J Am Soc Nephrol,* **14**(7), 1731-1737.

Albert, A. P., & Large, W. A. (2003). Synergism between inositol phosphates and diacylglycerol on native TRPC6-like channels in rabbit portal vein myocytes. *J Physiol,* **552**(Pt 3), 789-795.

Ambudkar, I. S., & Ong, H. L. (2007). Organization and function of TRPC channelosomes. *Pflugers Arch*.

Amiri, H., Schultz, G., & Schaefer, M. (2003). FRET-based analysis of TRPC subunit stoichiometry. *Cell Calcium,* **33**(5-6), 463-470.

Arikawa, K., Hicks, J. L., & Williams, D. S. (1990). Identification of actin filaments in the rhabdomeral microvilli of Drosophila photoreceptors. *J Cell Biol,* **110**(6), 1993-1998.

Asanuma, K., Yanagida-Asanuma, E., Faul, C., Tomino, Y., Kim, K., & Mundel, P. (2006). Synaptopodin orchestrates actin organization and cell motility via regulation of RhoA signalling. *Nat Cell Biol,* **8**(5), 485-491.

Benzing, T. (2004). Signaling at the slit diaphragm. *J Am Soc Nephrol,* **15**(6), 1382-1391.

Berridge, M. J., Bootman, M. D., & Lipp, P. (1998). Calcium--a life and death signal. *Nature,* **395**(6703), 645-648.

Bezzerides, V. J., Ramsey, I. S., Kotecha, S., Greka, A., & Clapham, D. E. (2004). Rapid vesicular translocation and insertion of TRP channels. *Nat Cell Biol,* **6**(8), 709-720.

Boulay, G., Zhu, X., Peyton, M., Jiang, M., Hurst, R., Stefani, E., et al. (1997). Cloning and expression of a novel mammalian homolog of Drosophila transient receptor potential (Trp) involved in calcium entry secondary to activation of receptors coupled by the Gq class of G protein. *J Biol Chem,* **272**(47), 29672-29680.

Boute, N., Gribouval, O., Roselli, S., Benessy, F., Lee, H., Fuchshuber, A., et al. (2000). NPHS2, encoding the glomerular protein podocin, is mutated in autosomal recessive steroid-resistant nephrotic syndrome. *Nat Genet,* **24**(4), 349-354.

Bradford, M. M. (1976). A rapid and sensitive method for the quantitation of microgram quantities of protein utilizing the principle of protein-dye binding. *Anal Biochem,* **72**, 248-254.

Cayouette, S., Lussier, M. P., Mathieu, E. L., Bousquet, S. M., & Boulay, G. (2004). Exocytotic insertion of TRPC6 channel into the plasma membrane upon Gq protein-coupled receptor activation. *J Biol Chem,* **279**(8), 7241-7246.

Cheng, H. W., James, A. F., Foster, R. R., Hancox, J. C., & Bates, D. O. (2006). VEGF activates receptor-operated cation channels in human microvascular endothelial cells. *Arterioscler Thromb Vasc Biol,* **26**(8), 1768-1776.

Chubanov, V., Waldegger, S., Mederos y Schnitzler, M., Vitzthum, H., Sassen, M. C., Seyberth, H. W., et al. (2004). Disruption of TRPM6/TRPM7 complex formation by a mutation in the TRPM6 gene causes hypomagnesemia with secondary hypocalcemia. *Proc Natl Acad Sci U S A,* **101**(9), 2894-2899.

Clapham, D. E. (2003). TRP channels as cellular sensors. *Nature,* **426**(6966), 517-524.

Cohen, C. D., Frach, K., Schlondorff, D., & Kretzler, M. (2002). Quantitative gene expression analysis in renal biopsies: a novel protocol for a high-throughput multicenter application. *Kidney Int,* **61**(1), 133-140.

Corey, D. P., Garcia-Anoveros, J., Holt, J. R., Kwan, K. Y., Lin, S. Y., Vollrath, M. A., et al. (2004). TRPA1 is a candidate for the mechanosensitive transduction channel of vertebrate hair cells. *Nature,* **432**(7018), 723-730.

Cosens, D. J., & Manning, A. (1969). Abnormal electroretinogram from a Drosophila mutant. *Nature,* **224**(5216), 285-287.

Coward, J., Maisey, N., & Cunningham, D. (2005). The effects of capecitabine in Raynaud's disease: a case report. *Ann Oncol,* **16**(5), 835-836.

Crousillac, S., LeRouge, M., Rankin, M., & Gleason, E. (2003). Immunolocalization of TRPC channel subunits 1 and 4 in the chicken retina. *Vis Neurosci,* **20**(4), 453-463.

Cybulsky, A. V., Bonventre, J. V., Quigg, R. J., Lieberthal, W., & Salant, D. J. (1990). Cytosolic calcium and protein kinase C reduce complement-mediated glomerular epithelial injury. *Kidney Int,* **38**(5), 803-811.

Cybulsky, A. V., Quigg, R. J., & Salant, D. J. (2005). Experimental membranous nephropathy redux. *Am J Physiol Renal Physiol,* **289**(4), F660-671.

Dahm, R., Schonthaler, H. B., Soehn, A. S., van Marle, J., & Vrensen, G. F. (2007). Development and adult morphology of the eye lens in the zebrafish. *Exp Eye Res,* **85**(1), 74-89.

Dai, C., Yang, J., Bastacky, S., Xia, J., Li, Y., & Liu, Y. (2004). Intravenous administration of hepatocyte growth factor gene ameliorates diabetic nephropathy in mice. *J Am Soc Nephrol,* **15**(10), 2637-2647.

Daskalakis, N., & Winn, M. P. (2006). Focal and segmental glomerulosclerosis. *Cell Mol Life Sci,* **63**(21), 2506-2511.

Deen, W. M., Lazzara, M. J., & Myers, B. D. (2001). Structural determinants of glomerular permeability. *Am J Physiol Renal Physiol,* **281**(4), F579-596.

Dietrich, A., Chubanov, V., Kalwa, H., Rost, B. R., & Gudermann, T. (2006). Cation channels of the transient receptor potential superfamily: their role in physiological and pathophysiological processes of smooth muscle cells. *Pharmacol Ther,* **112**(3), 744-760.

Dietrich, A., Kalwa, H., Fuchs, B., Grimminger, F., Weissmann, N., & Gudermann, T. (2007). In vivo TRPC functions in the cardiopulmonary vasculature. *Cell Calcium,* **42**(2), 233-244.

Dietrich, A., Mederos y Schnitzler, M., Emmel, J., Kalwa, H., Hofmann, T., & Gudermann, T. (2003). N-linked protein glycosylation is a major determinant for basal TRPC3 and TRPC6 channel activity. *J Biol Chem,* **278**(48), 47842-47852.

Dietrich, A., Mederos, Y. S. M., Gollasch, M., Gross, V., Storch, U., Dubrovska, G., et al. (2005). Increased vascular smooth muscle contractility in TRPC6-/- mice. *Mol Cell Biol,* **25**(16), 6980-6989.

Ding, G., Reddy, K., Kapasi, A. A., Franki, N., Gibbons, N., Kasinath, B. S., et al. (2002). Angiotensin II induces apoptosis in rat glomerular epithelial cells. *Am J Physiol Renal Physiol,* **283**(1), F173-180.

Drenckhahn, D., & Franke, R. P. (1988). Ultrastructural organization of contractile and cytoskeletal proteins in glomerular podocytes of chicken, rat, and man. *Lab Invest,* **59**(5), 673-682.

Drummond, I. (2003). Making a zebrafish kidney: a tale of two tubes. *Trends Cell Biol,* **13**(7), 357-365.

Drummond, I. A. (2000). The zebrafish pronephros: a genetic system for studies of kidney development. *Pediatr Nephrol,* **14**(5), 428-435.

Durvasula, R. V., & Shankland, S. J. (2006). Podocyte injury and targeting therapy: an update. *Curr Opin Nephrol Hypertens,* **15**(1), 1-7.

Elizondo, M. R., Arduini, B. L., Paulsen, J., MacDonald, E. L., Sabel, J. L., Henion, P. D., et al. (2005). Defective skeletogenesis with kidney stone formation in dwarf zebrafish mutant for trpm7. *Curr Biol,* **15**(7), 667-671.

Endlich, K., Kriz, W., & Witzgall, R. (2001). Update in podocyte biology. *Curr Opin Nephrol Hypertens,* **10**(3), 331-340.

Endlich, N., & Endlich, K. (2006). Stretch, tension and adhesion - adaptive mechanisms of the actin cytoskeleton in podocytes. *Eur J Cell Biol,* **85**(3-4), 229-234.

Eremina, V., & Quaggin, S. E. (2004). The role of VEGF-A in glomerular development and function. *Curr Opin Nephrol Hypertens,* **13**(1), 9-15.

Eremina, V., Sood, M., Haigh, J., Nagy, A., Lajoie, G., Ferrara, N., et al. (2003). Glomerular-specific alterations of VEGF-A expression lead to distinct congenital and acquired renal diseases. *J Clin Invest,* **111**(5), 707-716.

Estacion, M., Li, S., Sinkins, W. G., Gosling, M., Bahra, P., Poll, C., et al. (2004). Activation of human TRPC6 channels by receptor stimulation. *J Biol Chem,* **279**(21), 22047-22056.

Facemire, C. S., Mohler, P. J., & Arendshorst, W. J. (2004). Expression and relative abundance of short transient receptor potential channels in the rat renal microcirculation. *Am J Physiol Renal Physiol,* **286**(3), F546-551.

Fantozzi, I., Zhang, S., Platoshyn, O., Remillard, C. V., Cowling, R. T., & Yuan, J. X. (2003). Hypoxia increases AP-1 binding activity by enhancing capacitative Ca2+ entry in human pulmonary artery endothelial cells. *Am J Physiol Lung Cell Mol Physiol,* **285**(6), L1233-1245.

Foster, R. R., Satchell, S. C., Seckley, J., Emmett, M. S., Joory, K., Xing, C. Y., et al. (2006). VEGF-C promotes survival in podocytes. *Am J Physiol Renal Physiol,* **291**(1), F196-207.

Franz, S. (2005). Cyclosporin Protects Podocyte Stress Fibers through Stablization of Synaptopodin Protein Expression. Public presentation; 38th Renal Week Annual Meeting & Scientific Exposition, Philadelphia, Pennsylvania, United States; November 8-13.

Friedrich, C., Endlich, N., Kriz, W., & Endlich, K. (2006). Podocytes are sensitive to fluid shear stress in vitro. *Am J Physiol Renal Physiol,* **291**(4), F856-865.

Galeano, B., Klootwijk, R., Manoli, I., Sun, M., Ciccone, C., Darvish, D., et al. (2007). Mutation in the key enzyme of sialic acid biosynthesis causes severe glomerular proteinuria and is rescued by N-acetylmannosamine. *J Clin Invest,* **117**(6), 1585-1594.

Gawlik, A., & Quaggin, S. E. (2005). Conditional gene targeting in the kidney. *Curr Mol Med,* **5**(5), 527-536.

Georgijevic, S., Subramanian, Y., Rollins, E. L., Starovic-Subota, O., Tang, A. C., & Childs, S. J. (2007). Spatiotemporal expression of smooth muscle markers in developing zebrafish gut. *Dev Dyn,* **236**(6), 1623-1632.

Giulietti, A., Overbergh, L., Valckx, D., Decallonne, B., Bouillon, R., & Mathieu, C. (2001). An overview of real-time quantitative PCR: applications to quantify cytokine gene expression. *Methods,* **25**(4), 386-401.

Glassock, R. J. (2004). The rising tide of end-stage renal disease: what can be done? *Clin Exp Nephrol,* **8**(4), 291-296.

Goel, M., Sinkins, W., Keightley, A., Kinter, M., & Schilling, W. P. (2005). Proteomic analysis of TRPC5- and TRPC6-binding partners reveals interaction with the plasmalemmal Na(+)/K(+)-ATPase. *Pflugers Arch,* **451**(1), 87-98.

Goel, M., Sinkins, W. G., & Schilling, W. P. (2002). Selective association of TRPC channel subunits in rat brain synaptosomes. *J Biol Chem,* **277**(50), 48303-48310.

Goel, M., Sinkins, W. G., Zuo, C. D., Estacion, M., & Schilling, W. P. (2006). Identification and localization of TRPC channels in the rat kidney. *Am J Physiol Renal Physiol,* **290**(5), F1241-1252.

Goldenberg, A., Ngoc, L. H., Thouret, M. C., Cormier-Daire, V., Gagnadoux, M. F., Chretien, D., et al. (2005). Respiratory chain deficiency presenting as congenital nephrotic syndrome. *Pediatr Nephrol,* **20**(4), 465-469.

Gosling, M., Poll, C., & Li, S. (2005). TRP channels in airway smooth muscle as therapeutic targets. *Naunyn Schmiedebergs Arch Pharmacol,* **371**(4), 277-284.

Grimm, C., Kraft, R., Sauerbruch, S., Schultz, G., & Harteneck, C. (2003). Molecular and functional characterization of the melastatin-related cation channel TRPM3. *J Biol Chem,* **278**(24), 21493-21501.

Grunkemeyer, J. A., Kwoh, C., Huber, T. B., & Shaw, A. S. (2005). CD2-associated protein (CD2AP) expression in podocytes rescues lethality of CD2AP deficiency. *J Biol Chem,* **280**(33), 29677-29681.

Guan, F., Villegas, G., Teichman, J., Mundel, P., & Tufro, A. (2006). Autocrine VEGF-A system in podocytes regulates podocin and its interaction with CD2AP. *Am J Physiol Renal Physiol,* **291**(2), F422-428.

Gudermann, T. (2005). A new TRP to kidney disease. *Nat Genet,* **37**(7), 663-664.

Haas, M., Spargo, B. H., & Coventry, S. (1995). Increasing incidence of focal-segmental glomerulosclerosis among adult nephropathies: a 20-year renal biopsy study. *Am J Kidney Dis,* **26**(5), 740-750.

Hamano, Y., Grunkemeyer, J. A., Sudhakar, A., Zeisberg, M., Cosgrove, D., Morello, R., et al. (2002). Determinants of vascular permeability in the kidney glomerulus. *J Biol Chem,* **277**(34), 31154-31162.

Hara, M., Yanagihara, T., & Kihara, I. (2001). Urinary podocytes in primary focal segmental glomerulosclerosis. *Nephron Exp Nephrol,* **89**(3), 342-347.

Hardie, R. C., & Minke, B. (1992). The trp gene is essential for a light-activated Ca2+ channel in Drosophila photoreceptors. *Neuron,* **8**(4), 643-651.

Hassock, S. R., Zhu, M. X., Trost, C., Flockerzi, V., & Authi, K. S. (2002). Expression and role of TRPC proteins in human platelets: evidence that TRPC6 forms the store-independent calcium entry channel. *Blood,* **100**(8), 2801-2811.

Herweijer, H., & Wolff, J. A. (2007). Gene therapy progress and prospects: hydrodynamic gene delivery. *Gene Ther,* **14**(2), 99-107.

Hicks, G. A. (2006). TRP channels as therapeutic targets: hot property, or time to cool down? *Neurogastroenterol Motil,* **18**(8), 590-594.

Higuchi, N., Maruyama, H., Kuroda, T., Kameda, S., Iino, N., Kawachi, H., et al. (2003). Hydrodynamics-based delivery of the viral interleukin-10 gene suppresses experimental crescentic glomerulonephritis in Wistar-Kyoto rats. *Gene Ther,* **10**(16), 1297-1310.

Hisatsune, C., Kuroda, Y., Nakamura, K., Inoue, T., Nakamura, T., Michikawa, T., et al. (2004). Regulation of TRPC6 channel activity by tyrosine phosphorylation. *J Biol Chem,* **279**(18), 18887-18894.

Hodges, B. L., & Scheule, R. K. (2003). Hydrodynamic delivery of DNA. *Expert Opin Biol Ther,* **3**(6), 911-918.

Hofmann, T., Obukhov, A. G., Schaefer, M., Harteneck, C., Gudermann, T., & Schultz, G. (1999). Direct activation of human TRPC6 and TRPC3 channels by diacylglycerol. *Nature,* **397**(6716), 259-263.

Hofmann, T., Schaefer, M., Schultz, G., & Gudermann, T. (2002). Subunit composition of mammalian transient receptor potential channels in living cells. *Proc Natl Acad Sci U S A,* **99**(11), 7461-7466.

Hsu, Y. J., Hoenderop, J. G., & Bindels, R. J. (2007). TRP channels in kidney disease. *Biochim Biophys Acta,* **1772**(8), 928-936.

Hu, M., & Easter, S. S. (1999). Retinal neurogenesis: the formation of the initial central patch of postmitotic cells. *Dev Biol,* **207**(2), 309-321.

Huang, M., Gu, G., Ferguson, E. L., & Chalfie, M. (1995). A stomatin-like protein necessary for mechanosensation in C. elegans. *Nature,* **378**(6554), 292-295.

Huber, T. B., & Benzing, T. (2005). The slit diaphragm: a signaling platform to regulate podocyte function. *Curr Opin Nephrol Hypertens,* **14**(3), 211-216.

Huber, T. B., Hartleben, B., Kim, J., Schmidts, M., Schermer, B., Keil, A., et al. (2003). Nephrin and CD2AP associate with phosphoinositide 3-OH kinase and stimulate AKT-dependent signaling. *Mol Cell Biol,* **23**(14), 4917-4928.

Huber, T. B., Kottgen, M., Schilling, B., Walz, G., & Benzing, T. (2001). Interaction with podocin facilitates nephrin signaling. *J Biol Chem,* **276**(45), 41543-41546.

Huber, T. B., Kwoh, C., Wu, H., Asanuma, K., Godel, M., Hartleben, B., et al. (2006). Bigenic mouse models of focal segmental glomerulosclerosis involving pairwise interaction of CD2AP, Fyn, and synaptopodin. *J Clin Invest,* **116**(5), 1337-1345.

Ichimura, K., Kurihara, H., & Sakai, T. (2007). Actin filament organization of foot processes in vertebrate glomerular podocytes. *Cell Tissue Res,* **329**(3), 541-557.

Imai, H., Hamai, K., Komatsuda, A., Ohtani, H., & Miura, A. B. (1997). IgG subclasses in patients with membranoproliferative glomerulonephritis, membranous nephropathy, and lupus nephritis. *Kidney Int,* **51**(1), 270-276.

Inoue, T., Yaoita, E., Kurihara, H., Shimizu, F., Sakai, T., Kobayashi, T., et al. (2001). FAT is a component of glomerular slit diaphragms. *Kidney Int,* **59**(3), 1003-1012.

Jat, P. S., Noble, M. D., Ataliotis, P., Tanaka, Y., Yannoutsos, N., Larsen, L., et al. (1991). Direct derivation of conditionally immortal cell lines from an H-2Kb-tsA58 transgenic mouse. *Proc Natl Acad Sci U S A,* **88**(12), 5096-5100.

Jung, S., Strotmann, R., Schultz, G., & Plant, T. D. (2002). TRPC6 is a candidate channel involved in receptor-stimulated cation currents in A7r5 smooth muscle cells. *Am J Physiol Cell Physiol,* **282**(2), C347-359.

Kameda, S., Maruyama, H., Higuchi, N., Iino, N., Nakamura, G., Miyazaki, J., et al. (2004). Kidney-targeted naked DNA transfer by retrograde injection into the renal vein in mice. *Biochem Biophys Res Commun,* **314**(2), 390-395.

Kaplan, J. M., Kim, S. H., North, K. N., Rennke, H., Correia, L. A., Tong, H. Q., et al. (2000). Mutations in ACTN4, encoding alpha-actinin-4, cause familial focal segmental glomerulosclerosis. *Nat Genet,* **24**(3), 251-256.

Kashtan, C. E. (2005). Familial hematurias: what we know and what we don't. *Pediatr Nephrol,* **20**(8), 1027-1035.

Kestila, M., Lenkkeri, U., Mannikko, M., Lamerdin, J., McCready, P., Putaala, H., et al. (1998). Positionally cloned gene for a novel glomerular protein--nephrin--is mutated in congenital nephrotic syndrome. *Mol Cell,* **1**(4), 575-582.

Kim, J. M., Wu, H., Green, G., Winkler, C. A., Kopp, J. B., Miner, J. H., et al. (2003). CD2-associated protein haploinsufficiency is linked to glomerular disease susceptibility. *Science,* **300**(5623), 1298-1300.

Kim, Y. H., Goyal, M., Kurnit, D., Wharram, B., Wiggins, J., Holzman, L., et al. (2001). Podocyte depletion and glomerulosclerosis have a direct relationship in the PAN-treated rat. *Kidney Int,* **60**(3), 957-968.

Kirber, M. T., Ordway, R. W., Clapp, L. H., Walsh, J. V., Jr., & Singer, J. J. (1992). Both membrane stretch and fatty acids directly activate large conductance Ca(2+)-activated K+ channels in vascular smooth muscle cells. *FEBS Lett,* **297**(1-2), 24-28.

Kramer-Zucker, A. G., Wiessner, S., Jensen, A. M., & Drummond, I. A. (2005). Organization of the pronephric filtration apparatus in zebrafish requires Nephrin, Podocin and the FERM domain protein Mosaic eyes. *Dev Biol,* **285**(2), 316-329.

Kreidberg, J. A., Donovan, M. J., Goldstein, S. L., Rennke, H., Shepherd, K., Jones, R. C., et al. (1996). Alpha 3 beta 1 integrin has a crucial role in kidney and lung organogenesis. *Development,* **122**(11), 3537-3547.

Kretzler, M. (2005). Role of podocytes in focal sclerosis: defining the point of no return. *J Am Soc Nephrol,* **16**(10), 2830-2832.

Kretzler, M., Koeppen-Hagemann, I., & Kriz, W. (1994). Podocyte damage is a critical step in the development of glomerulosclerosis in the uninephrectomised-desoxycorticosterone hypertensive rat. *Virchows Arch,* **425**(2), 181-193.

Kriz, W. (2002). Podocyte is the major culprit accounting for the progression of chronic renal disease. *Microsc Res Tech,* **57**(4), 189-195.

Kriz, W. (2005). TRPC6 - a new podocyte gene involved in focal segmental glomerulosclerosis. *Trends Mol Med,* **11**(12), 527-530.

Kriz, W., Elger, M., Mundel, P., & Lemley, K. V. (1995). Structure-stabilizing forces in the glomerular tuft. *J Am Soc Nephrol,* **5**(10), 1731-1739.

Kriz, W., Gretz, N., & Lemley, K. V. (1998). Progression of glomerular diseases: is the podocyte the culprit? *Kidney Int,* **54**(3), 687-697.

Kriz, W., Hackenthal, E., Nobiling, R., Sakai, T., Elger, M., & Hahnel, B. (1994). A role for podocytes to counteract capillary wall distension. *Kidney Int,* **45**(2), 369-376.

Kuwahara, K., Wang, Y., McAnally, J., Richardson, J. A., Bassel-Duby, R., Hill, J. A., et al. (2006). TRPC6 fulfills a calcineurin signaling circuit during pathologic cardiac remodeling. *J Clin Invest,* **116**(12), 3114-3126.

Lepage, P. K., Lussier, M. P., Barajas-Martinez, H., Bousquet, S. M., Blanchard, A. P., Francoeur, N., et al. (2006). Identification of two domains involved in the assembly of transient receptor potential canonical channels. *J Biol Chem,* **281**(41), 30356-30364.

Li, H., Lemay, S., Aoudjit, L., Kawachi, H., & Takano, T. (2004). SRC-family kinase Fyn phosphorylates the cytoplasmic domain of nephrin and modulates its interaction with podocin. *J Am Soc Nephrol,* **15**(12), 3006-3015.

Li, Y., Jia, Y. C., Cui, K., Li, N., Zheng, Z. Y., Wang, Y. Z., et al. (2005). Essential role of TRPC channels in the guidance of nerve growth cones by brain-derived neurotrophic factor. *Nature,* **434**(7035), 894-898.

Lin, M. J., Leung, G. P., Zhang, W. M., Yang, X. R., Yip, K. P., Tse, C. M., et al. (2004). Chronic hypoxia-induced upregulation of store-operated and receptor-operated Ca2+ channels in pulmonary arterial smooth muscle cells: a novel mechanism of hypoxic pulmonary hypertension. *Circ Res,* **95**(5), 496-505.

Lin, S. Y., & Corey, D. P. (2005). TRP channels in mechanosensation. *Curr Opin Neurobiol,* **15**(3), 350-357.

Livak, K. J., & Schmittgen, T. D. (2001). Analysis of relative gene expression data using real-time quantitative PCR and the 2(-Delta Delta C(T)) Method. *Methods,* **25**(4), 402-408.

Lowik, M. M., Hol, F. A., Steenbergen, E. J., Wetzels, J. F., & van den Heuvel, L. P. (2005). Mitochondrial tRNALeu(UUR) mutation in a patient with steroid-resistant nephrotic syndrome and focal segmental glomerulosclerosis. *Nephrol Dial Transplant,* **20**(2), 336-341.

Mangos, S., Liu, Y., & Drummond, I. A. (2007). Dynamic expression of the osmosensory channel trpv4 in multiple developing organs in zebrafish. *Gene Expr Patterns,* **7**(4), 480-484.

Maroto, R., Raso, A., Wood, T. G., Kurosky, A., Martinac, B., & Hamill, O. P. (2005). TRPC1 forms the stretch-activated cation channel in vertebrate cells. *Nat Cell Biol,* **7**(2), 179-185.

Maruyama, H., Higuchi, N., Kameda, S., Nakamura, G., Iguchi, S., Miyazaki, J., et al. (2004). Rat kidney-targeted naked plasmid DNA transfer by retrograde injection into the renal vein. *Mol Biotechnol,* **27**(1), 23-31.

Mayer, G., Boileau, G., & Bendayan, M. (2003). Furin interacts with proMT1-MMP and integrin alphaV at specialized domains of renal cell plasma membrane. *J Cell Sci,* **116**(Pt 9), 1763-1773.

Miner, J. H. (1999). Renal basement membrane components. *Kidney Int,* **56**(6), 2016-2024.

Miner, J. H. (2005). Building the glomerulus: a matricentric view. *J Am Soc Nephrol,* **16**(4), 857-861.

Moeller, M. J., Sanden, S. K., Soofi, A., Wiggins, R. C., & Holzman, L. B. (2002). Two gene fragments that direct podocyte-specific expression in transgenic mice. *J Am Soc Nephrol,* **13**(6), 1561-1567.

Moller, C. C., Pollak, M. R., & Reiser, J. (2006). The genetic basis of human glomerular disease. *Adv Chronic Kidney Dis,* **13**(2), 166-173.

Moller, C. C., Wei, C., Altintas, M. M., Li, J., Greka, A., Ohse, T., et al. (2007). Induction of TRPC6 channel in acquired forms of proteinuric kidney disease. *J Am Soc Nephrol,* **18**(1), 29-36.

Monk, P. D., Carne, A., Liu, S. H., Ford, J. W., Keen, J. N., & Findlay, J. B. (1996). Isolation, cloning, and characterisation of a trp homologue from squid (Loligo forbesi) photoreceptor membranes. *J Neurochem,* **67**(6), 2227-2235.

Montell, C. (1997). New light on TRP and TRPL. *Mol Pharmacol,* **52**(5), 755-763.

Montell, C. (2005). The TRP superfamily of cation channels. *Sci STKE,* **2005**(272), re3.

Montell, C., & Rubin, G. M. (1989). Molecular characterization of the Drosophila trp locus: a putative integral membrane protein required for phototransduction. *Neuron,* **2**(4), 1313-1323.

Morigi, M., Buelli, S., Angioletti, S., Zanchi, C., Longaretti, L., Zoja, C., et al. (2005). In response to protein load podocytes reorganize cytoskeleton and modulate endothelin-1 gene: implication for permselective dysfunction of chronic nephropathies. *Am J Pathol,* **166**(5), 1309-1320.

Mosavi, L. K., Cammett, T. J., Desrosiers, D. C., & Peng, Z. Y. (2004). The ankyrin repeat as molecular architecture for protein recognition. *Protein Sci,* **13**(6), 1435-1448.

Mundel, P., & Kriz, W. (1995). Structure and function of podocytes: an update. *Anat Embryol (Berl),* **192**(5), 385-397.

Mundel, P., Gambaryan, S., Bachmann, S., Koesling, D., & Kriz, W. (1995). Immunolocalization of soluble guanylyl cyclase subunits in rat kidney. *Histochem Cell Biol,* **103**(1), 75-79.

Mundel, P., & Kriz, W. (1996). Cell culture of podocytes. *Exp Nephrol,* **4**(5), 263-266.

Mundel, P., Reiser, J., Zuniga Mejia Borja, A., Pavenstadt, H., Davidson, G. R., Kriz, W., et al. (1997). Rearrangements of the cytoskeleton and cell contacts induce process formation during differentiation of conditionally immortalized mouse podocyte cell lines. *Exp Cell Res,* **236**(1), 248-258.

Mundel, P., & Shankland, S. J. (2002). Podocyte biology and response to injury. *J Am Soc Nephrol,* **13**(12), 3005-3015.

Mukerji, N., Damodaran, T. V., & Winn, M. P. (2007). TRPC6 and FSGS: The latest TRP channelopathy. *Biochim Biophys Acta,* **1772**(8), 859-868.

Nauli, S. M., & Zhou, J. (2004). Polycystins and mechanosensation in renal and nodal cilia. *Bioessays,* **26**(8), 844-856.

Nilius, B. (2004). Store-operated Ca2+ entry channels: still elusive! *Sci STKE,* **2004**(243), pe36.

Nilius, B. (2007). TRP channels in disease. *Biochim Biophys Acta,* **1772**(8), 805-812.

Norgaard, J. O. (1976). A new method for the isolation of ultrastructurally preserved glomeruli. *Kidney Int,* **9**(3), 278-285.

Notredame, C., Higgins, D. G., & Heringa, J. (2000). T-Coffee: A novel method for fast and accurate multiple sequence alignment. *J Mol Biol,* **302**(1), 205-217.

O'Hagan, R., Chalfie, M., & Goodman, M. B. (2005). The MEC-4 DEG/ENaC channel of Caenorhabditis elegans touch receptor neurons transduces mechanical signals. *Nat Neurosci,* **8**(1), 43-50.

Oancea, E., Wolfe, J. T., & Clapham, D. E. (2006). Functional TRPM7 channels accumulate at the plasma membrane in response to fluid flow. *Circ Res,* **98**(2), 245-253.

Oh, J. (2007). Steigerung der podozytären TRPC6-Expression bei erworbenen proteinurischen Nephropathien. *Der Nephrologe,* **2**(3), 202-203.

Okada, T., Inoue, R., Yamazaki, K., Maeda, A., Kurosaki, T., Yamakuni, T., et al. (1999). Molecular and functional characterization of a novel mouse transient receptor potential protein homologue TRP7. Ca(2+)-permeable cation channel that is constitutively activated and enhanced by stimulation of G protein-coupled receptor. *J Biol Chem,* **274**(39), 27359-27370.

Owsianik, G., Talavera, K., Voets, T., & Nilius, B. (2006). Permeation and selectivity of TRP channels. *Annu Rev Physiol,* **68**, 685-717.

Pagtalunan, M. E., Miller, P. L., Jumping-Eagle, S., Nelson, R. G., Myers, B. D., Rennke, H. G., et al. (1997). Podocyte loss and progressive glomerular injury in type II diabetes. *J Clin Invest,* **99**(2), 342-348.

Patton, C., Thompson, S., & Epel, D. (2004). Some precautions in using chelators to buffer metals in biological solutions. *Cell Calcium,* **35**(5), 427-431.

Pavenstadt, H. (2000). Franz Volhard Award 2000: angiotensin II signalling in the podocyte. *Kidney Blood Press Res,* **23**(3-5), 156-158.

Pavenstadt, H., & Bek, M. (2002). Podocyte electrophysiology, in vivo and in vitro. *Microsc Res Tech,* **57**(4), 224-227.

Pavenstadt, H., Kriz, W., & Kretzler, M. (2003). Cell biology of the glomerular podocyte. *Physiol Rev,* **83**(1), 253-307.

Perkinson, D. T., Baker, P. J., Couser, W. G., Johnson, R. J., & Adler, S. (1985). Membrane attack complex deposition in experimental glomerular injury. *Am J Pathol,* **120**(1), 121-128.

Petermann, A. T., Pippin, J., Durvasula, R., Pichler, R., Hiromura, K., Monkawa, T., et al. (2005). Mechanical stretch induces podocyte hypertrophy in vitro. *Kidney Int,* **67**(1), 157-166.

Pippin, J. W., Durvasula, R., Petermann, A., Hiromura, K., Couser, W. G., & Shankland, S. J. (2003). DNA damage is a novel response to sublytic complement C5b-9-induced injury in podocytes. *J Clin Invest,* **111**(6), 877-885.

Pocock, T. M., Foster, R. R., & Bates, D. O. (2004). Evidence of a role for TRPC channels in VEGF-mediated increased vascular permeability in vivo. *Am J Physiol Heart Circ Physiol,* **286**(3), H1015-1026.

Pollak, M. R. (2002). Inherited podocytopathies: FSGS and nephrotic syndrome from a genetic viewpoint. *J Am Soc Nephrol,* **13**(12), 3016-3023.

Praetorius, H. A., & Spring, K. R. (2005). A physiological view of the primary cilium. *Annu Rev Physiol,* **67**, 515-529.

Putaala, H., Soininen, R., Kilpelainen, P., Wartiovaara, J., & Tryggvason, K. (2001). The murine nephrin gene is specifically expressed in kidney, brain and pancreas: inactivation of the gene leads to massive proteinuria and neonatal death. *Hum Mol Genet,* **10**(1), 1-8.

Ramsey, I. S., Delling, M., & Clapham, D. E. (2006). An introduction to TRP channels. *Annu Rev Physiol,* **68**, 619-647.

Rebibou, J. M., He, C. J., Delarue, F., Peraldi, M. N., Adida, C., Rondeau, E., et al. (1992). Functional endothelin 1 receptors on human glomerular podocytes and mesangial cells. *Nephrol Dial Transplant,* **7**(4), 288-292.

Regele, H. M., Fillipovic, E., Langer, B., Poczewki, H., Kraxberger, I., Bittner, R. E., et al. (2000). Glomerular expression of dystroglycans is reduced in minimal change nephrosis but not in focal segmental glomerulosclerosis. *J Am Soc Nephrol,* **11**(3), 403-412.

Reiser, J., Kriz, W., Kretzler, M., & Mundel, P. (2000). The glomerular slit diaphragm is a modified adherens junction. *J Am Soc Nephrol,* **11**(1), 1-8.

Reiser, J., & Mundel, P. (2004). Danger signaling by glomerular podocytes defines a novel function of inducible B7-1 in the pathogenesis of nephrotic syndrome. *J Am Soc Nephrol,* **15**(9), 2246-2248.

Reiser, J., Oh, J., Shirato, I., Asanuma, K., Hug, A., Mundel, T. M., et al. (2004). Podocyte migration during nephrotic syndrome requires a coordinated interplay between cathepsin L and alpha3 integrin. *J Biol Chem,* **279**(33), 34827-34832.

Reiser, J., Polu, K. R., Moller, C. C., Kenlan, P., Altintas, M. M., Wei, C., et al. (2005). TRPC6 is a glomerular slit diaphragm-associated channel required for normal renal function. *Nat Genet,* **37**(7), 739-744.

Reiser, J., von Gersdorff, G., Loos, M., Oh, J., Asanuma, K., Giardino, L., et al. (2004). Induction of B7-1 in podocytes is associated with nephrotic syndrome. *J Clin Invest,* **113**(10), 1390-1397.

Reiser, J., von Gersdorff, G., Simons, M., Schwarz, K., Faul, C., Giardino, L., et al. (2002). Novel concepts in understanding and management of glomerular proteinuria. *Nephrol Dial Transplant,* **17**(6), 951-955.

Ronco, P., & Debiec, H. (2006). Molecular dissection of target antigens and nephritogenic antibodies in membranous nephropathy: towards epitope-driven therapies. *J Am Soc Nephrol,* **17**(7), 1772-1774.

Sanger, F. (1981). Determination of nucleotide sequences in DNA. *Science,* **214**(4526), 1205-1210.

Sato, Y., Miyasaka, N., & Yoshihara, Y. (2005). Mutually exclusive glomerular innervation by two distinct types of olfactory sensory neurons revealed in transgenic zebrafish. *J Neurosci,* **25**(20), 4889-4897.

Schaefer, L., Babelova, A., Kiss, E., Hausser, H. J., Baliova, M., Krzyzankova, M., et al. (2005). The matrix component biglycan is proinflammatory and signals through Toll-like receptors 4 and 2 in macrophages. *J Clin Invest,* **115**(8), 2223-2233.

Schiffer, M., Bitzer, M., Roberts, I. S., Kopp, J. B., ten Dijke, P., Mundel, P., et al. (2001). Apoptosis in podocytes induced by TGF-beta and Smad7. *J Clin Invest,* **108**(6), 807-816.

Schindl, R., Frischauf, I., Kahr, H., Fritsch, R., Krenn, M., Derndl, A., et al. (2007). The first ankyrin-like repeat is the minimum indispensable key structure for functional assembly of homo- and heteromeric TRPC4/TRPC5 channels. *Cell Calcium*.

Schliwa, M. (1982). Action of cytochalasin D on cytoskeletal networks. *J Cell Biol,* **92**(1), 79-91.

Schmid, H., Henger, A., Cohen, C. D., Frach, K., Grone, H. J., Schlondorff, D., et al. (2003). Gene expression profiles of podocyte-associated molecules as diagnostic markers in acquired proteinuric diseases. *J Am Soc Nephrol,* **14**(11), 2958-2966.

Schnabel, E., Anderson, J. M., & Farquhar, M. G. (1990). The tight junction protein ZO-1 is concentrated along slit diaphragms of the glomerular epithelium. *J Cell Biol,* **111**(3), 1255-1263.

Schwarz, K., Simons, M., Reiser, J., Saleem, M. A., Faul, C., Kriz, W., et al. (2001). Podocin, a raft-associated component of the glomerular slit diaphragm, interacts with CD2AP and nephrin. *J Clin Invest,* **108**(11), 1621-1629.

Seri, M., Pecci, A., Di Bari, F., Cusano, R., Savino, M., Panza, E., et al. (2003). MYH9-related disease: May-Hegglin anomaly, Sebastian syndrome, Fechtner syndrome, and Epstein syndrome are not distinct entities but represent a variable expression of a single illness. *Medicine (Baltimore),* **82**(3), 203-215.

Sever, S., Altintas, M. M., Nankoe, S. R., Moller, C. C., Ko, D., Wei, C., et al. (2007). Proteolytic processing of dynamin by cytoplasmic cathepsin L is a mechanism for proteinuric kidney disease. *J Clin Invest,* **117**(8), 2095-2104.

Shankland, S. J. (2006). The podocyte's response to injury: role in proteinuria and glomerulosclerosis. *Kidney Int,* **69**(12), 2131-2147.

Shankland, S. J., Pippin, J., Pichler, R. H., Gordon, K. L., Friedman, S., Gold, L. I., et al. (1996). Differential expression of transforming growth factor-beta isoforms and receptors in experimental membranous nephropathy. *Kidney Int,* **50**(1), 116-124.

Shankland, S. J., Pippin, J. W., Reiser, J., & Mundel, P. (2007). Podocytes in culture: past, present, and future. *Kidney Int,* **72**(1), 26-36.

Shi, J., Mori, E., Mori, Y., Mori, M., Li, J., Ito, Y., et al. (2004). Multiple regulation by calcium of murine homologues of transient receptor potential proteins TRPC6 and TRPC7 expressed in HEK293 cells. *J Physiol,* **561**(Pt 2), 415-432.

Shih, N. Y., Li, J., Karpitskii, V., Nguyen, A., Dustin, M. L., Kanagawa, O., et al. (1999). Congenital nephrotic syndrome in mice lacking CD2-associated protein. *Science,* **286**(5438), 312-315.

Shirato, I., Sakai, T., Kimura, K., Tomino, Y., & Kriz, W. (1996). Cytoskeletal changes in podocytes associated with foot process effacement in Masugi nephritis. *Am J Pathol,* **148**(4), 1283-1296.

Sidi, S., Friedrich, R. W., & Nicolson, T. (2003). NompC TRP channel required for vertebrate sensory hair cell mechanotransduction. *Science,* **301**(5629), 96-99.

Singh, B. B., Lockwich, T. P., Bandyopadhyay, B. C., Liu, X., Bollimuntha, S., Brazer, S. C., et al. (2004). VAMP2-dependent exocytosis regulates plasma membrane insertion of TRPC3 channels and contributes to agonist-stimulated Ca2+ influx. *Mol Cell,* **15**(4), 635-646.

Sinkins, W. G., Goel, M., Estacion, M., & Schilling, W. P. (2004). Association of immunophilins with mammalian TRPC channels. *J Biol Chem,* **279**(33), 34521-34529.

Smith, P. R., Saccomani, G., Joe, E. H., Angelides, K. J., & Benos, D. J. (1991). Amiloride-sensitive sodium channel is linked to the cytoskeleton in renal epithelial cells. *Proc Natl Acad Sci U S A,* **88**(16), 6971-6975.

Smyth, J. T., Lemonnier, L., Vazquez, G., Bird, G. S., & Putney, J. W., Jr. (2006). Dissociation of regulated trafficking of TRPC3 channels to the plasma membrane from their activation by phospholipase C. *J Biol Chem,* **281**(17), 11712-11720.

Somlo, S., & Mundel, P. (2000). Getting a foothold in nephrotic syndrome. *Nat Genet,* **24**(4), 333-335.

Sours, S., Du, J., Chu, S., Ding, M., Zhou, X. J., & Ma, R. (2006). Expression of canonical transient receptor potential (TRPC) proteins in human glomerular mesangial cells. *Am J Physiol Renal Physiol,* **290**(6), F1507-1515.

Spassova, M. A., Hewavitharana, T., Xu, W., Soboloff, J., & Gill, D. L. (2006). A common mechanism underlies stretch activation and receptor activation of TRPC6 channels. *Proc Natl Acad Sci U S A,* **103**(44), 16586-16591.

Steffes, M. W., Schmidt, D., McCrery, R., & Basgen, J. M. (2001). Glomerular cell number in normal subjects and in type 1 diabetic patients. *Kidney Int,* **59**(6), 2104-2113.

Strubing, C., Krapivinsky, G., Krapivinsky, L., & Clapham, D. E. (2001). TRPC1 and TRPC5 form a novel cation channel in mammalian brain. *Neuron,* **29**(3), 645-655.

Strubing, C., Krapivinsky, G., Krapivinsky, L., & Clapham, D. E. (2003). Formation of novel TRPC channels by complex subunit interactions in embryonic brain. *J Biol Chem,* **278**(40), 39014-39019.

Takeda, T., McQuistan, T., Orlando, R. A., & Farquhar, M. G. (2001). Loss of glomerular foot processes is associated with uncoupling of podocalyxin from the actin cytoskeleton. *J Clin Invest,* **108**(2), 289-301.

Tanaka, E., & Sabry, J. (1995). Making the connection: cytoskeletal rearrangements during growth cone guidance. *Cell,* **83**(2), 171-176.

Thisse, C., & Thisse, B. (1999). Antivin, a novel and divergent member of the TGFbeta superfamily, negatively regulates mesoderm induction. *Development,* **126**(2), 229-240.

Thompson, J. D., Higgins, D. G., & Gibson, T. J. (1994). CLUSTAL W: improving the sensitivity of progressive multiple sequence alignment through sequence weighting, position-specific gap penalties and weight matrix choice. *Nucleic Acids Res,* **22**(22), 4673-4680.

Thorsen, D. H., & Hale, M. E. (2005). Development of zebrafish (Danio rerio) pectoral fin musculature. *J Morphol,* **266**(2), 241-255.

Thorsen, D. H., & Hale, M. E. (2007). Neural development of the zebrafish (Danio rerio) pectoral fin. *J Comp Neurol,* **504**(2), 168-184.

Tiruppathi, C., Minshall, R. D., Paria, B. C., Vogel, S. M., & Malik, A. B. (2002). Role of Ca2+ signaling in the regulation of endothelial permeability. *Vascul Pharmacol,* **39**(4-5), 173-185.

Topala, C. N., Bindels, R. J., & Hoenderop, J. G. (2007). Regulation of the epithelial calcium channel TRPV5 by extracellular factors. *Curr Opin Nephrol Hypertens,* **16**(4), 319-324.

Topham, P. S., Haydar, S. A., Kuphal, R., Lightfoot, J. D., & Salant, D. J. (1999). Complement-mediated injury reversibly disrupts glomerular epithelial cell actin microfilaments and focal adhesions. *Kidney Int,* **55**(5), 1763-1775.

Tossidou, I., Kardinal, C., Peters, I., Kriz, W., Shaw, A., Dikic, I., et al. (2007). CD2AP/CIN85 balance determines receptor tyrosine kinase signaling response in podocytes. *J Biol Chem,* **282**(10), 7457-7464.

Trachtman, H., Schwob, N., Maesaka, J., & Valderrama, E. (1995). Dietary vitamin E supplementation ameliorates renal injury in chronic puromycin aminonucleoside nephropathy. *J Am Soc Nephrol,* **5**(10), 1811-1819.

Trebak, M., Vazquez, G., Bird, G. S., & Putney, J. W., Jr. (2003). The TRPC3/6/7 subfamily of cation channels. *Cell Calcium,* **33**(5-6), 451-461.

Tryggvason, K., & Wartiovaara, J. (2001). Molecular basis of glomerular permselectivity. *Curr Opin Nephrol Hypertens,* **10**(4), 543-549.

Tsiokas, L., Arnould, T., Zhu, C., Kim, E., Walz, G., & Sukhatme, V. P. (1999). Specific association of the gene product of PKD2 with the TRPC1 channel. *Proc Natl Acad Sci U S A,* **96**(7), 3934-3939.

Vazquez, G., Wedel, B. J., Kawasaki, B. T., Bird, G. S., & Putney, J. W., Jr. (2004). Obligatory role of Src kinase in the signaling mechanism for TRPC3 cation channels. *J Biol Chem,* **279**(39), 40521-40528.

Venkatachalam, K., & Montell, C. (2007). TRP channels. *Annu Rev Biochem,* **76**, 387-417.

Verma, R., Kovari, I., Soofi, A., Nihalani, D., Patrie, K., & Holzman, L. B. (2006). Nephrin ectodomain engagement results in Src kinase activation, nephrin phosphorylation, Nck recruitment, and actin polymerization. *J Clin Invest,* **116**(5), 1346-1359.

Verma, R., Wharram, B., Kovari, I., Kunkel, R., Nihalani, D., Wary, K. K., et al. (2003). Fyn binds to and phosphorylates the kidney slit diaphragm component Nephrin. *J Biol Chem,* **278**(23), 20716-20723.

Vincenti, F., & Ghiggeri, G. M. (2005). New insights into the pathogenesis and the therapy of recurrent focal glomerulosclerosis. *Am J Transplant,* **5**(6), 1179-1185.

Walz, G. (2005). Slit or pore? A mutation of the ion channel TRPC6 causes FSGS. *Nephrol Dial Transplant,* **20**(9), 1777-1779.

Warnock, D. G. (2005). Fabry disease: diagnosis and management, with emphasis on the renal manifestations. *Curr Opin Nephrol Hypertens,* **14**(2), 87-95.

Warnock, D. G. (2007). Enzyme replacement therapy and Fabry kidney disease: quo vadis? *J Am Soc Nephrol,* **18**(5), 1368-1370.

Wasserstein, A. G. (1997). Membranous glomerulonephritis. *J Am Soc Nephrol,* **8**(4), 664-674.

Wedel, B. J., Vazquez, G., McKay, R. R., St, J. B. G., & Putney, J. W., Jr. (2003). A calmodulin/inositol 1,4,5-trisphosphate (IP3) receptor-binding region targets TRPC3 to the plasma membrane in a calmodulin/IP3 receptor-independent process. *J Biol Chem,* **278**(28), 25758-25765.

Weissmann, N., Dietrich, A., Fuchs, B., Kalwa, H., Ay, M., Dumitrascu, R., et al. (2006). Classical transient receptor potential channel 6 (TRPC6) is essential for hypoxic pulmonary vasoconstriction and alveolar gas exchange. *Proc Natl Acad Sci U S A,* **103**(50), 19093-19098.

Welsch, T., Endlich, N., Gokce, G., Doroshenko, E., Simpson, J. C., Kriz, W., et al. (2005). Association of CD2AP with dynamic actin on vesicles in podocytes. *Am J Physiol Renal Physiol,* **289**(5), F1134-1143.

Welsh, D. G., Morielli, A. D., Nelson, M. T., & Brayden, J. E. (2002). Transient receptor potential channels regulate myogenic tone of resistance arteries. *Circ Res,* **90**(3), 248-250.

Westerfield, O. (1995). A prescription for hospital safety: treating workplace violence. *Healthc Facil Manag Ser*, 1-8.

Wharram, B. L., Goyal, M., Gillespie, P. J., Wiggins, J. E., Kershaw, D. B., Holzman, L. B., et al. (2000). Altered podocyte structure in GLEPP1 (Ptpro)-deficient mice associated with hypertension and low glomerular filtration rate. *J Clin Invest,* **106**(10), 1281-1290.

Wiggins, R. C. (2007). The spectrum of podocytopathies: a unifying view of glomerular diseases. *Kidney Int,* **71**(12), 1205-1214.

Winn, M.P. (2004). A new gene in proteinuria. Public presentation; 5th International Podocyte Conference, Seattle, Washington, United States; June 18-20.

Winn, M. P., Conlon, P. J., Lynn, K. L., Farrington, M. K., Creazzo, T., Hawkins, A. F., et al. (2005). A mutation in the TRPC6 cation channel causes familial focal segmental glomerulosclerosis. *Science,* **308**(5729), 1801-1804.

Winn, M. P., Daskalakis, N., Spurney, R. F., & Middleton, J. P. (2006). Unexpected role of TRPC6 channel in familial nephrotic syndrome: does it have clinical implications? *J Am Soc Nephrol,* **17**(2), 378-387.

Wissenbach, U., Niemeyer, B. A., & Flockerzi, V. (2004). TRP channels as potential drug targets. *Biol Cell,* **96**(1), 47-54.

Wu, G., & Somlo, S. (2000). Molecular genetics and mechanism of autosomal dominant polycystic kidney disease. *Mol Genet Metab,* **69**(1), 1-15.

Wyszynski, M., Lin, J., Rao, A., Nigh, E., Beggs, A. H., Craig, A. M., et al. (1997). Competitive binding of alpha-actinin and calmodulin to the NMDA receptor. *Nature,* **385**(6615), 439-442.

Yao, J., Le, T. C., Kos, C. H., Henderson, J. M., Allen, P. G., Denker, B. M., et al. (2004). Alpha-actinin-4-mediated FSGS: an inherited kidney disease caused by an aggregated and rapidly degraded cytoskeletal protein. *PLoS Biol,* **2**(6), e167.

Yu, Y., Fantozzi, I., Remillard, C. V., Landsberg, J. W., Kunichika, N., Platoshyn, O., et al. (2004). Enhanced expression of transient receptor potential channels in idiopathic pulmonary arterial hypertension. *Proc Natl Acad Sci U S A,* **101**(38), 13861-13866.

Yuan, J. P., Kiselyov, K., Shin, D. M., Chen, J., Shcheynikov, N., Kang, S. H., et al. (2003). Homer binds TRPC family channels and is required for gating of TRPC1 by IP3 receptors. *Cell,* **114**(6), 777-789.

Zhang, L., & Saffen, D. (2001). Muscarinic acetylcholine receptor regulation of TRP6 Ca2+ channel isoforms. Molecular structures and functional characterization. *J Biol Chem,* **276**(16), 13331-13339.